

**Indentation Curve Prediction and Inverse Material
Parameters Identification of Hyperfoam Materials Based
on Intelligent ANN Method**

Xiaoxiang Su

**A thesis submitted in partial fulfilment of the requirement of the
Liverpool John Moores University for the degree of Doctor of
Philosophy**

May 2014

ACKNOWLEDGEMENTS

I would like to take this opportunity to express my deepest gratitude and sincerest thanks to my supervisors Prof. James Ren, Dr Jamie Finlay and Prof. Ian Jenkinson for their inspiring supervision of my study and guidance during the production of this thesis.

Many other academic, secretarial and technical members of staff have facilitated the realisation of this thesis and I express them all my gratitude. I would like to thank Mr. Clive Eyre and Mr. Steven Gotts for their invaluable technical support with modifying the testing machine and material testing.

I acknowledge the Liverpool John Moores University and the School of Engineering for the facilities and support provided.

Special thanks also to my group mates, Mr J. Aw, Mr A. Norbury, Dr F. Elkut, Dr L. Li and Dr. Y. Gu for their friendship and sharing the experience of being a postgraduate student. I am also grateful of the help of my friends, who gave me help in many ways and shared a great time in my studies and life at Liverpool John Moores University.

Finally, I would like to thank my family for sustained encouragement that gave me motivation during my studies, continuous and unselfish love and support.

Xiaoxiang (Justin) Su

ABSTRACT

In this work, an ANN program has been developed to predict the indentation P-h curves with known properties (hyperfoam material parameter, μ and α). An interactive parametric FE model and python programming based data extracting program has been developed and used to develop data for the ANN program. Two approaches have been proposed and evaluated to represent the P-h curve. One is using 2nd order polynomial trendline approach ($P=a_2h^2+a_1h$), the other is to use the forces at different indentation depth. The performance of the ANN based on the trendline approach is evaluated with MSE and relative error of the coefficient 'a2' and 'a1' and the average error in forces over different depths. A frequency method is used to analyse the data, which provided important data/base to further enhanced the accuracy of the P-h curve based on averaging multiple ANN tests. This approach effectively taking use of the fact that ANN prediction is not continuous around any property point. The ANN program with the depth based approach showed similar accuracy in predicting P-h curves of hyperfoam materials. The program was validated in blind tests with numerical data and experimental data on two EVA foams with known properties. Comparison with other approaches (including surface mapping and direct data space fitting process) showed that the ANN program is accurate and much quicker than some other approaches and direct FE modeling.

The feasibility of using ANN to directly predict the material properties is evaluated including assessing its capacity to predict trained data and untrained data. The use of single indenter approach and dual indenter approach is assessed. It was found that the approach with 2nd order polynomial fitting of the P-h curves is not able to predict the material parameters. Using 3rd order fitting showed much improvement and it is able to predict the trained data accurately but could not be used to predict untrained data. Works on dual indenter approach with R4 and R6 showed some improvement in predicting untrained data but could not produce data with reasonable accuracy of the full dataset.

A new approach utilising the direct ANN program for P-h curve prediction is developed. A computerised program (with Web based interface) has been developed including data

generation through ANN, data storage, interface for input and viewing results. A searching program is developed which enables the identification of any possible materials property sets that produce P-h curves matching the experiment data within a predefined error range. The approach is applied to analysis single and dual indenter methods through blind tests with model materials (with known material properties). A new approach using foams of different thickness is also proposed. The results showed that in a single indenter approach, there are multiple materials property sets that can produce similar P-h curves, thus the results are not unique. Dual indenter size approach showed a significant improvement in mapping out all potential material sets matching the test data. The new program successfully identifies additional material property sets that can produce P-h curves that match both R4 and R6 data, which was not identified previously with other inverse programs. The new approach proposed of using the tested data on samples of different thickness showed that the uniqueness of the prediction can be improved. The accuracy and validity of the program is firstly assessed with blind tests (using numerical data as input/target) then used to predict the properties of the EVA foam samples. Some key results of the real foam data is compared to the target and prediction results from other programs and data processing method, the comparison results showed that the new ANN based computer program has clear improvement in accuracy, robustness and efficiency in predicting the parameters of EVA foams. Future work is to transfer the program and methodology developed to other material systems and testing conditions and further develop the computer program for material developments and research.

Nomenclature

Upper case

| | | |
|-----------------|------------------------------|-----|
| C | Curvature of the P-h curve | |
| E ₁ | Young's Modulus (Material 1) | GPa |
| F | Indentation force | N |
| F _M | Major loading | N |
| F _m | Minor loading | N |
| G | Objective function | |
| J | Jacobian matrix | |
| P | Indentation load | N |
| P _{av} | Indentation load average | N |
| P _m | Indentation peak force | N |
| P _u | Unloading force | N |
| R | Radius of the indenter | mm |
| R ² | Coefficient of determination | |
| W _e | Elastic work | KJ |
| W _p | Plastic work | KJ |
| W _t | Total work | KJ |

Lower case

| | | |
|----------------|---|----|
| a ₁ | first order curve fitting coefficient of the P-h curve | |
| a ₂ | Second order curve fitting coefficient of the P-h curve | |
| b | Bias in a neural network | |
| <i>f</i> | Transfer function in ANN | |
| h | Depth of Indentation | mm |
| h _p | Penetration measured at the circle of contact | mm |
| h _r | Residual indentation depth | mm |
| h _s | Maximum depth of penetration | mm |
| n | Work hardening coefficients | |
| <i>v</i> | Poisson's ratio | |
| u _z | Vertical displacement z direction | mm |
| wp | Weight factor in ANN | |

Greek

| | | |
|-----------------------------------|---------------------------------------|-----|
| σ | Stress | MPa |
| E | Young's Modulus | |
| ε_e | The engineering measurement of strain | |
| $\lambda_1, \lambda_2, \lambda_3$ | Principle stretches | |
| J^{el} | Elastic volume ratio | |
| μ | Shear modulus | GPa |

Abbreviations

| | |
|--------|--|
| ANN | Artificial Neural Networks |
| CAE | Computer Aided Engineering |
| EVA | Ethylene vinyl acetate |
| FE | Finite Element |
| FEM | Finite Element Models |
| MLP | Multilayer perceptron |
| MSE | Mean-Square-Error |
| MSEREG | Mean-Squared-Error with Regularization |
| P-h | Force-displacement curve |
| QNA | Quasi Newton Algorithm |
| TANSIG | Tangent sigmoid |

Contents

| | |
|--|---------------|
| Acknowledgement | |
| Abstract | |
| Nomenclature | |
| List of Figures | |
| Chapter 1 Introduction | 1-8 |
| 1.1 Introduction | 1 |
| 1.2 Aims and objectives | 4 |
| 1.3 Outline of the thesis | 7 |
| Chapter 2 Literature Review | 9-70 |
| 2.1 Indentation tests and its applications | 10 |
| 2.2 Linear and nonlinear material behaviours and energy functions for EVA foams | 19 |
| 2.3 Inverse problems and its application in material testing and properties prediction | 24 |
| 2.4. Introduction to ANN and its applications. | 31 |
| 2.4.1 The structure and working process of ANN | 31 |
| 2.4.2 Transfer (activation) functions for ANNs | 34 |
| 2.4.3 Different types of ANN | 37 |
| 2.4.4 Learning rules and their applications | 42 |
| 2.5 Testing and validation of an ANN for practical applications | 49 |
| 2.5.1 Parameter for testing and validation of performance of an ANN | 49 |
| 2.5.2 Generalisation of ANN and influencing factors | 50 |
| 2.5.3 Key Factors affecting the ANN performance | 52 |
| 2.6 FE modelling methods and data processing | 57 |
| 2.7 Applications of ANN in engineering and indentation tests | 60 |
| 2.8 Potential application of ANN in indentation testing of EVA foams and main challenges | 65 |
| Chapter 3 Prediction of indentation force displacement curves of hyperfoams based ANN | 71-129 |
| 3.1 Introduction and research structure | 72 |
| 3.2 Experimental test and numerical models | 71 |
| 3.2.1 Experimental and typical results | 75 |
| 3.2.2 FE indentation model and validation | 75 |
| 3.3 ANN Program development for predicting indentation force displacement curve | 80 |
| 3.3.1 Key technical works and programs | 80 |
| 3.3.2 The structure of the ANNs and proposed input data based on indentation P-h curves. | 83 |
| 3.3.3 Development of data space for ANN training, testing and validation. | 87 |
| 3.3.4 The optimisation of the activation functions, number of neurons and development of early stopping mechanisms | 93 |

| | |
|--|---------|
| 3.4 ANN prediction result with the trendline approach: Results and analysis | 96 |
| 3.5 ANN program based on the force at depth approach and results | 116 |
| 3.6 Use of ANN in the prediction of P-h curves of EVA foams of known properties. | 125 |
| 3.7 Summary | 128 |
| | |
| Chapter 4 Inverse Materials Parameters Identification Based on Indentation Tests | 130-192 |
| 4.1 Introduction | 131 |
| 4.2 Evaluation ANN based approach to predict material properties based on indentation curves. | 135 |
| 4.2.1 Structure of the ANN and data process | 135 |
| 4.2.2 Preliminary evaluation of the data using nftool and comparison between 2nd and 3rd order polynomial fitting. | 144 |
| 4.2.3 ANN based inverse with different data intensity | 150 |
| 4.2.4 ANN prediction of material parameters based on dual indenter approach | 156 |
| 4.3 Materials properties identification based on data mapping approach, computer program and results | 160 |
| 4.3.1 Structure of the inverse materials parameter identification approach and computer program. | 160 |
| 4.3.2 Inverse FE modelling based on the data of single indenter | 165 |
| 4.3.3 Inverse FE modelling based on data from dual indenters of different sizes | 170 |
| 4.4 Inverse FE modelling based on the tests data on sample of different thickness and dual thickness approach | 175 |
| 4.5 Prediction of EVA foam properties based on experimental data | 184 |
| 4.6 Summary | 191 |
| | |
| Chapter 5 Discussions | 193-205 |
| 5.1 Use of ANN in prediction of P-h curves based on different approaches and its applications | 194 |
| 5.2 Comparison of the ANN approach with other methods | 198 |
| 5.3 Inverse modelling and data analysis method | 203 |
| | |
| Chapter 6 Conclusion and future work | 206-210 |
| 6.1 Conclusion | 206 |
| 6.2 Future works | 209 |
| | |
| References | 210-218 |

List of Figures

Chapter 2

| | |
|---|----|
| Figure 2.1 Schematic to show an indentation testing process and typical load (P) – indentation depth (h) data of the loading curve . | 14 |
| Figure 2.2 Schematics showing different shapes of indentation tips. | 15 |
| Figure 2.3 Use of indentation tests in different areas. | 16 |
| Figure 2.4 <i>In vivo</i> indentation test and simulation of the human foot tissue | 17 |
| Figure 2.5(a) Schematic illustration of a typical force (P) indentation depth (h) response of an elasto-plastic material to instrumented sharp indentation showing that the loading curve can be expressed by a simple mathematical expression (C is the curvature). | 18 |
| Figure 2.5 (b) Schematic shows typical continuous indentation curves of foam/rubber materials. | 18 |
| Figure 2.6 Schematics showing linear elastic and nonlinear material behaviours in loading | 22 |
| Figure 2.7 Deformation modes of various experimental tests for defining nonlinear material parameters | 23 |
| Figure 2.8 Flow chart illustrating typical procedures of an interactive inverse FE modelling method. | 28 |
| Figure 2.9 Flow chart of Kalman Filter procedure to determine the unknown parameters using instrumented indentation records | 29 |
| Figure 2.10 A typical parametric modelling approach to extract the elastic material properties based on surface tension tests | 30 |
| Figure 2.11 The structure and working process of ANN. | 33 |
| Figure 2.12 Typical transfer (activation) functions for ANNs | 36 |
| Figure 2.13 Feedforward and feedback system | 39 |
| Figure 2.14 A typical unsupervised learning networks: Kohonen SOMs (Self-Organizing Maps) for ecological modeling | 40 |
| Figure 2.15 Supervised learning and a typical supervised learning networks of a multilayer feed-forward neural network for weld joint strength prediction | 41 |
| Figure 2.16 (a) Schematic to illustrate finding the minimum of a function | 48 |
| Figure 2.16 (b) Typical example to illustrate the concept of The Newton Method. | 49 |
| Figure 2.17 Typical examples showing using MSE to assessing effect of number of hidden units | 54 |
| Figure 2.18 Typical data showing the improvement of ANN approximating capability with increases of the number of neurons in the hidden layer of in a feed-forward artificial neural network | 55 |
| Figure 2.19 Schematic to show the concept of fitting and over fit | 56 |
| Figure 2.20 The main steps in a Finite Element modelling process | 59 |
| Figure 2.21 A two ANN system used in predicting plastic properties of metals based on conical indentation | 63 |
| Figure 2.22 A single ANN system used in predicting plastic properties based on conical indentation and the equations. | 64 |

| | |
|--|----|
| Figure 2.23 Schematics to show the structure of the sport shoe design and the application of EVA materials | 68 |
| Figure 2.24 Manufacture of the midsole with different materials to illustrate the use of EVA foam. | 69 |
| Figure 2.25 FE model for simulating the effect of EVA foams on shoe heel interaction to highlight the importance of EVA testing and properties. | 70 |

Chapter 3

| | |
|--|-----|
| Figure 3.1 Flow chart showing the main research work. | 74 |
| Figure 3.2 The indentation testing system used and typical force displacement curve of a sample EVA foam. | 77 |
| Figure 3.3 FE model of indentation process with a spherical indenter and typical displacement fields. | 78 |
| Figure 3.4 FE model validation based on the experimental data of materials of with known solution. | 79 |
| Figure 3.5 Flow chart to show the research structure and programming to predict the indentation force displacement curve under different conditions. | 82 |
| Figure 3.6 Proposed feed-forward neural network with back propagation Algorithm for predicting the indentation force-displacement data. | 84 |
| Figure 3.7 Schematic to show the two different approaches to process the indentation curves for the ANN (Approach 1: Point method; Approach 2: Trendline approach). | 85 |
| Figure 3.8 The structure of the multilayer neural networks for the Coefficient approach (2nd order polynomial) and force at depth approach | 86 |
| Figure 3.9 The matrix of training and testing data for the ANN program. | 90 |
| Figure 3.10 Typical FE indentation data and curve fitting with 2nd order polynomial trendline. | 92 |
| Figure 3.11 Typical training curves to show the influence of different activation functions in the hidden layer. | 95 |
| Figure 3.12 Typical ANN training and validation curve with early stopping (trendline approach, training and validation: material data set-1, R4mm). | 102 |
| Figure 3.13 MSE for training and validation showing the effect of the number of neurons | 103 |
| Figure 3.14 Error of the 2nd and 1st order fitting coefficient (a_2 and a_1) using the training data (Material data set-1) as test data. | 104 |
| Figure 3.15 Typical Error of the 2nd and 1st order coefficient using the un-trained data as test data. | 105 |
| Figure 3.16 Typical data showing the variation of ANN predicted data in different ANN tests using untrained data as test data | 106 |
| Figure 3.17 Averaged relative error and maximum error of a_2 and a_1 based ANN with 10 and 20 neurons (Test data Material data set 3) | 107 |
| Figure 3.18 (a) Sample data showing the predicted force at different indentation depth based on the ANN predicted curve coefficients (a_1 and a_2) with maximum error | 108 |
| Figure 3.18 (b) Average error (among 4 depth) in the forces based on ANN predicted curve coefficients (a_1 and a_2) with maximum error (Neuron 10). | 109 |

| | |
|--|-----|
| Figure 3.18 (c) Average error in the forces based on ANN predicted curve coefficients (a1 and a2) with maximum error.(Neuron 10). | 109 |
| Figure 3.19 Frequency of data of different error range showing that the prediction with different neuron number. | 110 |
| Figure 3.20 Comparison between average force-displacement curve based on ANN predicted parameters and FE data. | 111 |
| Figure 3.21(a) averaged relative error of the ANN predicted curve coefficient (a2 and a1) with maximum and minimum value of the all the test data. (20 neurons). | 112 |
| Figure 3.21(b) Relative error of the ANN predicted curve coefficient (a2 and a1) with maximum and minimum value of the all the test data. (10 neurons). | 112 |
| Figure 3.22 (a) Relative error of indentation force based on ANN predicted curve fitting parameter for materials Data set-2. (20 neurons). | 113 |
| Figure 3.22 (b) Relative error of indentation force based on ANN predicted curve fitting parameter for materials Data set-2. (10 neurons). | 113 |
| Figure 3.22(c) Frequency of error range for predicting gradient data (data set-2) with neuron 10 and 20. | 114 |
| Figure 3.23 Typical data showing the influence of error (5% or 10%) in material properties on the ANN predicted indentation force-displacement curve. | 115 |
| Figure 3.24 Performance and regression based on the depth approach using material set-1 as the training data (Neuron number =10 and 20). | 118 |
| Figure 3.25 Typical ANN (neuron 20) predicted forces at different indentation depth and relative error to illustrate the way the data processing method. | 119 |
| Figure 3.26 Error in the forces at different depth using untrained data (data set-3) showing the effect of number of neurons. | 121 |
| Figure 3.27 Typical ANN test data with neuron=10 showing the repeatability of each ANN simulation. (Training material set-1; Test materials set-3). | 122 |
| Figure 3.28 (a) Plot of average error (each test 4 depth points over 5 tests) for different material data point and the frequency of different error range. (Depth approach, Test data: material data set-3). | 123 |
| Figure 3.28 (b) Frequency of the error range with neuron 20 and neuron 10 based on the depth method. | 123 |
| Figure 3.29 Comparison of predicted force-displacement curves with material sets of different level of relative error. | 124 |
| Figure 3.30 Comparison between ANN predicted P-h curves with the testing data of R4 and R6. EVA-1 and EVA-2. | 127 |

Chapter 4

| | |
|--|-----|
| Figure 4.1 Flow chart showing the research in inverse prediction of material properties. | 134 |
| Figure 4.2 Proposed feed-forward neural network with back propagation Algorithm for estimating the material parameters (μ and α) based on indentation test data. | 137 |
| Figure 4.3 Schematic to show the two polynomial fitting approach. | 138 |
| Figure 4.4 The structure of the multilayer neural networks for the trend line method. | 139 |
| Figure 4.5 The matrix of training data for the ANN program. | 141 |

| | |
|---|-----|
| Figure 4.6 Typical FE p-h curves fitted with 3 rd order polynomial equation. (2 nd order polynomial fitting was shown in Figure 3.10) | 143 |
| Figure 4.7 Typical result data when using nftool function in NN box with second order curve fitting coefficients. | 146 |
| Figure 4.8 Effect of neuron number on the training MSE. (nftool) based on 2 nd and 3 rd order fitting data. | 147 |
| Figure 4.9 Typical data showing the effect of neuron numbers on the training results | 148 |
| Figure 4.10 Typical results with Material data set-1 as the training data (Neuron 100). | 149 |
| Figure 4.11 Typical ANN prediction results with trained high density data (Materials data set 4) and different neuron number showing that the neuron number needs to be increased when use high density data. | 153 |
| Figure 4.12 Typical results of ANN using the gradient data (Materials data set-2) in predict trained data showing the effect of neuron number on MSE and the value of goal on the prediction accuracy. | 154 |
| Figure 4.13 Typical fine training data with 10% increase and ANN prediction results showing this approach could be used to inversely predict the material parameters based on trained data. | 155 |
| Figure 4.14 The structure of the multilayer neural networks for dual indenter approach (a) and typical regression data (b). (Materials data set-1). | 157 |
| Figure 4.15 (a) Effect of neuron on MSE based on dual indenter approach. | 159 |
| Figure 4.15(b) Predict trained data with dual indenter . | 159 |
| Figure 4.15 (c) Predict untrained data with dual indenter. | 160 |
| Figure 4.16 Flow chart showing the inverse FE modelling approach based on the data from ANNN direct p-h curve prediction. | 163 |
| Figure 4.17 Screen shot to illustrate the data generating function of the computer program developed based on the ANN direct p-h curve prediction. | 164 |
| Figure 4.18 Screen shot to show the structure, input and error setting of the computer program developed. | 164 |
| Figure 4.19 Typical prediction data with R=4mm using a FE data as input | 168 |
| Figure 4.20 Typical prediction data with R=6mm using a FE data as input | 169 |
| Figure 4.21 Dual Indenter approach (R4+R6) using data within predefined error . | 172 |
| Figure 4.22 Typical result with approach using limited number of material point with lower error for the dual indenter approach. | 173 |
| Figure 4.23 FE P-h curves using materials data point 2 in Figure 4. | 174 |
| Figure 4.24 FE model of thin samples and results. | 178 |
| Figure 4.25 Correlation coefficients for 2 nd order polynomial fitting of force-displacement curves of a thin EVA foam. | 180 |
| Figure 4.26 (b) Comparison between the FE P-h curves based on the material properties predicted and the target data. | 181 |
| Figure 4.27 Typical predicted results based on dual sample thickness data (t12 and t20mm) and two different approaches to identify the optimum material properties: fixed error range approach and fixed data number approach. | 182 |
| Figure 4.28 Combination of t24R4, t24R6 and t12R4 with different number of materials sets of lower relative error. | 183 |
| Figure 4.29 Material properties with different error range for Foam 1 using the | |

| | |
|--|-----|
| experimental as input. (Target: $\mu=0.62$; $\alpha=8$). | 185 |
| Figure 4.30 Predicted results based on different range. (Target based on experimental tests: $\mu=0.62$, $\alpha=8$). | 186 |
| Figure 4.31 Comparison between the predicted properties based on the ANN methods, experimental data and results from other methods. | 188 |
| Figure 4.32 Typical Interception point of trendline approach for the dual indenter and dual thickness approach. | 189 |
| Figure 4.33 Sample property identification results showing a situation that the trendline approach is not feasible, while the prediction using overlapping point showed good agreement with standard experimental data. | 190 |

Chapter 5

| | |
|--|-----|
| Figure 5.1 Sample figure to illustrate the process of 3D surface mapping and typical data showing the error range. | 200 |
| Figure 5.2 (a) Program for polynomial point fitting. | 201 |
| Figure 5.2(b) Comparison between the original FE P-h curve, ANN predicted and curve predicted directly though polynomial point fitting. | 202 |

Chapter One Introduction

1.1 Introduction

In a continuous indentation process, an indenter is pressed onto the surface of a material and the force and displacements are recorded. This method is increasingly being used to test materials, and the force/load displacement ($P-h$) curve represents the indentation resistance of the material (Nakamura et al, 2000; Ren et al 2002; Ullner et al, 2002; Tho et al, 2004; Li 2011). The Conventional hardness method only provides information about the hardness of a sample, which could not be directly used to simulate the detailed behaviours of the material in service. The continuous force-displacement data could direct reflect the deformation of the materials and, in some case, the performance of the material in service. In addition, the force displacement data could potentially provide data to extract material parameters from indentation tests. This is particular important for materials such as foams which has a complex material model. Close cell foams, such as Ethylene Vinyl Acetate (EVA) foam are widely used in engineering, sport and biomedical fields (Mills and Zhu, 1999; Petre et al, 2007; Gu 2010). The indentation resistance of the material directly reflects the deformation of the material under load. Detailed properties of the foam are very important for both material development and design. In a product development process, the engineer has to select foam from a range of products; in some cases a combination of material has to be used. Two research areas are very important for EVA foams. One is to predict the performance of the material with known properties; the other is to extract the material parameters from indentation tests. In both cases, ANNs could potentially provide an effective tool.

The artificial neural network (ANN) has been widely used in many engineering fields and recently is has been used in material research and development (Zaw et al, 2009; Esfahani et al, 2009; Partheepan et al 2011; Gong et al, 2012). Use of ANN in materials behaviour prediction or property estimation could be a complex process, in many cases, some physical based analysis or data process has to be implemented. Given the wide application of EVA and the use of indentation testing, it is important to explore the use of ANN in indentation testing and property estimation of EVA materials. The prediction of the

material behaviour represented by the P-h curve will help the engineer/researcher to estimate the potential performance when comparing different materials with known properties. Another area of the case where the nonlinear material parameters are not available, it will be great advantage if the material parameter can be predicted inversely from indentation tests as a quick way of predicting the properties since standard tests are complicated and time consuming. In addition, research is also required to establish an effective way to further develop direct or inverse programs into a computerised program accessible through internet and multimedia to further expand the application these methods in material testing, research and development.

Despite its successful application in many material areas, the use of ANN on hyperfoam materials has not been explored and established. The material represents a much more challenging research topic than metallic materials. For example, in testing metallic materials with shaped indenter, the P-h curve can be represented by a power law relationship (Dao et al 2001). But for EVA foams, a more complex way has to be used to represent the data. The choice of mathematical representation of the curve has to be properly selected to be able to aid the direct or inverse engineering. In addition, the accuracy/robustness in direct (predict indentation curves from known properties) and inverse (predict properties from indentation curves) has to be established. The practice in some of the published work in materials oriented projects has been focused on a limited number of testing cases, which could not satisfy the need of materials research and development or could not be used by material researchers with no direct experience in ANN. In addition, there are possible issues with nonuniqueness, where more than one set of variables fit the target data equally well; this has been a major issue in preventing wider application of the inverse program. One approach to improve this is to use testing data of different conditions (e.g. indenter size, thickness) to improve the robustness. The basic concept is that the true material property should match test data of different conditions. To evaluate these approaches, a methodology and computational tool needs to be developed that is capable of mapping out all possible solutions in a direct/inverse program, which will ultimately give the user the confidence in the inverse results and select the optimum solution. When data from multiple tests are used, an effective way of identifying the target

property needs to be developed, which also needs to be implemented in computing programs. The behaviour of EVA materials are representative of a range of materials including biomedical materials, so the program developed and evaluated with EVA (as a model material) will be transferable to other material systems in the future based on the research framework.

1.2 Aims and Objectives

This work aims to investigate the use of ANN technique in studying indentation tests of EVA foams and establish a computational program to predict the force-displacement data with known properties and/or inverse identification of material parameters from indentation tests.

Main objectives are:

- To develop and optimise an ANN program/methodology to predict the force displacement curves of indentation of hyperfoams models;
- To apply the approach to predict the P-h curves of EVA foams with known material properties and compare the method with other approaches;
- To systematically evaluate the feasibility of using ANN in inverse prediction of material properties based on indentation tests with single and dual indenters;
- To develop an effective method to identify material properties from indentation tests of different conditions and investigate the factors affecting the accuracy and robustness of the inverse FE indentation approach;
- To convert the approach into a computerised program for inverse material property identification;

Many of the work in related field of inverse material properties identification has been focusing on using interactive searching techniques, such as Kalman filter, interactive parameter changing approach, etc, which can predict the materials' behaviour under relatively well defined condition. But there are still uncertainties with the completeness of solution due to the nature of material test or ill conditioning. The focus of the work is to develop a computational program to map out any possible material properties, which can give the user a full picture of all possible solutions in order to make a sound choice with confidence. This is more useful to the material characterisation practice. With such a tool, the factors that affect the accuracy and robustness of an inverse program can be established and new method to improve the performance of an inverse program can be developed though combination of different testing

mode or conditions. One long term focus of the work is to develop a way to represent/analyse the indentation data effectively to make it possible to develop a computerised program (potentially with multi media) to enhance the use of inverse modelling in material works.

In this work, hyperfoam materials (EVA) is to be used as the main test materials. Detailed studies of the EVA foams are very important for many product developments in particular in sport technology. EVA foams are widely used in sport footwear and equipment such as the midsole of sport shoes, providing the shock absorbing and cushioning capacity (Mills 2003; Ruiz-Herrero et al, 2005). The properties of EVA foams are highly nonlinear and viscoelastic (Verdejo and Mills, 2004). Any method to predict the P-h curves from known material properties will make materials tests and comparison easier as some existing model can only deal with elastic model with very small indentation depth. Determination of the material parameters is important to provide data for the simulation of their in-service performances, product design and quality control. The work uses hyperfoam model as a model materials, but in a longer term, this should be transferable to other material systems to be used as a tool to support material research and development or design in related fields.

1.3 Outline of the thesis

In Chapter 2, background information and current research on indentation tests, inverse modelling and their applications in materials characterisation have been reviewed. It covers different types of indentation tests and their applications in studying different materials. A summary of current testing methods for foams is presented. The strain energy functions of foams are reviewed with key controlling material parameters highlighted. The theory of ANN and its application is reviewed and discussed in the context of materials testing. Different inverse FE modelling methods and optimisation programs are compared. The difficulties and challenge for the inverse FE modelling approach based the indentation tests are reviewed and discussed.

Chapter 3 consists of two main parts of work. The first part is development of FE models and data processing of indentation tests. The second part involves developing an ANN program to predict the force indentation displacement curves with known materials properties (μ and α) for different indenter sizes. The ANN work enables the prediction of force displacement data without re-running the FE modelling. The work provides a framework for developing an inverse material property prediction program, which is presented in the next chapter. In the ANN development section, two approaches of representing the P-h curves have been proposed and evaluated; one is to use polynomial trendline to represent the P-h curves (designated as trendline approach); the other is to use force at different indentation depth (designated as depth approach). The validity and accuracy of each ANN is assessed using trained data and new data (not used in training or validation) using Mean-Square-Error (MSE) and relative error as performance indicator and new approach is developed to improve the robustness of the prediction through frequency analysis. The sensitivity of the estimated mechanical properties to variations of the input parameters (e.g. potential perturbation of the load) is also investigated.

Chapter 4 consists of two main parts. In the first part, the feasibility of using ANN directly to predict the material properties with single and dual indenter approach is evaluated. In

the second part of this chapter, a new approach utilising the direct ANN program developed (presented in Chapter 3) is proposed. The work involves developing a large data base using the high efficiency of ANN in predicting P-h curves. A computerised program (through Web interface) including data generation through ANN, data storage, interface for input and viewing results. A search program is developed which enables the identification of any possible materials property sets that match the experiment data within a predefined error range. This will help the user to identify any possible materials sets that are a close match to the target, thus give full confidence in the inversely identified material properties. The program is evaluated with blind tests (i.e. using FE data) then used to investigate analyse real EVA foams.

Chapter 5 discusses the key feature and technical improvement of the program. The P-h prediction is compared to other approach including surface mapping and direct data fitting. The key factor that may affect direct and inverse processes is discussed. The outcome of the work is compared to other inverse modelling approaches and the main improvements identified. The advantages and disadvantages of using the new approach proposed in thesis in dealing with data from different test condition against other approaches are identified. Finally, current and potential future application of the program developed in researching other material system/testing method is discussed.

In Chapter 6, overall conclusions were given and future works were highlighted.

Chapter Two

Literature Review

2.1 Indentation tests, its applications and characteristics of indentation curves

Indentation tests have been employed to measure the material properties of engineering or biological materials/systems for a wide range of applications (Ren et al, 2002; Ullner et al, 2002; Tho et al, 2004; Luo and Lin, 2007; Briody et al, 2012; Budiarsa et al, 2013). In an indentation test, an indenter is pressed onto a sample surface to certain depth, the resistance of the material to deformation could be represented by the size of the residual impression on the surface or the force-indentation depth data, normally designated as P-h curves (Figure 2.1). The main reason for the wide use of indentation tests lies in its experimental simplicity in terms of facilities and sample preparation requirements. The tests can be performed with small samples and can be conducted several times on a single specimen at different locations. In addition, indentation tests can also be performed at different environments (e.g. temperatures or humidities) with complicated loading histories (Ren et al 2002; Petre et al 2005).

Figure 2.2 schematically shows some typical types of indenters of different shapes, these have been developed for different situations and materials. Sharp indenters, such as conical indenter and pyramidal tip, are normally used for harder materials such as metals or ceramics. With these materials, different hardness systems have been developed based on the average pressure underneath the indenters (Dao et al, 2001). Softer materials such as foams and biological tissues are normally tested using flat indenter and spherical indenters to avoid damage. For foams, the hardness is tested commonly by Shore hardness tester using a flat surface and a tapered tip, as shown in Figure 2.2(c). In the shore test, a dead load is applied, and then the depth at major and minor load is measured to represent the resistance of the foam to indentation (Kunz and Studer, 2006). The hardness method only provides indicative information about the resistance of a sample, but could not be directly used to simulate the material behaviours in service (Petre et al, 2007), as in modelling, detailed materials parameter are required (Abaqus 6.10).

Recent developments of advanced instruments have made it possible to record continuously the force and displacement (as shown in Figure 2.1 (b)) rather than measuring

the residual impressions based on a single reading. This approach is particularly useful for materials such as foams and biological materials (Petre et al, 2005). These tests can provide much more data but the curve is not easily represented with a mathematical form and it is difficult to develop link between P-h curve and materials properties of physical meaning. Research is required to develop methods to represent the data and link the curve fitting coefficients to material properties. This is a general goal of this research, as only after a proper way of representation of the indentation curve has been developed, it can be used in estimating the material performance if the material properties are known. On the other side, proper characterization of the indentation curve could help the development of practical inverse tools (i.e. determine the properties from nonstandard test such as indentation tests). This is particularly important for materials of nonlinear material laws with complex structures/loading conditions, such as foams (Mills and Zhu, 1999; Nakamura et al, 2000; Petre et al, 2007) as no robust mathematical solution is available.

There are many application examples of continuous indentation (Giannakopoulos et al, 2006; Jordan et al, 2009; Gu 2010). It can be used in material development, comparing materials in design, providing data for computer simulation, etc. One major application is in testing soft materials such as biological materials and foams. Work in this area is becoming more and more important in order to provide data for computer aided design in areas such as biomechanics, sport and medical engineering, where foams including EVA foams are increasingly being used. Another application of indentation tests and inverse properties prediction is in biological materials, where standard samples cannot be made or are not available. Figure 2.3 (a) shows a typical application of indentation method for characterising soft tissues. In this work, an indenter is pressed into the liver tissue, and force-displacement is measured, which can provide important information on the property of the material or its change with medical condition through the indentation curve (Jordan et al, 2009). Continuous indentation based tests are also more suitable for *in vivo* or *in situ* tests than tests based on static hardness tests. *In vivo* tests are performed on biological tissue in its natural state with the material behaviour close to the real physiological condition. *In vivo* tests with different methods are increasingly used to study the

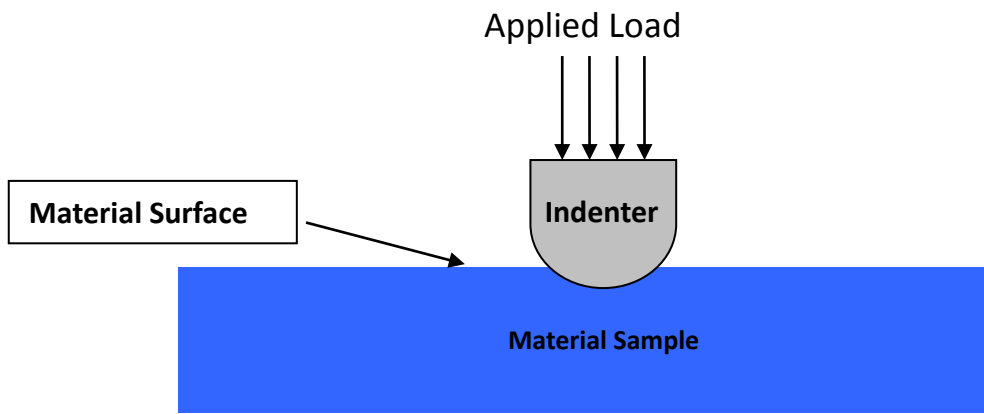
deformation of biological tissue such as human skin, biological organs, heel pad as well some internal organs, with indentation type of test is one of the most common one being explored (Tong et al., 2003; Petre et al, 2007). Figure 2.3 (b) shows a typical set-up of *in vivo* compression testing of the human foot tissue (Tong et al., 2003). The test rig used includes a base plate, a support frame with a see-through Perspex foot mount plate. A force transducer and linear variable displacement transducer (LVDT) measured the indentation force and displacement. Figure 2.4(a) shows the set of indentation used in testing human heel (Lisa 2009; Gu, 2011). In the work, the human heel pad is tested by pressing the indenter to the heel pad. The data can then be used to estimate the material property for developing finite element modelling of human foot and the interaction between human foot and EVA foam or sport shoes (Figure 2.4 (b)).

As shown by these cases, indentation tests are promising and useful techniques. However, there are many technical challenges to make full use of the method. Among the technical challenges could be machine design, data processing and most importantly processing and interpretation of the force-displacement data, which is the main measurable outcome from continuous indentation tests representing the behaviour of the material tested. It will be very useful if the curve can be represented by a simple mathematical formula with curve fitting coefficients linked to the properties. For example, as shown in Figure 2.5(a), in metal material as such as steel, the curvature (C) of the force-displacement data is found to be linked to the yield stress and strain hardening coefficients. The loading part of an instrumented sharp indentation generally follows (Dao 2001).

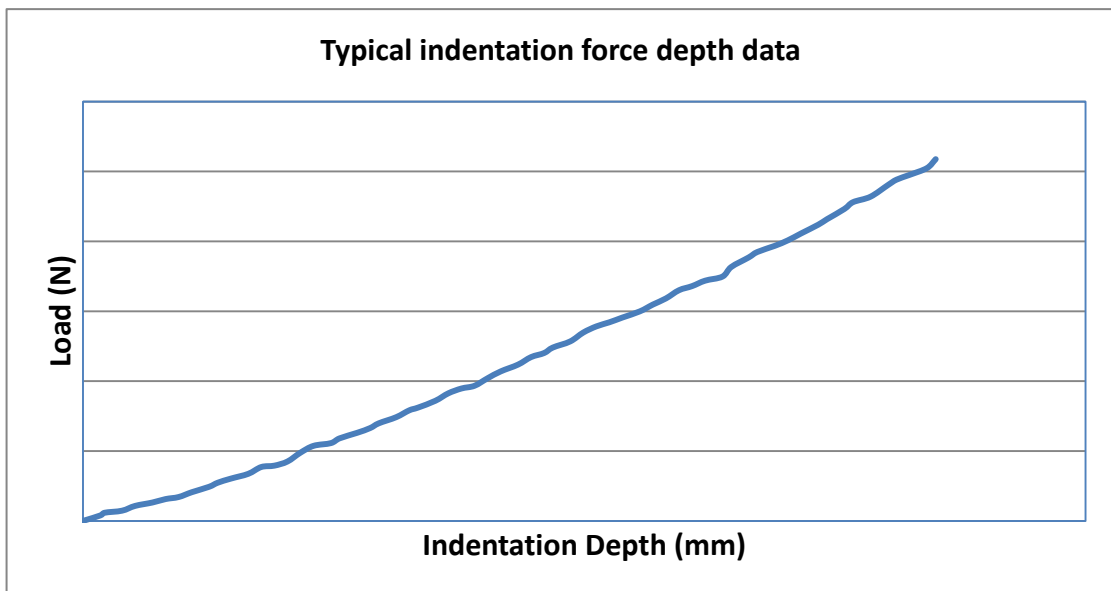
$$P=Ch^2, \tag{2.1}$$

where P is the indentation load, h is the penetration depth measured from the original surface of the sample and C is a constant representing the curvature of the P-h curve, which known to be a function of the plastic materials properties (yield stress and working hardening coefficients) (Dao et al, 2001; Tho et al, 2004). The indentation P-h curve represents the resistance of the materials to elastic and plastic deformation. The existence of this formula and establishment of the relationship has helped to development of many

works associated with indentation of steel and other metal materials, including direct prediction of the force-displacement data from known properties and inverse property prediction. However, the situation with spherical indentation of soft materials such as foam is more complicated as a higher order fitting with more than one coefficient has to be used. As shown in Figure 2.1 (b) and illustrated in Figure 2.5(b), the force displacement curve for foam and rubber like materials are nonlinear. The loading part didn't follow the equation for metals; a more complex approach has to be developed. This makes it more challenging in data process and analysis. Any work that could bring improvement in characterising the force-indentation depth data or extract to more information from the curve would further advance the understanding of the material behaviours. In addition, a way to represent the data (e.g. the loading curve) and potential way of extracting the materials properties will help to quantify the effect of factors such as different materials, temperature, humidity etc. This is part of the general direction of this project using EVA foam as a typical example. The methodology can then be transferred to other material systems



(a)



(b)

Figure 2.1 Schematic to show an indentation testing process (a) and typical load-indentation depth data of the loading curve (b) (P-h curve).

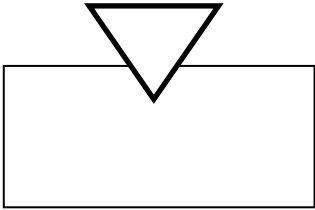
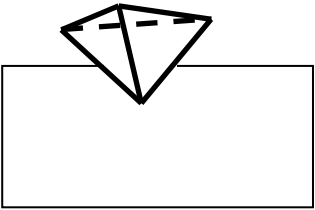
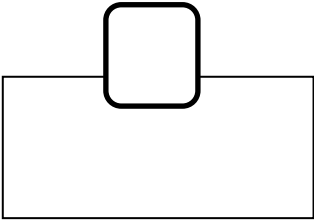
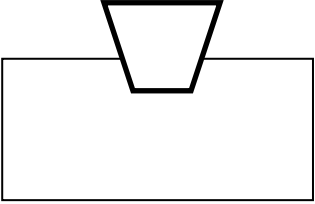
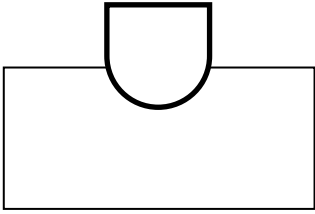
| | |
|---|--|
|  |  |
| <p>(a) Conical indenter.</p> | <p>(b) Sharp (pyramidal tip) indenter; (e.g. Vickers)</p> |
|  |  |
| <p>(c) Flat indenter.</p> | <p>(d) Tapered tip for Shore Hardness Tester.</p> |
|  | |
| <p>(e) Spherical indenter.</p> | |

Figure 2.2 Schematics showing different shapes of indenter tips.

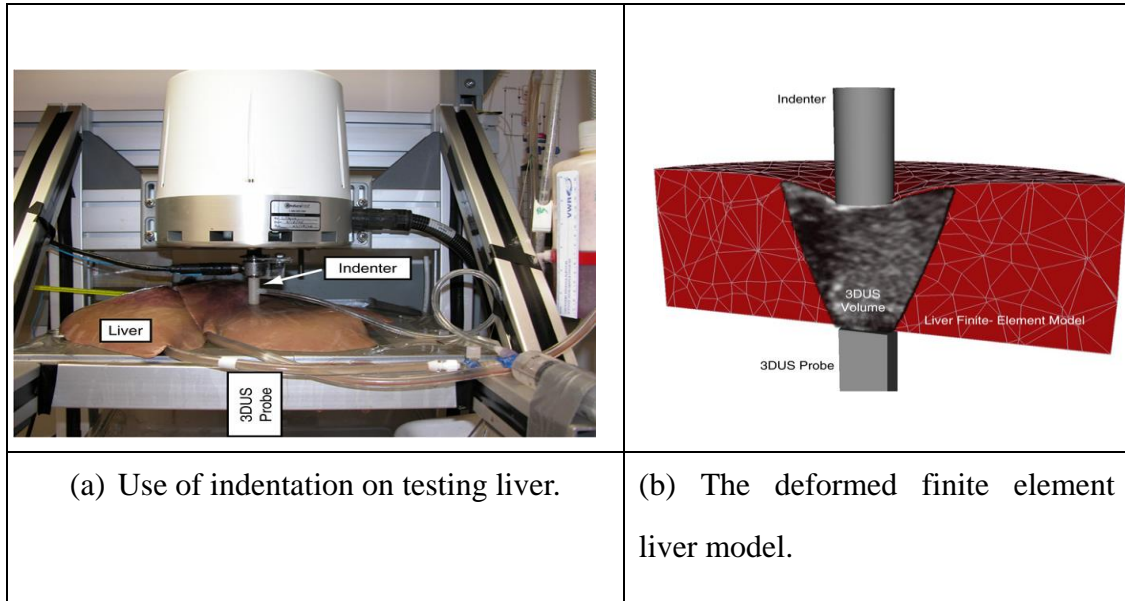


Figure 2.3 (a) Use of indentation tests in studying soft liver tissues (Jordan *et al*, 2009; Elkult, 2012).

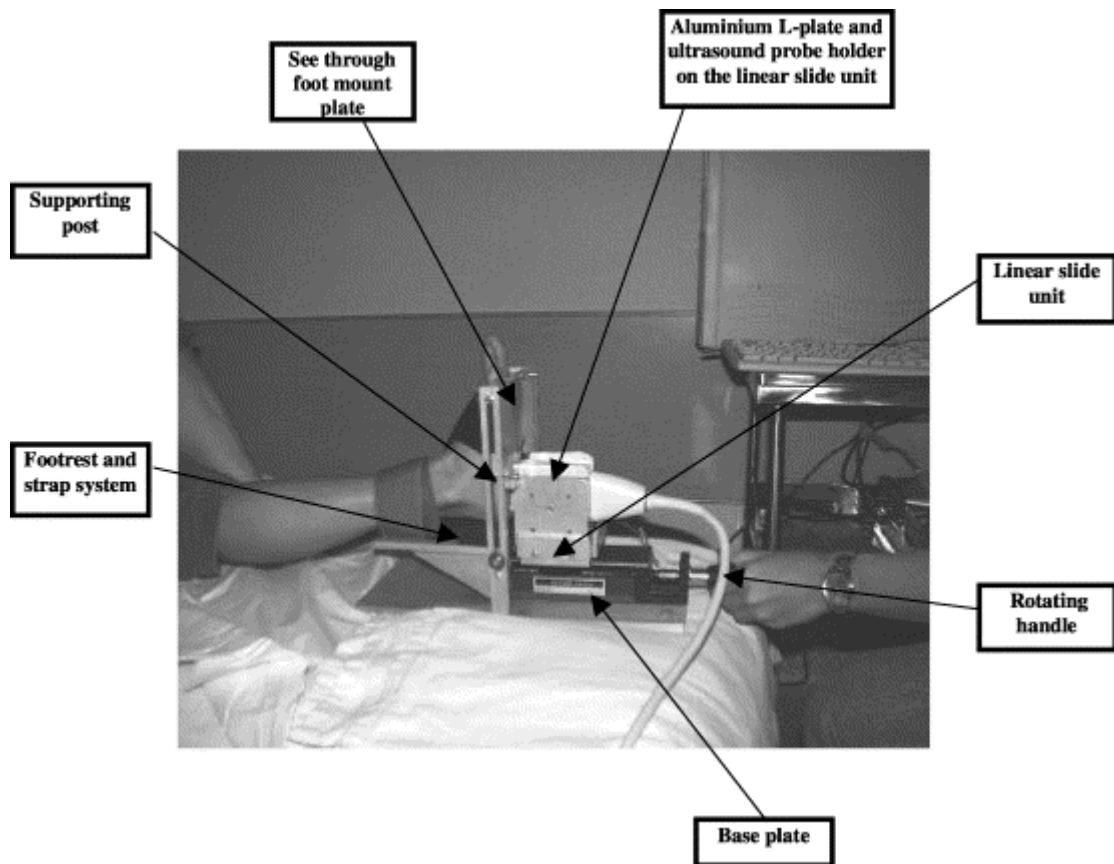
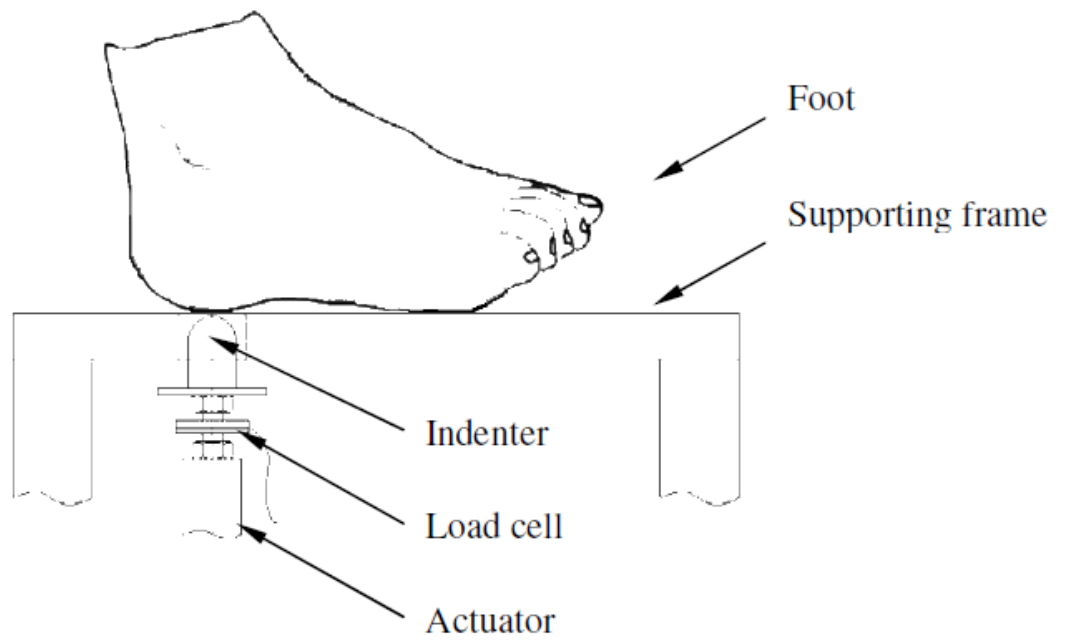
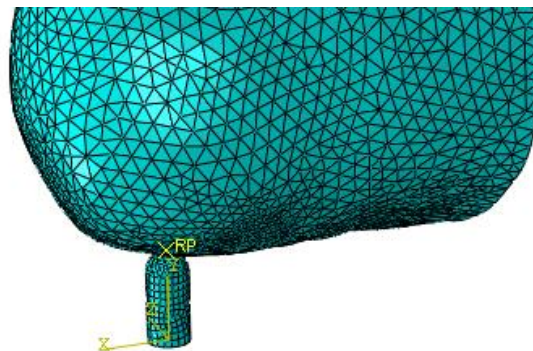


Figure 2.3 (b) Use of indentation tests in testing human foot (Tong *et al.*, 2003, Gu 2010).



(a) Set-up of the *in vivo* indentation testing on the human heel pad



(b) FE models of the *in vivo* indentation test.

Figure 2.4 *In vivo* indentation test and simulation of the human foot tissue (Li, 2009; Gu, 2010).

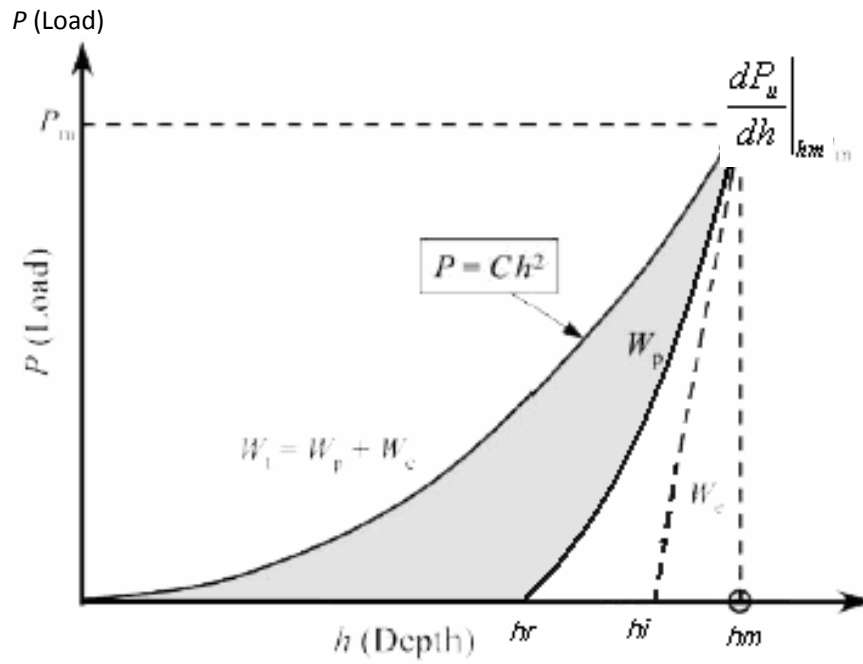


Figure 2.5(a) Schematic illustration of a typical force (P) indentation depth (h) response of an elasto-plastic material to instrumented sharp indentation showing that the loading curve can be expressed by a simple mathematical expression (C is the curvature). (Dao *et al*, 2001)

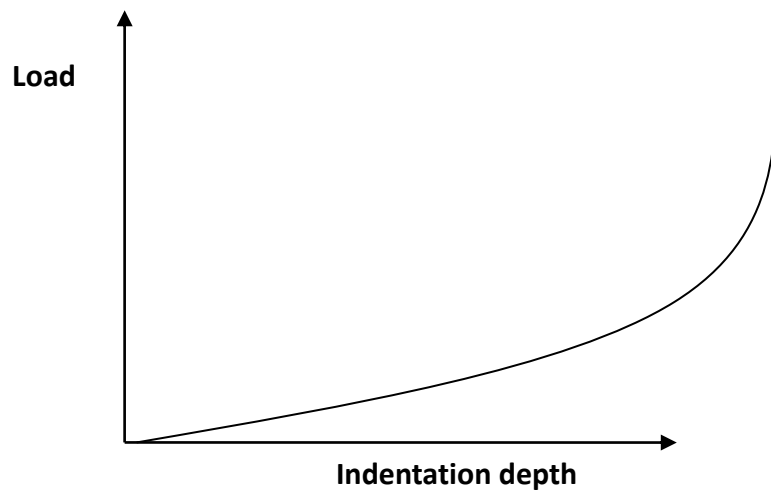


Figure 2.5 (b) Schematic shows typical continuous indentation curves of foam/rubber materials.

2.2 Linear and nonlinear material behaviours and energy functions for EVA foams

The behaviour of materials subject to tensile/compression forces can be described by a stress-strain graph. Figure 2.6 shows schematically the two main type of stress strain relationships of soft materials (such as rubber, foams and biological tissues) in the loading phase, namely linear elastic (a), elastically non-linear (b). For an elastic material, the stress is proportional to the strain and the strain is recoverable if the stress is removed, i.e. the specimen returns to its original dimensions. This occurs in the initial linear region of the stress-strain curve of flexible foams (open cell foam) and some rigid foam (closed cell foam). A linear elastic relationship (Figure 2.6(a)) between compressive or tensile stress (σ) and strain (ε) in the loading direction can be described by:

$$\sigma_x = E\varepsilon_x \quad (2.2)$$

where the constant E is the Young's modulus.

The absolute value of the ratio of the lateral strain to the longitudinal strain is the Poisson's ratio:

$$\nu = -\frac{\varepsilon_y}{\varepsilon_x} \quad (2.3)$$

At small strain, for both compression and tension, the average experimentally observed Poisson's ratio, ν , of foams is very low close to 0, while the Poisson's ratio for rubber is close to 0.5 (Verdejo and Mills, 2004). Foam is highly compressible while rubber is incompressible.

Figure 2.6 (b) shows the non-linear relationships between stress and strain. For foam or biological tissues, the non-linearity occurs due to changes in its geometry at different strain levels (Ren and Silberschmidt, 2008). At small strains the material deforms in a linear, elastic manner as a result of cell wall bending. The region with lower stress (plateau region) increase is the buckling zone. At large strain, the cell walls rotate and align, resulting in an increased stiffness. Most foam materials and biological material exhibited highly nonlinear behaviours (Mills *et al*, 2003), which have to be understood based on the nonlinear mechanics. Many different function/material models have been developed to simulate

different materials (ABAQUS 6.10 User's Manual). EVA foam used in the work was described by hyperfoam material model. The strain energy function (U) represented by in first term strain energy (ABAQUS 6.10 User's Manual):

$$U = \frac{2\mu}{\alpha^2} \left[\lambda_1^\alpha + \lambda_2^\alpha + \lambda_3^\alpha - 3 + \frac{1}{\beta} ((J^{el})^{-\alpha\beta} - 1) \right] \quad (2.4)$$

Where $\lambda_1, \lambda_2, \lambda_3$ are the principal stretches; J^{el} is the elastic volume ratio; μ, α and β are the material properties representing the compressible foam behaviours. β is related to the effective Poisson's ratio (ν) following

$$\beta = \frac{\nu}{1 - 2\nu} \quad (2.5)$$

This energy function was widely used to describe the stress-strain response of EVA foams. The inverse program in this work is to predict the values for the two parameters ' μ ' and ' α ' as in many cases, the first order form is sufficient.

As illustrated in the material model for EVA foams, the materials behaviours can be described with more than one material parameter. It is a challenging task to accurately derive these functions which are mainly mathematical based without direct physical meanings. Conventionally, the determination of material parameters is based on the use of test samples of a standardised geometry and strain state as shown in Figure 2.7, so particular conditions on the stress and strain field are satisfied in the sample/or part of the sample. Then the unknown model parameters are obtained through curve fitting from experimental data. These methods are inconvenient or even impossible where large scale standard specimens are not readily available (such as biological tissues), or for *in situ* monitoring the mechanical strength of the materials. It is important to use localised tests such as indentation tests, which potentially could be an effective alternative approach by combining experimental and numerical works. In addition, in a standard test, such as shear test, the sample has to be assembled to the plate using adhesives, this makes the process very time consuming. In addition, when testing materials in different environments (such as temperatures) the work becomes very difficult due to the uncertainty with the

deformation of the adhesives used (e.g. in shear tests). One potential approach is to develop a way to inversely identify the materials parameters from indentation tests through program in direct or inverse modelling.

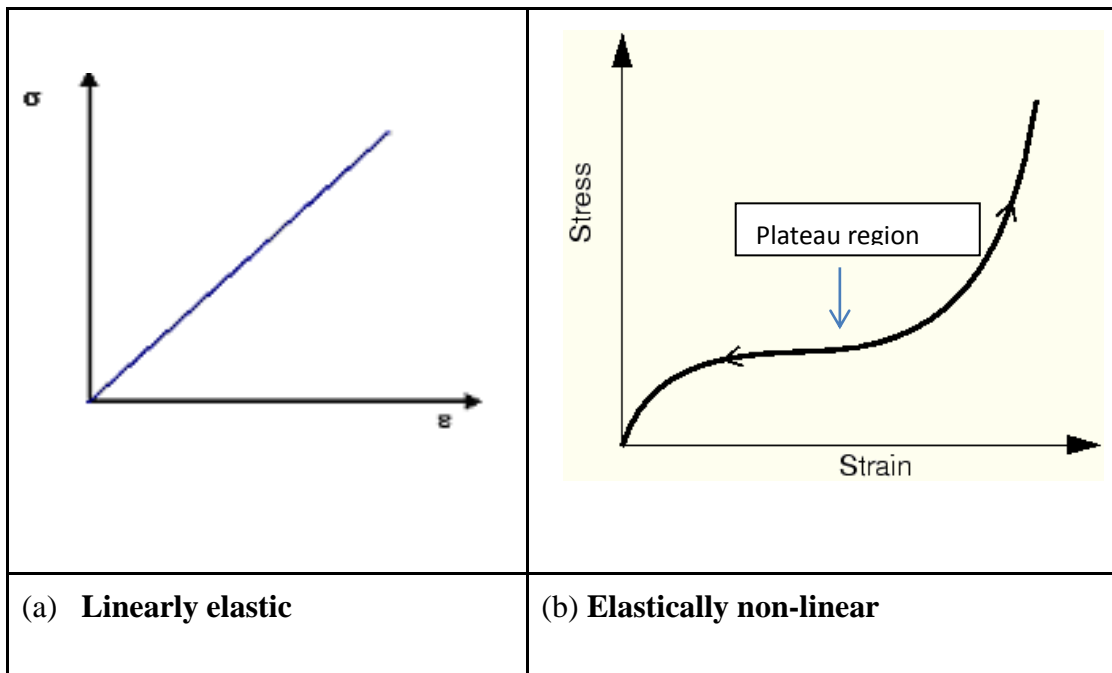


Figure 2.6 Schematics showing linear elastic and nonlinear material behaviours in loading (ABAQUS manual, V6.10).

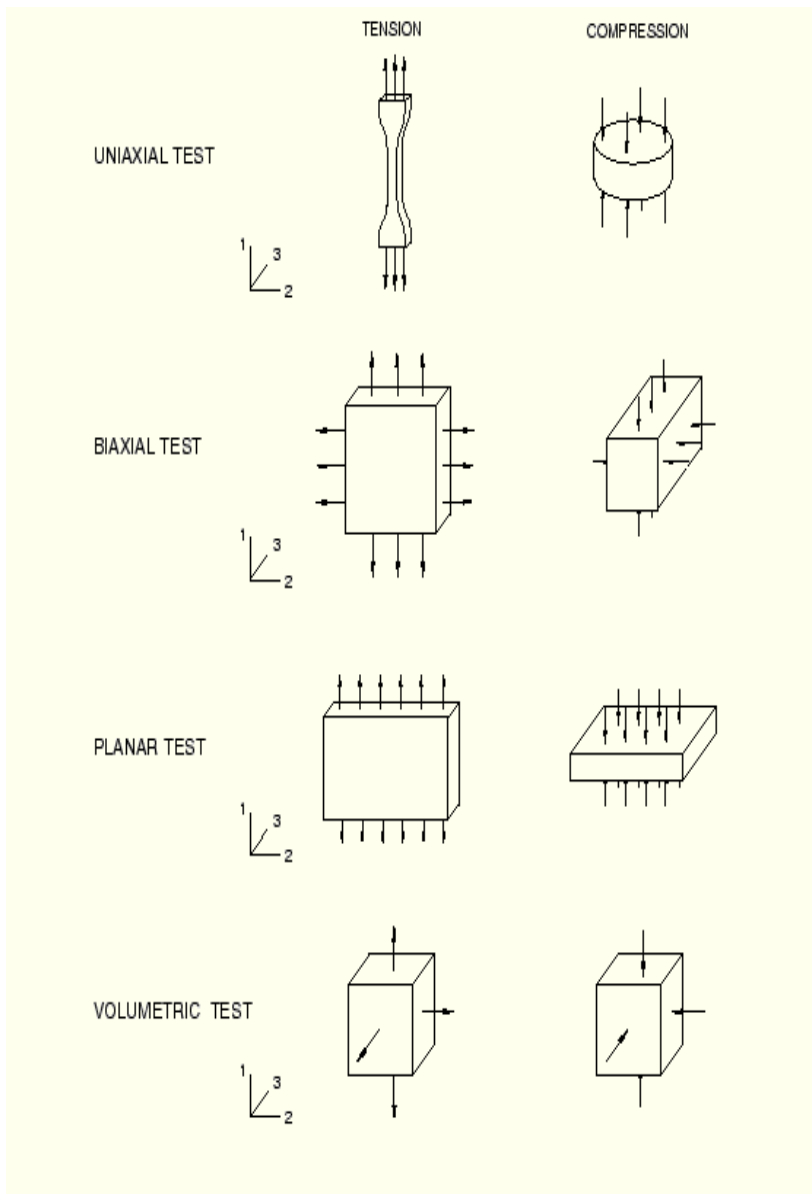


Figure 2.7 Deformation modes of various experimental tests for defining nonlinear material parameters (ABAQUS Manual, V6.10)

2.3 Inverse problems and its application in material testing and properties prediction

Parameter estimation is one form of inverse problem of optimisation, in which unknown material properties (or other parameters) is determined from the knowledge of response to given loading or boundary conditions. A successful program for predicting material parameter has to be accurate, efficient and robust and this depends on testing method used, inverse program, optimisation method etc. The performance of an inverse process has to consider the time/computational resources used, data process, accuracy and robustness.

Figure 2.8(a) shows the structure of typical inverse modelling approach based on an interactive method (Meuwissen et al, 1998). In this process, the parameters to be predicted (e.g. material properties) are interactively changed in the FE models until the predicted results match the experimental results. A user defined objective function could be used to measure the difference between predicted and target parameters until an optimal fit between the simulated data to the experimental is reached. Figure 2.8(b) is a chart illustrating the basic process in an interactive parameter fitting with FE modelling. In this process, the FE modelling is repeated with changing material parameters until an optimum combination of material properties are found. Similar approach has been used for different materials including metals, polymeric foam and bio-materials (Kauer 2001; Bolzon et al, 2004; Gerard et al, 2005; Hendriks et al, 2006). This is procedure easy to understand and can be developed using computer programming environments such as python (Aw, 2013). This approach requires re-running of the FE models during the optimisation process, which may take a large amount of time to reach the optimal solution, thus increasing the computational cost. In some cases, the work may converge at a local minimum rather than a global minimum. So different initial value have to be assigned to approach the target from different direction/domains. In some complex models, for example, fracture model of metals (Kong 2008); Welding model (Norbury, 2012), this process can be time consuming and expensive in terms of computational resources. In addition, this work requires the use of FE package all the time, so it could be more costly in terms of software cost and analyst time.

Another approach is a post modelling approach, i.e. the inverse is done after the FE modelling has been completed. In this process, a data space (simulation space) can be developed, then the optimum property can be found by searching through the database to match the experimental result without re-run the FE modelling. Several methods could be employed. [Nakamura et al \(2000\)](#) have developed a Kalman Filter method for the optimal inverse analysis to estimate effective material properties of functional gradient materials (FGMs), in which the material properties changes across the section of the sample that can only be measured using indentation tests. Figure 2.18 shows a flow chart showing the main component of inverse modelling using Kalman Filter method ([Nakamura et al, 2000](#)). Similar approach has been used in predicting nonlinear material properties from spherical indentation tests ([Delalleau, 2006](#); [Gu et al 2003](#); [Li, 2009](#)), it require updating the material parameters using the Kalman filter method. It is an effective method in the cases reported but it is not very good at dealing with complex data and the program could be time consuming in the case of complex models. For example, since the searching starts from one depth point and updating the data through each point, Kalman filter based program could not deal with indentation data at lower depth. In addition, in the program developed by [Li \(2009\)](#), different random error (noise) has to be introduced. Due to this complex mathematical frame work, it is not very easily used by researchers without in-depth programming background. In addition as the program relies on convergence to one final point, so there is uncertainty with the completeness of the final results. All these features limited its wide application and development of potential computer program to automatically determine the materials properties.

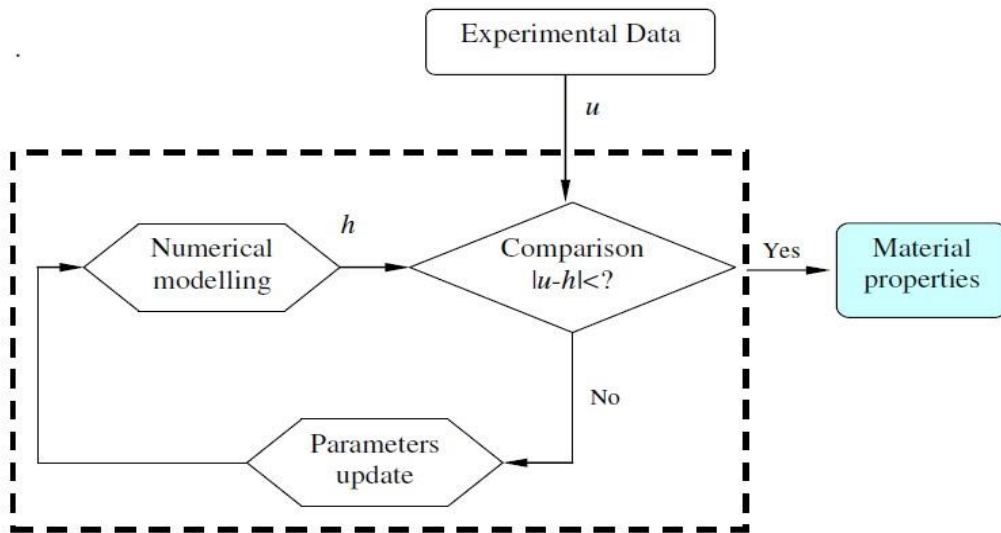
The parametric study method is another type of post modelling method, which is easy to understand and follow. A typical example ([Ren et al, 2006](#)) for testing rubber materials is shown in Figure 2.10(a). In the test, two double sided tapes are used to apply a tension on the surface of soft materials, then the force-displacement data is used to represent the resistance of materials to deformation. The work developed a parametric approach for determining the results from *in vivo* surface testing. The method involves a two-staged

approach using a rough range data first and then refining the material. This method could effectively reduce the amount of computational works required but the approach has to be based on a good pre-knowledge of the materials and the testing variables has to be limited to a few numbers.

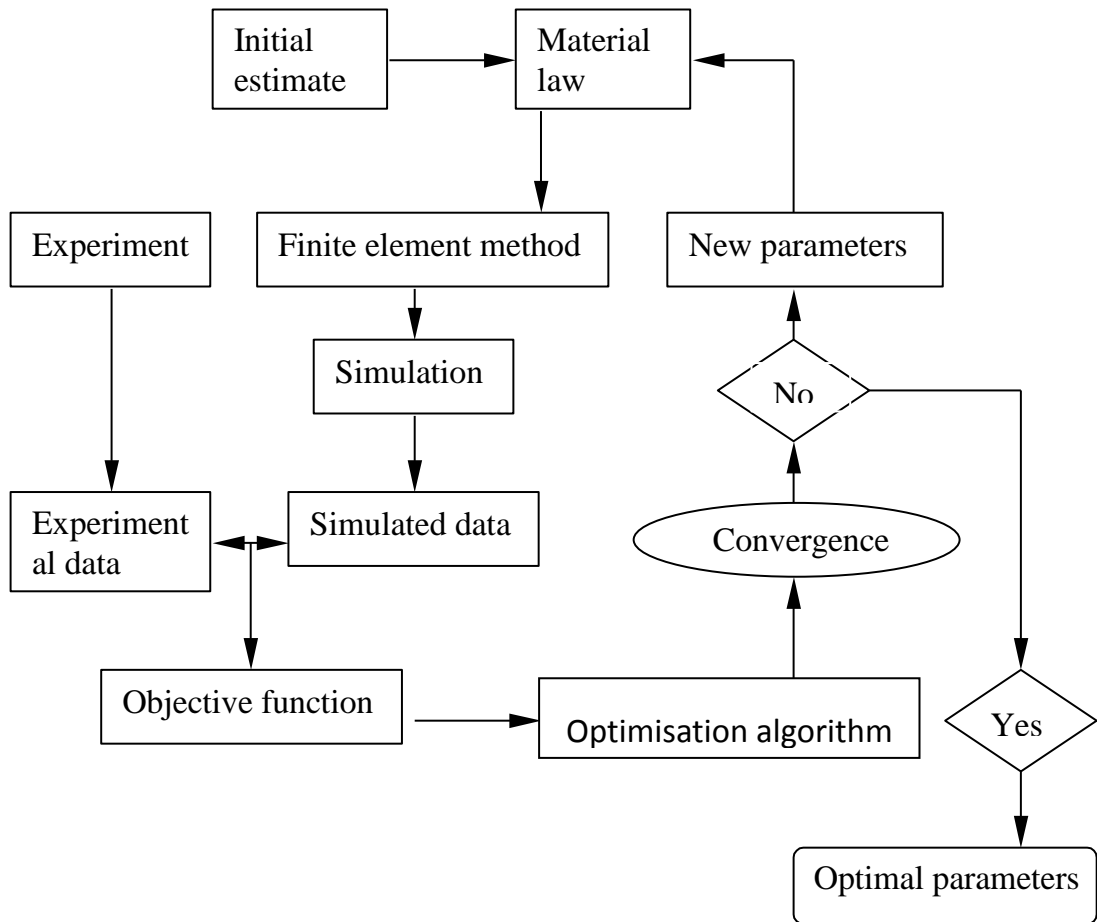
Another potential method for materials characterisation is the Artificial Neural Networks (ANN) (Zaw et al, 2009; Esfahani et al, 2009). The ANN method is known to be able to deal with complex problems with multiple parameters, which is normally the case for material parameters characterisation. Zaw et al (2009) has used a rapid inverse analysis ANN approach to identify the “unknown” elastic modulus (Young’s modulus) of the interfacial tissue between a dental implant and the surrounding bones. In 2009, Esfahani et al presented an ANN to model the influences of chemical composition and process features on the yield strength of hot strip steels, in which the ANN prediction showed good agreements with experimental data. The ANN method potentially can be used for characterising foam materials and similar materials from indentation tests. ANN programs are easy to use and once successfully trained, they can be packaged into a computer program with a proper interface allowing the user to input and extract data.

A successful inverse FE modelling method requires the combination of FE modelling and data analysis for different applications. The suitability of each approach to be used in material parameter estimation based on indentation test data depends on the material system and the parameters being determined. The parametric approach is time consuming but represents the most robust approach (as it could effectively cover any possible material properties within the domain to be searched on) for systems with limited number of variables or a good pre-knowledge about the material. The main time and resource consuming part is in the development of the simulation space/database. The interactive method can be used for multiple parameters but requires significant re-running of the FE programs. The method is also sensitive to problem of stopping at local minimum rather than global minimum point. Method such as Kalman filter is an effective approach for a well defined problem. As the kalman filter converges on a single value, the user must

ensure that the result is independent of initial conditions in order to be absolutely sure of the final result. This study of starting point independence is not without lost. A practical way is to run the modelling many time with different initial guessed values (Li, 2009). ANNs represent a method capable of dealing with multiple variables, which can potentially be used to analyse complex material systems. Most of the published work in this field has been focused on materials with well-defined material laws having simplified geometry (such as metals). The suitability of these approaches for materials with nonlinear behaviour requires a systematic study. In addition, as this work also aims to develop a method that could be easy to put into a practical computer program, so an effective way of representing and processing also needs to be investigated and explored.



(a) General structure of interactive inverse approach based on updating FE modelling ('u' is the target; 'h' is the prediction) (Meuwissen et al, 1998).



(b) A framework of interactive modelling approach.

Figure 2.8 Flow chart illustrating typical procedures of an interactive inverse FE modelling method.

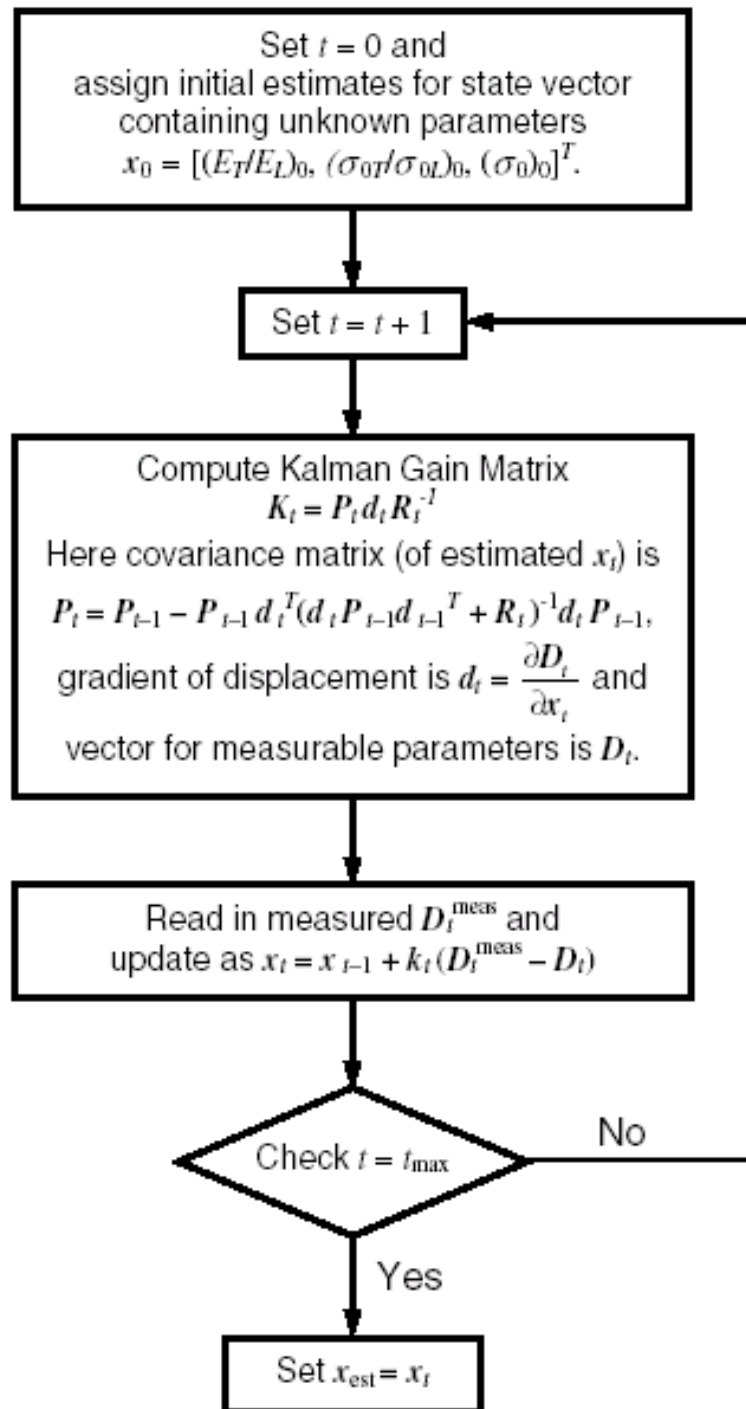
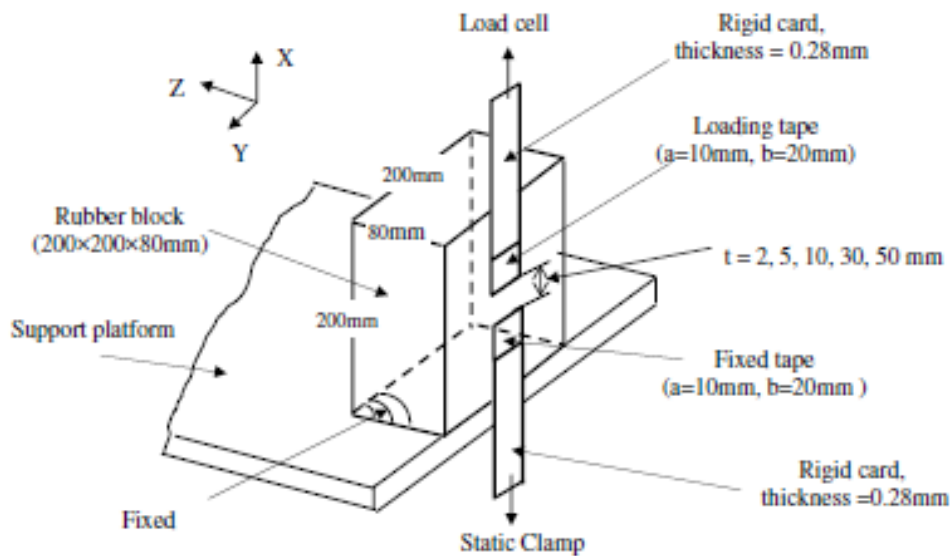
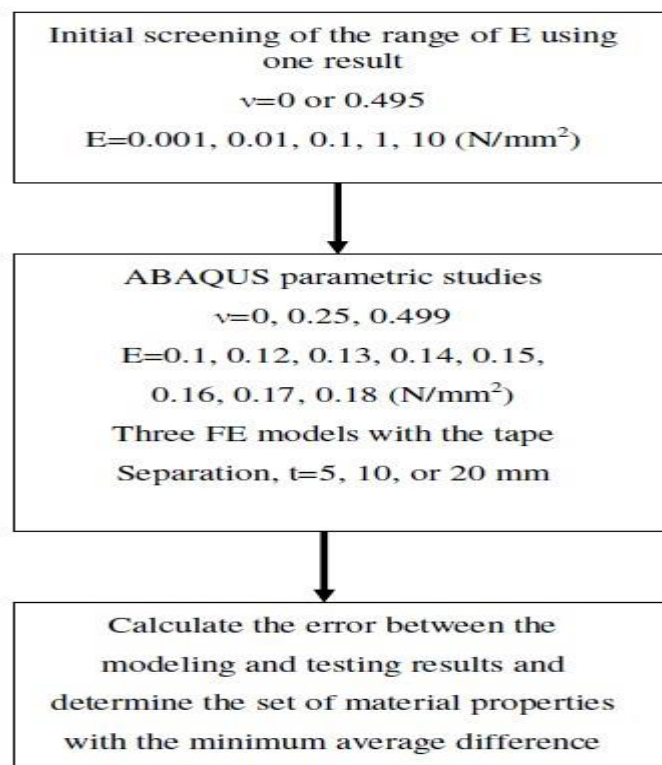


Figure 2.9 Flow chart of Kalman Filter procedure to determine the unknown parameters using instrumented indentation records (Nakamura and Gu, 2007).



(a) Surface tension tests where two adhesive tapes are used to test soft materials (rubber, human skin etc.)



(b) Parametric modelling approach to extract the material properties.

Figure 2.10 A typical parametric modelling approach to extract the elastic material properties based on surface tension tests (Ren *et al*, 2006).

2.4. Introduction to ANN and its applications.

2.4.1 The structure and working process of ANN

Artificial neural networks (ANN) are non-linear mapping structures based on a working mechanism similar to the functions of the brain (Lek and Guegan, 1999; Lippman, 1987, Harkins, 1994, Sibi et al, 2013) as shown in Figure 2.11(a). The parallelism of the biological neural system provides an ability to deal with different tasks and processes. The working process of an artificial neuron is illustrated in Figure 2.11(b). The scalar input 'p' is transmitted through a connection that multiplies its strength by the scalar weight 'w' to form a scalar product 'wp'. The scalar output 'a' is produced with weighted input 'wp' being the argument of the transfer function 'f'. A scalar bias, 'b', of the neuron is simply being added to the product 'wp'. It is well documented that a single neuron is not much use, in many case, a working system needs many neuron in different layers as shown in Figure 2.11(c) to be able to process complex issues.

If there are R input, the inputs on the left hand of the diagram, are multiplied by the weights and summed as

$$n = \sum_{n=1}^R (p_n W_n) \quad (2.6)$$

The bias, b, is in the form of a constant value and is applied to the sum, so the total input to the transfer function becomes:

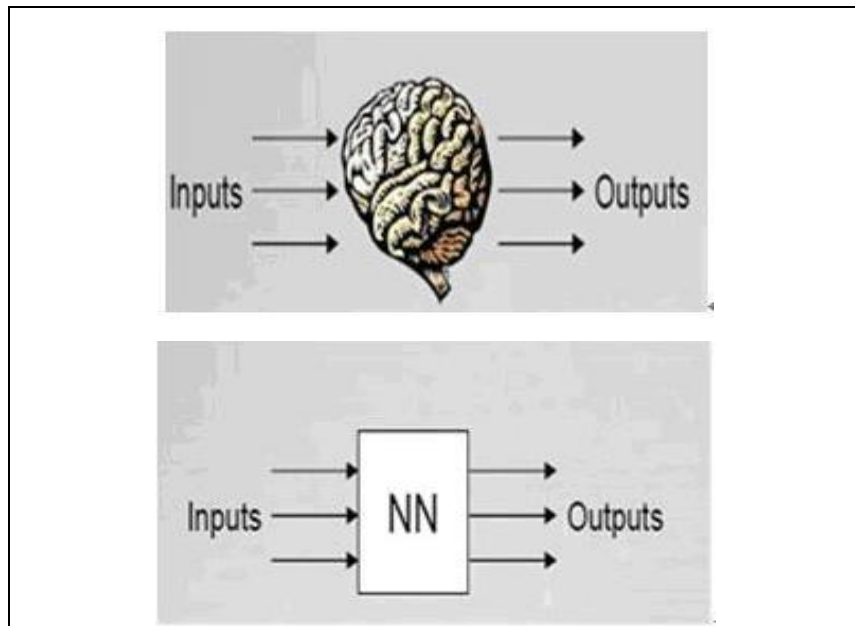
$$n = Wp + b \quad (2.7)$$

The final output, a, is the sum of the weighted input with the added bias transformed through a transfer function f (to be explained in detail in the next section). The weights of neurons are determined by means of training algorithms (to be detailed in the next section). Equation 2.8 shows the relationship between the output and inputs, weight, bias and transfer function as:

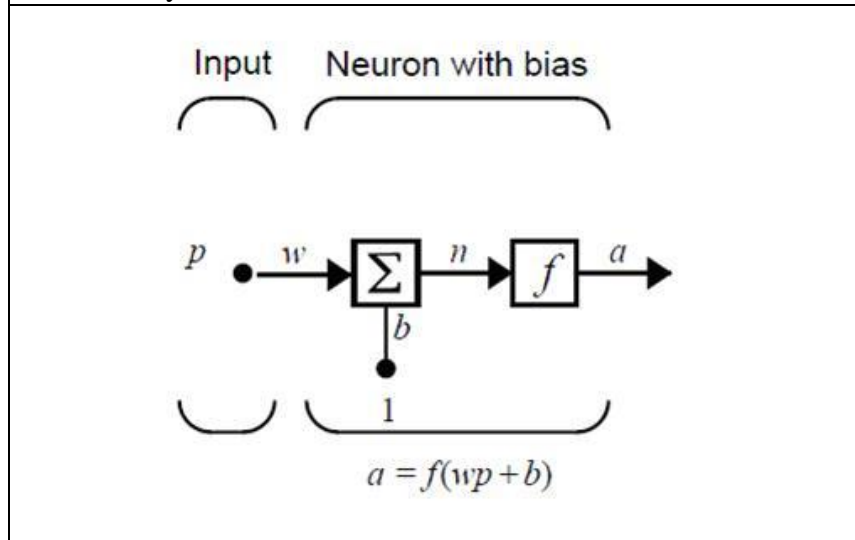
$$\mathbf{a} = f(Wp + b) \quad (2.8)$$

The performance of the system depends on the structure, individual neurons, activation

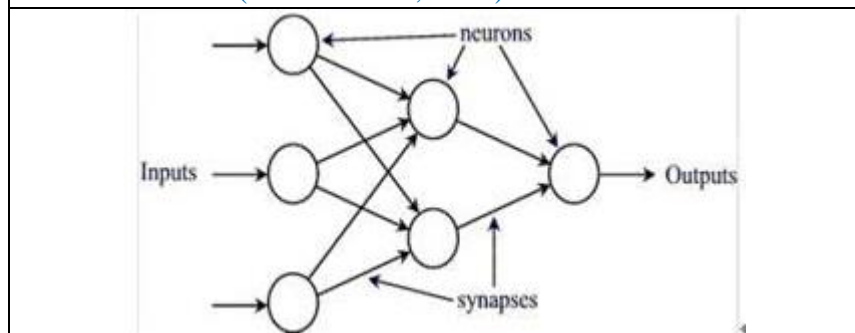
function/transfer functions, training/learning mechanism and quality of the input data (accuracy, diversity, validity, uniqueness etc.). Some of these are to be briefly presented in the next section of the thesis, these will help with deciding structure of the ANN and focus of the research in the context of indentation testing of nonlinear materials and related area.



(a) Schematics showing comparison between the human brain and ANN system.



(b) A schematic model showing the working process of an artificial neuron (Demuth *et al*, 2008).



(c) Structure and data of ANN system.

Figure 2.11 The structure and working process of ANN.

2.4.2 Transfer (activation) functions for ANNs

The transfer/activation function is one of the most important/critical factor for an effective ANN, it is used to convert the net input values to the node's output value. An activation function specifies the output of a neuron for a given input state. Figure 2.12 illustrates different transfer functions (activation functions) (Karlik and Olgac, 2006; Demuth et al, 2008). A hard limit transfer function (Figure 2.12 (a)) is restricted to Boolean operations and, can only output an value of '0' or '1'. When the neuron is on, the value is '1', when the neuron is off, the value is '0'. Figure 2.12 (b) illustrates a linear transfer function that cannot perform non-linear computations. For nonlinear problems, Sigmoid functions (Figures 2.12 (c&d)) are most commonly used in neural networks, this function overcomes the limitations of both hard limit and linear activation functions.

As shown in Figure 2.12 (c), Logsig is a uni-polar sigmoid function the output value is between between 0 and +1 in the form of

$$f(x) = \frac{1}{1+e^n} \quad (2.9)$$

The logistic form of the equation maps the interval $(-\infty, \infty)$ onto $(0,1)$.

Figure 2.12(d) shows the form of tangent sigmoid (Tansig), this is a bi-polar sigmoid function, which maps the interval $(-\infty, \infty)$ onto output value is between -1 and +1 in the form of hyperbolic tangent sigmoid:

$$\tanh(x) = \frac{\sinh(n)}{\cosh(n)} = \frac{e^n - e^{-n}}{e^n + e^{-n}} \quad (2.10)$$

Or in another equivalent form (Meng and Lin, 2008; Matlab Menu, 2013) as

$$f(n) = \frac{2}{1+e^{-2n}} - 1 \quad (2.11)$$

This is mathematically equivalent to $\tanh(N)$. It differs in that it runs faster than the MATLAB implementation of \tanh , but the results can have very small numerical differences. This function is a good tradeoff for neural networks, where speed is important and the exact shape of the transfer function is not (Matlab Menu, 2013).

The activation functions shown in Figure 2.12 are the most common ones relevant to the problem to be studied in this work. There are other forms of activation function such as Radial Basis Function, which can perform better in some other applications ([Wu et al, 2006](#); [Karlik and Olgac, 2006](#)).

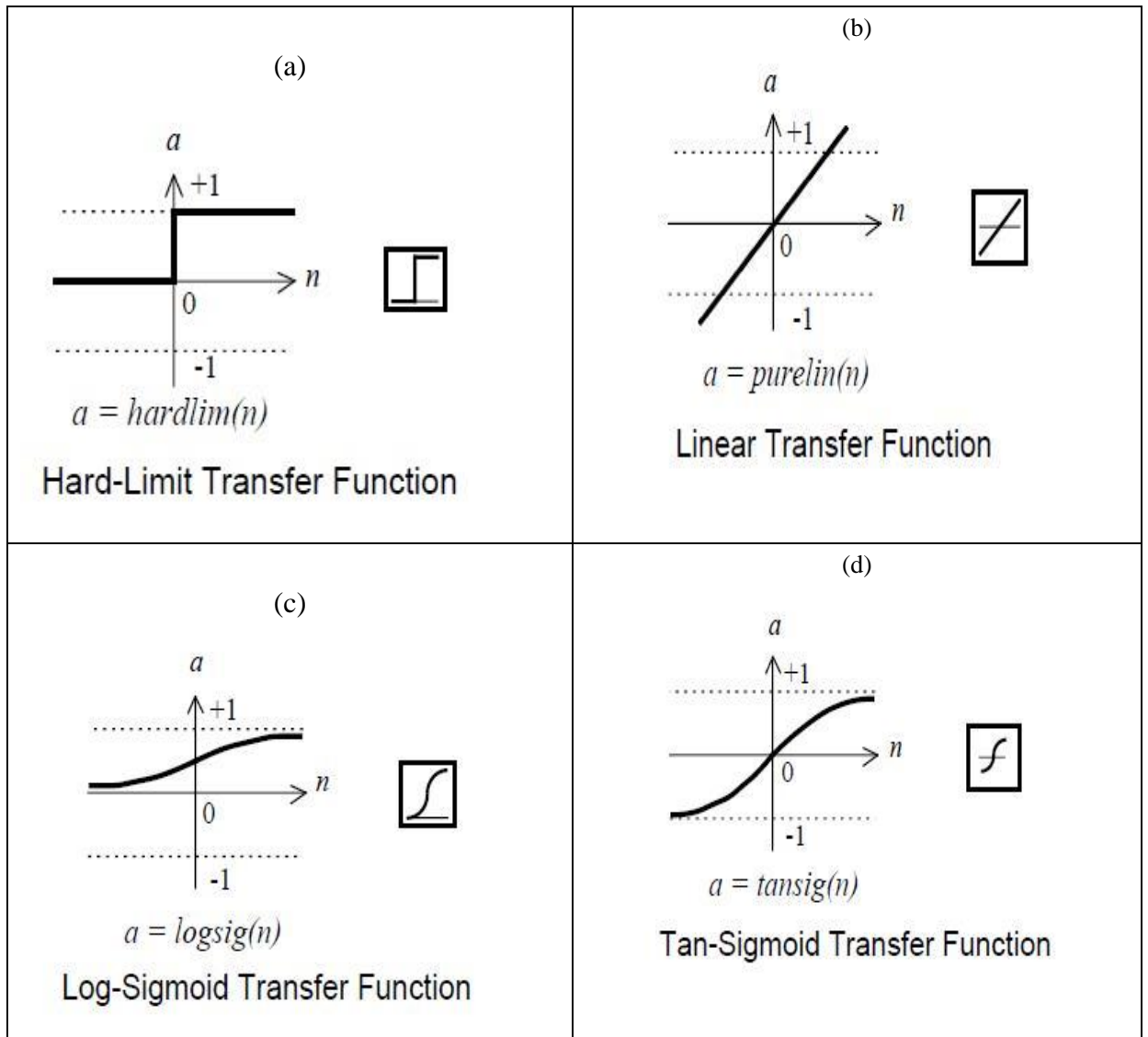


Figure 2.12 Typical transfer (activation) functions for ANNs (Demuth *et al.*, 2008; Neural Network Toolbox™ Users' Guide)

2.4.3 Different types of ANN

Feed-Forward and Recurrent Neural Networks

Feed-forward neural networks provide a general framework for representing nonlinear functional mappings between a set of input variables and a set of output variables (Bishop, 2006; Brescia, 2012). As illustrated in Figure 2.13(a) (Gualano, 2007), in a Feed-forward Artificial Neural Networks (FANNs), the input signals are fed into a first layer of neurons and the output(s) from these neurons are forwarded to the following layers in the ANN until the last layer (output layer) is reached. In this structure, information exchange only occurs in one direction passing through any eventual hidden layer. With a structure of a feed-forward neural network, both the number of layers and the number of neurons in each layer affects the ANN performance. Every node in the previous layer is connected to each of the nodes in the next layer. There is one problem for this structure; it does not have feedback connection, so it can only produce outputs which are directly related to the inputs.

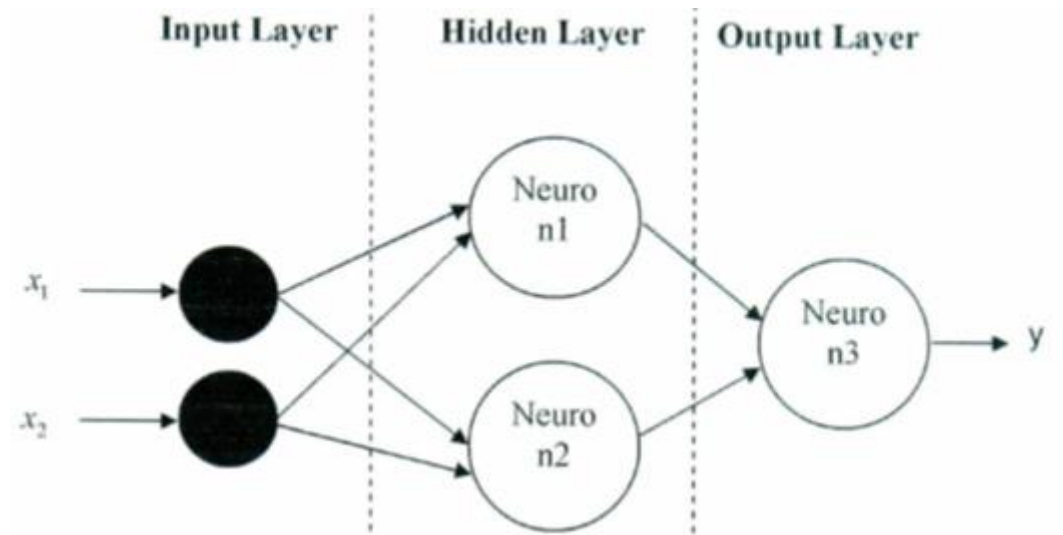
To overcome this problem with non-linear system modelling, past observations at the input and output of the feed-forward artificial neural networks (FANNs) are supplied to the FANNs themselves as inputs. Typical systems are in the form of a Recurrent Neural Network (RNN) method. As show in Figure 2.13(b), an RNN has the output(s), from one or more of its neurons, delayed and fed back (directly or indirectly) to the same neuron(s). The feedback signals include a delay of one time step for updating the variables, in other words, the feedback input to a neuron at a certain time 't', represents the output of the neuron from where the feedback is generated at time 't-1' (Gualano, 2007).

Different method of training: Unsupervised and supervised network

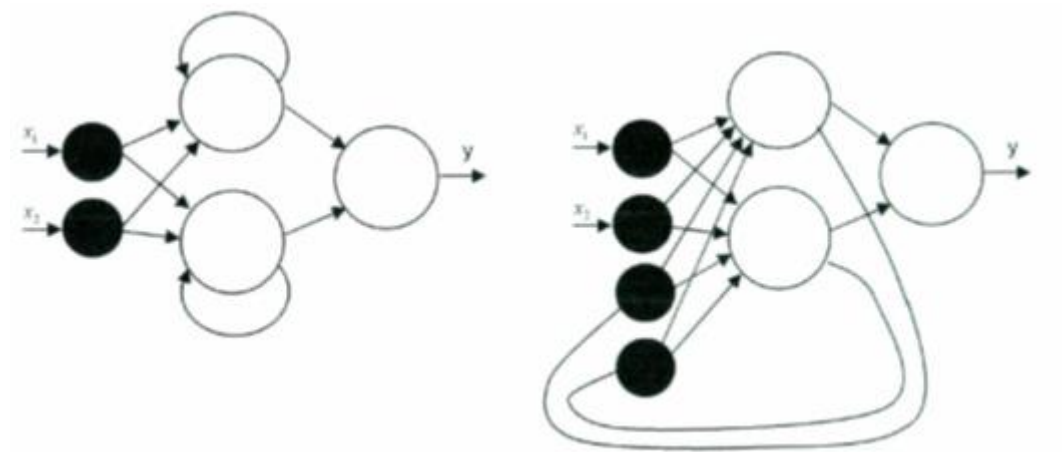
Learning is one of the most important and critical features influencing the performance of an ANN. There are many types of Neural Network Learning Rules. Based on the way the training has been conducted, it can be classified into two types: supervised learning, and unsupervised learning (Masters, 1993; Benchebra, 2008), which is shown Figure 2.14 and

2.15, respectively together with published application cases. As shown in Figure 2.14(a), in unsupervised learning, the weights and biases are updated in response to network input only. There are no target outputs used. Unsupervised learning is often used to perform operations such as clustering (Benchebra, 2008). In learning without supervision the desired response is not known; thus, explicit error information cannot be used to improve network behaviour. Since no information is available as to correctness or incorrectness of responses in a unsupervised learning, learning has to be accomplished based on observations of responses to inputs with marginal or no knowledge about. Figure 2.14 (b) shows a typical of unsupervised learning: Kohonen SOMs (self organising mapping) commonly used for ecological modelling (Lek and Guegan, 1999). Unsupervised learning can easily result in finding the boundary between classes of distributed input patterns. Apparently, this approach will not be suitable for materials parameters identification based on the indentation test as the problem to be studied in this work.

In supervised learning, as shown in Figure 2.15 (a), the learning rule is provided with a set of examples (the training set), the network outputs are compared with the targets for given corresponding inputs, The learning rule is then used to adjust the weights and the biases of the network in order to move the network outputs closer to the targets. Supervised learning can be applied in either feedforward NN and feedback NN (Gualano, 2007). Figure 2.15(b) schematically shows a typical feedforward structure of supervised learning with a multilayer feed-forward neural network (Pal et al, 2008). The network will be trained with target data corresponding to a set of inputs before being used to predict results for trained data or untrained input data.

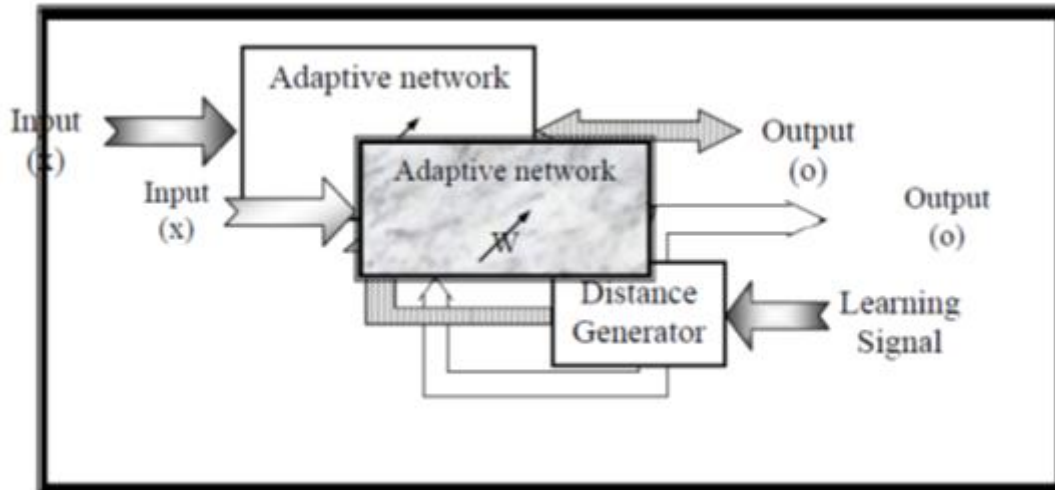


(a) Schematic to show a feed forward structure.



(b) Two example of recurrent/feedback method.

Figure 2.13 Feedforward and feedback system (Gulano, 2008).



(a) Blockdiagram to show the principal of unsupervised learning (The Categories of Neural Network Learning Rules; <http://www.uotechnology.edu.iq/>; Accessed 12/2013)

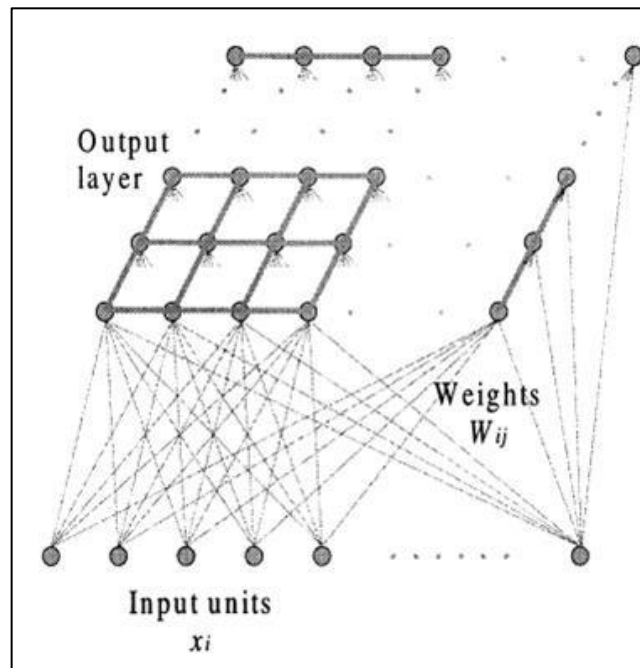
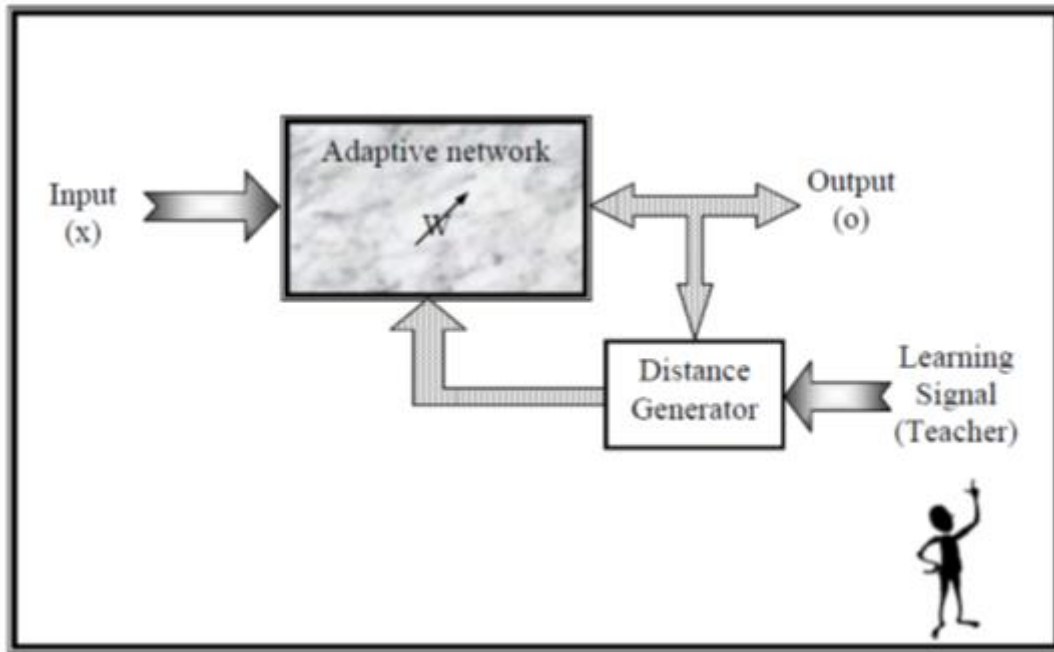
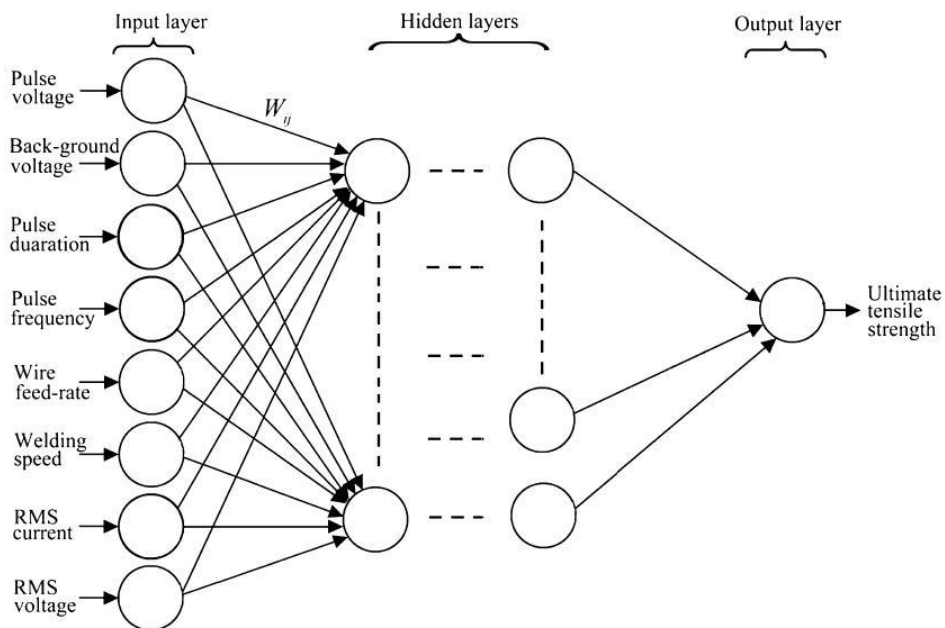


Figure 2.14 (b) A typical unsupervised learning networks: Kohonen SOMs (Self-Organizing Maps) for ecological modelling (Lek *et al.*, 1999).



(a) Supervised learning (The Categories of Neural Network Learning Rules); <http://www.uotechnology.edu.iq/>; Accessed 12/2013)



(b) a multilayer feed-forward neural network for weld joint strength prediction.

Figure 2.15 Supervised learning (a) and a typical supervised learning networks (b) (Pal *et al.*, 2008).

2.4.4 Learning rules and their applications

As shown in previous sections, the learning process involving updating the weights of a neuron or a group of neurons in the system. Many learning rules/algorithms have been developed and have found applications in different areas (Maier et al, 2000; Pal et al, 2008; Zaw et al, 2009). These algorithms are different from each other in the way the weights in a network are modified/adjusted. The error-correction rule is one of the most common methods, which works by minimizing the error outputs generated by the network with respect to the targets by modifying the synaptic weights (Maier et al 2000; Mansour et al, 2004). In supervised learning, the inputs are processed through the corresponding weights and neurons, the output and the target output are compared. The difference is known as the error that needs to be minimized to a level that is sufficiently accurate. Many methods have been developed to find the minimum error, including Gradient descent method, Newton method, Quasi Newton Algorithm method, Levenberg–Marquardt etc (Finlay, 2004; Adeloye and Munari,2006;). The choice of the approach should be selected within the context of the technical problem to be studied, nature of the input and output data including the accuracy and computational resources requirements.

Gradient Descent Approach

The techniques of calculating the slope of a function towards a function minimum is known as gradient descent (Masters, 1993; Baldi, 1995, Finlay, 2004, Gong et al, 2012; Zhao 2013). Figure 2.16 illustrates the concept of the gradient descent approach. As shown in the graph of function $y(x)$, if the changes in y due to x are considered small $\delta_y \approx \Delta_y$, it can be shown that the gradient of the slope $\frac{\Delta y}{\Delta x}$ can be evaluated following (Master, 1993):

$$\Delta x = -a \left(\frac{dy}{dx} \right)^2 \quad (2.12)$$

Where the learning rate, ‘a’ is greater than zero but small enough that $\delta_y \approx \Delta_y$ still holds true. If ‘a’ is a small non-zero value, the direction of the descent is always

towards the minimum of the function, thus bring convergence to a minimum (at least locally).

For a complex function, there are more variables:

$$y = y(x_1, x_2 \dots x_n) \quad (2.13)$$

Partial differentiation has to be used to analyse the situation with multiple variables, the gradient of each variable can be determined for each variable, x_i , following equation:

$$\Delta x_i = -a \left(\frac{\delta y}{\delta x_i} \right) \quad (2.14)$$

The error on output of a given neuron is a function of weights:

$$E = E(w_1, w_2, \dots, w_x). \quad (2.15)$$

If the function has more than one variable (more than 1 weight), the error in terms of the weights can be expressed as:

$$\Delta w_i = -a \frac{\delta E}{\delta w_i} \quad (2.16)$$

It is known that the error in a network can be expressed in terms of the difference between a target and output value pair under the supervised learning ([Pal et al, 2008](#)). For a nonlinear problem, the error can only be expressed in terms of a selected target vector and a corresponding activation vector:

$$E = \frac{1}{N} \sum_{p=1}^N \frac{1}{2} (t^p - a^p)^2 \quad (2.17)$$

In this equation, the superscript, p, indicates the current input pattern, t, is the target vector and, a, is the activation output.

Newton and Quasi Newton Algorithm Method

The most commonly used approach in engineering program is the multilayer perceptron (MLP) approach, the learning rule of which is the Quasi Newton Algorithm (QNA). A general Quasi Newton Algorithms (QNA) are variable metric methods used to find local maxima and minima of functions (Davidon 1968; 1991; Shanno, 1970; Gibert and Lemarichal 1989; Brescia, 2012). In the case of MLP's, it can be used to find the stationary (i.e. the zero gradient) point of the learning function. QNA is based on the Newton method, the basis of which is finding the roots of an equation by computing recursive function approximations. It is a good alternative for high order functions when a formula for finding the roots of the function is not available (Aldrich 2002; Gualano, 2008; Brescia, 2012).

For a function $f(x)$, by using the equation of the straight lines defining the derivative of the function to the root approximations, the root x_n can be approximated following equation:

$$x_n = x_{n-1} - \frac{f'(x_{n-1})}{f''(x_{n-1})} \quad (2.18)$$

Comparing equation 2.12 and 2.18, the newton method is different from the gradient method. Gradient descent tries to find such a minimum 'x' by using information from the first derivative of function 'f', simply following the steepest descent from the current point. Newton's method tries to find a point satisfying $f'(x) = 0$ by approximating f' with a linear function and then solving for the root of that function. When approximating f' , Newton's method makes use of f'' (the curvature of f). This means it has higher requirements on the smoothness of data of 'f', but it also means that (by using more information) it will converges faster (Aldrich 2002, Brescia, 2012). The Newton method is a very powerful technique for finding the roots of any-order equations in a very simple manner. The main drawback of the Newton rule is that the program may diverge from the true solution. When approximations *diverge* from the root of the function, another guess has to be made until series of Newton's successive approximations is found, causing *diverge* rather than full convergence to the root r of the function. In practice, an ANN system may include many

layers and neurons. A training algorithm has to consider that more than one weights is associated with a neuron , and when the weights are all considered, the format of the Newton's rule take the form of

$$x_n = x_{n-1} - [Hf(x_{n-1})]^{-1} \nabla f(x_{n-1}) \quad (2.19)$$

With this form, the weights could be considered all together instead of ‘one by one’, so the derivative $f'(x_{n-1})$ in the Newton equation is replace by a gradient $\nabla f(x_{n-1})$, and $(1/f'(x_{n-1}))$ is replaced by the inverse of Hessian matrix ($Hf(x_{n-1})$) of $f(x)$ (Likas, 2000; Gualano, 2008). Hessian is a matrix of second derivatives and finding the inverse of the Hessian matrix is difficult, which may require a lot of computational power and is unpractical for the training of an ANN. The implementation of QNA is based on a statistical approximation of the Hessian by cyclic gradient calculation through Back Propagation method (Bishop 2006).

Accordingly to (Brescia, 2012). the Newton method uses local square approximation of the error function to determine the minimum position. The gradient in every point w can be given as:

$$\nabla E = H \times (w - w^*) \quad (2.20)$$

where w^* corresponds to the minimum of the error function, which satisfies the condition:

$$w^* = w - H^{-1} \times \nabla E \quad (2.21)$$

The vector $H^{-1} \times \nabla E$ is known as Newton direction and it is the base for a variety of optimization strategies, such as for instance the QNA, which instead of calculating the H matrix and its inverse, uses a series of intermediate steps of lower computational cost to generate a sequence of matrices which are more accurate approximations of H^{-1} . Details of the process can be found in (Brescia, 2012).

Based on the Newton formula, the weight vectors on steps t and $t+1$ are correlated to the correspondent gradients by the formula known as *Quasi Newton Condition* .:

$$w^{(t+1)} - w^{(t)} = -H^{-1}(g^{(t+1)} - g^{(t)}) \quad (2.22)$$

The approximation of gradient G is therefore built to satisfy this condition. Details of the G and implementation of the process can be found in reference (Brescia 2012). General speaking, by using such system, the weight updating can be calculated following:

$$w^{(t+1)} = w^{(t)} + \alpha^{(t)} G^{(t)} g^{(t)} \quad (2.23)$$

where α is obtained by the *line search*.

$$\alpha^{(t)} = -\frac{d^{(t)T} g^{(t)}}{d^{(t)T} H d^{(t)}} \quad (2.24)$$

One of main advantage of QNA, compared with conjugate gradients, is that the *line search* does not require the calculation of α with a high precision, because it is not a critical parameter. On the contrary, the downside is that it requires a large amount of memory to calculate the matrix G $|w| \times |w|$ for large $|w|$ (Brescia 2012).

Levenberg–Marquardt method

Like the quasi-Newton methods, the Levenberg–Marquardt algorithm was designed to approach second-order training speed without having to compute the Hessian matrix (Hagan 1994; Mirzaee, 2009; Liu 2010). When the performance function has the form of a sum of squares (as is typical in training feed-forward networks), then the Hessian matrix can be approximated as:

$$H = J^T J \quad (2.25)$$

where H is the an Hessian matrix, J is a Jacobian matrix (the matrix of all first-order partial derivatives of a vector-valued function) and J^T is the transpose of the Jacobian matrix.

So equation 2.19 becomes:

$$x_n = x_{n-1} - [J^T J]^{-1} \nabla f(x_{n-1}) \quad (2.26)$$

and the gradient can be computed as:

$$\nabla f(x_{n-1}) = J^T E \quad (2.27)$$

In this case, the Jacobian matrix 'J' contains first derivatives of the network errors with respect to the weights and bias; E is the vector of network errors. The Jacobian matrix can be computed through a standard back-propagation technique. The process is much less complex than computing the Hessian matrix in full scale (Mirzaee, 2009). Details of the process of the approximation of the Hessian matrix in the Levenberg–Marquardt algorithm can be found in (Mirzaee, 2009). It is reported that this algorithm appears to be the fastest method for training moderate-sized feed-forward neural networks (up to several hundred weights). (Coulibaly,2000; Gulano 2008; Altun et al, 2008; Mirzaee, 2009)

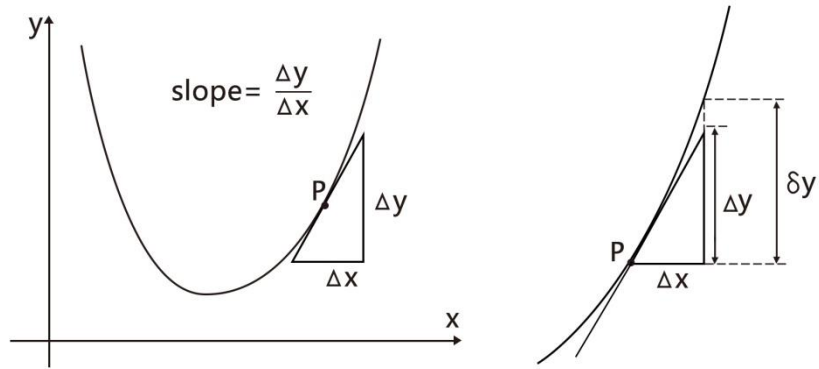


Figure 2.16 (a) Schematic to illustrate finding the minimum of a function (Adapted from Finlay, 2004).

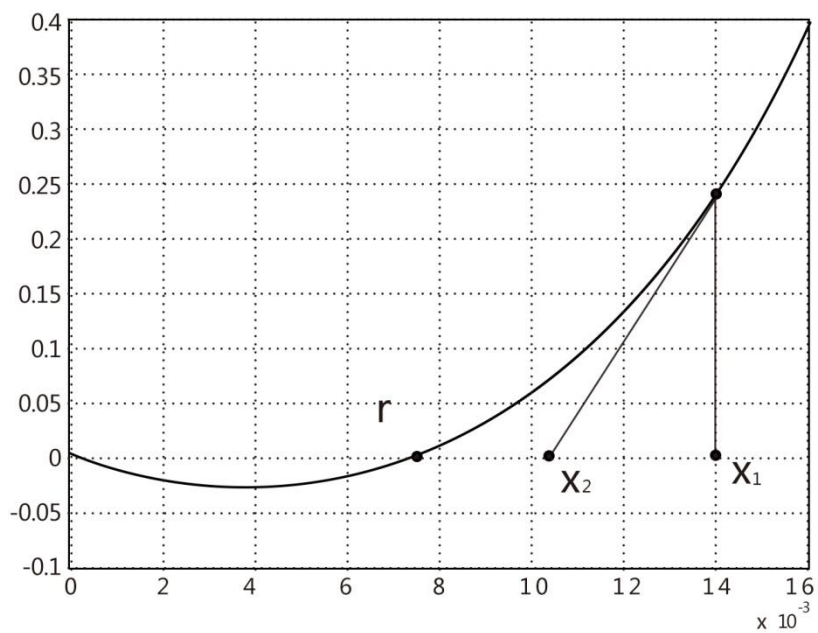


Figure 2.16(b) Typical example to illustrate the concept of The Newton Method. (Adapted from Gualano, 2008).

2.5 Testing and validation of an ANN for practical applications

ANN is a useful technique in many applications, but there are limitations. One key factor in developing ANN is to develop a practical method to evaluate the performance in a problem specific way, as each different case has different requirements on the accuracy, robustness or reliability. The evaluation of the performance of an ANN program needs to cover two aspects. One is the accuracy of the training process, then, the results may need to be further extended into a physical meaningful way with measurable parameters.

2.5.1 Parameter for testing and validation of performance of an ANN

Testing and validation of an ANN is an important part in the development of an ANN. The most common approach is the Mean-Square-Error (MSE), which is in the form of:

$$MSE = \frac{1}{Q} \sum_{k=1}^Q (t(k) - a(k))^2 \quad (2.28)$$

where Q is the number of samples of the target output set, t(k) is the output of the target model to a certain input, and a(k) is the output of the ANN to the same input. This function produces an average of the squares of the errors between the target output and the ANN output. The objective a training process is to minimise this. Another form is Mean-Squared-Error with Regularization (MSEREG) which is the SUM of the MSE and the mean squared weight and bias values, both of these being first multiplied by some "damping" factors which are arbitrary and often vary with different software implementations of ANN performance measurement techniques ([Matlab Menu, 2013](#)). The MSE function provides a measure of the prediction accuracy of the ANN by calculating a single value representing the mean of the squares of the errors occurring between the ANN output and the target system output. However, there are aspects of the ANN responses which cannot be assessed by using the MSE function alone. Further analysis is required in the context of the work and nature of the data. For example, for material testing related works, certain levels of error is acceptable, but the range of error for all the data should be within certain limits. This may require training the ANN with a different focus. This is an area directly relevant to this project.

2.5.2 Generalisation of ANN and influencing factors

Generalisation with respect to neural network training refers to the ability of a network to produce the correct outputs for inputs in a test set (or a majority) that was not used in the training (Masters, 1993; Lawrence et al, 1996; Finlay 2004; Wan et al, 2009). In other word, the capacity of ANN in predicting results using data not used in training or validation. A fully generalised ANN could predict based on non-training data from the same class. This is a more useful feature but technically more challenging than the ability of the ANN to produce output of a supervised neural network to approximate the target values for data in the training set. In some case, 100% generation is not necessarily achievable depending on the nature of the problem and the way the training was designed and performed. This may pose a problem with materials testing as the material has to be 100% reliable for the ANN to be useful in particular to be routinely used by users with no in-depth ANN experiences.

There are two types of generalisations; one is interpolation and extrapolation (Barnard and Wessels, 1992). Interpolation applies to cases that the data are within the range or domain of the training cases or close to the training sets; while extrapolation situation refers to condition of fitting data outside the range of the training data (Lawrence et al 1996; Pala et al, 2007). Interpolation is much easier to achieve while extrapolation is difficult and in many cases impossible and unreliable, so most of the common engineering applications of ANN is concerned with interpolation. With FEA based data, it can always cover a wide range data so the ANN can be developed for interpolation problem effectively avoiding the need for extrapolation. So FE modelling is useful in this sense and should be used as an alternative method to methods purely based on experimental data. Many practical methods could help with achieving generalisation such as sufficient information linking the input to the target with desired accuracy through a general mathematic relationship (Trend). (Finlay, 2004). It is commonly known that ANNs are data dependent. In other words, it does not impose functional relationship between the independent and dependent variables. The functional relationship is determined by the data in the training (or calibration) process.

The advantage of such an approach is that a network with sufficient hidden units is able to approximate any continuous function to a certain degree of accuracy, if efficient training is performed ([Coulibaly et al 2000](#)).

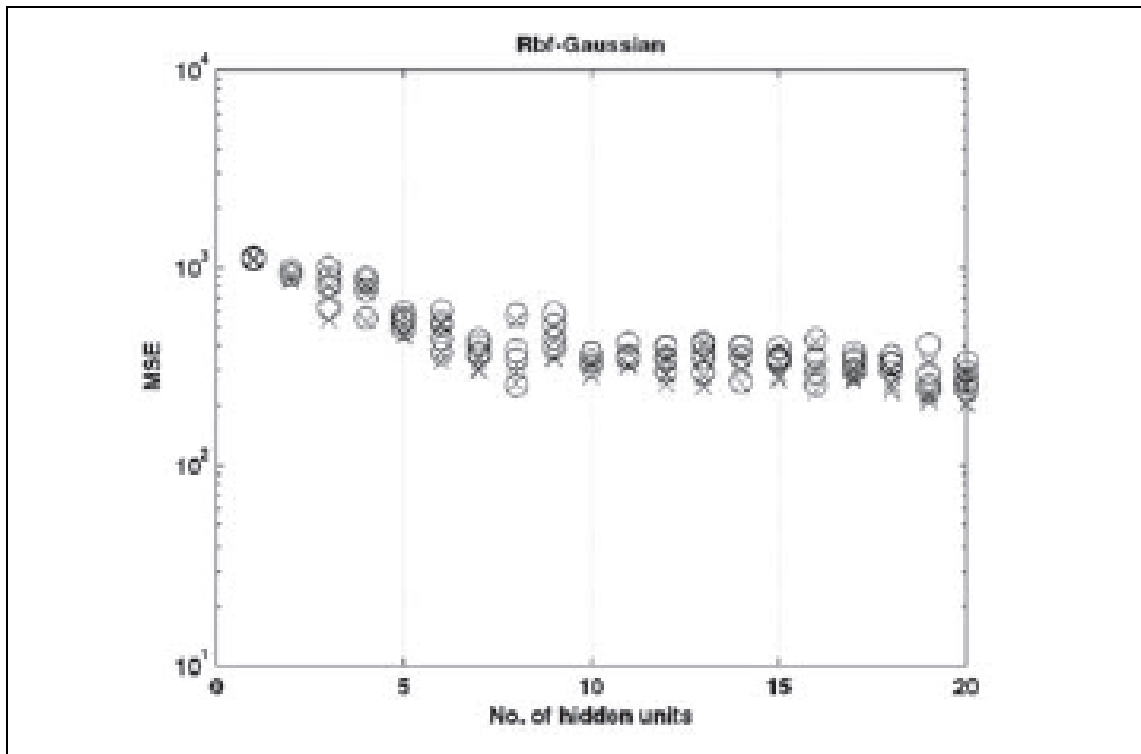
2.5.3 Key Factors affecting the ANN performance

The performance of an ANN depends on many issues and factors depending on the priority of the technical problem. Some key factors commonly evaluated in engineering ANNs included choice of number of neurons, choice of the activation function, over fitting, early stopping, w partition of the data, etc. (Finlay, 2004 ; Ince,2004). In most cases, MSE is normally the main performance indicator when evaluating the effects of these factors.

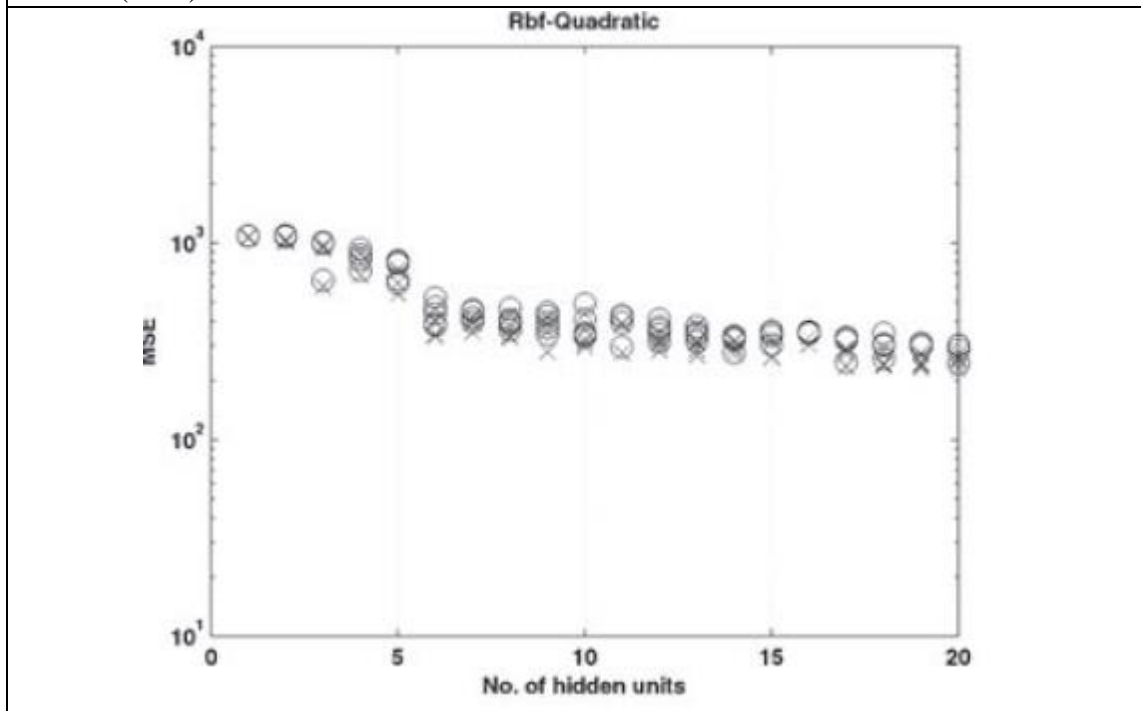
As detailed in the previous sections on the structure and working mechanism of ANN, the number of neurons directly influence the performance and the demand on computing resources of an ANN system. The rule for proper selection of neuron number is that the number of neurons should be sufficient in producing results of acceptable accuracy in the meantime avoid over fitting. Many works use MSE as an indicator to assess the effect of number of neurons (Wu et al 2006; Meng and Lin 2008), which has been very effective through trial- and-error methods. A typical example of using MSE to evaluate the performance of ANN is shown in Figure 2.17. In this work on developing a neural network and real genetic algorithm combined tool for an engine test bed, the change of MSE with increasing number of hidden units of an NN model (from 1 to 20) is established to select the optimum condition. In the work, for each fixed hidden unit, several runs are arranged with different initial conditions for the network parameters. The optimal network structure is determined by the minimum error for the validation set over all these runs. In another work by Meng and Lin (2008), in order to clarify the effect of neuron number on the approximation capability, the work compared the performance of ANNs with 1–10 neurons in the hidden layer. Considering only the predictive performance, 90% of the entire data set was used to establish ANNs and the remaining 10% was used for testing the predictive accuracy of these established ANNs. The 90% data were further randomly divided into a training subset (80%) and a validating subset (10%) to meet the requirement of the early-stopping technique. Figure 2.18 shows a typical relationship, between MSE and the neuron number for both the training+validating subsets and the testing subset (Meng and Lin, 2008). In contrast to the persistent reduction of MSE in the training+validating subsets,

the MSE in the testing subset began decreasing only marginally and even stopped decreasing when the neuron number exceeded 4 and 6, respectively. Thus, more than 6 neurons were considered redundant, and the ANN with 6 neurons in the hidden layer was accepted.

Over training could be a major problem in ANN. In this situation even though the accuracy of the training may increase but the overall accuracy of the ANN will decrease in particular for predicting untrained data. If the complexity of the network is too high for the problem being considered, the NN system will learn all the details of the training patterns, potentially including the noise, which doesn't reflect the nature of the material or system. One major condition causing over training is excessive number of neurons in the hidden layer. As illustrated in Figure 2.19, when the network has too much freedom (i.e. too many resources such as neurons) that it focus on fitting the details (even noises) of the training data rather than the underlying trend/function (Masters, 1993). With a new set of test data, the ANN will try to match/find output values from the trained data rather than trying to interpolate to a new output values. (Finlay, 2004). Typical methods to avoid over training could include proper selection of number (normally through trials); partition of the data, incorporating early stopping mechanism, etc. (Coulibaly et al 2000; Meng and lin 2008, Prechelt, 1998).



(a) Effect of Number of hidden units on MSE with radial basis function (RBF)-Gaussian function.



(b) Effect of Number of hidden units on MSE with radial basis function (RBF)-Quadratic function.

Figure 2.17 Typical examples showing using MSE to assessing effect of number of hidden units (Wu et al 2006).

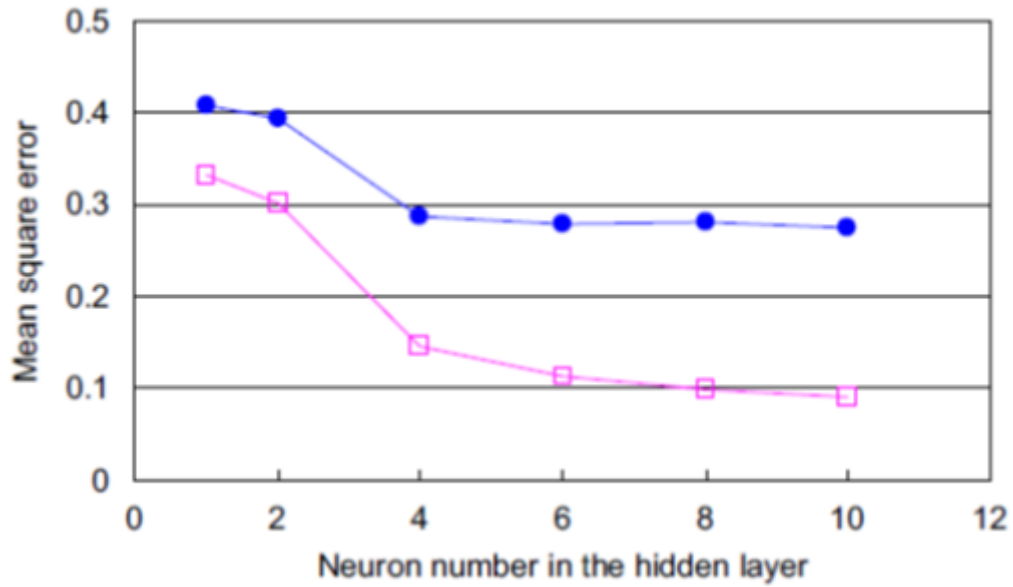


Figure 2.18 Typical data showing the improvement of ANN approximating capability with increases of the number of neurons in the hidden layer of in a feed-forward artificial neural network for prediction of the aquatic ecotoxicity of alcohol ethoxylate incorporating early stopping (Meng and Lin 2008).

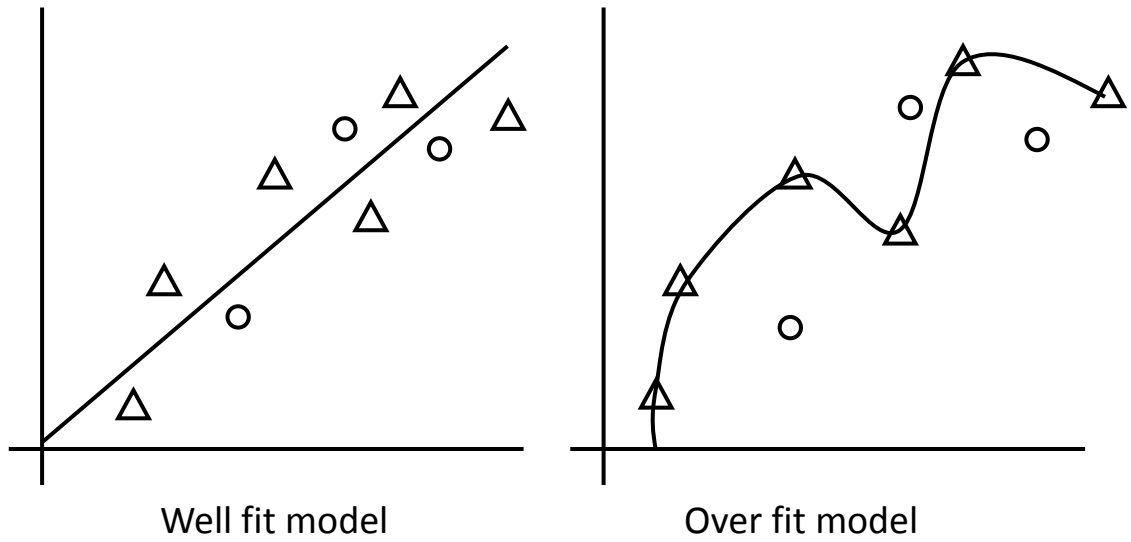


Figure 2.19 Schematic to show the concept of fitting and over fit (Adapted from Maters 1993; Finlay, 2004).

2.6 FE modelling methods and data processing

In many engineering and material related works, FE is increasingly being used to provide data for NN works in addition to experimental data (Tho et al 2004; Ince 2004, Khin 2009, Luo et al 2007; Harsono, 2009). The advantage of FE lies in the fact, once it was validated with experimental data, it will be able to produce much large scale of data than pure experimental methods. This could potentially enhance the use of ANN in materials related works. However, both FE and ANN have their limitations which have to be considered to be able to combine these two techniques. The basic structure and theories of Finite element modelling is briefly summarized here, with a particular focus on the data and information from FE modelling at different stages. Understanding of nature of data and processing is important for ANN development based on FE data, post modelling database development and potential development of computer based program, which is directly relevant to this project.

Finite Element methods are now widely used by engineers and scientists to simulate very complex problems (Dao et al, 2001; Tho et al 2004; Ren et al 2008; Gu, 2010; Norbury 2014). In general, the Finite Element approach involves dividing the continuum into elements which are small enough for factors such as stress or displacement fields (or other physical parameters) to be approximated satisfying the problem's boundary conditions. There are many different commercial packages available such as the ABAQUS, ANSYS etc. This work will focus on the data and main factors that affect the modelling process, which may relevant when using them in ANN, including demand on computational resources and time.

Figure 2.20 shows the main steps in structural FE modelling. It starts with input of dimensions, part and assembly, material properties, meshing, boundary and loading conditions, then meshing. Through the meshing process, the model is discretised in space, i.e., converted to a discrete model of a finite number of elements, taking into consideration degrees of freedom (DOF), loading, boundary conditions and different material properties. After the problem has been discretised, the governing equations for each element are

calculated and then assembled to give the system equation. The details of the calculation process and theory can be found in many references (e.g. Fagan 1992).

One of the main aspects of FE with ANN is data process in a FE modelling process. The data requirement for an FE process is complex. The input maybe dimensions, shape, material properties and boundaries condition such as contact, friction, etc. The accuracy of these is important to the accuracy of the model. The input data can be entered interactively, it can also be done using parametric program, or recently for ABAQUS via. A .RPY file based on python programming, which can systematically change the properties or dimensions through loop or optimisation function (ABAQUS 6.10 Manual). This potentially could produce a program to generate a large quantity of data covering a wide range of properties. This could enhance the data quality if used for ANN training. The calculation time of FE varies with the problem; some calculation can be done very quickly while some models can be very time consuming depends on the number of elements or if the material model is complicated. In addition, FE modelling is also an expensive process on software requirement in comparison with ANN based processes. ANN programs may take time to train but once trained the calculation could be much faster than FE modelling. Combining the two approaches could be advantageous. Recently, the post processing of FE results is being rapidly developed; many different ways can be used to extract data through interactive, python or subroutine, the output can be typical materials deformation, force, etc., all these may potentially provide more comprehensive data for ANN than using pure experimental data. An effective process would be using experimental to validate the FE model, then use the FE model to produce more data for the training of ANN, then use both FE and experimental data to validate the ANN program.

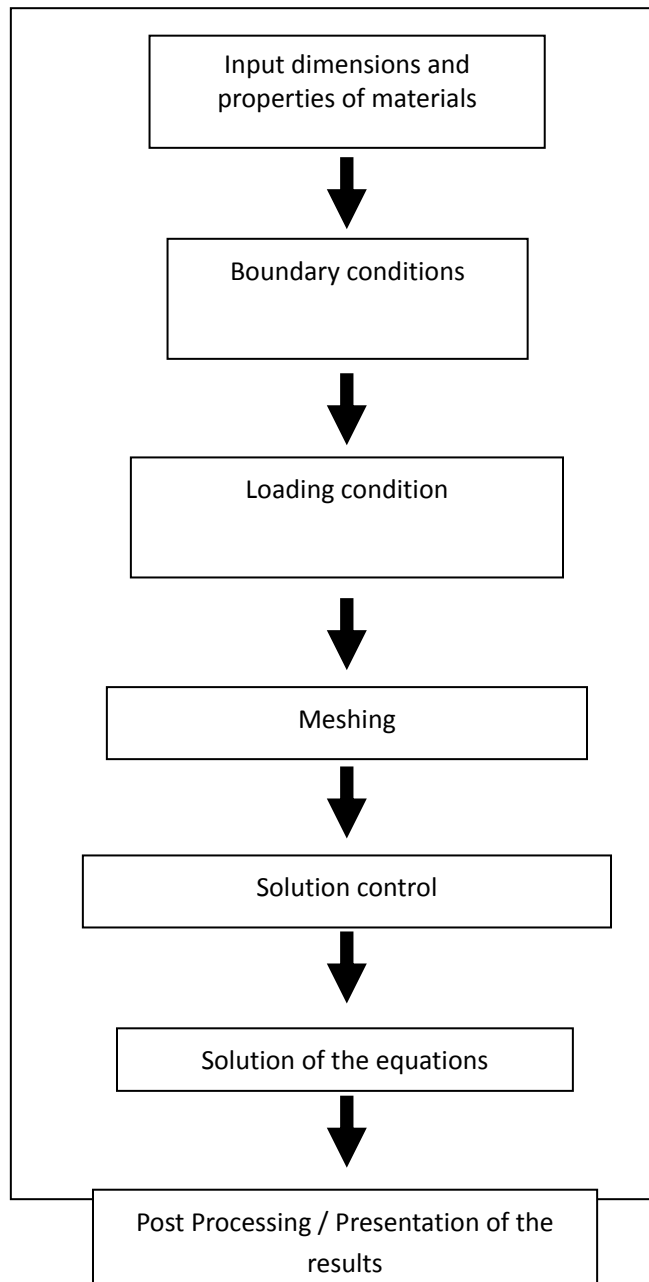


Figure 2.20 The main steps in a Finite Element modelling process (Adapted from Fagan 1992).

2.7 Applications of ANN in engineering and indentation tests

ANNs have been used in many different areas in different technical industries (Huber et al 2000; Zaw et al 2009; Lee 1998, Scott et al 2007; Coulibaly 2000; Harsono 2009; Demir et al, 2008; Maier 2000; Partheepan, 2011). Many of these works is concerned or associated with the use ANN in material testing. As discussed in section 2.3, ANNs represent a simple and quick method without repeated running of FE program; this could provide a significant computational advantage. Zaw et al (2009) proposed a rapid inverse analysis approach based on artificial neural network to identify the “unknown” elastic modulus (Young’s modulus) of the interfacial tissue between a dental implant and the surrounding bones. In another study, Esfahani et al (2009) presented an artificial neural network to model the influences of chemical composition and process features on the properties (yield stress) of hot strip steels. In all these works, ANN approach showed significant advantages over other inverse and optimization approaches in dealing with complex material systems.

General speaking, there are several advantages of the ANN method in comparison to other method such as the interactive and parametric method (Section 2.3). A major advantage of the use of neural networks for data modelling is that they are able to fit complex nonlinear models and these models do not have to be specified in advance. This is directly relevant on material characterisation as in many cases, the materials is unknown or may change with time/conditions. Neural networks are composed of elements operating in parallel, which allows increased speed of calculation compared to slower sequential processing, this can be important for complex material models or systems. As explained in section 2.6, some FE models may take a long time to run, if the data has been used to develop an ANN, the calculation will be much faster. In addition, neural networks have the ability to detect many possible interactions between variables: The hidden layer of a neural network gives it the power to detect interactions or interrelationships between all of the input variables; this is a commonly case as the material parameters could be interlinked in many cases. ANNs are robust in the sense that, should part of a network lose connectivity, the remainder will continue to function, thus a partial loss of function is not catastrophic in the same way it would be for conventional models based on the physical process. In addition, as a post

modelling approach, another advantage of this method is that it does not require re-running the FE modelling during the optimisation process. All of these features made ANN an attractive option for material testing either for predicting the material response or estimating material parameters by combining FE modelling and experimental testing, in particular for systems with nonlinear properties such as foams and related structures.

Use of ANN in materials property estimation could be a complex process, in many cases, the program or structure of ANN has to be designed to suit the problem, this could be deciding what input to use or what will be used as output if the physical parameters/properties could not be used. Some specific data process has to be implemented. For example, the main measurement result in indentation is force-indentation depth curves, but the parameter describing P-h curves not necessary can be linked mathematically to the property parameters. For ANN, the more meaning for data as input the better, so sometimes, some factor that may not necessarily directly relevant to material work, but it can be very useful to the ANN program. A typical example by [Tho et al. \(2004\)](#) on use of cone indenter in predicting material properties of metals (yield stress and work hardening coefficients) is shown in Figure 2.21 (a). The work requires the construction of 2 artificial neural networks (ANN1 and ANN2) as two stages of mapping have to be performed. Each ANN model created by Neural Network Toolbox (Matlab V6.5) comprises 3 layers, namely, (i) an input, (ii) a hidden and (iii) an output layers. The tangent sigmoid transfer function is employed in the hidden layer while the output layer uses the linear transfer function. In the work, the number of neurons in the hidden layer is calibrated based on the training and validation processes. The work has been successfully used to predict the plastic properties of a range of metals including Aluminium and steel based on dual indenter approach. Harsono (2009) used a single neural network approach (Figure 2.22 (a)) study the prediction of yield stress and work hardening coefficients based on a single indenter approach, while the input are the surface of ratio between work done and total energy (W_R/W_t) and the ratio of the curvature ratio of the curves of two different indenter angles (C_1/C_2) (Figure 2.22(b)). The comparison between the ANN predictions is listed in Table 2.1 in comparison with the target value. The yield strength shows a good agreement but the

work hardening coefficients showed a very high deviation. This shows that ANN can be used to predict the materials properties but not necessary will achieve high accuracy for all the material parameters. This does not imply that program is not useful but to highlight the fact that when developing ANN, the goal should be try to achieve the best than can be achieved rather than purely to produce accurate number on limited cases. It will be interesting to investigate this with other more complex material models such as EVA foams.

Table 2.1 Comparison of the predicted material properties obtained from ANNs algorithm with inputs for various combinations of three-sided pyramidal indenter tips. (Tho et al, 2004)

| | Al6061 | Al7075 |
|--------------------------------|----------|----------|
| E^* [GPa] | | |
| Actual | 70.2 | 73.4 |
| ANN | 56.5 | 75.7 |
| [% deviation] | [-19.52] | [+3.13] |
| Oliver and Pharr Method (1992) | | |
| Actual | 85.0 | 86.2 |
| ANN | 85.0 | 86.2 |
| [% deviation] | [+21.1] | [+17.4] |
| Y [MPa] | | |
| Actual | 284.0 | 500.0 |
| ANN | 283 | 498 |
| [% deviation] | [-0.35] | [-0.40] |
| n | | |
| Actual | 0.080 | 0.122 |
| ANN | 0.0957 | 0.0944 |
| [% deviation] | [+19.63] | [-22.62] |

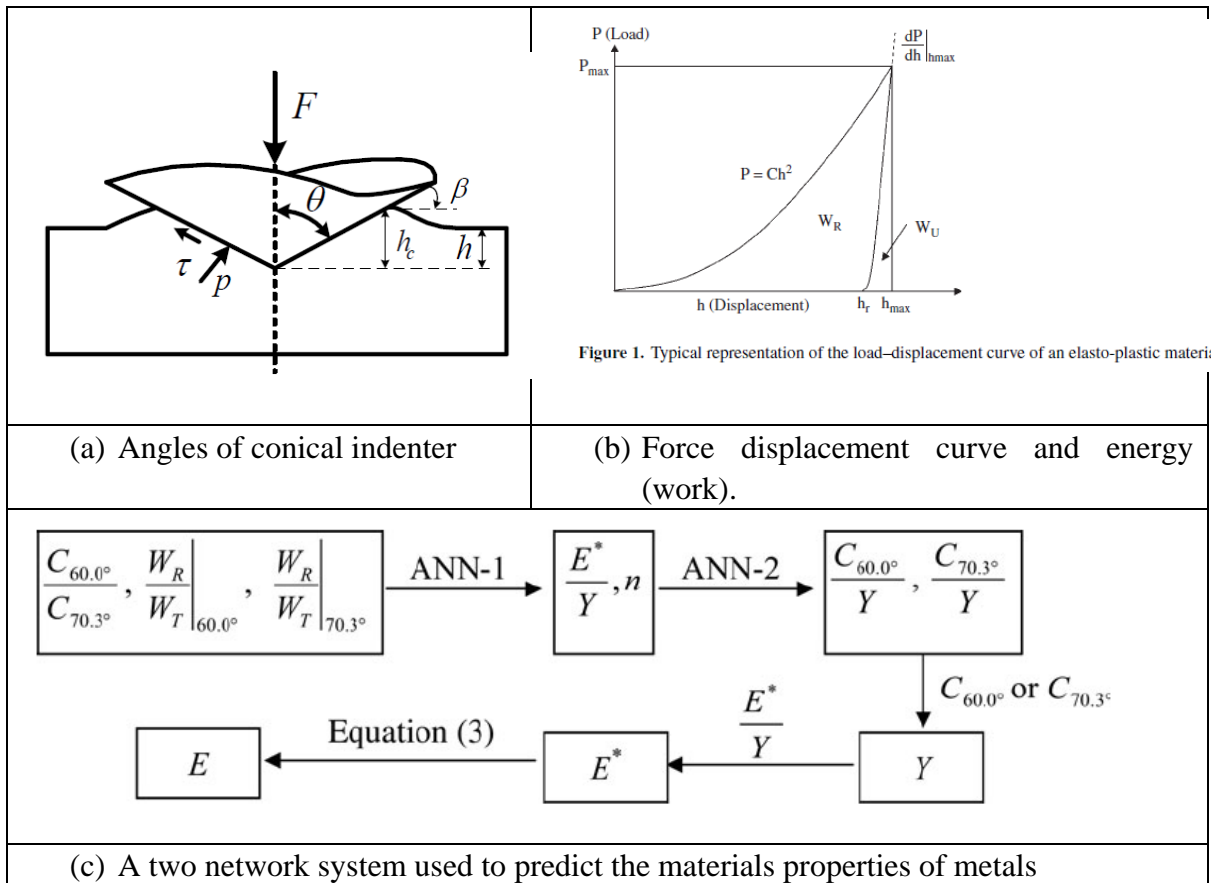
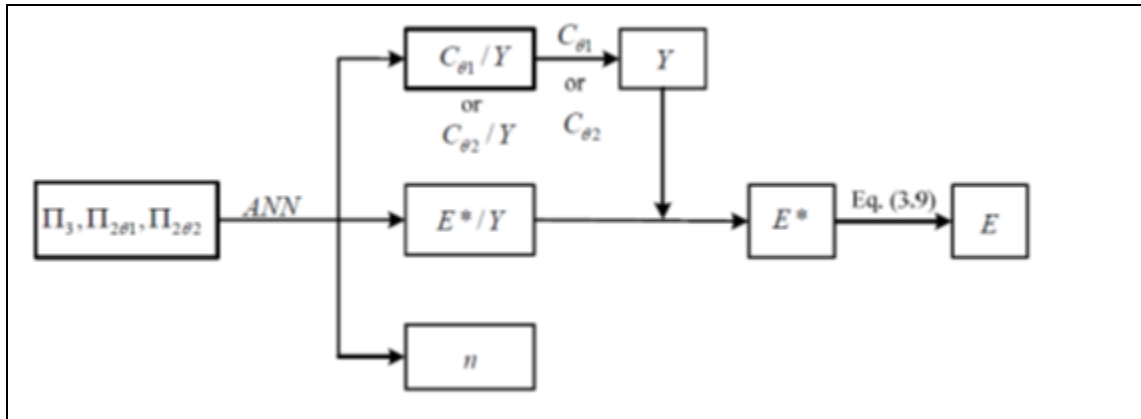


Figure 2.21A two ANN system used in predicting plastic properties of metals based on conical indentation (Tho et al 2004).



(a) Flow chart of proposed ANN based on a single ANN model.

$$\left. \frac{C}{Y} \right|_{\theta_1} = \Pi_{1\theta_1} \left(\frac{E^*}{Y}, n \right)$$

$$\left. \frac{C}{Y} \right|_{\theta_2} = \Pi_{1\theta_2} \left(\frac{E^*}{Y}, n \right)$$

$$\left. \frac{W_R}{W_T} \right|_{\theta_1} = \Pi_{2\theta_1} \left(\frac{E^*}{Y}, n \right)$$

$$\left. \frac{W_R}{W_T} \right|_{\theta_2} = \Pi_{2\theta_2} \left(\frac{E^*}{Y}, n \right)$$

$$\frac{C_{\theta_1}}{C_{\theta_2}} = \frac{\Pi_{1\theta_1}}{\Pi_{1\theta_2}} = \Pi_3$$

(b) Surface function (Π) used in the ANN inverse program.

Figure 2.22 A single ANN system used in predicting plastic properties based on conical indentation (a) and the equations (b) (Harsono, 2009).

2.8 Potential application of ANN in indentation testing of EVA foams and main challenges

Close cell foams, such as Ethylene vinyl acetate (EVA) foam are widely used in engineering, sport and biomedical fields (Mills et al, 2003; Moreu and Mills, 2004). EVA foam is made up of tiny gas bubbles, which give the material a unique mechanical behaviour, which is difficult to characterise. A typical application for EVA foam is in footwear, where a range of EVA materials of different hardness are used (Verdejo and Mills, 2004; Gu et al 2011). As illustrated in Figure 2.23, sports shoes can be broken down into 4 main areas; upper shoe, inserts, mid-soles and the outsole. While the upper shoe functions are mainly to hold the sports shoe together, it also helps to stabilize the foot during running (Gu et al 2011). The midsole of a sports shoe, which commonly made by EVA foam, aims to help spread the impact forces so the peak ground reaction force is not placed directly to the foot, leg and knee, which is how most injuries have occurred (Gu, 2010). The indentation resistance of the material directly reflect the deformation of the material under load and the comfort of the shoe, etc. EVA foam could provide the mid-sole cushioning properties. Detailed properties of the foam is very important for both material development and the design. In a product development process, the engineer has to select material form a range of product, in some case combination of material has to be used. Figure 2.24 illustrate an example in developing midsole using different EVA foams (Gu, 2011). In this case, EVA foams of different hardness is used in different areas of the midsole. The effect of these different designs has to be simulated with finite element modelling as shown in Figure 2.25, which requires detailed material parameters.

Given the wide application of EVA and the use of indentation testing, it is important to explore the use of ANN in indentation of EVA materials. Two main areas need to be studied for both industrial application and academic research. One area is direct estimation of the indentation curves for material of known properties, this will help the engineer/researcher to estimate the potential performance when comparing different materials with known properties. As explained in the hyperfoam models, the property of

EVA foam is governed by two parameters (equation 2.4) (as compared to metallic materials, the P-h curve of which can be represented by only one coefficient (equation 2.1)), so it is very difficult to tell how the material is going to perform under indentation as the two parameters influence the P-h curves in a different way. FE modelling has to be performed which is not very convenient in particular when the software or modelling expertise are not available. In addition, an ANN program validated with standard indentation tests may be able to be transferred into more complex loading to study the effect of material properties such as foot-shoe interaction. Another area to be investigated is to inversely estimate the material parameters from indentation tests as it is much more easier than standard approach (i.e. combination of shear and compression tests), it will be a great advantage if the material parameter can be predicted inversely from indentation tests as a quick way of predicting the properties with full confidence. As detailed in section 2.2 and illustrated in Figure 2.7, use of standard tests are complicated and time consuming. In addition, it will be difficult to conduct materials testing at different temperatures with the setup of standard tests.

There are some challenges for both research directions (i.e. direct P-h curve prediction and inverse material property estimation). The material represents a much more challenging research topic than metal materials. The indentation curve of metals can be represented by a simple curvature (as in Eq. 2.1), but for EVA foams, a more complex way has to be used to represent the data. Polynomial fitting could be a way to describe the curves, but there are issues of nonuniqueness in using polynomial fitting. More challengingly, the choice of mathematical representation of the curve has to be properly selected to be able to aid the direct or inverse engineering. In addition, the accuracy/robustness in direct (predict indentation curves from known properties) and inverse (predict properties from indentation curves) has to be established. The practice in some of the published work in materials oriented projects has been focus on limited number of testing cases, which could not satisfy the need of materials research and development or to be used by material researchers without direct experience in ANN. There may be non-uniqueness issues, where more than one set material parameters fit the target of P-h curves; this and the uncertainty

associated with this has been a major barrier in preventing wider application of inverse program. One direction of this work is to explore situation where testing data of different situation (e.g. indenter size, thickness) can be used to improve the robustness. Another aim on program development is to establish methodology and computational tool that is capable of mapping out all possible solution in a direct/inverse program, which will ultimately give the user the confidence in the inverse results and select the optimum/best available solution based on pre-knowledge or experience in case that no unique properties can be defined, this will be suitable for the nature of materials testing. The material behaviour of EVA material is representative of a range of materials including biomedical materials, so the program developed and evaluated with EVA as a model material will be transferable to other material systems in the future based on the research framework (including the use of different ANN tools (nftool, nntol and code based), programming language and curve fitting/searching approach to be established in this project). Some of these will be highlighted in the discussion and future work section.



Figure 2.23 Schematics to show the structure of the sport shoe design and the application of EVA materials (Nigg et al., 2006).

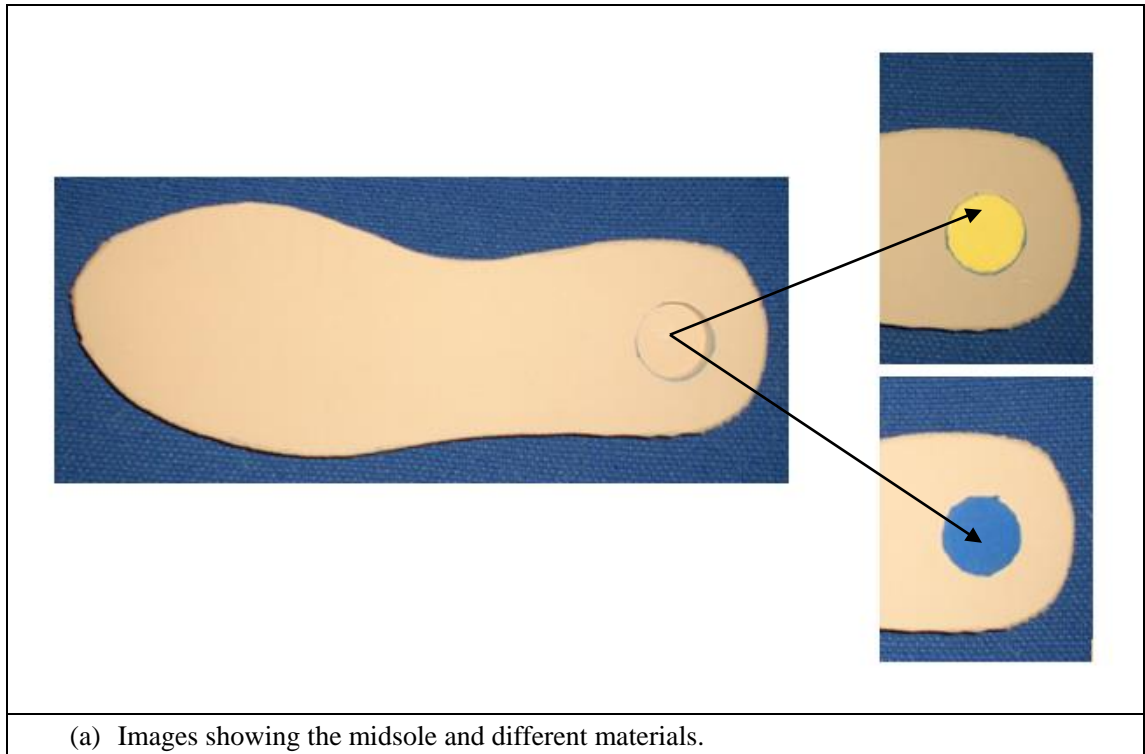


Figure 2.24 Manufacture of the midsole with different materials to illustrate the use of EVA foam (Gu et al, 2011).

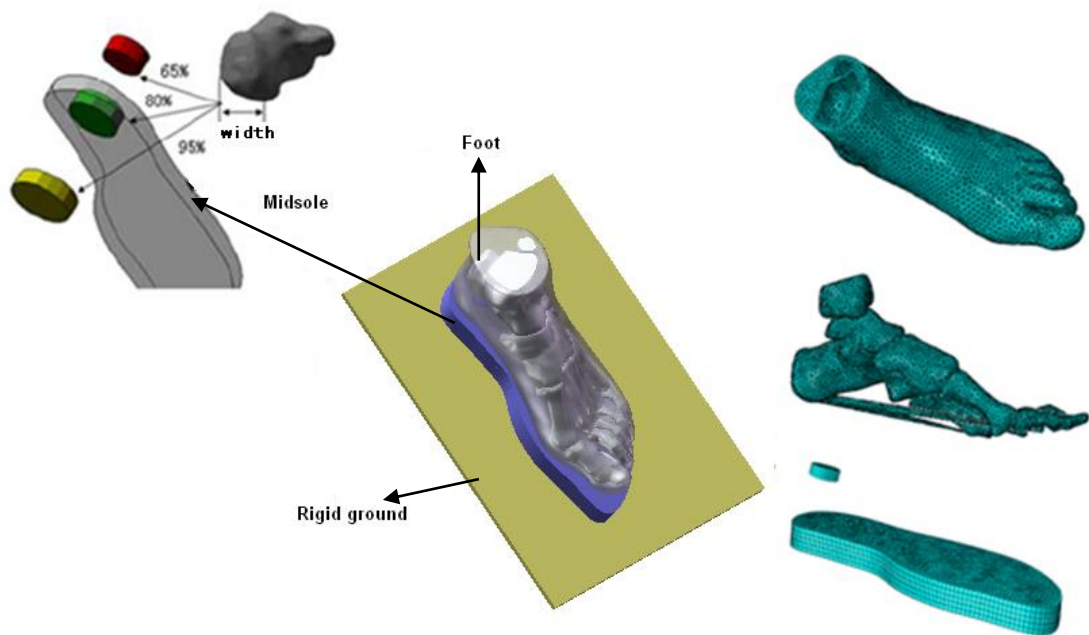


Figure 2.25 FE model for simulating the effect of EVA foams on shoe heel interaction (Gu et al 2010) to highlight the importance of EVA testing and properties.

Chapter Three
Prediction of indentation force displacement curves
(P-h) of hyper foams based ANN

3.1 Introduction and research structure

Figure 3.1 shows the main research work reported in the thesis, consisting three main parts: FE modelling and data process; development of ANN for direct prediction of indentation $P-h$ curves and inverse material property identification. Chapter 3 consists of first two main parts of works. The first part is development of FE models and data processing. The second part involves developing an ANN program to predict the force indentation displacement curves with known materials properties (μ and α) for different indenter sizes. The ANN work will enable the prediction of Force displacement data without re-running the FE modelling. The work will provide a base for developing inverse material property prediction program, which to be presented in the next chapter.

In the FE modelling part, a parametric FE .inp file is developed which is able to change the key material properties and dimensions, including indenter size, sample size and thickness. This will make the data processing process a lot easier compared to interactively changing these in the FE model. The effects of some key modelling parameters (such as mesh density, etc.) on the indentation curves are investigated using parametric studies in ABAQUS and the optimum modelling conditions are established. The FE model is validated with experimental test data with EVA foam with known properties. The FE model is then used to map the effects of material properties on the loading curves using parametric studies in ABAQUS. Based on the parametric studies, simulation spaces covering a wide range of potential material properties are constructed. Two methods are used to generate the material property matrix data: one is to use regular fixed increment in μ and α ; the other is to use increment in percentage. These provide essential systematic data for the ANN training, validation and test data.

In the ANN part, two approaches have been proposed and evaluated to represent the $P-h$ curves; one is to use polynomial trendline to represent the $P-h$ curves (designated as trendline approach); the other is to use force at different indentation depth (designated as depth approach). The validity and accuracy of each ANN is assessed using trained data and

new data (not used in training or validation) using MSE and relative error as performance indicator. A new approach is developed to improve the robustness of the prediction through frequency analysis. The sensitivity of the estimated mechanical properties to variations of the input parameters (e.g. potential perturbation (error or noise) of the load) is also investigated. The prediction of ANN is extensively validated with FE data, the prediction is also compared to experimental testing data. The ANN approach is also compared to other methods including surface mapping and direct data searching programming using Matlab Polyfit functions. The frame work of the ANN program developed is then used to develop a computerised method for inverse foam properties identification (to be presented in the next chapter).

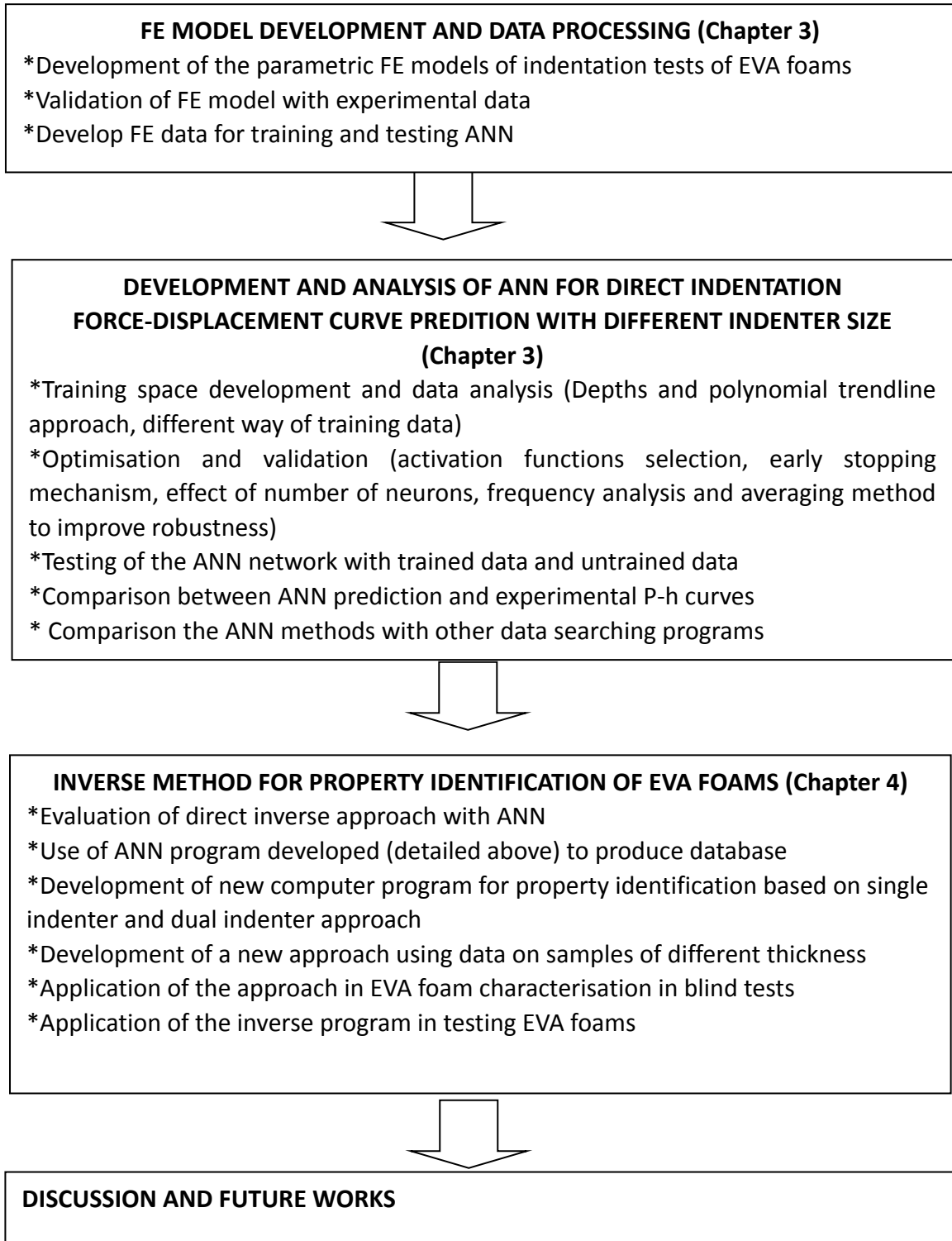


Figure 3.1 Flow chart showing the main research work of the thesis.

3.2 Experimental test and numerical models

3.2.1 Experimental and typical results

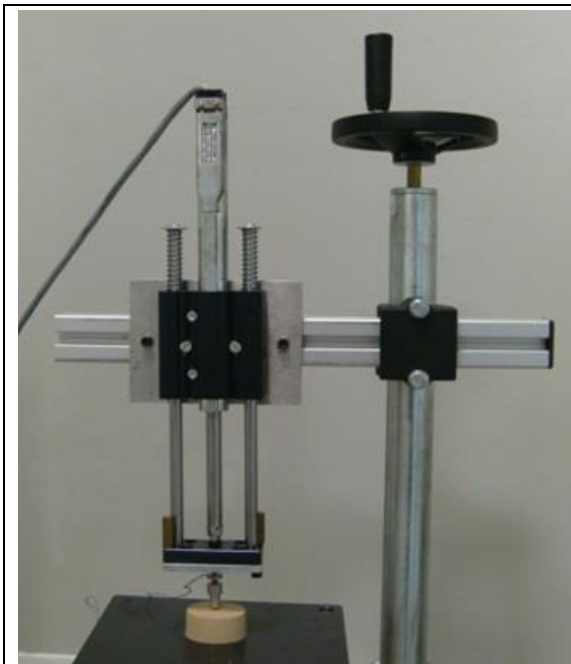
Figure 3.2(a) shows the testing machine used. The indentation test system used an actuator as the driving system mounted on a strong supporting frame and allows tests in both vertical and horizontal directions. A sensitive load cell (model: LCMS-D12TC-10N) is attached to the moving head of the actuator to monitor the forces during the test. The indentation tests were performed using a spherical indenter made of stainless steel. The machine was developed in a previous project, some modification has been made to allow for both tension and compression tests. Figure 3.2 (b) shows a shore hardness tester used to assess the hardness of the EVA foams. Tests have been performed on two EVA samples with indenter size, 4mm and 6mm. A typical force indentation depth data is shown in Figure 3.2(c) to illustrate the loading curves (P-h curves). In the test, both loading and unloading curve can be captured, but this work will be focusing on the loading curve only, which is governed by the hyperfoam parameters. Indentation test data can be used to validate the FE model then the FE models is used in producing input and validation data for the development of ANN program. All the experimental data (two samples (thickness 20mm) and two indenter sizes) will also be used to validate the ANN programs to assess its accuracy in predicting indentation P-h curves, which are to be presented in later sections.

3.2.2 FE indentation model and validation.

As shown in Figure 3.3(a), a 2-D axial symmetric model was used due to the symmetry of the spherical indenter. The indenter was assumed to be an analytically rigid body as it is much harder than the indented material. The element type of the material used is CAX4R (an axisymmetric element) and finer meshes have been applied around the indenter to improve the accuracy. The thickness and width of the model is 20 mm and 25mm respectively mimicking the sample and test condition; both are about 4 times larger than the indenter radius to avoid potential sample size and boundary effects. The bottom base of

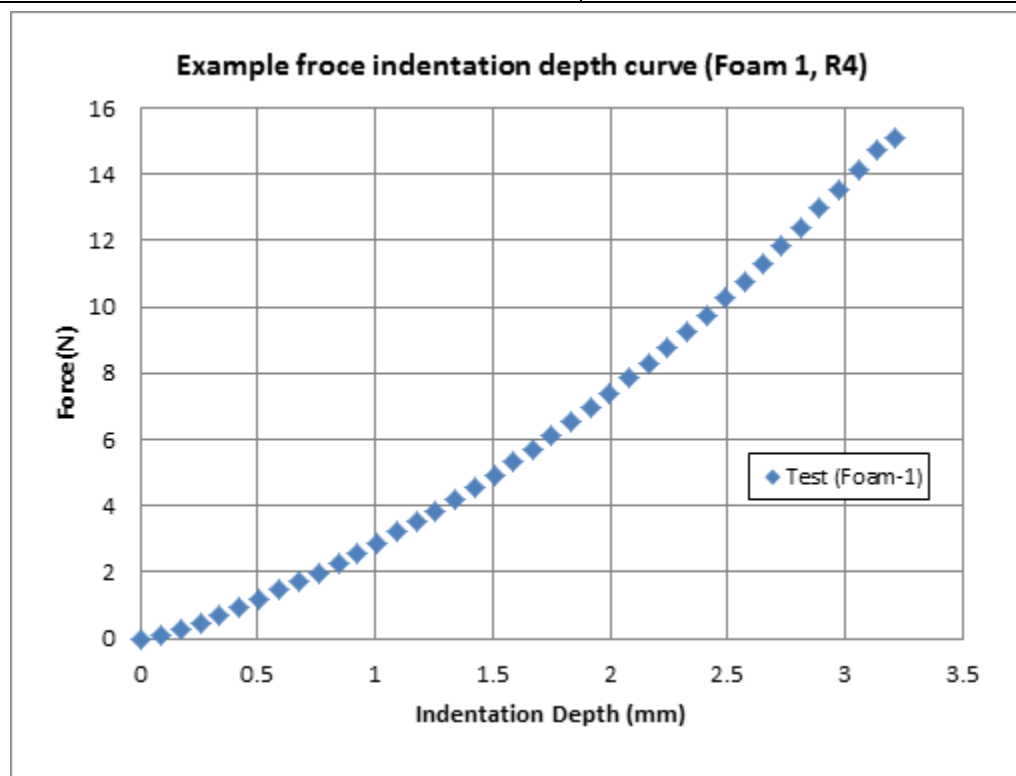
the material was fixed in all degrees of freedom (DOF). Contact has been defined between the indenter surface and sample surface with a coefficient of friction of 0.5. The material of interest is allowed to move and the contact between the indenter surface and the material surface was maintained at all the times.

In FE modelling, the accuracy of the results is influenced by many factors such as the mesh density, frictional condition and validation of the boundary conditions. The most relevant factors for the simulation of indentation process are the mesh density and frictional conditions (Taljat and Zacharia, 1998). The friction coefficient used is 0.5, which is commonly used in indentation testing of soft materials. The potential influence of mesh size on the accuracy of the modelling process has all been assessed to ensure that the model produce accurate results and in the meantime require optimum computational time. This is performed by refining the mesh size in different FE models until no further significant influence of mesh size on the P-h curves was observed. Figure 3.3 (b) shows the displacement field (vertical displacement U2) under the indenter. The force at each indentation depth can be extracted to represent the indentation resistance of the materials. In the early part of the work, the P-h curve is extracted from the program interactively, which was time consuming and slow when generating large number of models for ANN training. Towards later stage of the work, a python program was developed to automatically extract P-h curves from multiple FE parametric simulations. This is very useful for developing ANN as a large number of dataset are required. Figure 3.4 compares the numerically predicted force-displacement curved and experimental data of a model EVA foam with known material properties. The properties used were determined using a standard approach combining compression and shear test from a previous study. Several tests have been performed and three test data from the same foam sample are plotted, which showed slight variation. This is natural for such tests, as many factors may affect the results such as initial contact, position accuracy, etc. The reasonably close agreement between the numerical and experimental result suggested that FE model was accurate for the purpose of generating training and test data. This validation is very important before using the FE for developing ANN program.



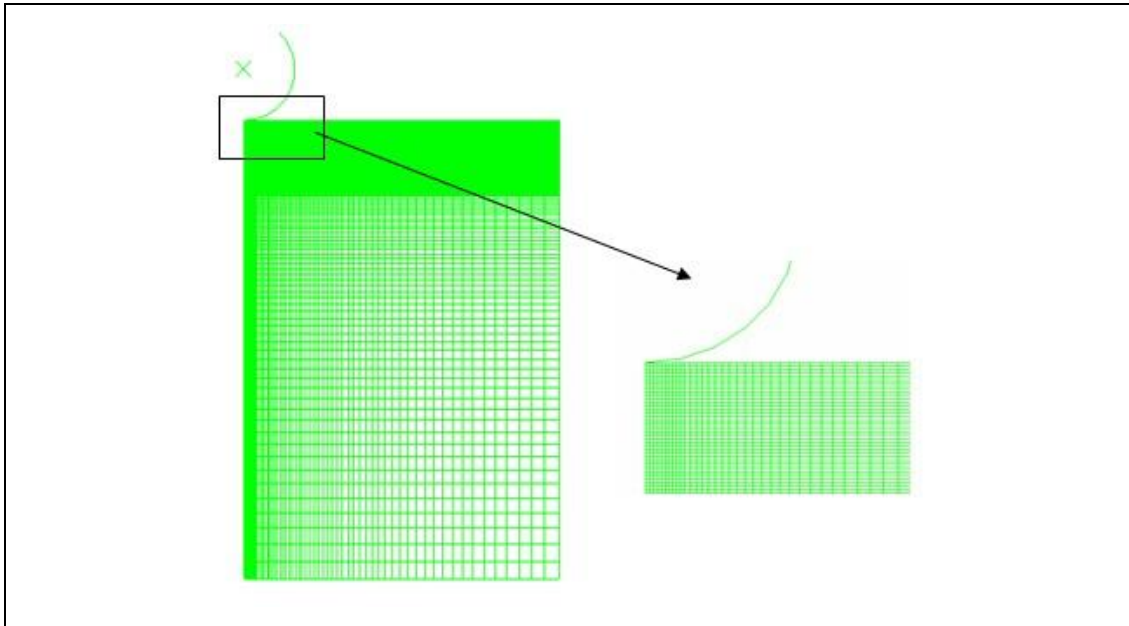
(a) The indentation testing system used to test foam specimen.

(b) Shore hardness tester.

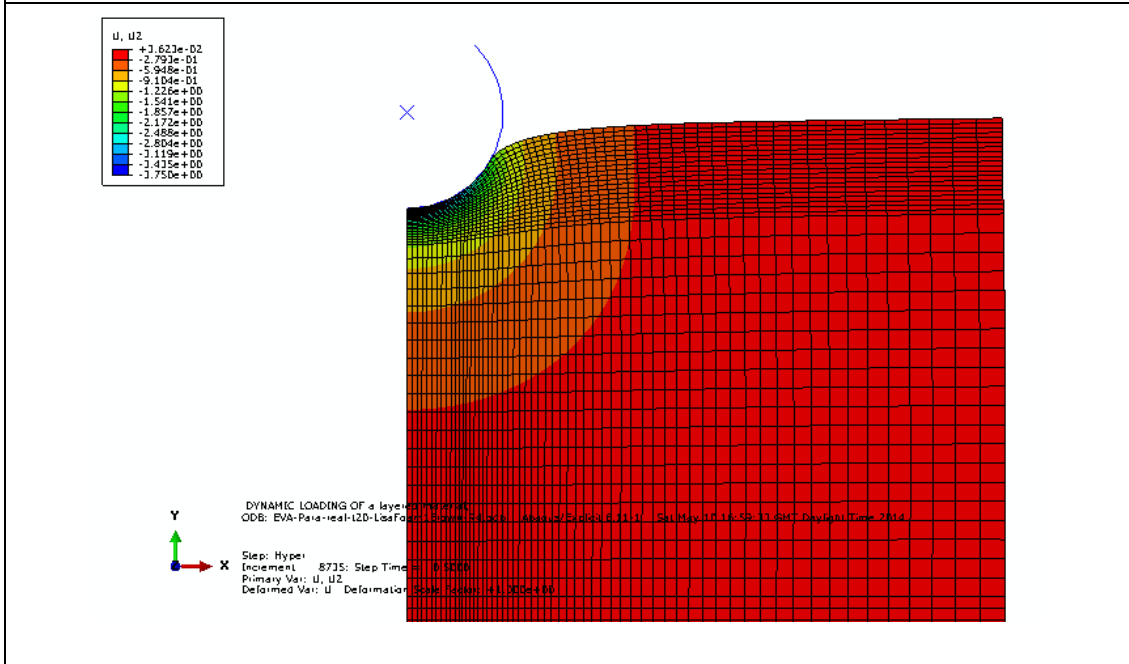


(c) Typical force indentation depth data of foam 1 (R=4mm).

Figure 3.2 The indentation testing system used and typical force displacement curve of a sample EVA foam.



(a) FE model of indentation process with a spherical indenter.



(b) Typical displacement fields (R4, Vertical displacement (Y axis): U2)

Figure 3.3 FE model of indentation process with a spherical indenter and typical displacement fields (U2, vertical direction).

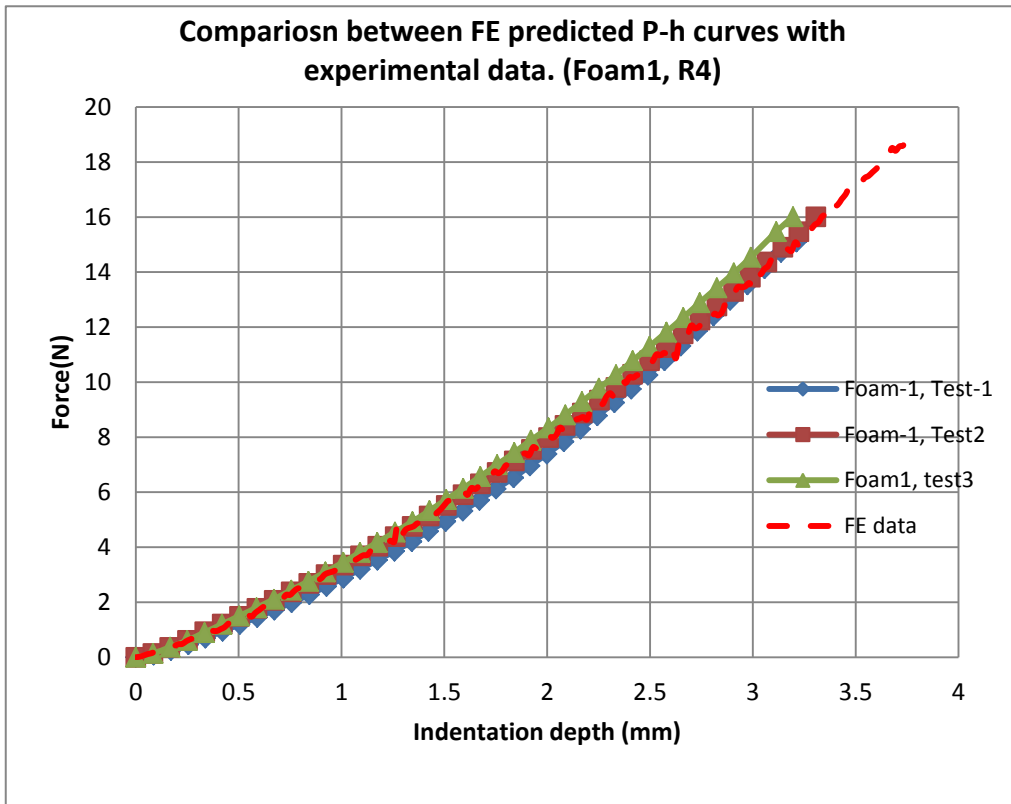


Figure 3.4 FE model validation based on the experimental data of materials of with known solution.

3.3 ANN Program development for predicting indentation force displacement curve and results

3.3.1 Key technical works and programs

As highlighted in literature review in Chapter 2, the nature of the data input is critical to the performance of an ANN program, which requires a systematic investigation. Figure 3.5 shows the main development and research works. In the first part, FE parametric modelling was developed through ABAQUS parametric, in which the multiple FE models can be run by defining the range of material properties. This function allows production of data for ANN in an effective way. It also allows the assessing the performance of ANN systematically rather than based on limited number of data. Table 1 lists the key parameters of the .inp file developed, which allows change the indenter size, sample size, mesh and material properties. In the program, the sample is built by different layers (4 layers in this case); in this work, the purpose of this approach is purely to control the mesh in a practical and controllable way. As far as each layer has the same materials properties, then the end results is the same as building the FE model as one component.

Table 3.1 Defining key parameters in ABAQUS .inp files.

```
*PARAMETER
d=8
v1 = 0 # 'X' coordinates of the start point of indenter
w1 = 0 # 'Y' coordinates of the start point of indenter
r=d/2
v2=r*0.707
w2=r+r*0.707
dis=3.75#indentation depth
t1=2# Position of the bottom line of the top layer
t2=t1+2 # Position of the bottom line of the 2nd layer
t3=t2+10*1 # Position of the bottom line of the 3rd layer
t4=t3+10*1 # Position of the bottom line of the 4th layer
x1=r/2 # area under the indenter, used to control the mesh size
x2=25 # boundary of the sample to control sample width
mu1=0.6# materials parameters
alfa1=5# material parameter
.....
```

For ANN, a large number of data will be required. This was achieved by using ABAQUS parametric functions, in which multiple models can be produced by changing the materials properties. A python program with loop function is used for the purpose of extracting P-h curves from multiple models. The program will automatically open ABAQUS .odb files from the parametric studies, extract the P-h curve, and save them as text file, which can then processed using Excel or other file reading programs. This program has greatly help developing different data for the ANN program.

As show in Figure 3.5, two approaches have been proposed to represent the P-h curves. One is using trendline method, the other is to use force at different depth. Details will be presented the next section. The use of both approaches is analysed in detail. The optimisation of the ANN has been focused on selection of transformation function, use of early stopping, number of neurons, etc. One key work is to develop an effective way of assessing the ANN performance to suit the specific purpose of predicting P-h curves to overcome the problem of nonuniqueness of polynomial curve fitting. These works will provide a framework helping the development of inverse methodology and computer program, the results of which are to be presented in Chapter 4.

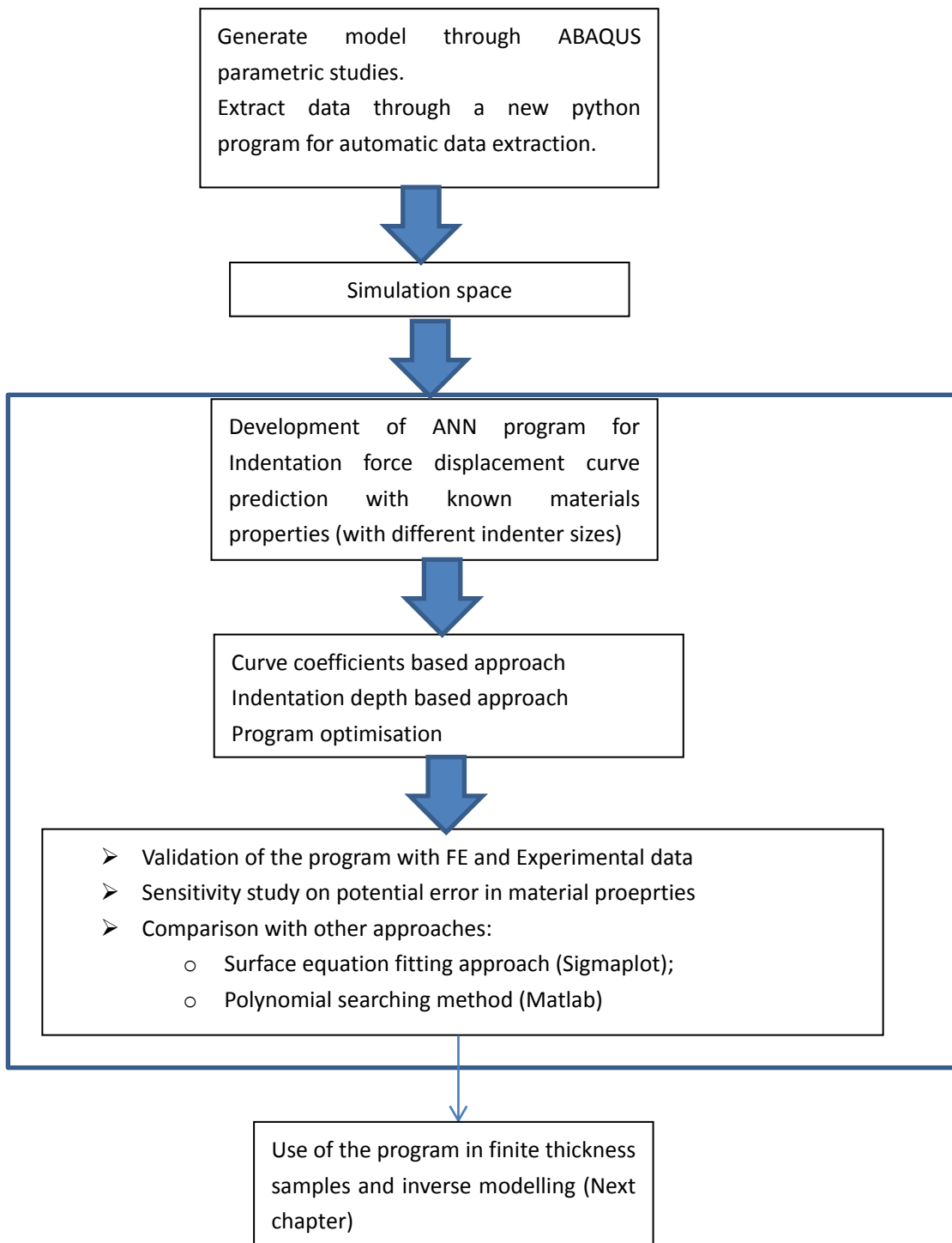


Figure 3.5 Flow chart to show the research structure and programming to predict the indentation force displacement curve under different conditions.

3.3.2 The structure of the ANNs and input/out data for indentation P-h curves prediction.

Figure 3.6 shows the general structure of the ANN program used in the work. The program used the back-propagation learning method, which is applicable to a multilayer network that uses differentiable activation functions and supervised training. The optimization procedure in the program is based on Levenberg–Marquardt (L–M) algorithm that adjusts weights to reduce the system error or cost function (Esfahani et al, 2009). As illustrated in the figure, the forward connections are used for both the learning and the operational phases, while the backward linkages are used only for the learning phase. Each training pattern is propagated forward layer by layer until an output pattern is computed. The computed output is then compared to a desired or target output and an error value is determined. The errors are then used as inputs to feedback connections from which adjustments are made to the synaptic weights layer by layer in a backward direction.

The input to the ANN are the material properties (μ and α), the output are the P-h curve in two different forms (either curve fitting coefficient for the trend line method or as for the different depth in the depth method). As schematically shown in Figure 3.7, two approaches have been analysed and their feasibilities for the material models used in this work were assessed. As illustrated in the figure, the two approaches were designated as trendline method and depth method and, respectively. In the point method, the indentation was divided into discrete points and the force and displacement for each point were used as an individual input. While for the trend line method, the whole curve was fitted with a second order polynomial line and each indentation curve was represented by the coefficients ‘a2’ and ‘a1’. Figure 3.8 shows the structure of the multilayer layer feed-forward neural network for trend line method (a) and point method (b). In the ANN for each case, there were three layers in the neural networks: input layer hidden layer and output layer. The main difference was the output data and the neuron numbers. The point method used force at different depth data; the trend line one used the coefficients of the trend line. The depth method has more input neurons (each curve represent by n points) than the trend line method (represent by number of coefficient).

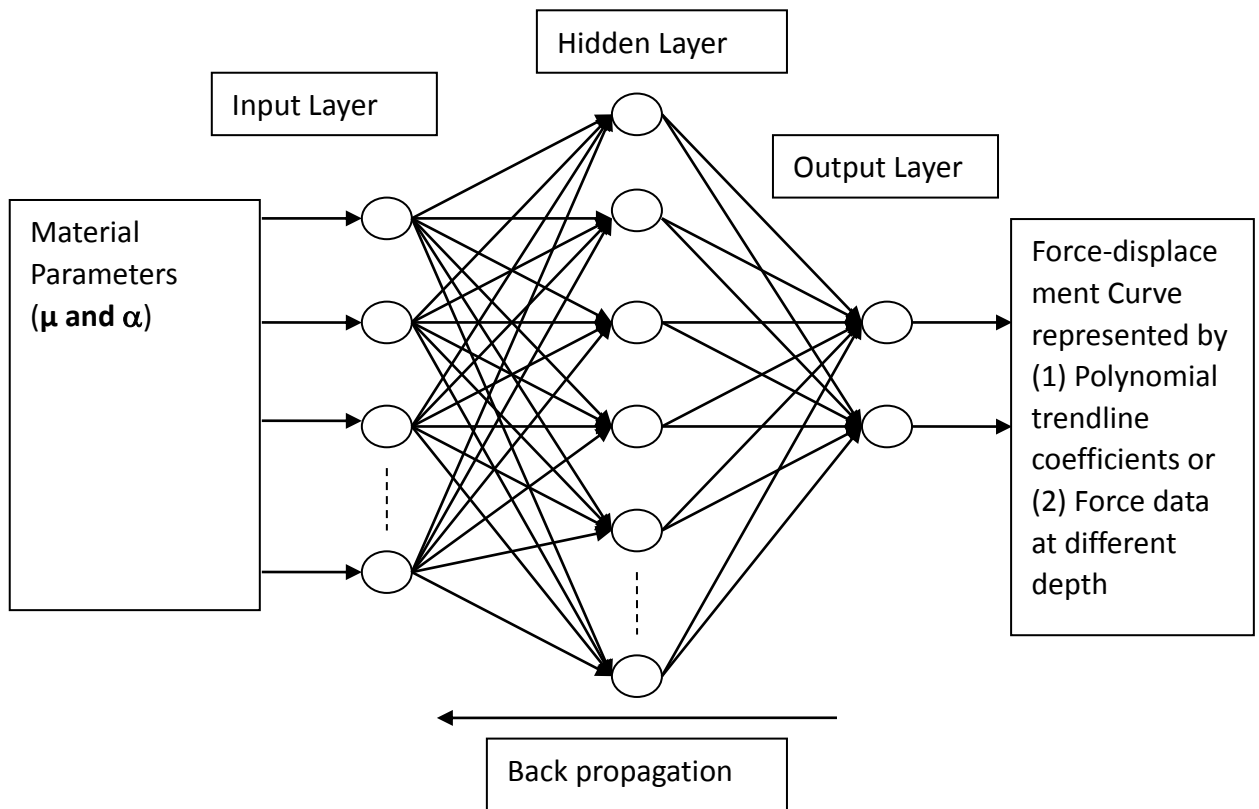


Figure 3.6 Proposed feed-forward neural network with back propagation Algorithm for predicting the indentation force-displacement data based on material parameters (μ and α).

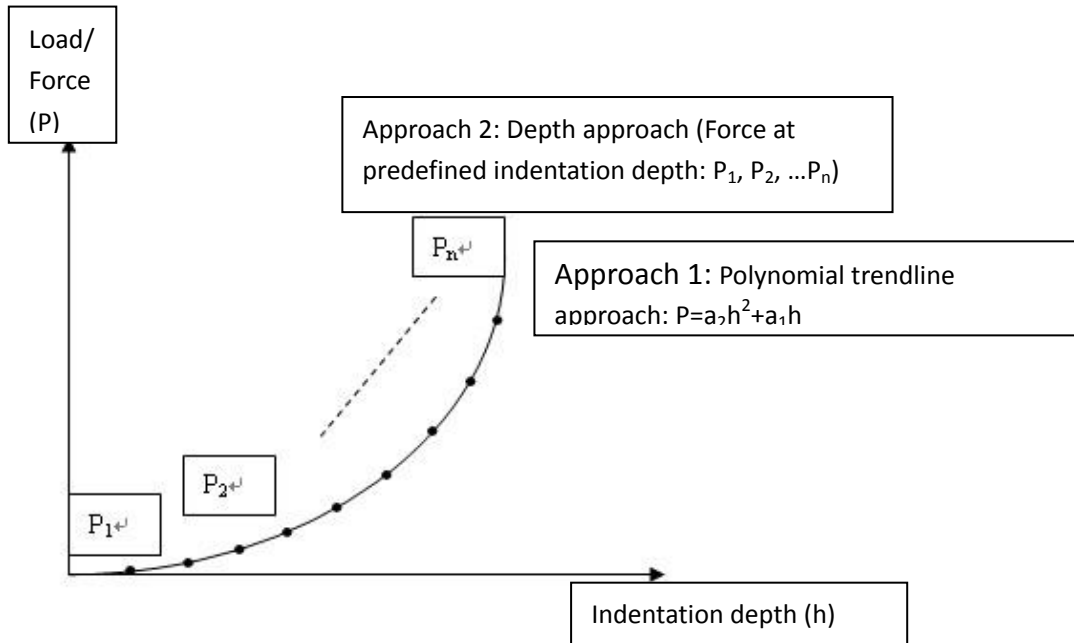
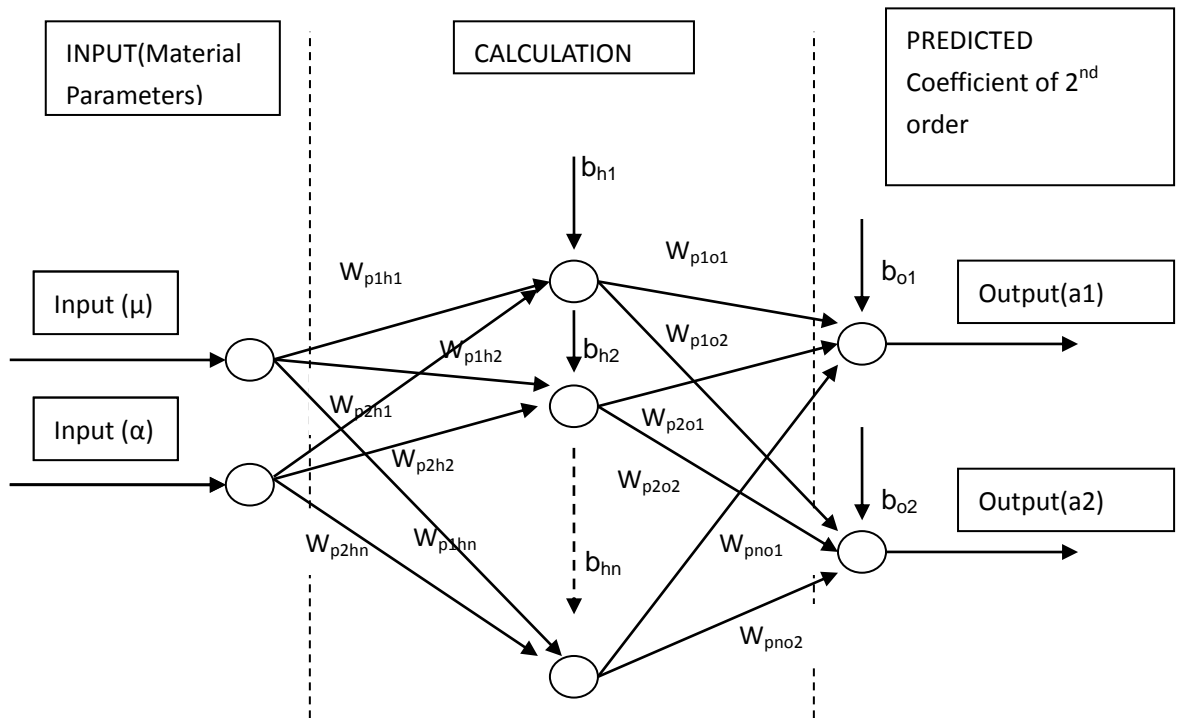
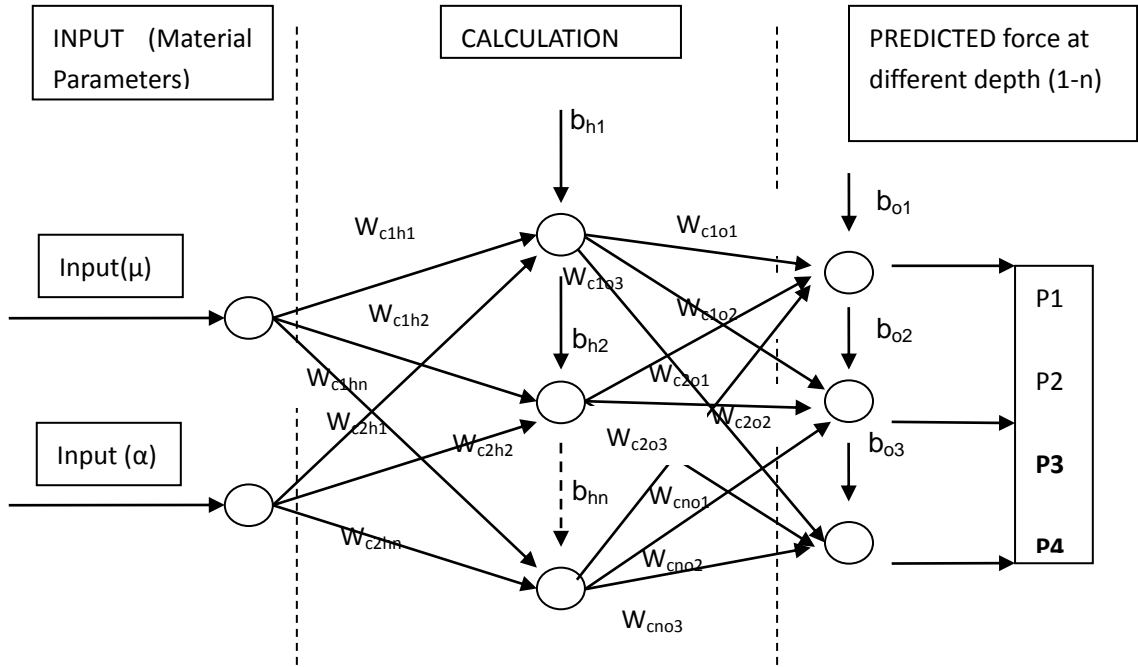


Figure 3.7 Schematic to show the two different approaches to process the indentation curves for the ANN (Approach 1: Depth approach; Approach 2: Trendline approach).



(a) The schematic diagram of multilayer neural network for trendline approach.



(b) The schematic diagram of multilayer neural network for the depth based method.

Figure 3.8 The structure of the multilayer neural networks for the Coefficient approach (2nd order polynomial) and depth approach

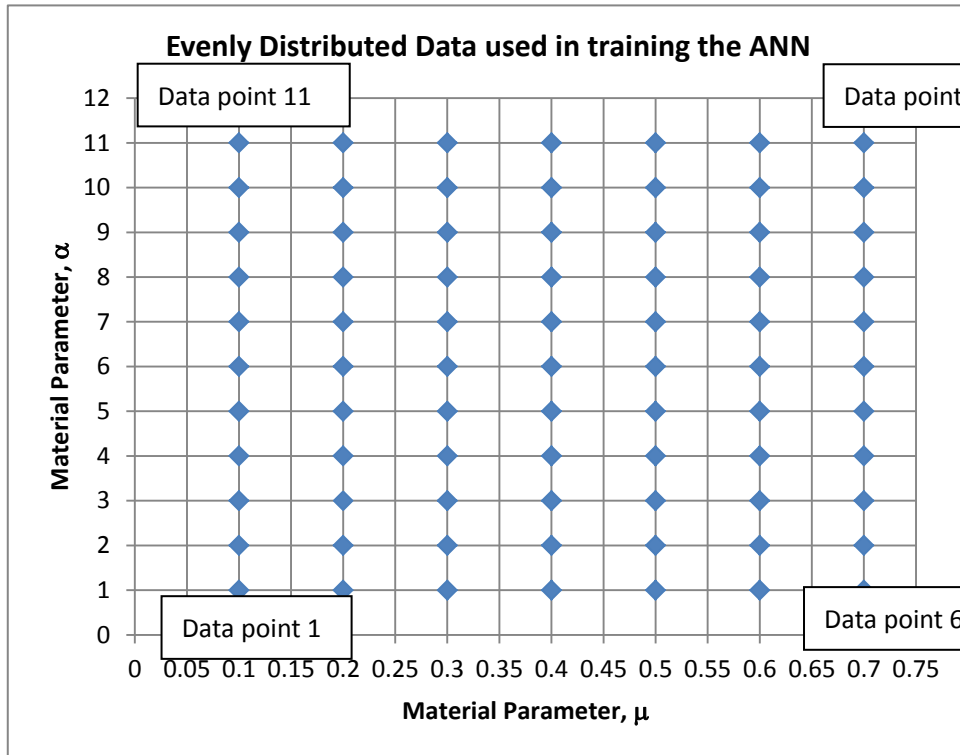
3.3.3 Development of data space for ANN training, testing and validation.

Figure 3.9 shows the main data sets used for training, validation and testing the ANNs. These data were obtained through finite element analyses encompassing a domain with α ranging between 1 and 11 and μ varying between 0.1 and 0.7. Figure 3.9(a) shows the data set of evenly distributed data with μ changed from 0.1 to 0.7, alpha changed from 1 to 11, in total 77 data points (designated as Material Data Set-1). The detailed parameter values are listed in Table 3.3. Figure 3.9(b) illustrate a set of data with progressive increase in percentage, with μ ranging from 0.1 to 0.7 and α ranging from 1 to 11, again 77 data being designated as Material data set-2.). As shown in table 3.3, The way the percentage is designed so the data set will have similar range and number of data as Mat set-1. Figure 3.9(c) illustrates a set of data similar to Material data set-1 with μ from 0.15 to 0.75, α from 1.5 to 11.5. As shown in Table 3.3, the difference between Material data set-1 and material data set-3 is '0.05' for μ and 0.5 for α . Material data set-1 is to be used as the main training and validation data, the ANN is then assessed by using Materials dataset-2 and 3 as the testing data. These will provide data to systematically assess the performance of the ANN rather than using limited property data, which may miss some key results. Detailed values of the three data sets are listed in Table 3.3, which is useful/required for checking the data properties when interpreting the error data presented in the next few sections.

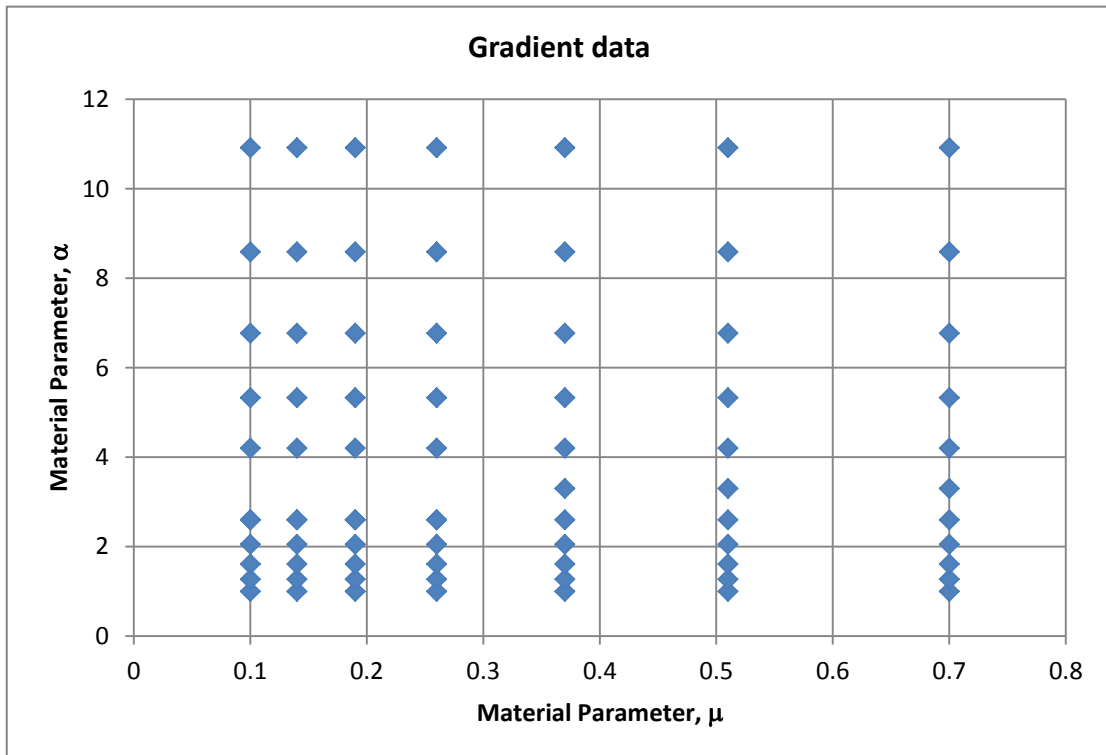
Figure 3.10 (a&b) shows some typical curves and trendlines. It is clearly shown that all the curves can be closely fitted by second order polynomial curve. Figure 3.10(c) plots the correlation coefficients for material data set -1, it is shown that all data can be fitted with 2nd order polynomial curves (also called a degree 2 polynomial, or quadratic) with the correlation coefficient over 98.5%. Curve fitting work has been performed on material data including sets 1, 2&3, generating a total of 231 P-h curves, similar level of correlation was observed for all curves. This suggests that 2nd order polynomial fitting is sufficient to represent the data with the two parameters 'a₁' and 'a₂'. Higher order fitting (3rd order) has been tried, it increased the fitting correlation coefficients slightly but it would have made the ANN more complex.

Table 3.3 Material parameters of the material data sets.

| | | Material data set 1 (Training data) | | | | | Material data set 2 (Test data) | | | | | | | | |
|-----|-------|-------------------------------------|-------|-------|-----|-------|---------------------------------|-------|-------|-----|-------|----------|-----|-------|----------|
| No. | μ | α | a_1 | a_2 | No. | μ | α | a_1 | a_2 | No. | μ | α | No. | μ | α |
| 1 | 0.1 | 1 | 0.90 | 0.20 | 40 | 0.5 | 6 | 2.45 | 0.61 | 1 | 0.1 | 1 | 40 | 0.37 | 3.3 |
| 2 | 0.2 | 1 | 1.49 | 0.47 | 41 | 0.6 | 6 | 2.84 | 0.77 | 2 | 0.14 | 1 | 41 | 0.51 | 3.3 |
| 3 | 0.3 | 1 | 1.81 | 0.81 | 42 | 0.7 | 6 | 3.25 | 0.92 | 3 | 0.19 | 1 | 42 | 0.7 | 3.3 |
| 4 | 0.4 | 1 | 2.12 | 1.18 | 43 | 0.1 | 7 | 0.68 | 0.07 | 4 | 0.26 | 1 | 43 | 0.1 | 4.2 |
| 5 | 0.5 | 1 | 2.44 | 1.54 | 44 | 0.2 | 7 | 1.18 | 0.15 | 5 | 0.37 | 1 | 44 | 0.14 | 4.2 |
| 6 | 0.6 | 1 | 2.74 | 1.90 | 45 | 0.3 | 7 | 1.59 | 0.27 | 6 | 0.51 | 1 | 45 | 0.19 | 4.2 |
| 7 | 0.7 | 1 | 3.07 | 2.27 | 46 | 0.4 | 7 | 1.98 | 0.40 | 7 | 0.7 | 1 | 46 | 0.26 | 4.2 |
| 8 | 0.1 | 2 | 0.94 | 0.16 | 47 | 0.5 | 7 | 2.34 | 0.54 | 8 | 0.1 | 1.27 | 47 | 0.37 | 4.2 |
| 9 | 0.2 | 2 | 1.47 | 0.38 | 48 | 0.6 | 7 | 2.72 | 0.68 | 9 | 0.14 | 1.27 | 48 | 0.51 | 4.2 |
| 10 | 0.3 | 2 | 1.84 | 0.66 | 49 | 0.7 | 7 | 3.08 | 0.82 | 10 | 0.19 | 1.27 | 49 | 0.7 | 4.2 |
| 11 | 0.4 | 2 | 2.19 | 0.96 | 50 | 0.1 | 8 | 0.65 | 0.06 | 11 | 0.26 | 1.27 | 50 | 0.1 | 5.33 |
| 12 | 0.5 | 2 | 2.53 | 1.27 | 51 | 0.2 | 8 | 1.11 | 0.14 | 12 | 0.37 | 1.27 | 51 | 0.14 | 5.33 |
| 13 | 0.6 | 2 | 2.88 | 1.58 | 52 | 0.3 | 8 | 1.51 | 0.24 | 13 | 0.51 | 1.27 | 52 | 0.19 | 5.33 |
| 14 | 0.7 | 2 | 3.25 | 1.88 | 53 | 0.4 | 8 | 1.88 | 0.36 | 14 | 0.7 | 1.27 | 53 | 0.26 | 5.33 |
| 15 | 0.1 | 3 | 0.88 | 0.13 | 54 | 0.5 | 8 | 2.22 | 0.49 | 15 | 0.1 | 1.61 | 54 | 0.37 | 5.33 |
| 16 | 0.2 | 3 | 1.44 | 0.30 | 55 | 0.6 | 8 | 2.58 | 0.61 | 16 | 0.14 | 1.61 | 55 | 0.51 | 5.33 |
| 17 | 0.3 | 3 | 1.83 | 0.54 | 56 | 0.7 | 8 | 2.94 | 0.74 | 17 | 0.19 | 1.61 | 56 | 0.7 | 5.33 |
| 18 | 0.4 | 3 | 2.21 | 0.79 | 57 | 0.1 | 9 | 0.59 | 0.06 | 18 | 0.26 | 1.61 | 57 | 0.1 | 6.77 |
| 19 | 0.5 | 3 | 2.59 | 1.04 | 58 | 0.2 | 9 | 1.04 | 0.13 | 19 | 0.37 | 1.61 | 58 | 0.14 | 6.77 |
| 20 | 0.6 | 3 | 2.97 | 1.29 | 59 | 0.3 | 9 | 1.42 | 0.22 | 20 | 0.51 | 1.61 | 59 | 0.19 | 6.77 |
| 21 | 0.7 | 3 | 3.37 | 1.55 | 60 | 0.4 | 9 | 1.74 | 0.34 | 21 | 0.7 | 1.61 | 60 | 0.26 | 6.77 |
| 22 | 0.1 | 4 | 0.84 | 0.10 | 61 | 0.5 | 9 | 2.10 | 0.45 | 22 | 0.1 | 2.05 | 61 | 0.37 | 6.77 |
| 23 | 0.2 | 4 | 1.39 | 0.24 | 62 | 0.6 | 9 | 2.45 | 0.57 | 23 | 0.14 | 2.05 | 62 | 0.51 | 6.77 |
| 24 | 0.3 | 4 | 1.81 | 0.43 | 63 | 0.7 | 9 | 2.80 | 0.68 | 24 | 0.19 | 2.05 | 63 | 0.7 | 6.77 |
| 25 | 0.4 | 4 | 2.21 | 0.64 | 64 | 0.1 | 10 | 0.56 | 0.06 | 25 | 0.26 | 2.05 | 64 | 0.1 | 8.59 |
| 26 | 0.5 | 4 | 2.60 | 0.85 | 65 | 0.2 | 10 | 0.96 | 0.13 | 26 | 0.37 | 2.05 | 65 | 0.14 | 8.59 |
| 27 | 0.6 | 4 | 3.00 | 1.06 | 66 | 0.3 | 10 | 1.33 | 0.21 | 27 | 0.51 | 2.05 | 66 | 0.19 | 8.59 |
| 28 | 0.7 | 4 | 3.38 | 1.28 | 67 | 0.4 | 10 | 1.64 | 0.32 | 28 | 0.7 | 2.05 | 67 | 0.26 | 8.59 |
| 29 | 0.1 | 5 | 0.78 | 0.08 | 68 | 0.5 | 10 | 1.98 | 0.42 | 29 | 0.1 | 2.6 | 68 | 0.37 | 8.59 |
| 30 | 0.2 | 5 | 1.34 | 0.20 | 69 | 0.6 | 10 | 2.31 | 0.53 | 30 | 0.14 | 2.6 | 69 | 0.51 | 8.59 |
| 31 | 0.3 | 5 | 1.75 | 0.36 | 70 | 0.7 | 10 | 2.64 | 0.63 | 31 | 0.19 | 2.6 | 70 | 0.7 | 8.59 |
| 32 | 0.4 | 5 | 2.16 | 0.53 | 71 | 0.1 | 11 | 0.51 | 0.06 | 32 | 0.26 | 2.6 | 71 | 0.1 | 10.92 |
| 33 | 0.5 | 5 | 2.55 | 0.71 | 72 | 0.2 | 11 | 0.89 | 0.13 | 33 | 0.37 | 2.6 | 72 | 0.14 | 10.92 |
| 34 | 0.6 | 5 | 2.94 | 0.90 | 73 | 0.3 | 11 | 1.25 | 0.21 | 34 | 0.51 | 2.6 | 73 | 0.19 | 10.92 |
| 35 | 0.7 | 5 | 3.33 | 1.08 | 74 | 0.4 | 11 | 1.59 | 0.29 | 35 | 0.7 | 2.6 | 74 | 0.26 | 10.92 |
| 36 | 0.1 | 6 | 0.74 | 0.07 | 75 | 0.5 | 11 | 1.89 | 0.40 | 36 | 0.1 | 2.6 | 75 | 0.37 | 10.92 |
| 37 | 0.2 | 6 | 1.25 | 0.17 | 76 | 0.6 | 11 | 2.20 | 0.50 | 37 | 0.14 | 2.6 | 76 | 0.51 | 10.92 |
| 38 | 0.3 | 6 | 1.68 | 0.31 | 77 | 0.7 | 11 | 2.49 | 0.60 | 38 | 0.19 | 2.6 | 77 | 0.7 | 10.92 |
| 39 | 0.4 | 6 | 2.06 | 0.46 | | | | 2.45 | 0.61 | 39 | 0.26 | 2.6 | | | |



(a) Materials data set-1 (μ and α) used generate the training and validation data. The number and arrow shows numbering system used. The data is evenly distributed. Detailed values and numbering can be found in Table 3.3.



(b) Materials data set-2 (μ and α) used in the training and testing data. Detailed values and numbering can be found in Table 3.3.

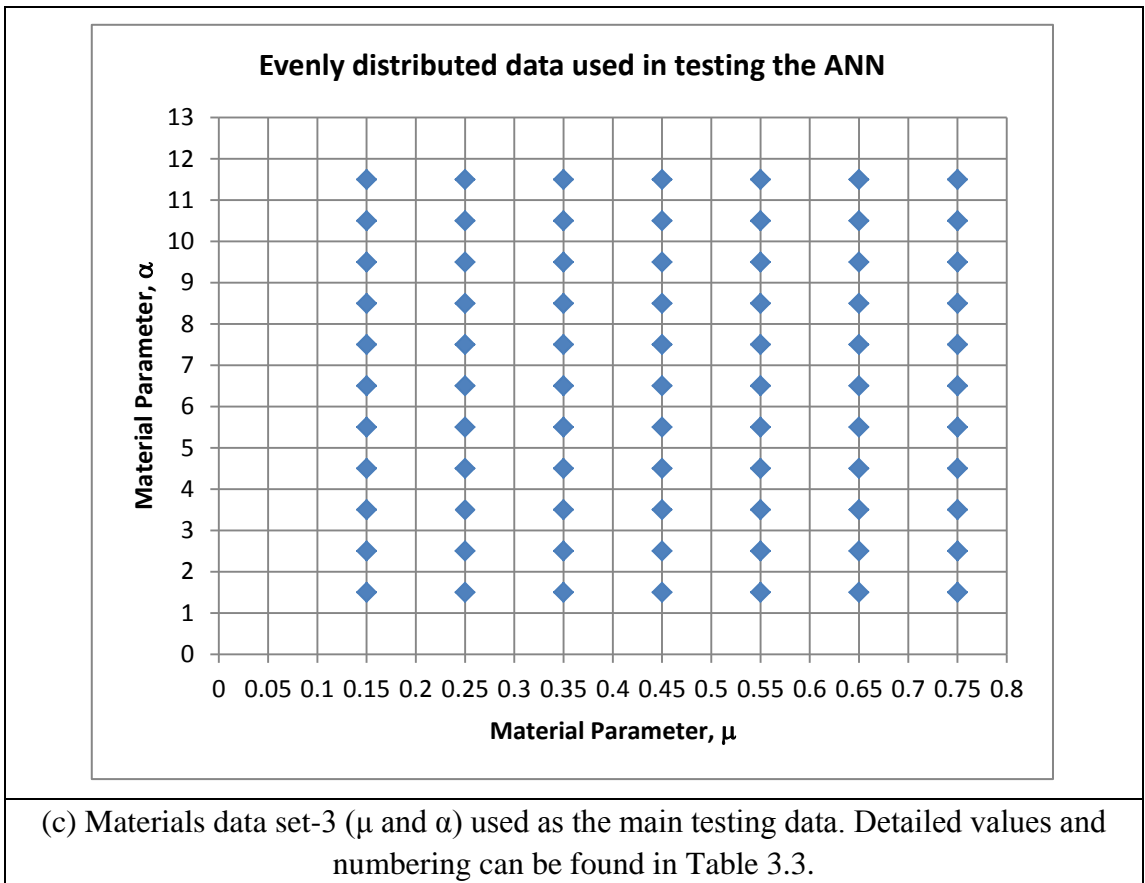
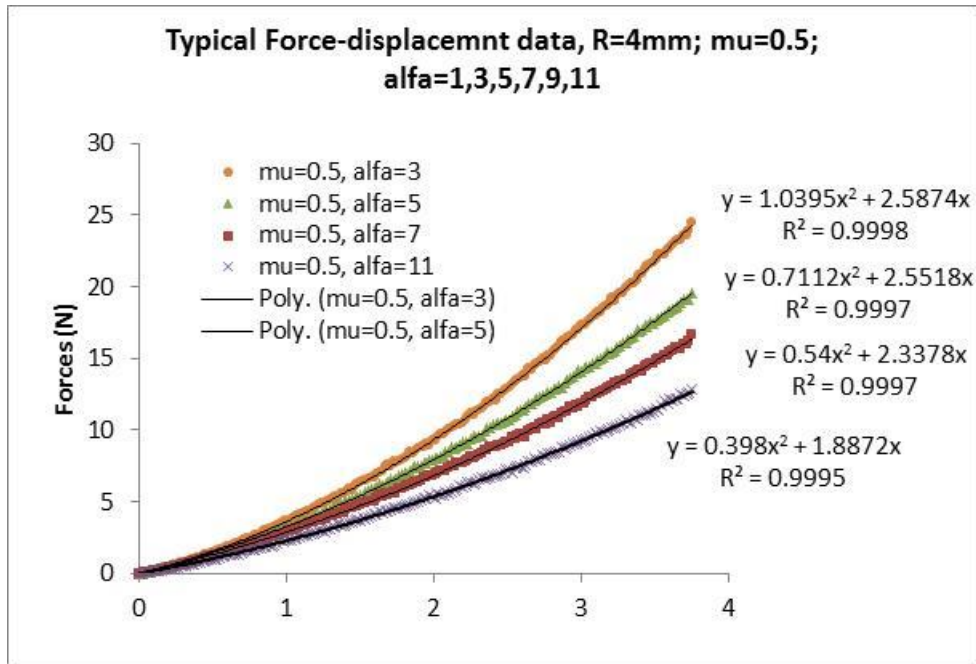
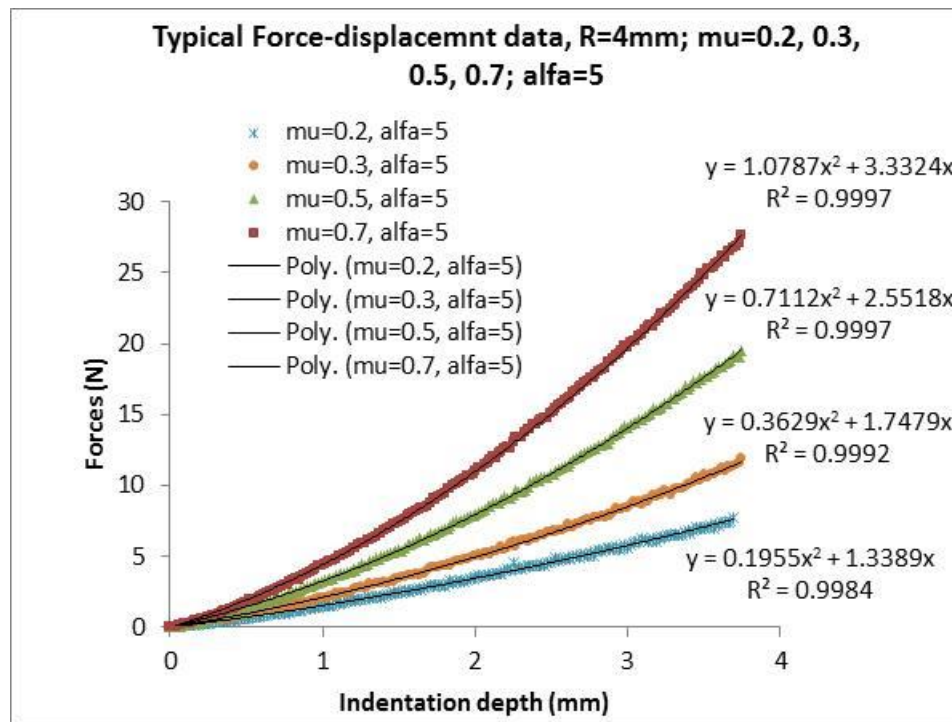


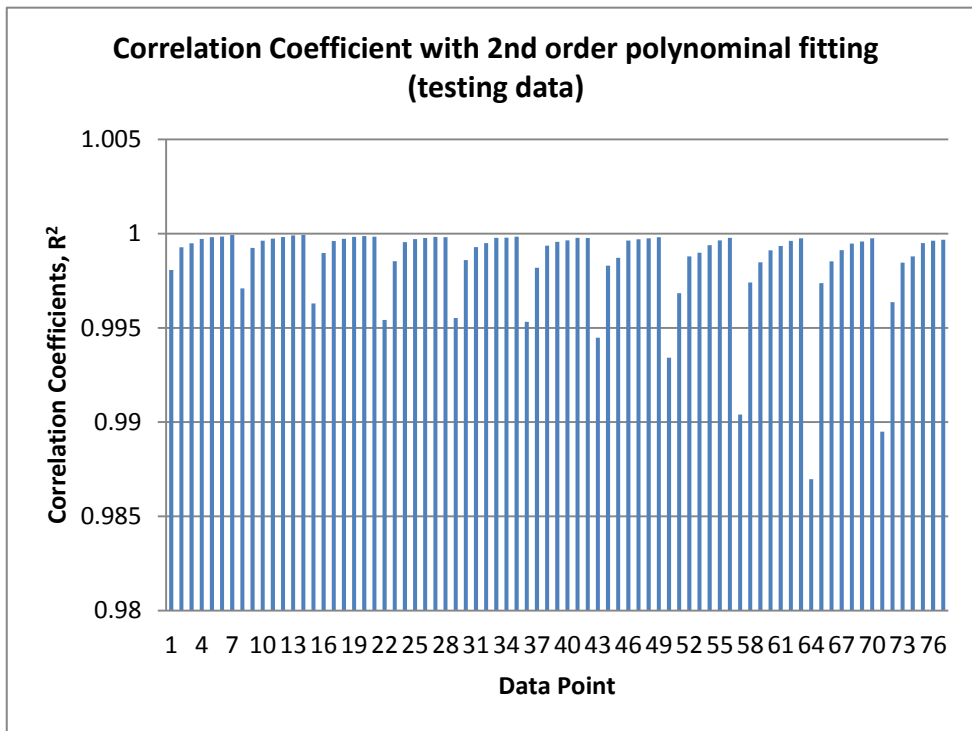
Figure 3.9 The data matrix of training and testing data for the ANN program.



(a) Typical FE indentation data and curve fitting, $\mu=0.5$, $\alpha=3, 5, 7, 11$;



(b) Typical FE indentation data and curve fitting, $\mu=0.5$, $\alpha=3, 5, 7, 11$;



(c) Correlation coefficients of with 2nd order polynomial fitting of material data set 1 (Figure 3.10a, evenly distributed data as in Figure 3.9(a)).

Figure 3.10 Typical FE indentation data and curve fitting with 2nd order polynomial trendline.

3.3.4 Optimisation of the activation functions, number of neurons and development of early stopping mechanisms

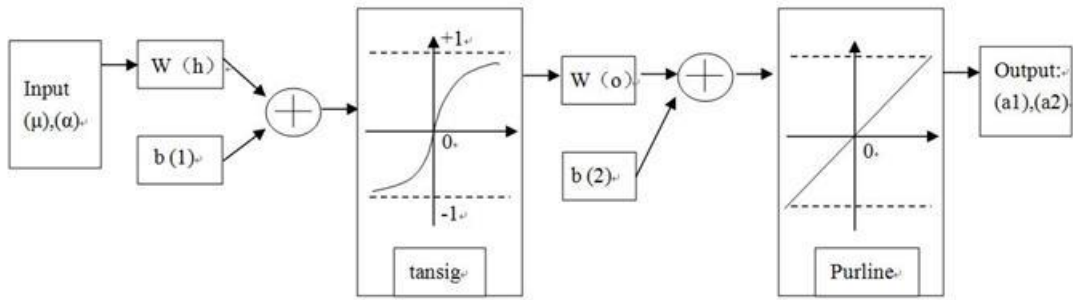
The effectiveness of the ANN is directly affected by the activation functions, number of neurons and the stopping criterions. These were assessed using the corresponding mean square of the network errors (MSE) calculated by

$$MSE = \frac{1}{N} \sum_{i=1}^N (t_k - a_k)^2 \quad (3.1)$$

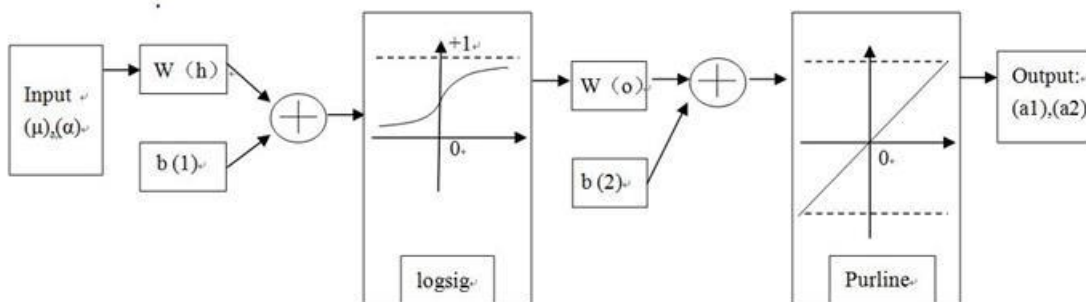
where N is the total number of training data, t_k is the target/desired value, and a_k is the network output value. This has been used to determine the optimal conditions for the ANNs for extracting material parameters from indentation tests. Figure 3.11 shows the training and validation curves based on different activation functions in the hidden and outer layer. Among the four activation function (Figure 2.12), the hard limit activation is not suitable as it generates an output of '0' or '1'. The linear function in the output layer was chosen since, when a regression problem is tackled by a neural network; all the neurons in the output layer should have a linear activation function (*Haykin, 1994*). This allows the range of the network outputs to be outside the range [0- 1] or [-1--+1] of the sigmoid function. Previously work (*Maier and Dandy, 2000; Finlay 2004*) suggested that using sigmoid-type functions in the hidden layer and linear functions in the output layer can be an advantage when it is necessary to extrapolate beyond the range of training data. This is directly relevant to the problem being investigated in this work. Figure 3.11 shows the structures with logistic (logsig) and tansig in the hidden layer and typical results for the training performance. The choice of activation function in the hidden layer (Figure 3.11(c)) showed some effect on the training process of the ANNs, but there were no major differences. Given the for a force-displacement data, the polynomial coefficient should not be negative (this is also confirmed with the curve fitting data of all three data sets) a logsig was used.

During the training process the error between the desired output and the actual output will continuously decrease until the error is close to a minimum. Ideally, the training should be stopped at the point where the error is at a minimum. However, this is not always the case

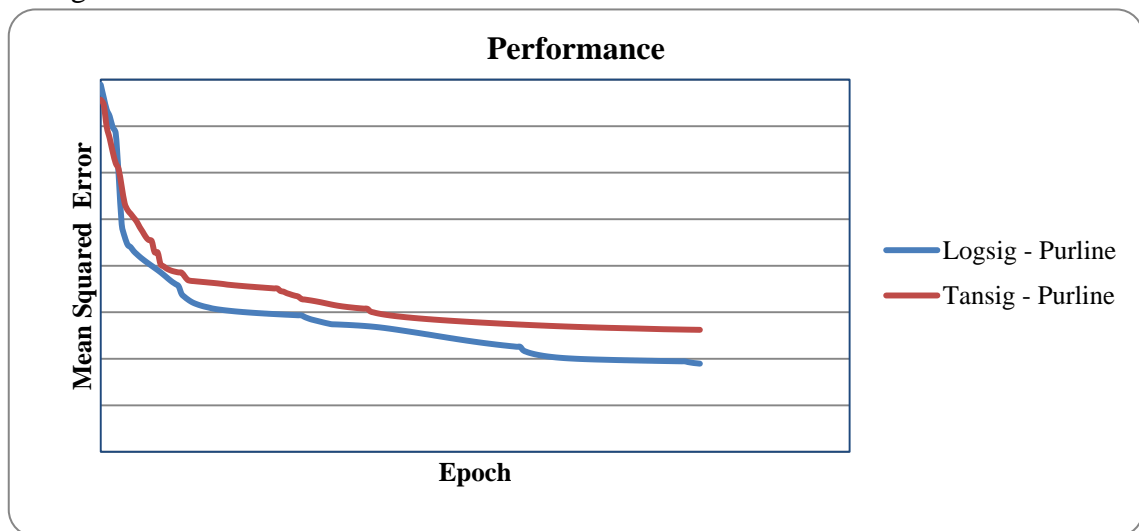
in real applications. At some point in the training the error in the test data stops falling and could even start to rise, causing over training and the network is starting to overfit. In many cases, the generalization curves could have more than one local minimum reducing the accuracy of the training and the prediction results. One way to improve this situation is to develop suitable early stopping mechanisms to ensure the training stops at a robust/stable minimum position to balance ANN performance and avoid over training. In this work, two methods have been tested/evaluated and their efficiency was compared . One method is to stop when the MSE values for training and verification, distinguished by the index T and V, respectively, are comparable, i.e. $MSE_T = MSE_V$. However, preliminary work showed that this did not always provide consistent result/accurate results. Another approach is to use a post minimal point by stopping the training process after a certain number of epochs to ensure the minimal is sustainable. In this method the training was stopped when the validation MSE start to continuously increase over several epoch. As shown in Figure 3.12(a), this validation process exhibited several increasing steps after the first local minimum and then reaches an improvement of validation set performance by second point. The result clearly showed that the new approach with defined stopping was able to accurately predict the real minimum point, therefore is much more robust than the approach which stops at the first unstable minimum point. This allows the assessment the effect of the number of neurons on the performance of the ANN more accurately.



(a) ANN program with a 'tansig' activation function in the hidden layer for the trendline fitting method.



(b) ANN program with a 'logsig' activation function in the hidden layer for the trend line fitting method.



(c) The training performance of the trend line approach with different activation functions.

Figure 3.11 Typical training curves to show the influence of different activation functions in the hidden layer. (Sample thickness $t=20\text{mm}$, $R=4\text{mm}$).

3.4 ANN prediction result with the trendline approach: Results and analysis

In the trendline based approach, the inputs are the material parameters (μ and α) and the output is the curve fitting coefficients (a_1 and a_2). A range of FE models has been conducted and the a_1 and a_2 values of the three data sets (as shown in Figure 3.9) were determined and used as training or test data. Materials data set-1 was used as the training and validation data, and materials data set-2 and set-3 as the test data; Most of the results reported is based on this case where four validation data has been picked from the dataset, 73 data was used as training data. Other format has been checked, which showed similar results. The effect of number of neuron is assessed and the ANN prediction accuracy when using trained data and untrained data as the test data is assessed.

As shown in the Figure 3.12, the training and validation data showed a similar trend. One key issue in practical application of ANN for this case is to establish a practical way to represent the performance of the ANN for the specific problem being investigated. This started with investigating the effect of neurons on the MSE of training and validation. To establish the effect of neurons on the performance of the ANN, a series of ANNs with different numbers of neuron were run multiple times and the MSE analysed and established. Figure 3.13 shows the effect of the number of neurons on the MSE. The results clearly show that the MSE is influenced by the number of neurons in the hidden layer. The best performance is found to be with the case of 20 neurons. This shows that MSE is a good indicator, however, for the problem studied in this work it will be easier to present the error in a more physically meaningful way in order to clearly tell the performance of the ANN when assessing the accuracy of the ANN tested with trained data and data not used in either the training or validation. To make it easier to understand the physically meaning in a simple way, the relative error between the predicted parameter ($'a_2'$ and $'a_1'$) and target is calculated

$$Relative\ Error = \frac{a_{Predict} - a_{Target}}{a_{Target}} \quad (3.2)$$

Figure 3.14 shows the relative error in the predicted results using the same data for ANN

training/testing (Material Data set 1) of 77 data from ANN with different neuron numbers. In all the cases, most the error level is low (within 0.05), but there are some material points with higher error values (over 0.1). To have a robust ANN for characterising materials, the maximum error value is the key to avoid causing problem even though it only appears at limited numbers. Comparing the three data, as shown in Figure (a), there are about 6 material points with error level over 10% for neuron number of 10 and relative error for one of them is over 0.2; while for Neuron number 20 (Figure (b), there is five cases of error over 10%.

For the case with neuron number of 25, there are only three data points having error over 10% but the maximum error value is much higher than the case of neuron 20. This higher error may cause problem when using the material to deal with real test data, so it is not suitable for this application.

Figure 3.15 shows the relative error of the predicted results using the data that has not been used in training (Material Data set 3) of 77 data from ANN with different neuron numbers. In all the cases, most of the error level are higher than the case for predicting trained data as shown in Figure 3.14. The case for neuron 20 is slightly better with maximum error within 15% but there are still a few data with error level over 10%. In the case of neuron=10, the error for several material point are above 20%. In the case of the neuron=25, the maximum error become as high as 100%.

Another key issue needs to be evaluated/established is the repeatability of the prediction as each ANN may randomly produce different output for the same input in different ANN simulation/test. The range of variation could be critical to the reliability/stability of the system. This can be assessed by re-running of the ANN (each run is a new simulation, the weighting values for previous ANN simulation is cleared by the program automatically). Figure 3.16 shows some typical examples showing the relative error of ANN simulation with neuron number of 20 (which shows the lower error from the study on the effects of neuron numbers). As shown in Figure 3.16, the predicted results showed a similar value range, but there is clear variation between each ANN test. Most of these tests have a few

material points with error over 10%. To further investigate the implication of this variation, repeatability of the ANN simulation was further evaluated by doing 5 tests for each neuron numbers, then the average relative error and maximum error values were determined, the results are shown in Figure 3.17. All the five tests were run under identical condition with the same input; the value represents the average value and the error bar for the maximum error value. The maximum error is used rather than the standard deviation, as this will show the worst case even though it only occurs once. This is important for material tests to eliminate any possible mis-prediction. As shown in the figure, in both cases, most of the average values are relatively low within 5%, but in the case of neuron 10, there are several data have error between 5%-10% and as indicated by the error bar, there are more data point with high error values than the case for ANN with neuron number of 20. This suggests that the approach using average data potentially could improve the ANN prediction accuracy when using un-trained data.

For the material problem being investigated, the relative error of the curve fitting coefficients is a better indication than the MSE as it is more relevant to the parameters associated with the P-h curves. It can directly tell how close the curve parameter to the corresponding target. But one problem with polynomial fitting is that the two parameters may have different effects on the curve, so it is still could not directly represent the accuracy of the indentation force displacement curve. a_1' and a_2' influence the curve in different way and it is known that the values of the curve fitting parameters are not unique. How this may affect the indentation force-displacement curve needs to be established. One way is to use the predicted curve fitting data to predict the force values, then use the comparison between the forces at some selected depth as the performance criterion. Further analysis is made to direct compare the indentation force displacement data based on the predicted values of a_1 and a_2 . With a given pair of polynomial coefficients predicted from ANN, the force displacement data (at selected depth) can be calculated, then the difference between the curve produced and the target curve using objective function:

$$G = \frac{\sum_{i=1}^N \left(\frac{F_{Ann} - F_{Target}}{F_{Target}} \right)}{N} \quad (3.3)$$

Where N is the indentation depth data, F_{Ann} is the force at an indentation depth point based on the curve fitting parameters (a2 and a1) predicted from ANN (averaged over 5 ANN tests), F_{Target} is the force data based on the original FE simulation. Relative error is used as it is directly more physically meaningful. In this work, 4 force depth points were used, more data point has been tried, which showed a similar results/accuracy.

Figure 3,18 (a) illustrated the process using the first five material data point of material data set-3 as example. Each bar represents the force at different indentation depth, with which the average error in the indentation force (over the four points) can be determined following Equation 3.3. The four displacement points used at 1,2,3,4 mm in depth respectively. The average error of the force over these four points are used to represent the error between ANN predicted P-h curve and the corresponding target. Figure 3.18 (b&c) shows average error in force for ANN with neuron 20 and 10, respectively. Most of the data is within 5% present, while a few data point has error values over 10%, which error value is less than that of the relative error of the a1 and a2 (the relative error of a1 and a2 could go over 20% as shown in Figure 3.17). Comparing the average value in Figure b & c, no major difference between ANN with 10 and 20 neurons. The results suggest that the average data approach is a reasonable to assess match between ANN predicted and target values. However, it can be seen on the error bars (maximum error), there are still a few data with high relative error which is not acceptable, and potentially causing problem in the reliability when using this in real material tests where the target is not known. This is to be assessed by looking at the frequency of occurrence for each ANN test data. Any ANN system (e.g. neuron number) which less likely produce prediction with high error will be a more reliable one.

The frequency is calculated following equation:

$$Frequency = \frac{\text{number of material data with erro lower that upper limit}}{\text{total number of data}} \quad (3.4)$$

The result is shown in Figure 3.19. The vertical axis represents the percentage of data which will fall within a certain error range for each ANN test. As shown in the Figure, in the case of 20 neurons, over 90% prediction is within 5% error, 95% prediction within 10% and almost 100% predicted data is within 12%. The case for Neuron 10 (curves in blue) is slightly different, it showed more scatter in the data but it is almost 100% within 12%. Frequency analysis has been conducted on more data, the trend is similar and the result is not shown to preserve clarity. For the test studied in this work, prediction data with 5% will be ideal, 10% error is probably acceptable given the large deformation involved in the test. This suggest that the ANN could produce accurate prediction and can be used to predicted P-h curves of hyper foam. However, it will be of significant importance to see if the prediction accuracy of the data with relatively high error could be further improved. One approach is to average the forces from multiple ANN tests; the other approach is to average the curve coefficients (a_2 and a_1). A typical example is shown in Figure 3.20. Figure 3.20(a) shows the indentation force displacement data for a selected material set with high error ($\mu=0.15$, $\alpha=7.5$, the maximum error is $\sim 12\%$, see Figure 3.18b). Figure 3.20(b) shows the comparison between force data following the two average approaches and the target data, it is clearly shown that, both averaging approach could effectively improve the ANN prediction. This is probably due the fact the ANN results is discrete rather than continuous, so the error will not frequently repeat at one data point, then more data will eventually increase the accuracy. Trials for the materials set showed that repeating 5 times is able to produce reliable data.

The approach established using mat set 3 as the testing data was further applied to Material data sets-2, which is data domain with gradient increment rather than evenly spaced, but the general range is the same. In this set of data, the μ is increased by about 38% each increment and α is increased by 27% each increment. This will ensure that the data will not coincident with the training data. It is also exploring a proper way of generating data mapping through materials property domain with gradient change that can be more useful/practical in producing material database. As in many cases, it is the relative accuracy rather than absolute value in materials that is useful. This will further assess the

accuracy of the ANN program developed. Some typical results are shown in Figures 3.21-22. Figure 3.21 shows the average of curve coefficients 'a₁' and 'a₂' based on five ANN tests and the maximum and minimum values. The range of maximum error is very similar between neuron 10 and neuron 20. Figure 3.22 plots the average error and maximum values of force following equation 3.3. It clearly shows that maximum error is within 10% and most of the data is within 5%. It also shows that the data for neuron 10 has more data with higher error (over 5%) Figure 3.22(c) shows the frequency of the error ranges. In the case of neuron 20, over 95% material; dat sets reached within error of 10%, while only 85-90% reached within 10% error for neuron 10. So it is reasonable to conclude with confidence that the ANN with 20 neuron is a better choice.

Sensitivity to Error in Material properties

For assess the robustness of the program, the effect of potential error or perturbation in the material properties. A prediction results need to be able to stable without jumping with error in the input. In this process, two error (5% and 10%) were introduced in the two materials parameters (μ and α), then the property is used as input in the ANN (20 neurons) and the curve coefficients (a₁ an d₂) is predicted, which then used to calculate the change of the force displacement data based properties with certain error/perturbation. A typical example is shown in Figure 3.23. The P-h curve changed to a certain extent but no significant move away from the target. This shows that the approach is robust.

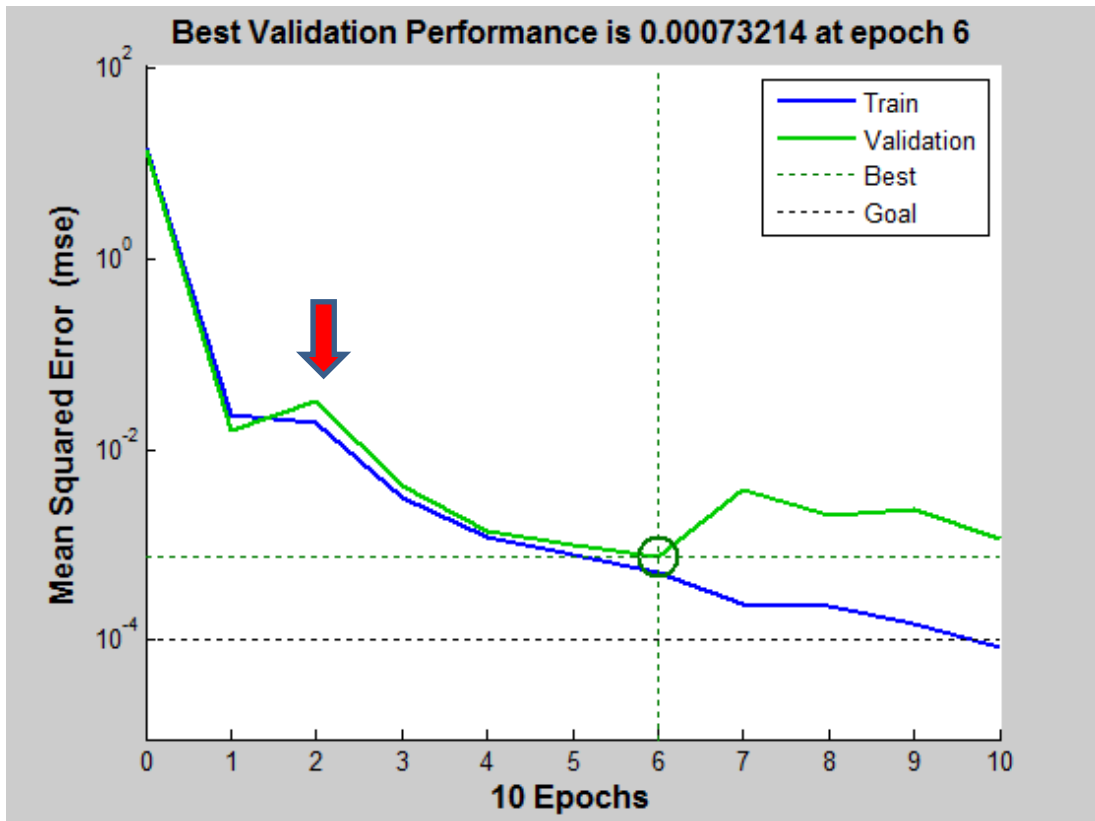


Figure 3.12 Typical ANN training and validation curve with early stopping (trendline approach, material data set-1, R4mm). The first dipping (labelled with the arrow) shows the effect of the setting of early stopping.

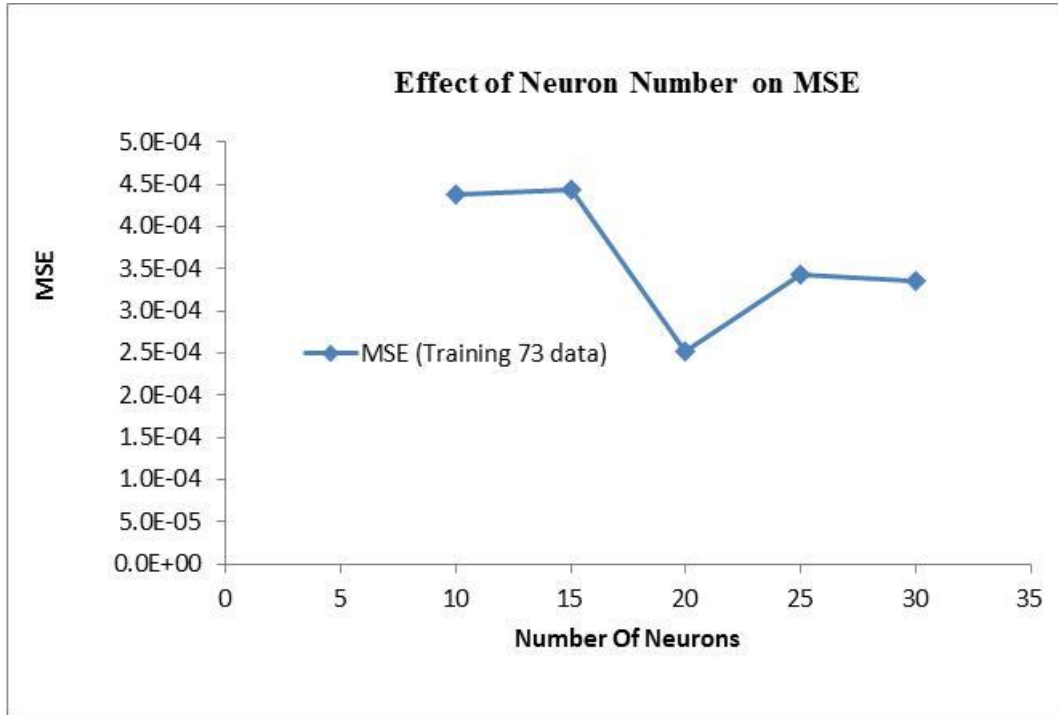


Figure 3.13 MSE for training and validation showing the effect of the number of neurons (material data set-1, Figure 3.9(a)). (Early stopping set at 6 epochs in the program)

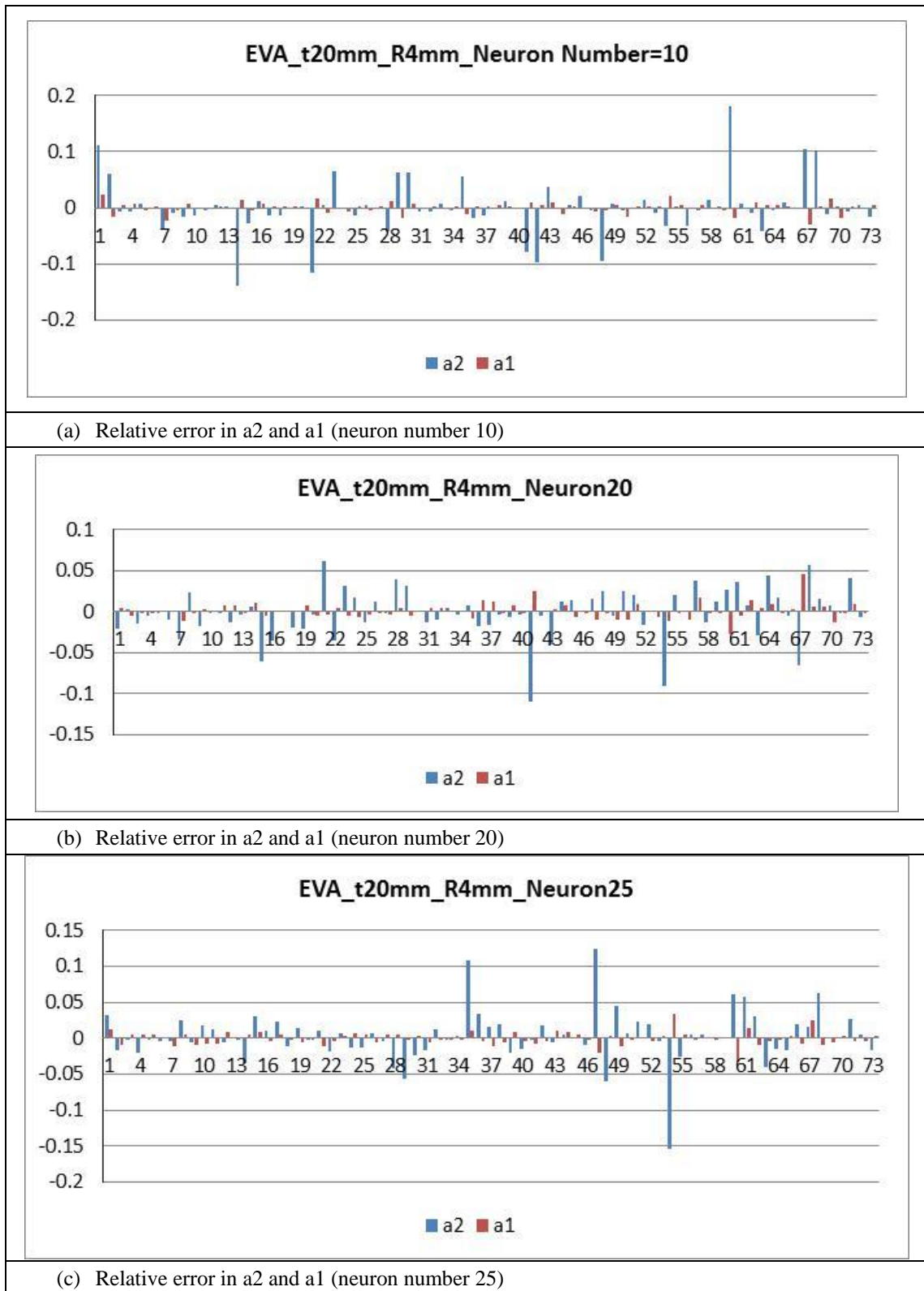
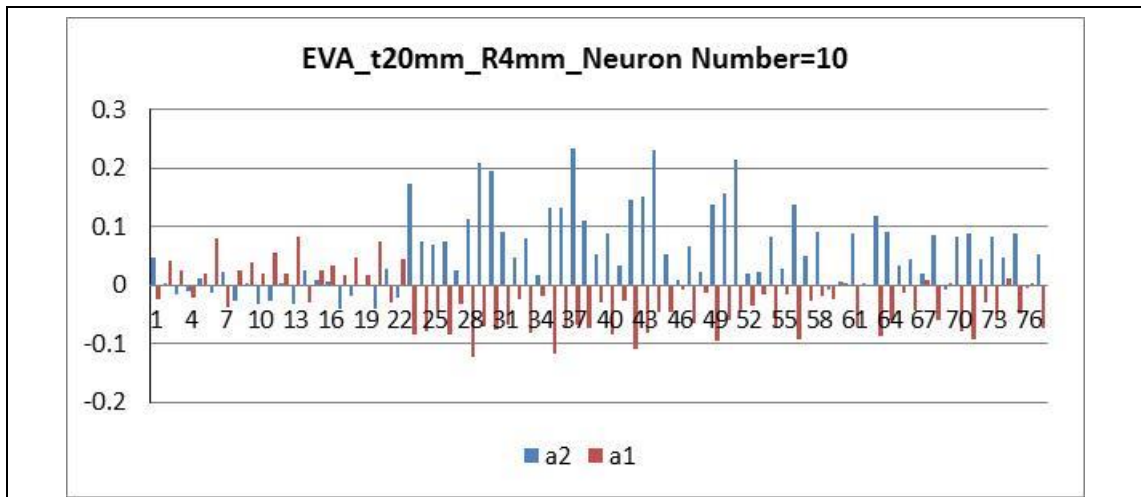
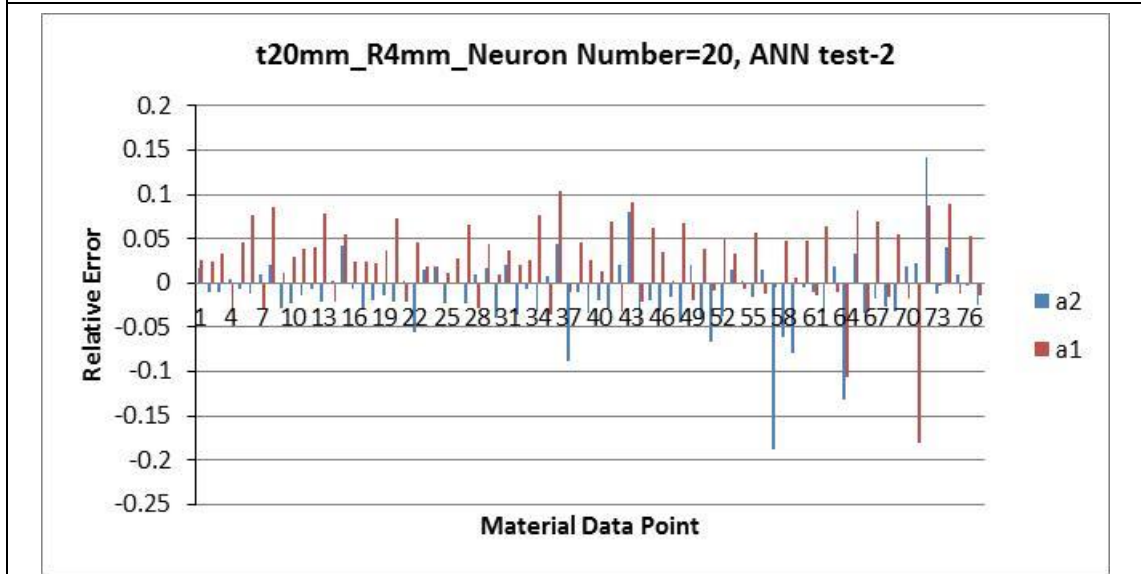


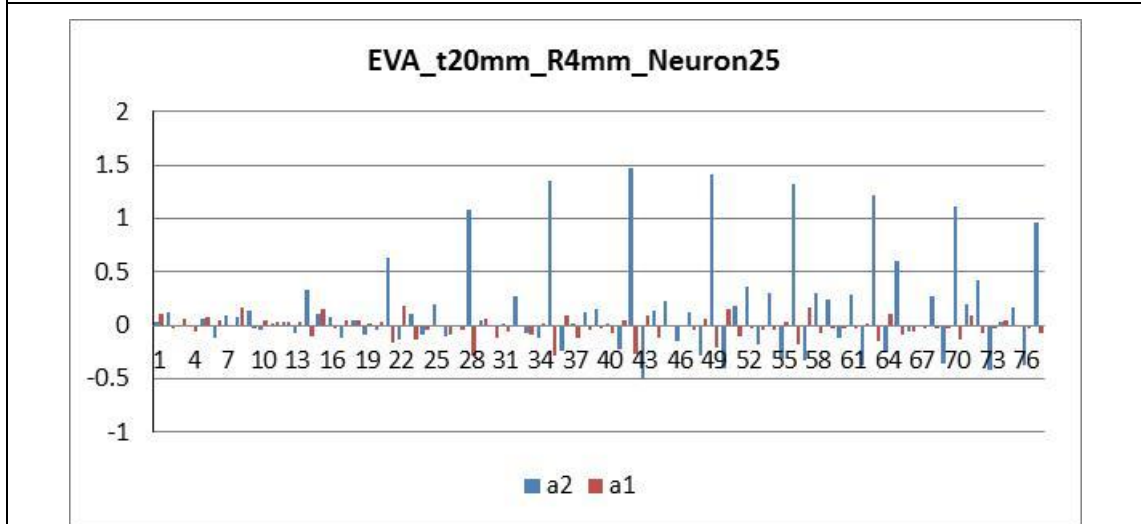
Figure 3.14 Error of the 2nd and 1st order fitting coefficient (a_2 and a_1) using the training data (Material data set-1) as test data.



(a) Relative error in a2 and a1 (neuron number 10)

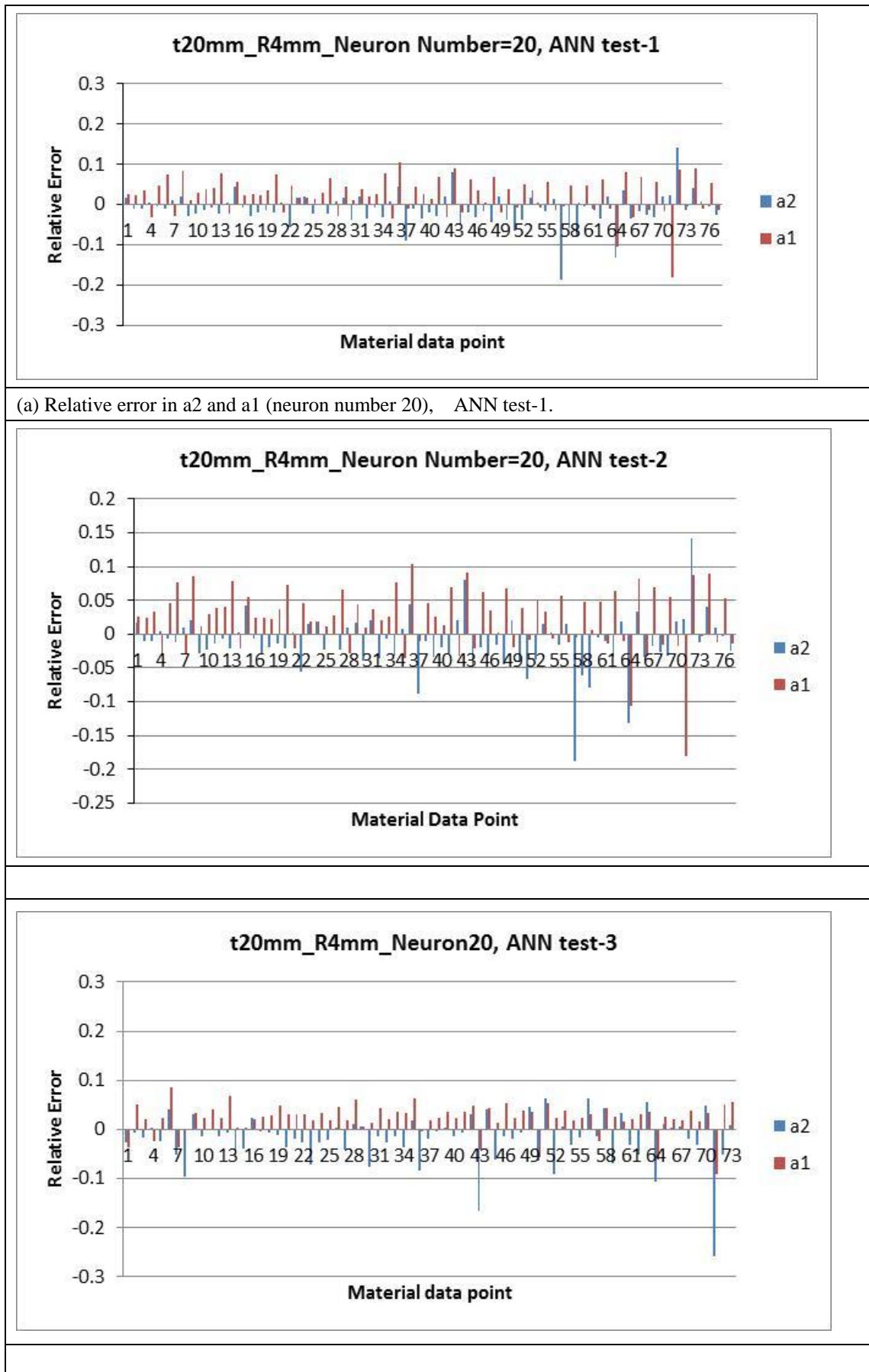


(b) Relative error in a2 and a1 (neuron number 20)



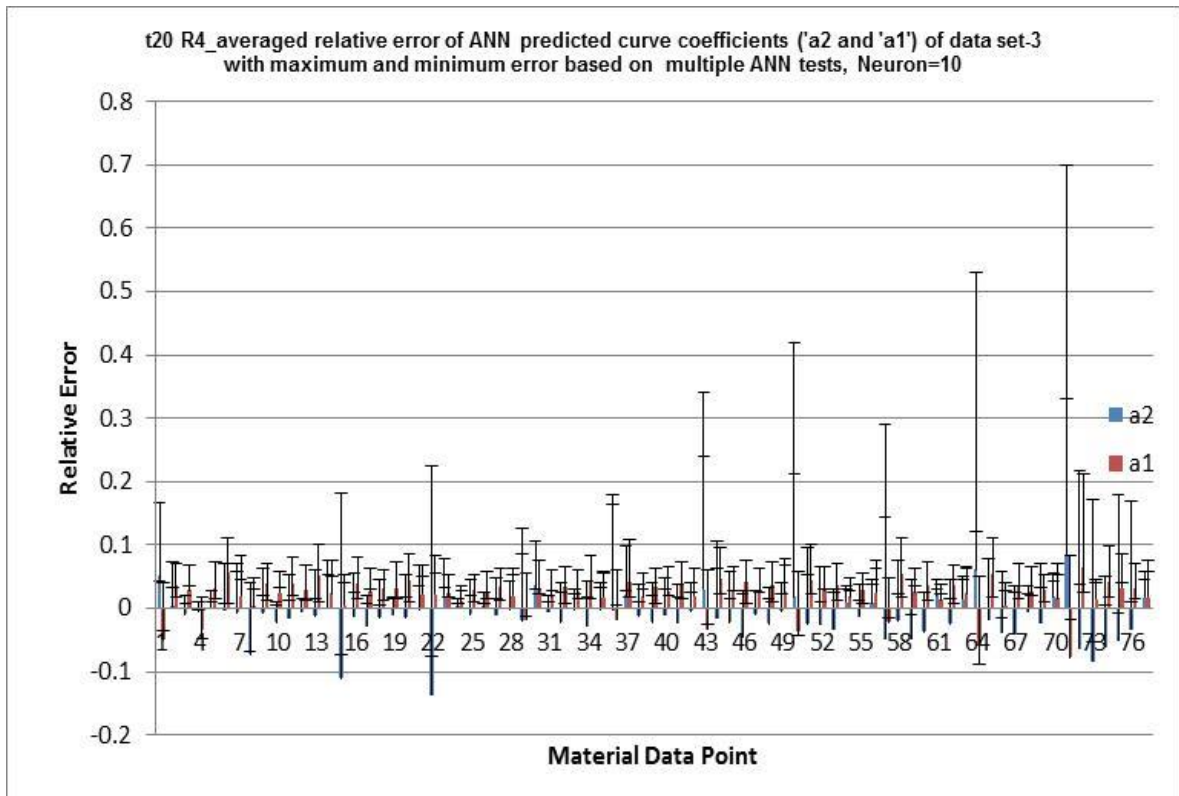
(c) Relative error in a2 and a1 (neuron number 25)

Figure 3.15 Typical Error of the 2nd and 1st order coefficient using the un-trained data (Mat data set3) as test data.

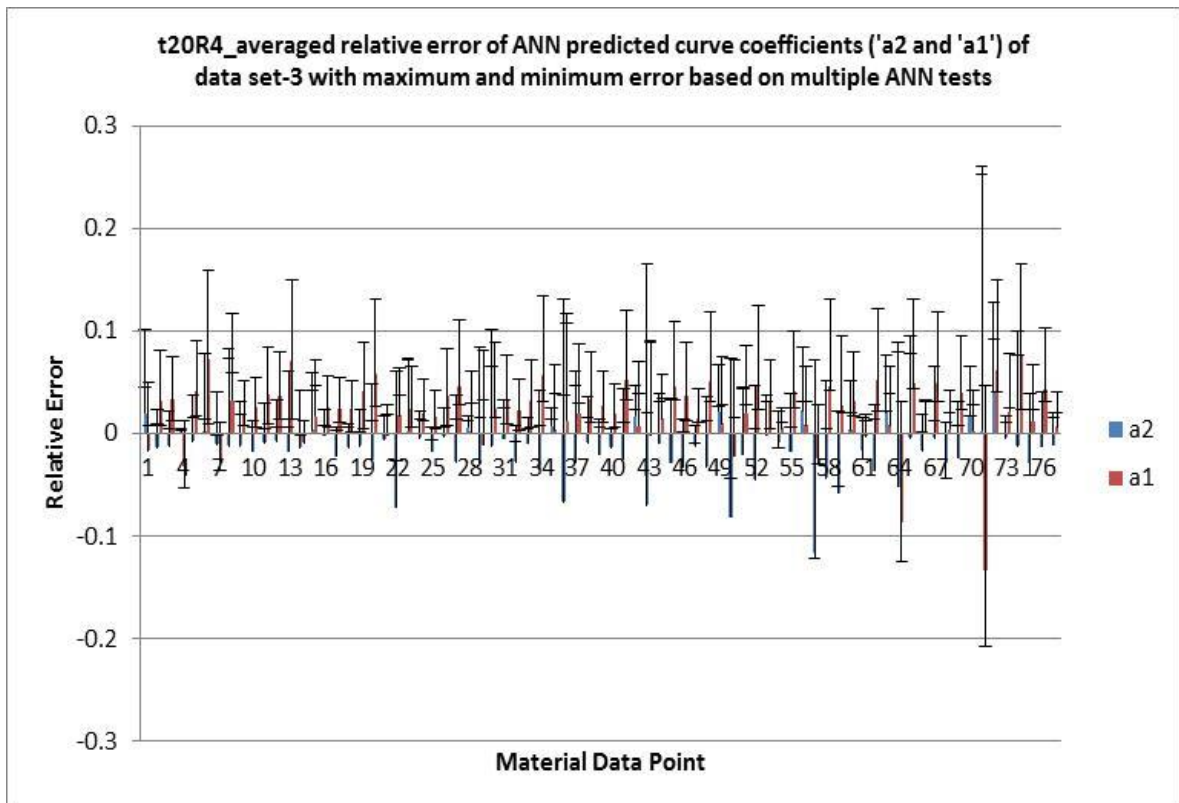


(a) Relative error in a2 and a1 (neuron number 20), ANN test-1.

Figure 3.16 Typical data showing the variation of ANN predicted data in different ANN tests using untrained data as test data (Materials data set 3).



(a) Neuron=10



(b) Neuron=20

Figure 3.17 Averaged relative error and maximum error of a2 and a1 based ANN with 10 and 20 neurons (Test data Material data set 3) showing neuron 20 data is better/robust as the maximum error is low.

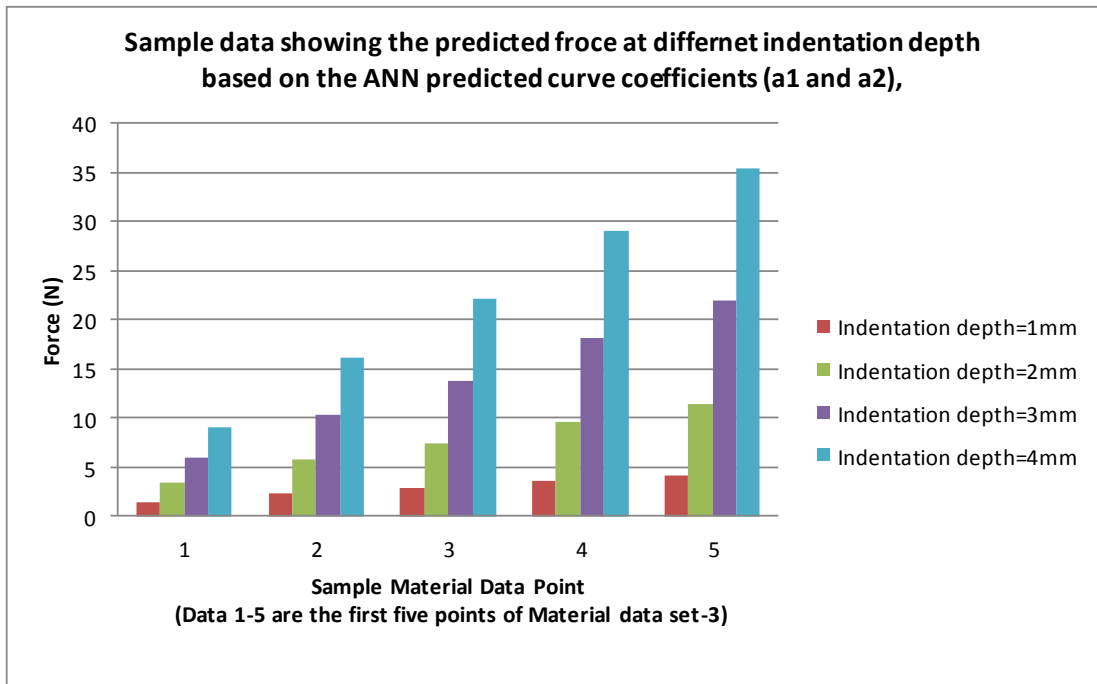


Figure 3.18 (a) Sample data showing the predicted force at different indentation depth based on the ANN predicted curve coefficients (a1 and a2). (Neuron number 20).

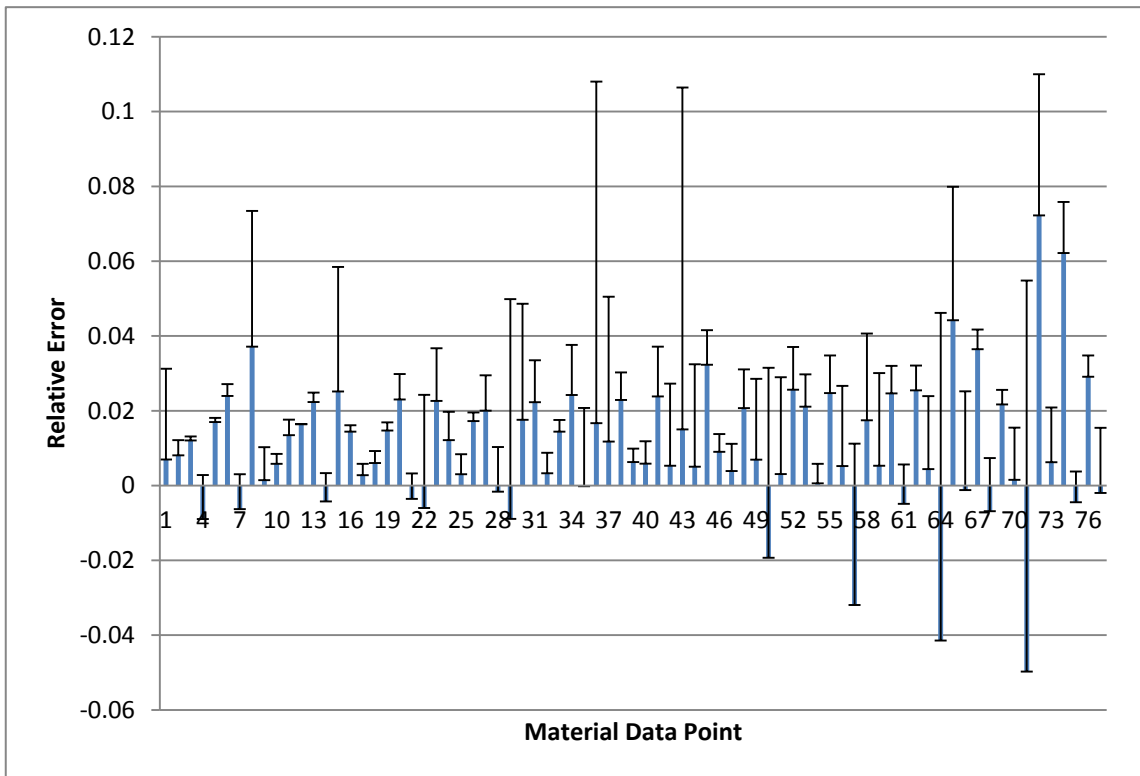


Figure 3.18 (b) Average error (among 4 depth) in the forces based on ANN predicted curve coefficients (a1 and a2) with maximum error (Neuron 10). (The error bars represent the maximum error among the 5 ANN simulations/tests) (Test data: material set 3).

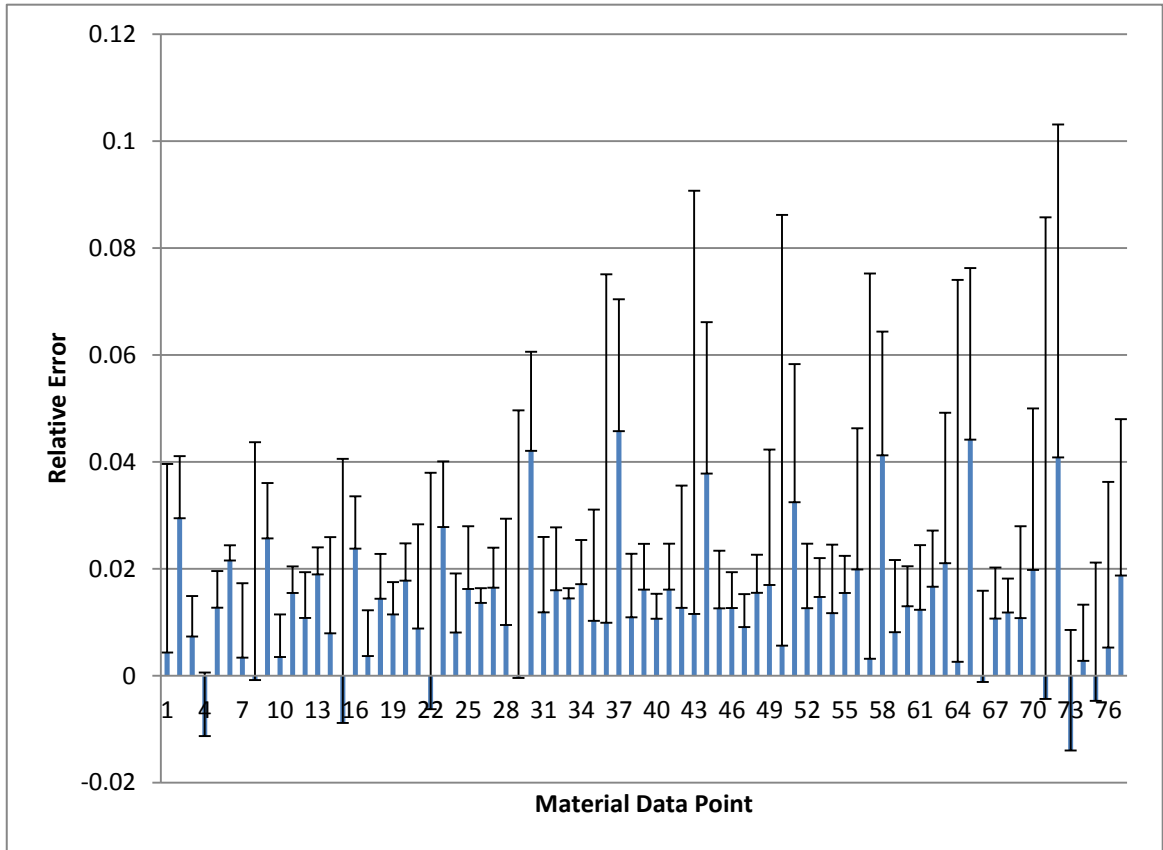


Figure 3.18 (c) Average error in the forces based on ANN predicted curve coefficients (a_1 and a_2) with maximum error.(Neuron 10). (Test data: Materials data set -3).

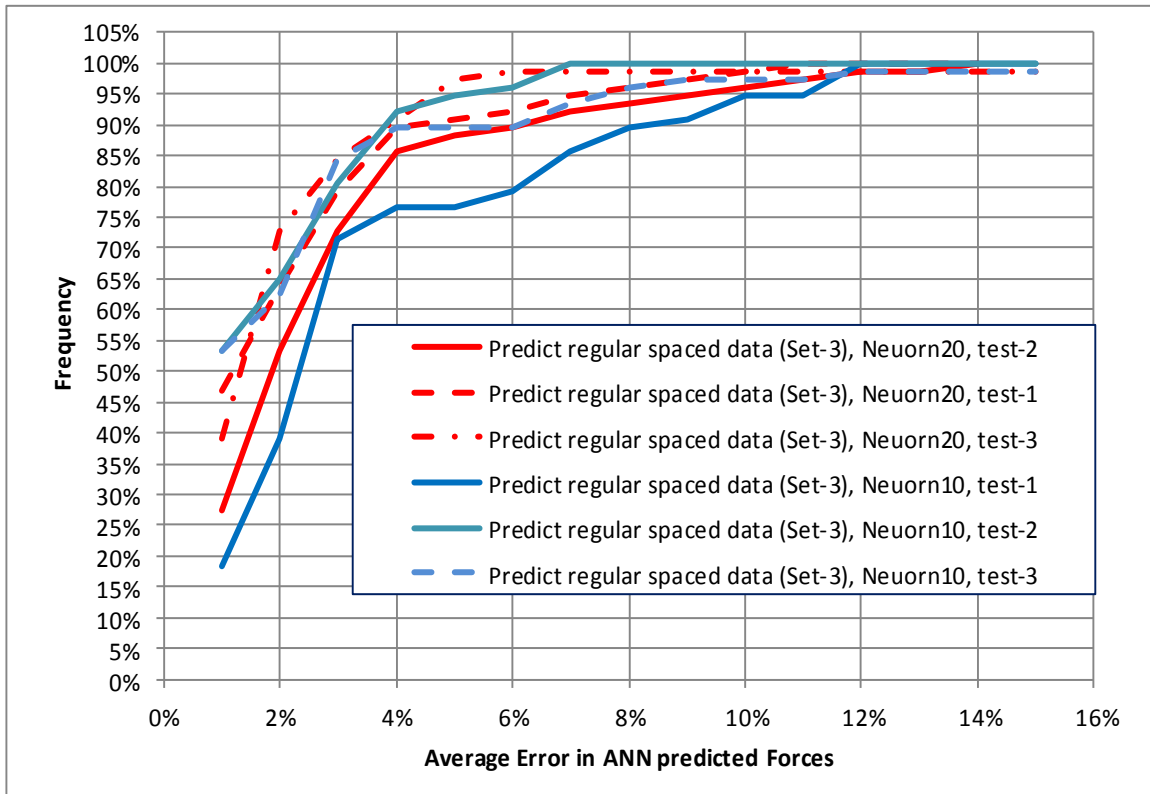
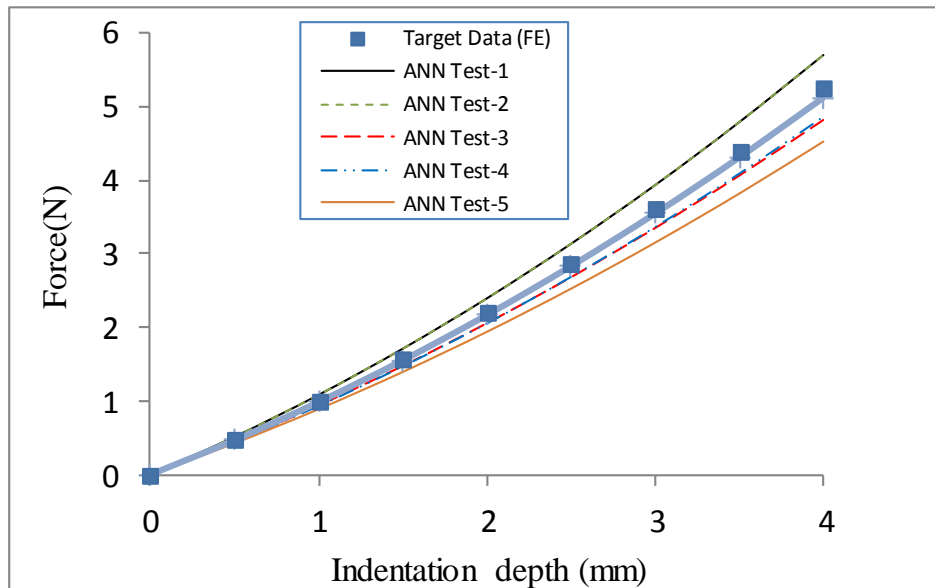
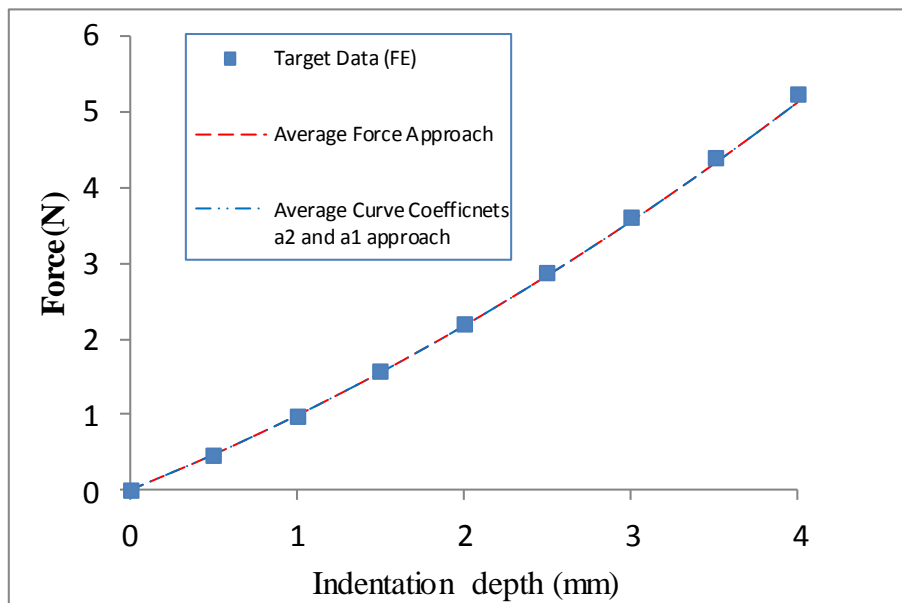


Figure 3.19 Frequency of prediction results of different error range. For relative error within 10%, ANN with 20 neurons achieved over 95%; ANN with 10 neurons is below 95%. Showing the ANN with 20 neuron is more robust than ANN with 10 neuron.



(a) Comparison between indentation force displacement curves based on the ANN predicted curve coefficients (a1 and a2) with high relative error in forces (Relative Error 0.122) between multiple ANN tests.(property $\mu=0.15$, $\alpha=7.5$).



(b) Comparison between indentation force and target data. One approach is to average the force data (in (a)) and another approach is to average curve parameters (a1 and a2) before produce the force data. (property $\mu=0.15$, $\alpha=7.5$)

Figure 3.20 Comparison between average force-displacement curve based on ANN predicted parameters and FE data showing that prediction accuracy of ANN can be further improved by using average data from multiple ANN tests.

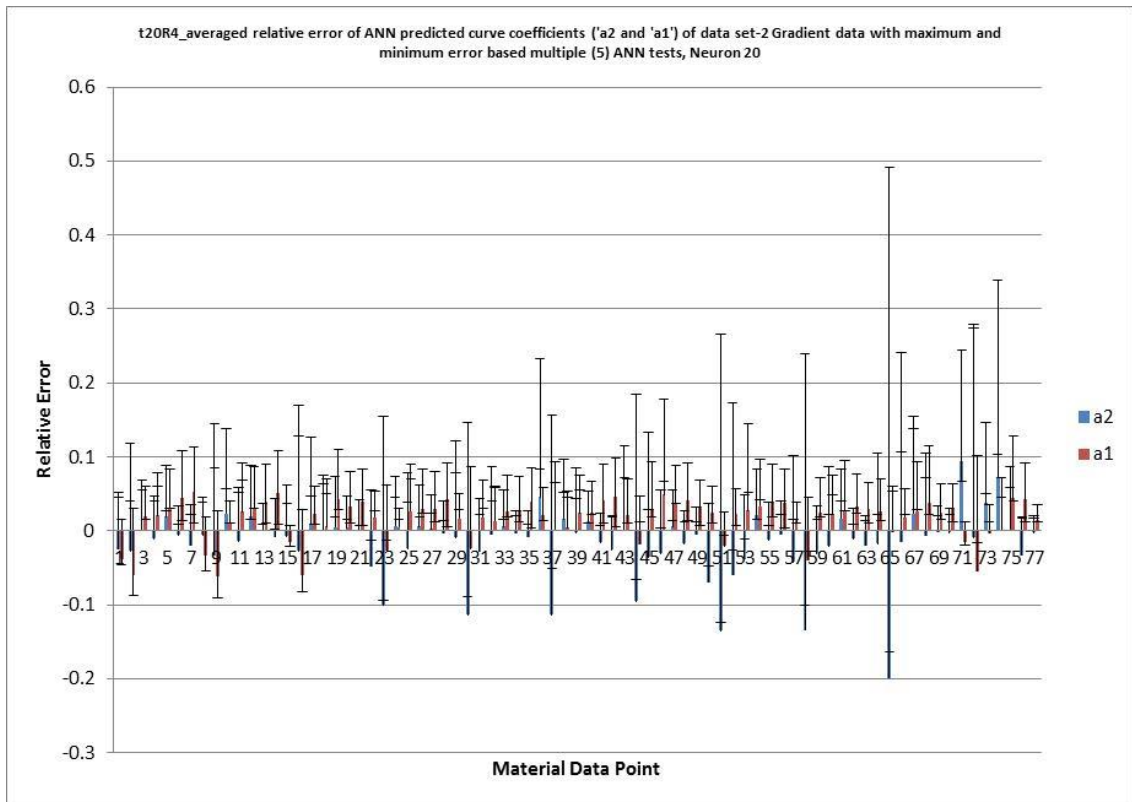


Figure 3.21(a) averaged relative error of the ANN predicted curve coefficient (a2 and a1) with maximum and minimum value of the all the test data. (Neuron number=20, Training data: Material set-1; test data: Materials data -2, gradient data).

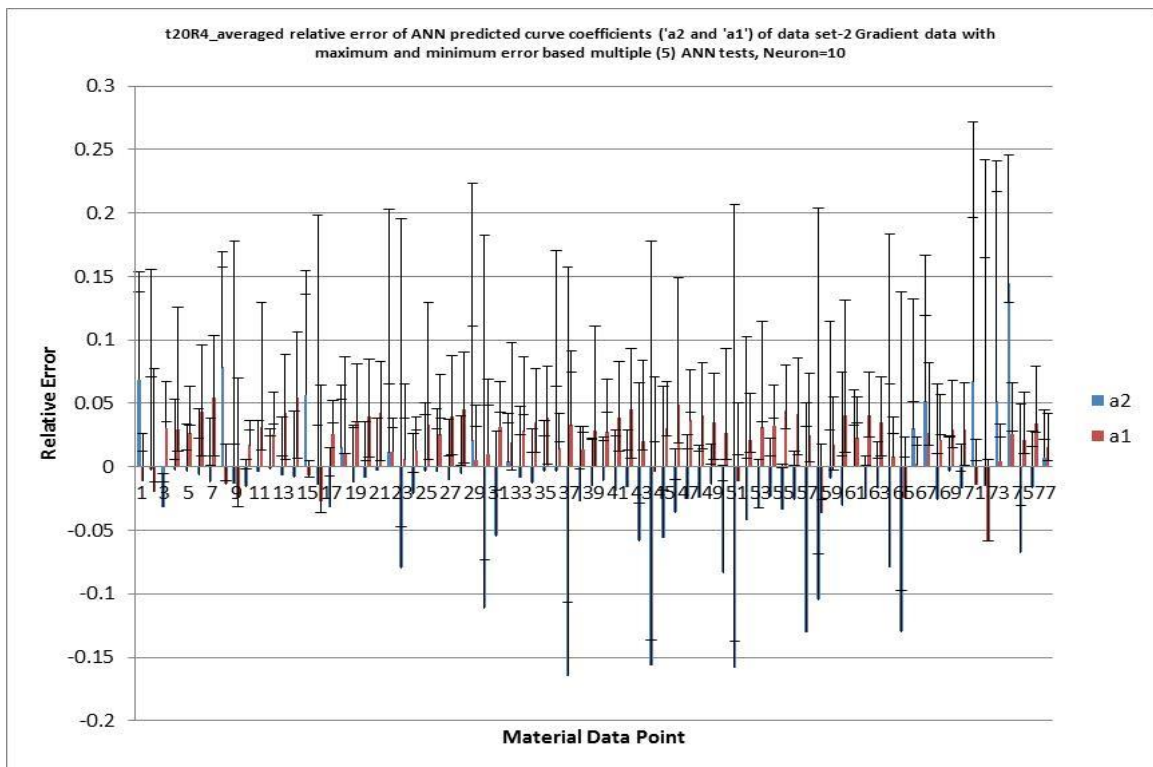


Figure 3.21(b) Relative error of the ANN predicted curve coefficient (a2 and a1) with maximum and minimum value of the all the test data. (Neuron number=10; Training data: Material set-1; Test data: Materials data -2, gradient data).

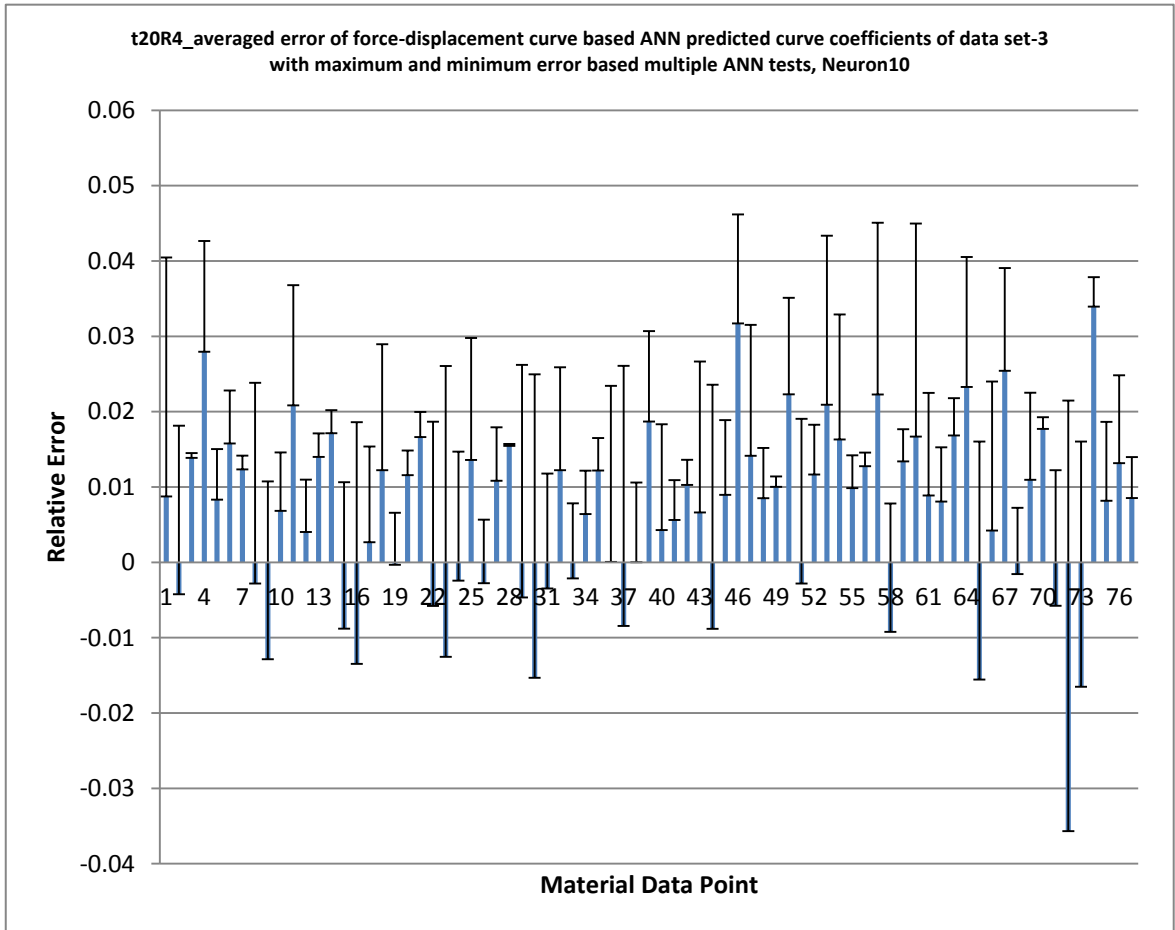


Figure 3.22 (a) Relative error of indentation force based on ANN predicted curve fitting parameter for materials Data set-2. (20 neurons).

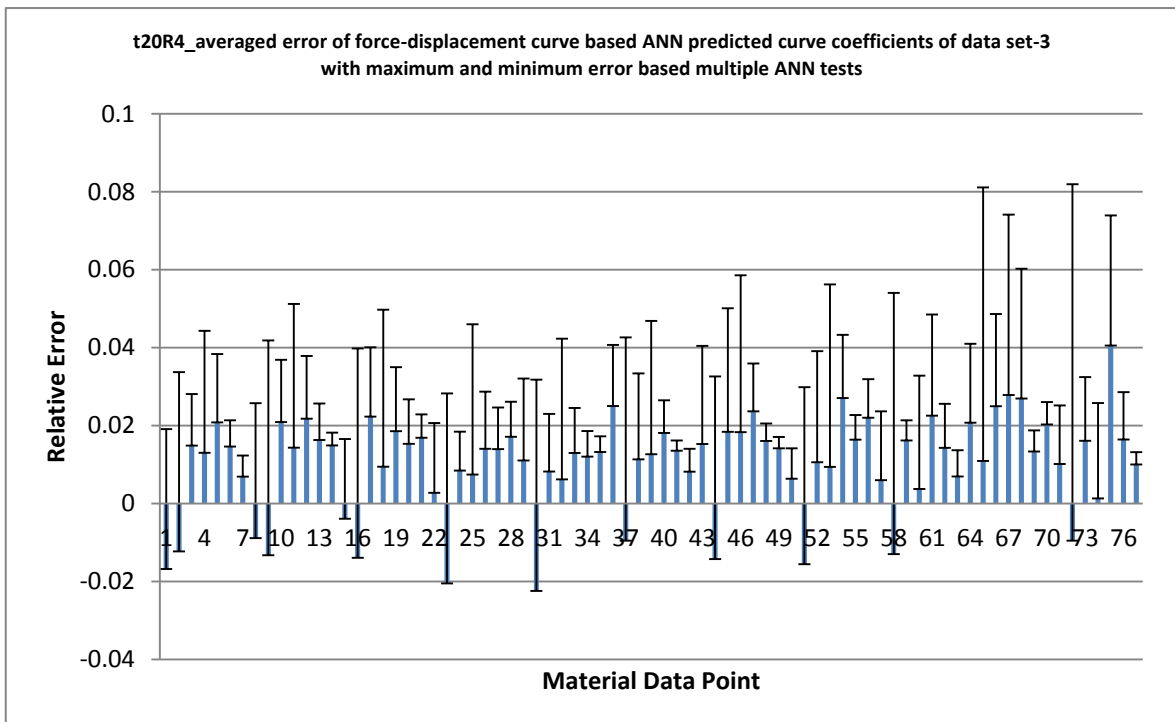


Figure 3.22 (b) Relative error of indentation force based on ANN predicted curve fitting parameter for materials Data set-2. (10 neurons).

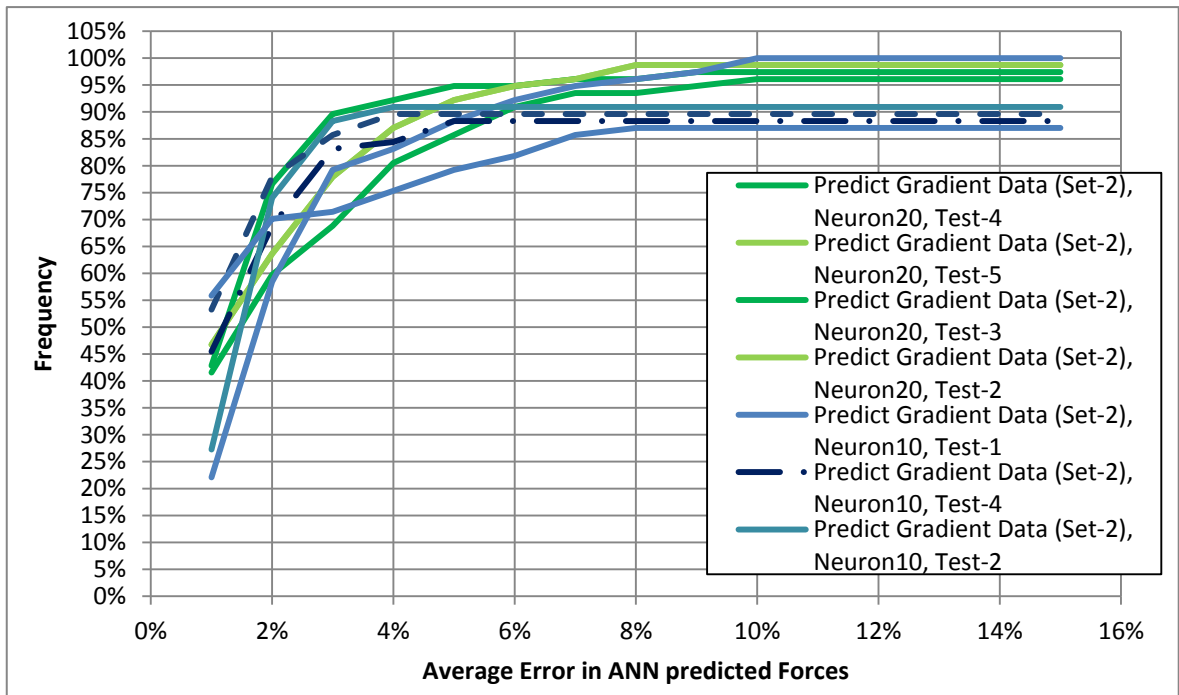


Figure 3.22(c) Frequency of error range for predicting gradient data (data set-2) with neuron 10 and 20. For relative error within 10%, ANN with 20 neurons achieved over 95%; ANN with 10 neurons is below 90%.

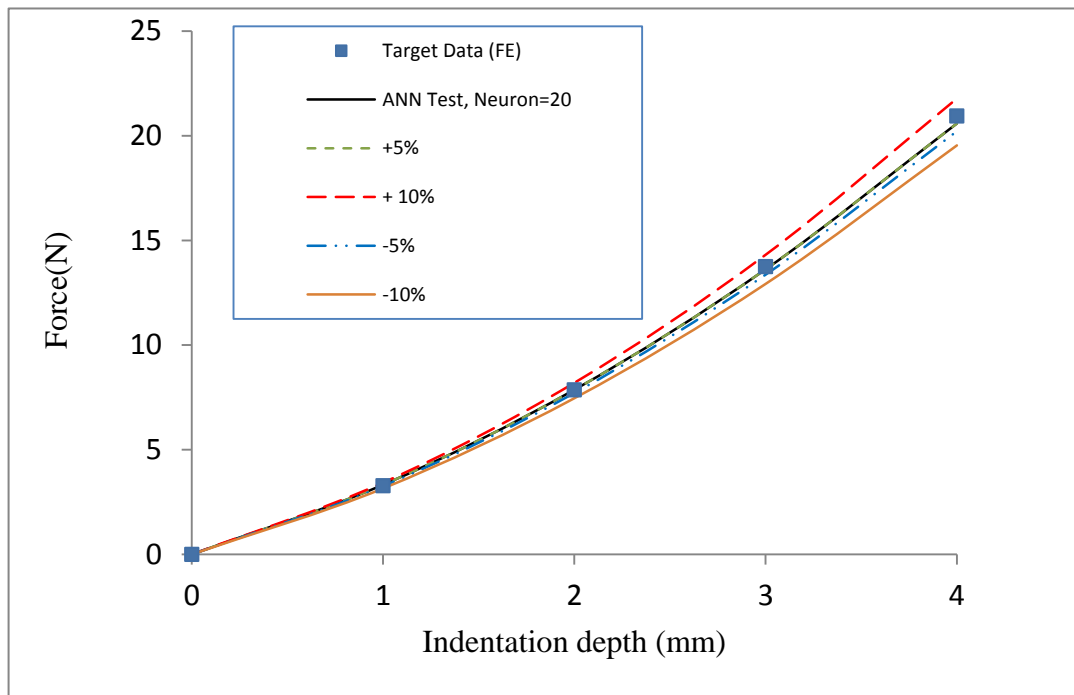


Figure 3.23 Typical data showing the influence of error (5% or 10%) in material properties on the ANN predicted indentation force-displacement curve illustrating the ANN based approach for P-h curve prediction is robust. (Property $\mu=0.65$, $\text{Alpha}=8.5$)

3.5 ANN program based on the force at depth approach and results.

As shown earlier in Figure 3.8(b), in the force at depth data approach, the output is force values at different indentation depth. In this work, the main depth was used 1, 2, 3 4mm. Given the curves are fitted with 2nd order polynomial; 4 point should be sufficiently accurate. This could balance the accuracy of the ANN prediction and the computational resources requirement, as when the number of depth increase, the computational time will increase. Figure 3.24 shows typical training process and regression results. In both cases with neuron number 10 and 20, the training and validation reach a sufficiently high accuracy. The training and validation is using material data set-1, then use material data sets 2&3 as the testing data.

Figure 3.25 shows some typical ANN predicted results (the first 7 materials points of data set-3) to show the concept and data processing process. Figure 3.25(a) plots the force at depth of 1, 2,3 and 4 mm. The relative error between the predicted force and target values is plotted in Figure 3.25 (b). It is clearly shown that the overall error is relative low, within 6% in all the cases. It would be naturally expected the relative error will be high at lower indentation depth as the force will be low, but error are random without a clear trend. This could be an advantage of ANN to avoid systematic error as the prediction between each point is not continuous. Similar data processing procedure is applied to larger material domains cover all the 77 material data points in the material data set-3. Figure 3.26 shows the relative error of the 77 points of materials data set-3 as the testing data. The figure is not very clear due to the large number of data present, material data point will be in the same format as in the previous figure (Figure 3.25(a)). The main info from these figure are the maximum error range. It is clearly shown that with neuron number=5, the maximum error is over 15% which is not acceptable. With neuron number 10, it reduced to within 6%; with neuron number 20, the error is slightly higher within 8%, both are acceptable. Further increase of the neuron number to 25, the error become much higher within 20%. Different from the trendline ANN approach, the outcome is force, which is directly meaningful to the material sets. From these, both neuron number 10 and 20 have produced acceptable results, with neuron 10 condition is slightly better. Repeatability test of the ANN prediction is

systematically assessed, the result for neuron 10 is shown in Figure 3.27.

The average error for each material point was calculated by averaging the relative error over the four depth data. As shown in Figure 3.28, the average error of predicted indentation forces is within 5% and the maximum error is 8%. Figure 3.28(b) compared the frequency of different error range, 95% data of the ANN with 10 neurons reaches an error within 6%; the frequency become close to 100% within an error range of 10%. But for the ANN with 20neurons, less than 85% reaches error range of 6%, and only over 90% reaches error within 10%. This clearly shows that the ANN with 10 neurons is better than the ANN program with 20 Neurons. Figure 2.9 shows the typical comparison between predicted indentation force data and the target. Figure (a) is for the first point on the Material data set-3 with an error range within 3% (as shown in Figure 3.28(a)). Figure (b) shows the force-displacement data for data 71, which has the highest error. The results is still reasonable close and acceptable for EVA materials. Similar ANN simulation has been conducted with Materials data set-2 as the testing data, the results is similar to the accuracy for that of material data set-3 presented. The ANN prediction of the forces is within 8%. The result is not shown to avoid repeating data of similar nature. These results show that the depth approach is a feasible method to predict indentation P-h curves but as robust as the trendline approach. The running time for each ANN simulation is also much longer than the trendline approach.

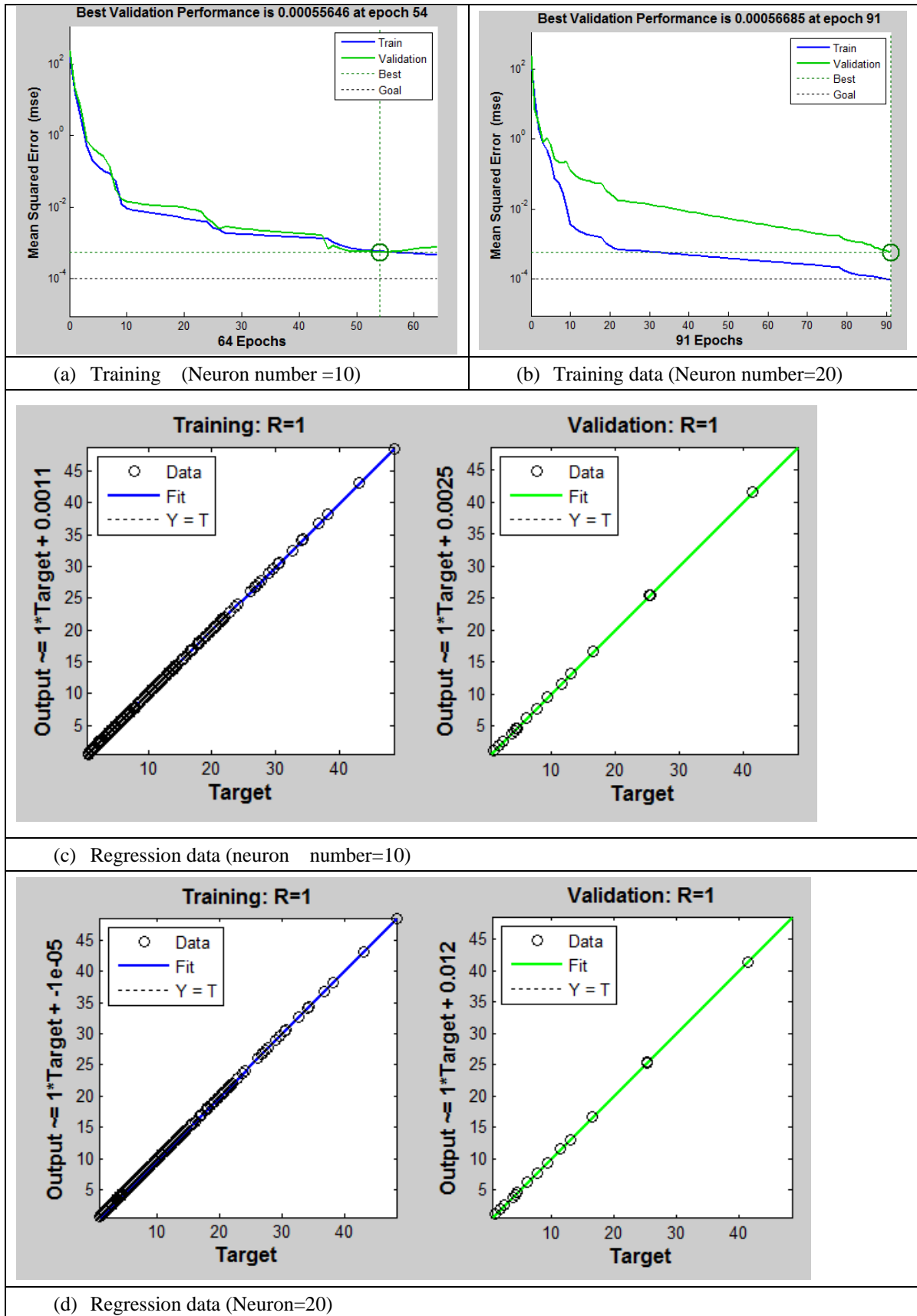
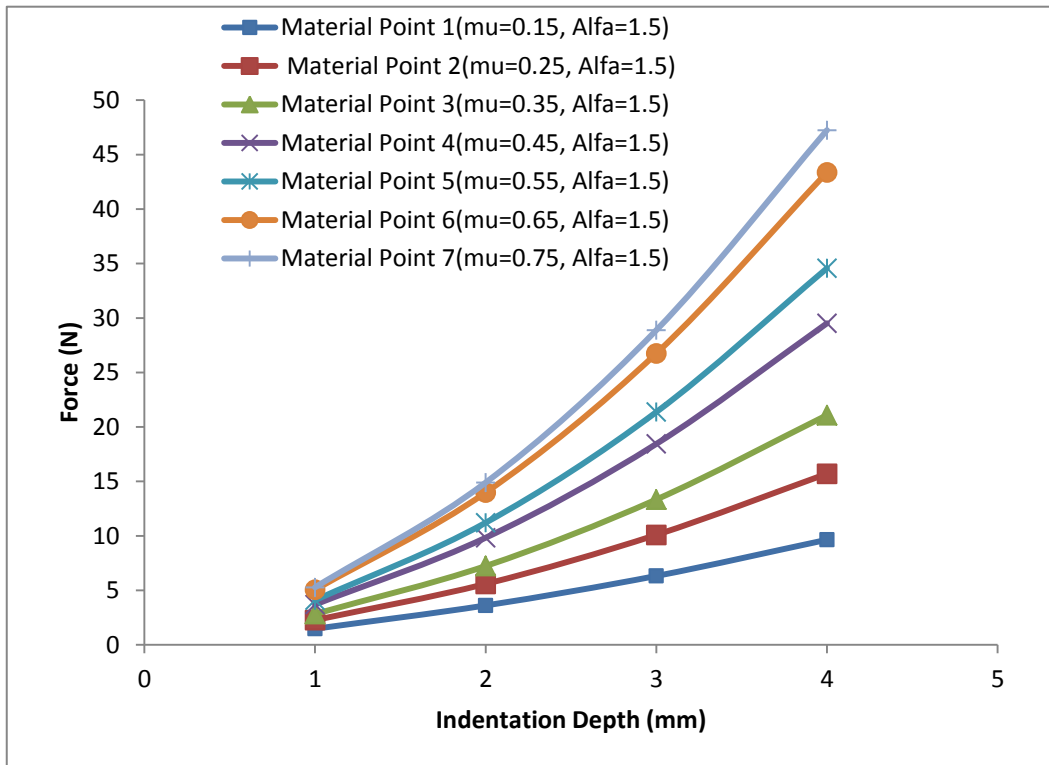
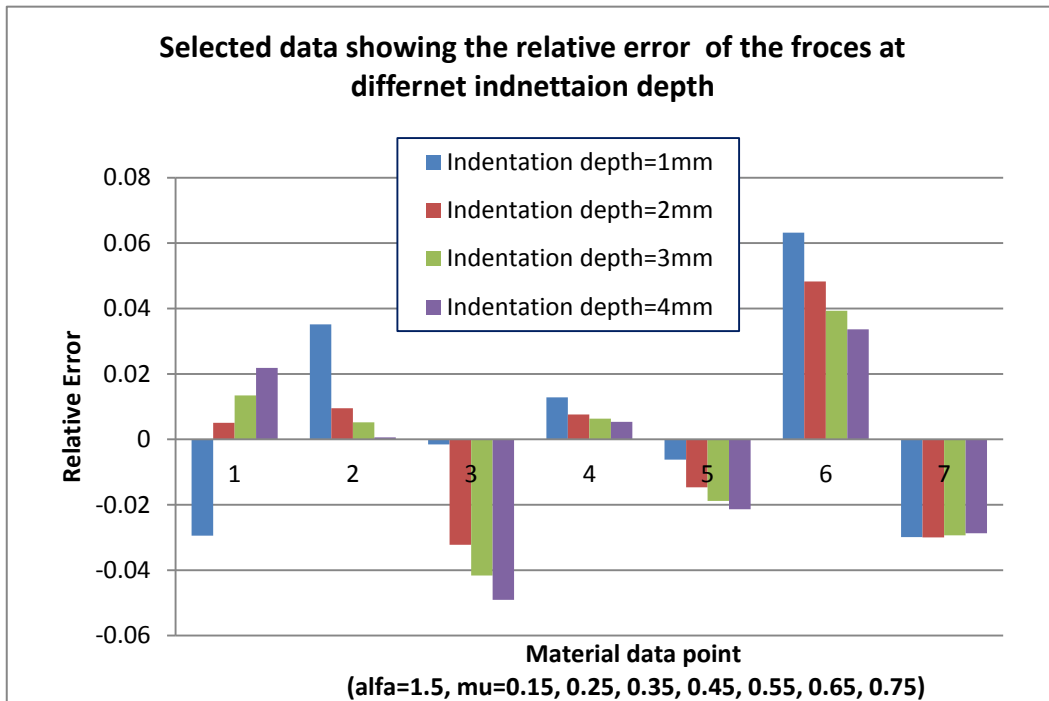


Figure 3.24 Performance and regression based on the depth approach using material set-1 as the training data (Neuron number =10 and 20).

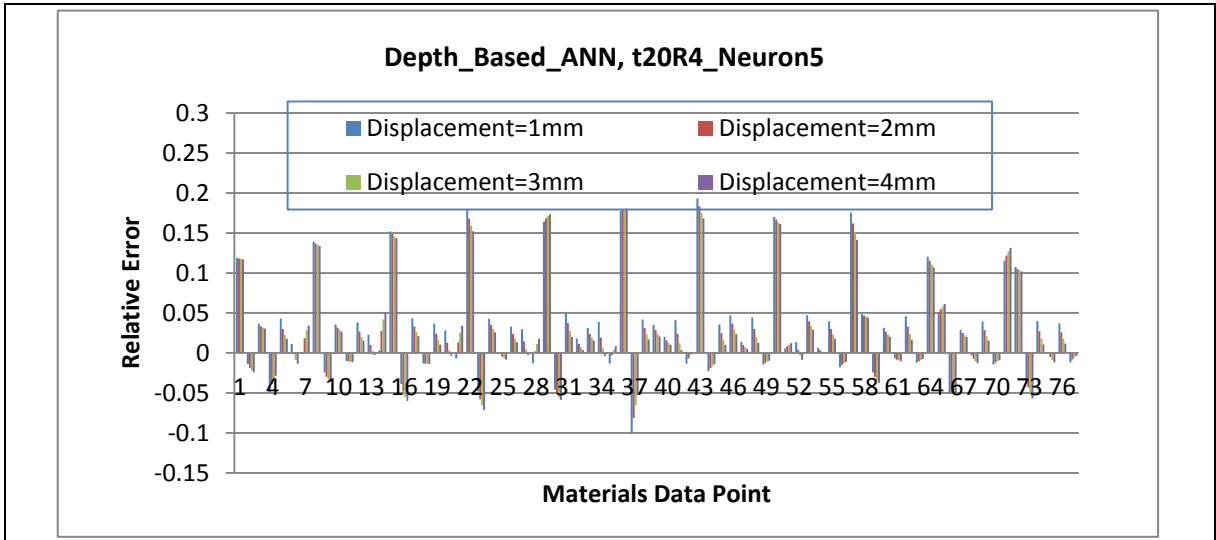


(a) Typical force at displacement of 1,2,3, 4 mm predicted by ANN (for the first 7 point of Material data set-3).

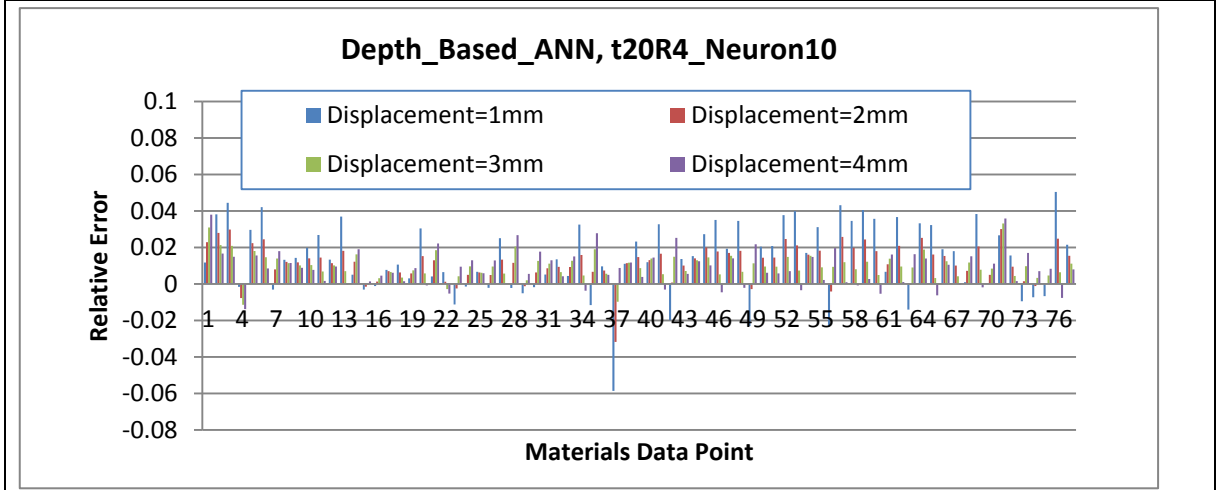


(b) Relative error of ANN (neuron 20) predicted force and the target values at different indentation depth (for the first 7 points in material set-3 only).

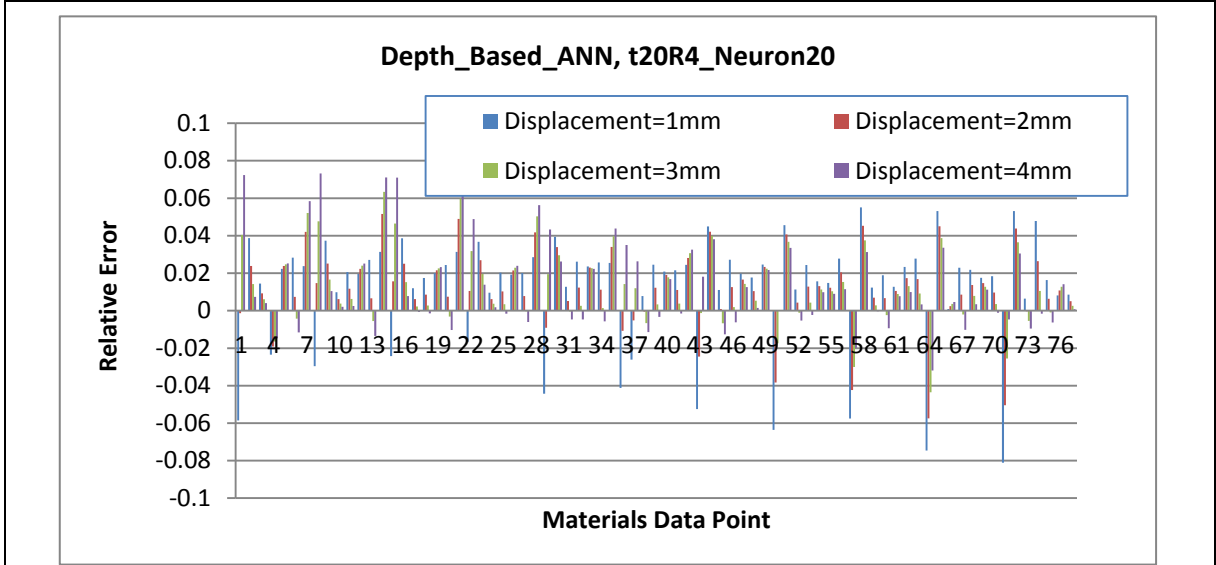
Figure 3.25 Typical ANN (neuron 20) predicted forces at different indentation depth and relative error to illustrate the way the data processing method.



(a) Neuron number=5



(b) Neuron number =10



(c) Neuron number=20

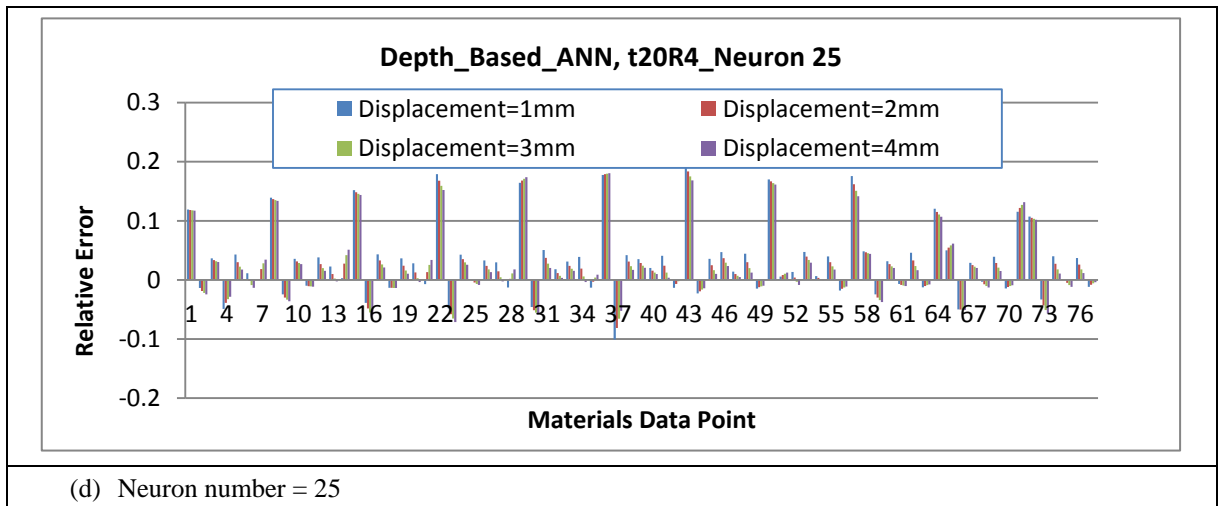
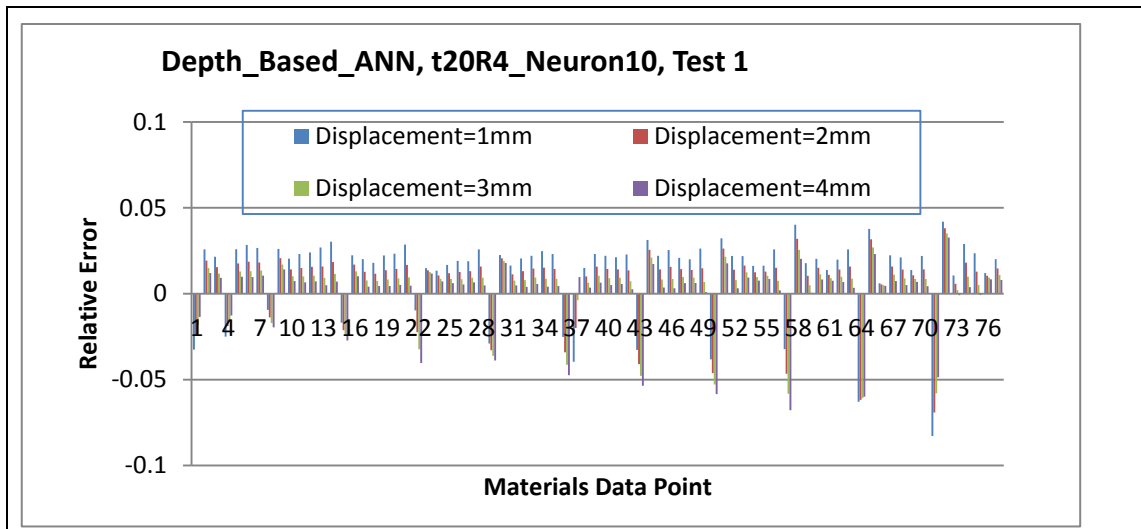
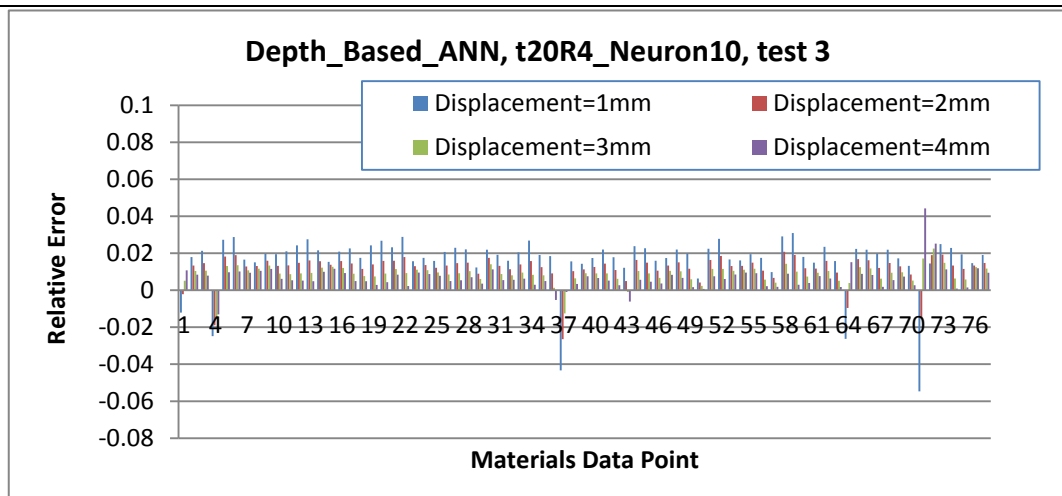


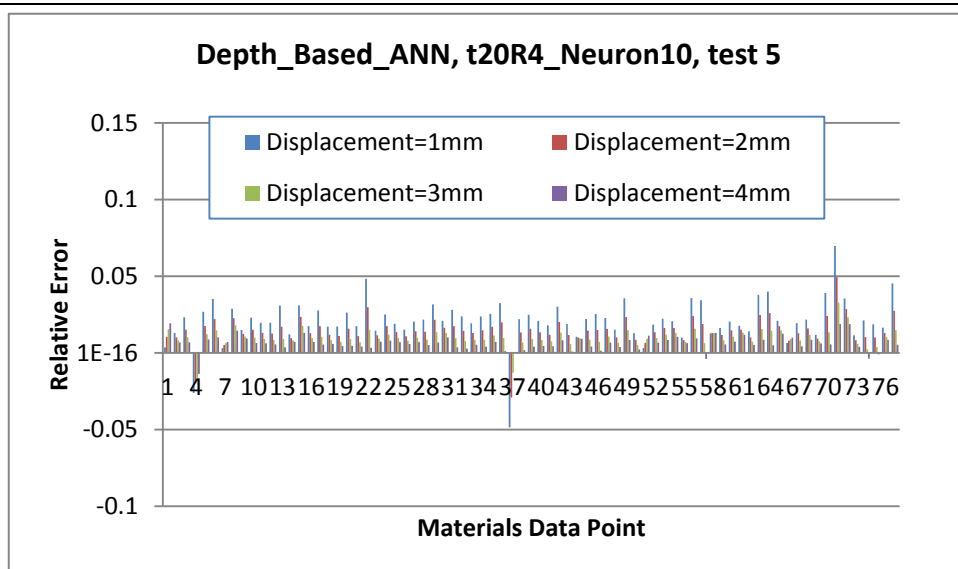
Figure 3.26 Error in the forces at different depth using untrained data (data set-3) showing the effect of number of neurons. The data illustrate that the error varies with material point but no significant variation with different depth for the same material property point.



(a) ANN test-1.



(b) ANN Test-3



(c) ANN Test-5

Figure 3.27 Typical ANN test data with neuron=10 showing the repeatability of each ANN simulation. (Training: material set-1; Test: materials set-3).

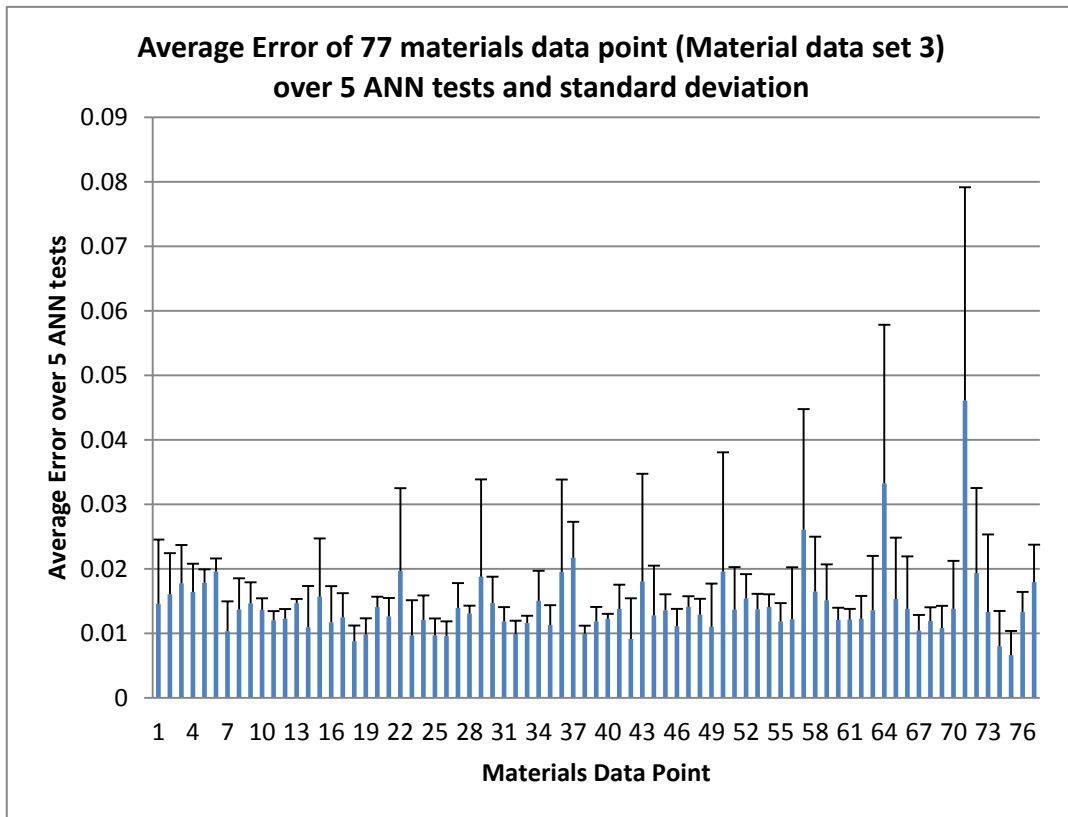


Figure 3.28 (a) Plot of average error (each test 4 depth points over 5 tests) for different material data point (Depth approach, Test data: material data set-3).

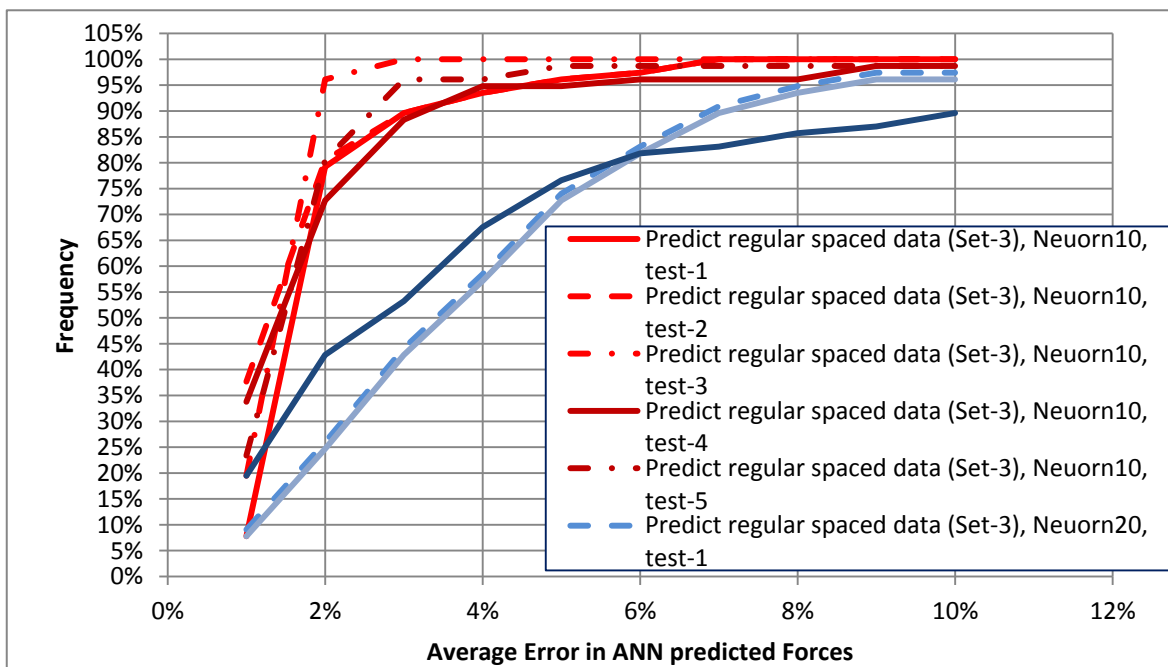
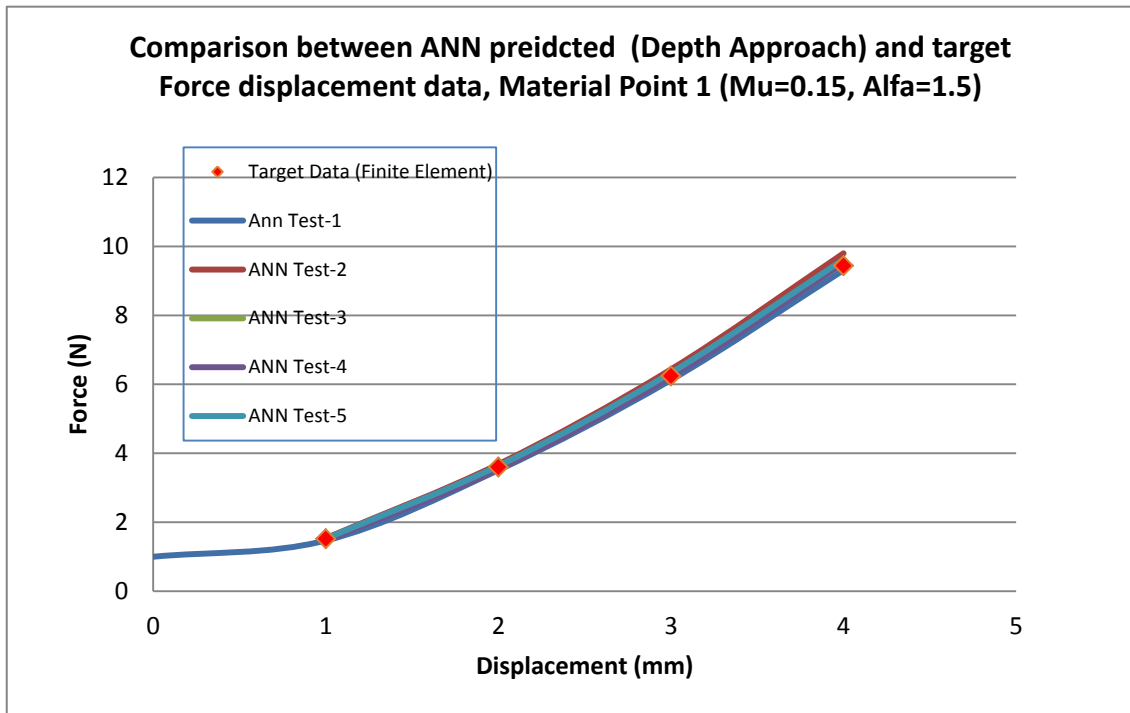
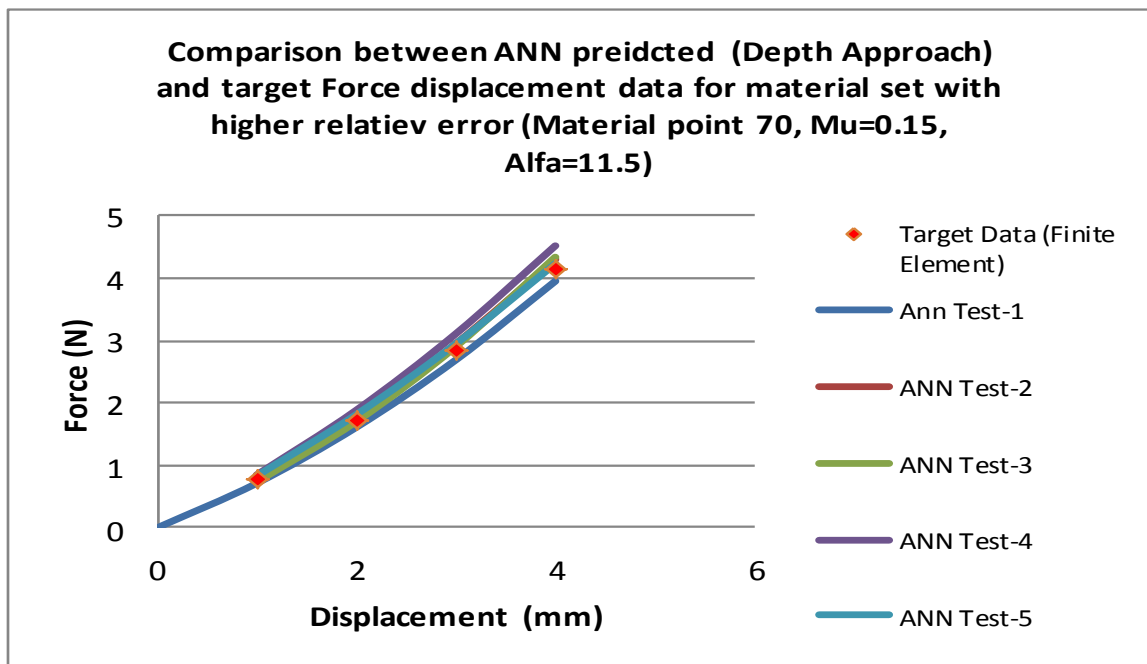


Figure 3.28 (b) Frequency of the error range with neuron 20 and neuron 10 based on the depth method. For ANN with 10 neurons, over 95% material data point reaches within an error 5%; For ANN with 20 neurons, over 85% material data reaches an error within 10%.



(a) Typical data showing the comparison between ANN predicted (Depth Approach) and target Force displacement data with lower relative error (Material Point 1, Mu=0.15, Alfa=1.5).

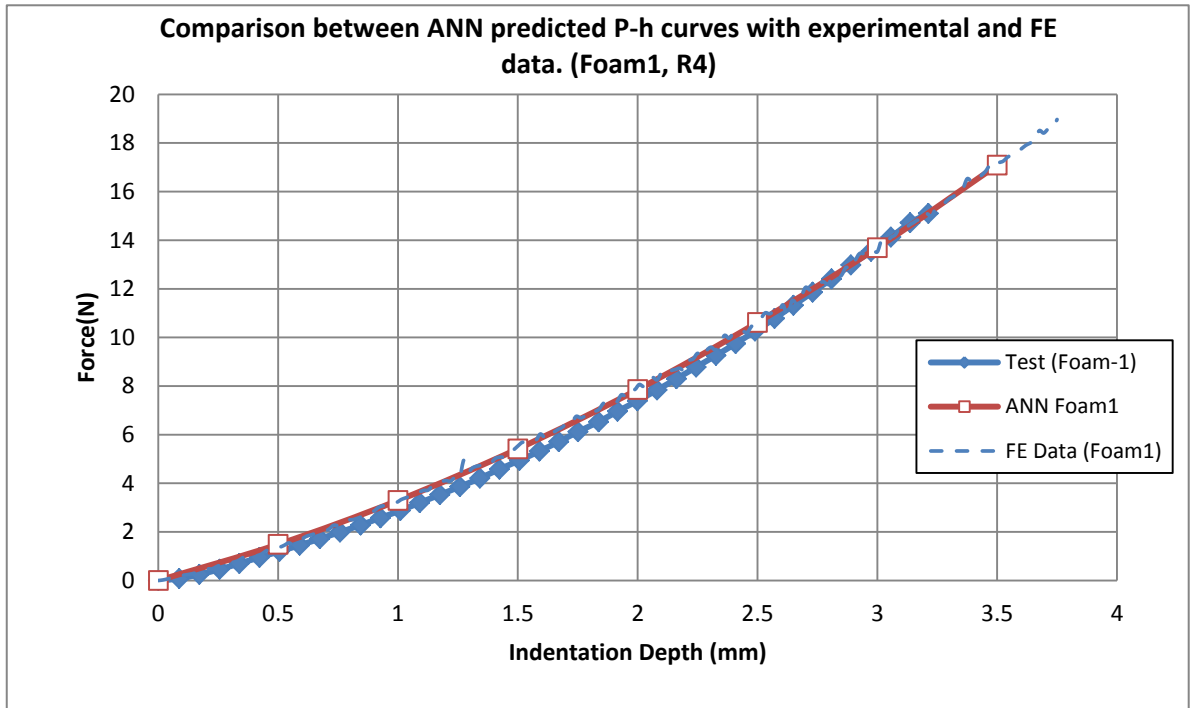


(e) Comparison between ANN predicted (Depth Approach) and target Force displacement data for material properties with higher error(b). The zero point for some tests were not plotted to show data more clearly).

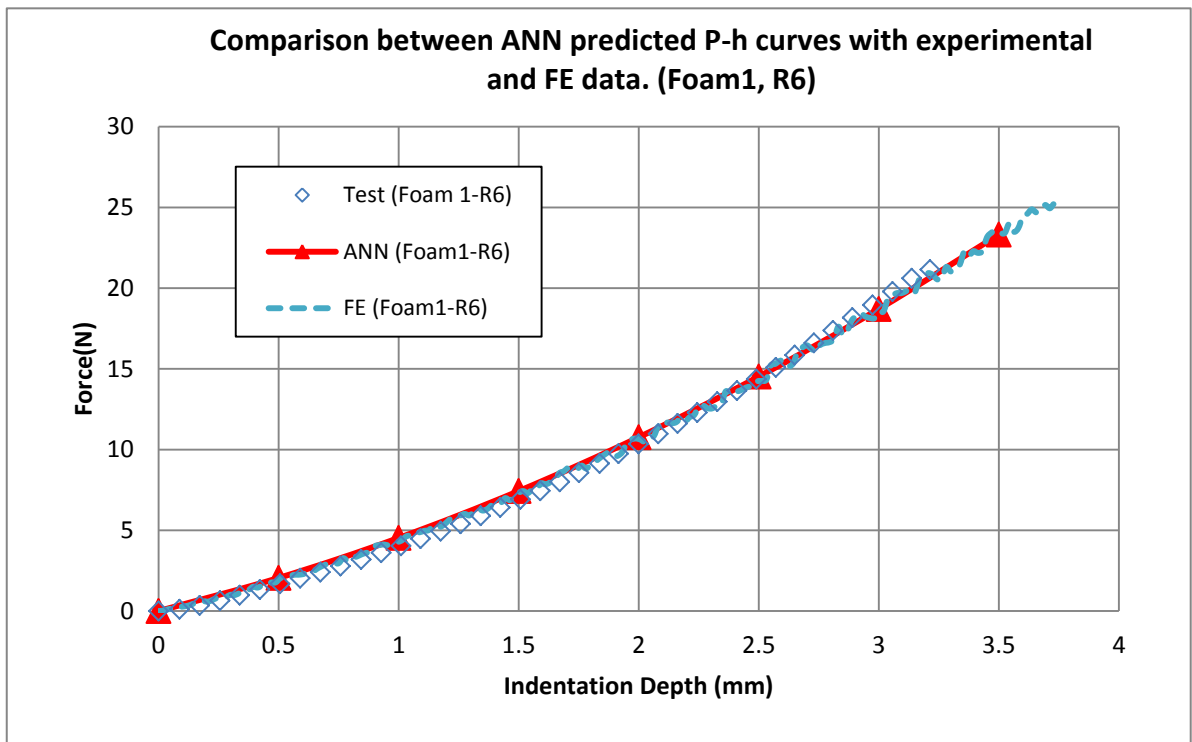
Figure 3.29 Comparison of predicted force-displacement curves with material sets of different level of relative error.

3.6 Use of ANN in the prediction of P-h curves of EVA foams of known properties.

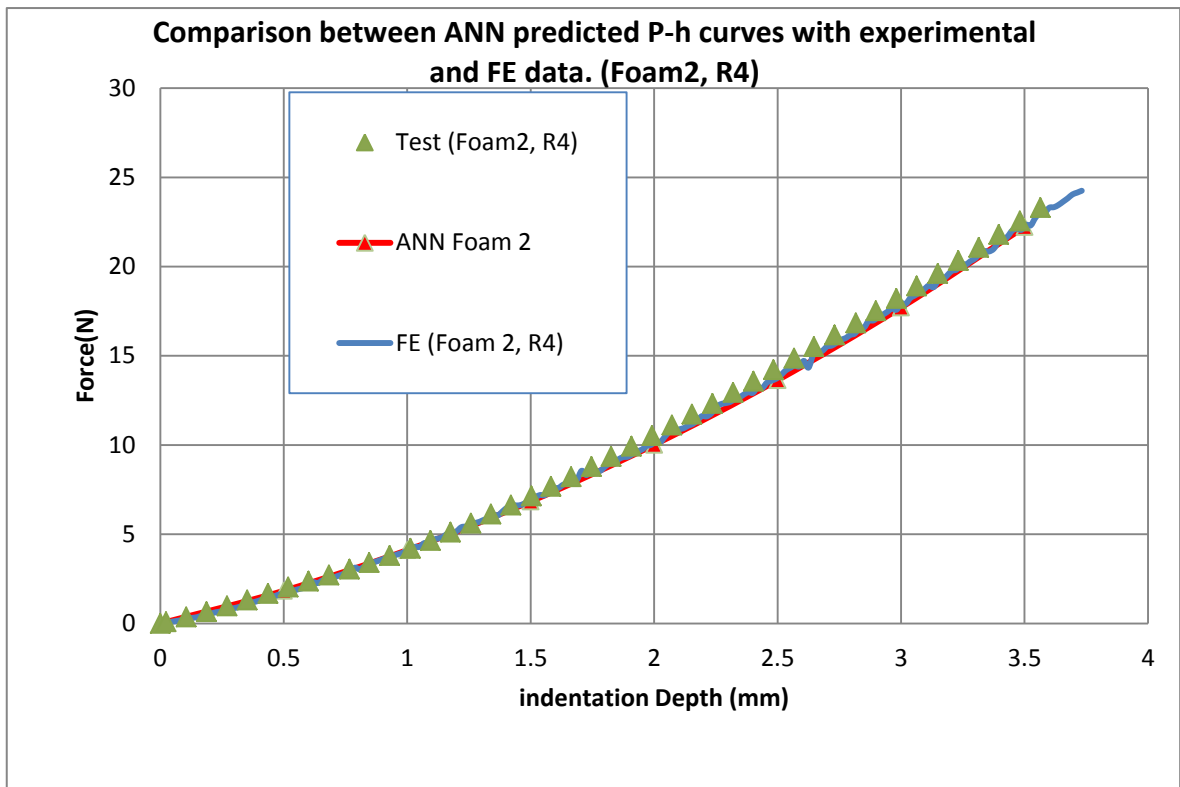
Sections 3.4 and 3.5 has evaluated the ANN program based numerical data and a workable procedure including the optimum number of neurons and average of multiple ANN tests was shown to be able to predict the P-h curves. All results presented in sections 3.4-66 is based on indenter size of R4. Similar work has been done with indenter size R6mm, the results showed a similar level of accuracy using the three material data set as the training and validation data. The results are not shown to preserve clarity and avoid repeating information of similar nature. Both ANN for R4 and R6 was used to test experimental data. The program has been used to analyse EVA foams with known properties determined from combined compression and shear tests. The results are shown in Figure 3.30. In each case, the ANN predicted curve is compared to the experimental data and the FE predicted data. The properties for foam is $\mu=0.62$, $\alpha=8$; the properties for foam 2 is $\mu=0.75$, $\alpha=6$. In the FE model, the property is input in the FE model with different indenter sizes (R4 and R6) and the P-h is directly predicted. In the ANN program, the material properties is used as input, then the coefficient 'a₂' and 'a₁' was predicted following the ANN procedure developed with the trendline method. In the ANN, material data set-1 was used as the training and validation data, then input the material properties of Foams1&2 as test data, re-run the ANN 5 times, then the average of prediction of 'a₂' and 'a₁' is determined, the P-h curve for the two foams is plotted. The results for foam1 with indenter size 4mm is shown in Figure (a); results for foam 1with indenter size of 6mm is shown in Figure (b). In both cases the ANN perdition showed a good agreement with the experimental and FE prediction. Figures (c&d) shows the results for foam 2, again, the Ann prediction showed a good agreement with the experimental data and FE prediction The depth based ANN approach is also evaluated and showed similar level of accuracy. These results further validate the ANN program developed.



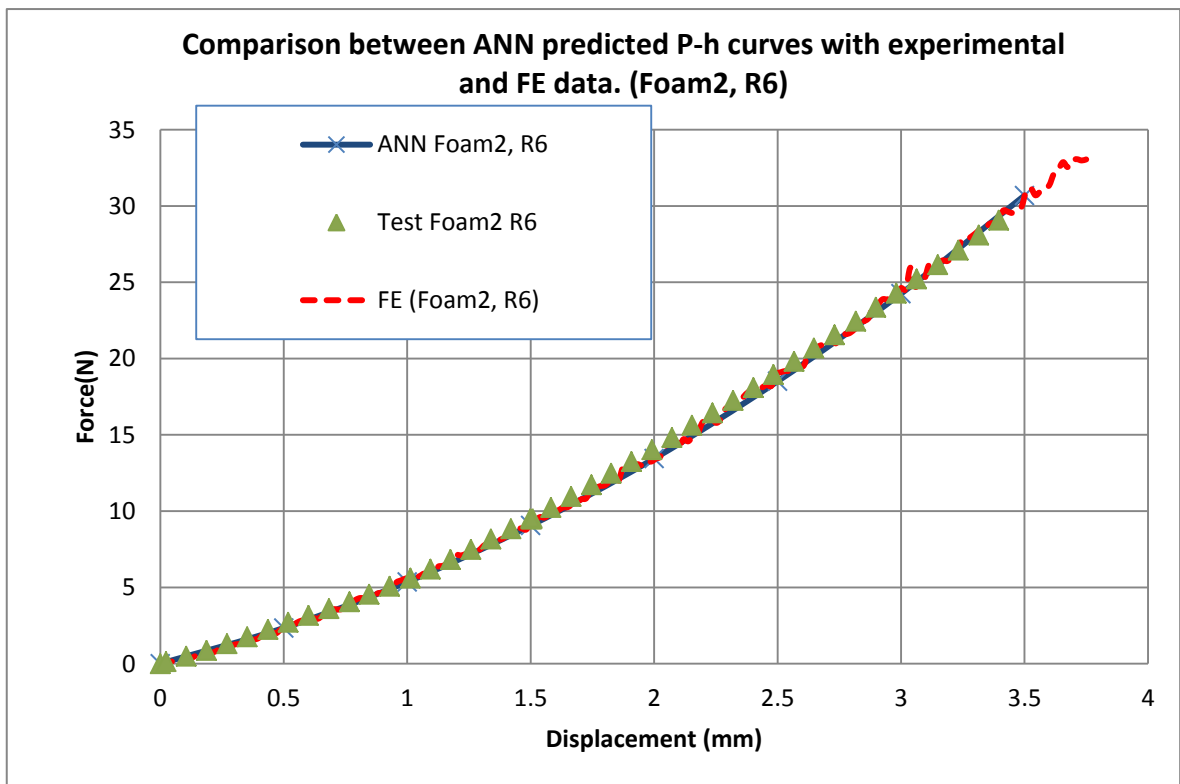
(a) EVA Foam-1 (R4).



(b) EVA Foam 1 (R6)



(c) EVA Foam 2 R4.



(d) EVA Foam 2, R6.

Figure 3.30 Comparison between ANN predicted P-h curves with the testing data of R4 and R6. EVA-1 and EVA-2.

3.7 Summary

In this chapter, an ANN program has been developed to predict the indentation P-h curves with known properties (hyperfoam material parameter, μ and α). An interactive parametric FE model and python programming based data extracting program has been developed and used to develop matrix data for the ANN program. Two approaches have been proposed and evaluated to represent the P-h curve. One is using 2nd order polynomial trendline approach ($P=a_2h^2+a_1h$), the other is to use the forces at different indentation depth. The ANN program is developed with early stopping mechanism, the effect of the transfer function and number of neurons was systematically analysed using three set of material matrix data. The performance of the ANN based on the trendline approach is evaluated with MSE and relative error of the coefficient 'a2' and 'a1' and the average error in forces over different depths. A frequency method is used to analyse the data, which provided important data/base about the robustness of the ANN program. It also helped with developing an approach to further enhanced the accuracy of the P-h curve based on averaging multiple ANN tests. This approach effectively taking use of the fact that ANN prediction is not continuous around any property point. Sensitivity tests with purposely introduced error in the input to ANN showed that the approach is accurate and robust. The ANN program with the depth based approach showed similar accuracy in predicting P-h curves of hyperfoam materials. The work used matrix of different structure to access the accuracy rather than single data point, all the test data showed good results. The work was initially developed based on indenter size of 4mm, it was then transferred to an indenter size of 6mm, both were then used to predict P-h curves and compared directly to experimental data on two EVA foams with known properties. The ANN prediction showed very good agreement with the FE prediction and experimental testing data.

Some of works has also been conducted in using surface mapping approach and direct interactive data search (similar to interpolation) as comparison to the Ann approach. Comparing with these approaches, the ANN approach is a much more accurate approach. Detailed are to be presented in the discussion chapter to highlight the significance of the work established in direct and inverse analysis of indentation data. The ANN program is

also extremely quicker than FE modelling, this provided a new tool to generate data over a wide range of material data. It is to be packaged into a computer program to predict P-h curves of different foams. Some of these are to be presented in the next chapter together with a new inverse program developed using the direct ANN program presented in this chapter. In addition, from the experience in developing data and ANN for different indenter sizes, it potentially can be easily/quickly transferred to other sample size (such as different thickness) if necessary, in particular the polynomial trendline approach, which is very flexible in fitting complex data. This will provide an important tool in analysis of form testing and development of new computerized inverse program, which are to be present in Chapter 4.

Chapter Four
Inverse Materials Parameters Identification Based
on Indentation Tests

4.1 Introduction

Following the successful establishment of the ANN method to predict the indentation force-displacement data presented in the last chapter, this chapter looks at developing a method to predict the material properties/parameter (μ and α) when the indentation force displacement data is known. The work in the previous chapter showed that the P-h curves can be effectively represented by polynomial curve fitting coefficients; this potentially will make it easier to develop inverse modelling programs through Neural Network as the input become simpler as the curve can be represented by coefficients numbers. As explained in the literature review, the inverse prediction of material properties is very useful as, once the properties are predicted, it can provide direct input to a simulation programs (e.g. ABAQUS model) to predict the behaviour of products or structure made of the material. Indentation test is simpler than other standard methods (e.g. combination of compression and shear tests), it can be routinely used in relatively small samples, which is an advantage in materials development and comparison. In addition the ability of the program to identify/map out all the possible material properties will help to analyse the full picture with inverse modelling which previously could not be done with other programs.

As listed in Figure 4.1 the work in this chapter consists of two main parts. In the first part, the feasibility of directly using ANN to predict the material properties is evaluated. Two main areas are investigated: one is to assess its capacity to predict trained data; the other is to predict untrained data, i.e. data not used in the training or validation. Both approaches can be relevant to materials testing. The use of 2nd order and 3rd order polynomial curve fitting of the force displacement curve is compared. In addition, the use of single indenter approach and dual indenter approach is assessed. The dual indenter approach has been reported to be able to improve the robustness of inverse program in different materials. It is necessary to assess if this will improve the performance of the ANN program and, to establish what is the most effective way to deal with data from different tests. Potential influences of some issues such as neuron numbers was systematically established, which will provide a clear understanding of the situation (such as uncertainty of the predicted

results) about the use of ANN in inverse material property prediction with EVA foams.

In the second part of this chapter, a new approach utilising the direct ANN program developed (presented in Chapter 3) is proposed. The work involves developing a large data space using the high efficiency of ANN. A computerised program (with Web interface) is developed including functions of data generation through ANN, data storage, interface for input and viewing results. A searching program is developed which will enable the identification of any possible materials property sets that may match the experiment data within a predefined error range. This will be able to help the user to identify any possible materials sets that has a close match to the target, thus has full confidence in the inversely identified material properties. The approach is applied to analysis data from single and dual indenter methods through blind tests (with known material properties). The problem with both approaches was identified as the new program has the capacity to map out all the potential material set, so it is able to identify some problem which could not be identified in other methods and previous works. A new approach using foam of different thickness is then proposed, as EVA foams are normally supplied in different thickness. This is based on a hypothesis/assumption that with the same indentation depth, the deformation/strain level within the foam may be different with different foam thickness. This may generate a situation that the data from different thickness tests will provide extra information to predict the material properties. In addition, it is more convenient to use sample of different thickness rather than changing the indenter sizes. Potential approach using both different indenter size and sample thickness is also presented. To assess this approach, series ANN for different indenter size and thickness has been developed following the procedure reported in Chapter 3. With both approaches, dual indenter and the newly proposed dual thickness approach, a major research focus is to work out an effective way to identify the material data set that match testing data from both conditions. This is very important for the development of inverse modelling in particular for developing computerised process.

The accuracy and validity of the program is firstly assessed with blind tests (using numerical data as input/target) then used to predict the properties of the EVA foam samples.

This is not only further validating the program and method but also identifying issue with real material test data as they are not as perfect as FE generated data. Some key results of the real foam data is compared to the target and predictions from other programs and data processing method towards the end of the chapter. Some further analysis is to be presented in the discussion section.

Evaluation of the feasibility of using ANN in inverse prediction of the nonlinear material parameters with different indenter size:

- 3rd order and 2nd order polynomial curve fitting,
- Effect of data density in the training data,
- Single and dual indenter approach



Development of database and computer program for inverse material properties identification combining ANN direct P-h prediction and data mapping

- Development of a computer program incorporating the P-h curve prediction of ANN
- Evaluation of single indenter approach
- Evaluation of dual indenter approach with new data identification method
- Development of ANN for finite thickness foams and dual thickness approach to predict material properties
- Use of the inverse program in testing EVA foams and comparison with other



Discussion and future works

Figure 4.1 Flow chart showing the research in inverse prediction of material properties.

4.2 Evaluation ANN based inverse approach to predict material properties based on indentation curves.

4.2.1 Structure of the ANN and data process

Figure 4.2 shows the general structure of the ANN program used in the work. The program used the back-propagation learning method, which is applicable to multilayer network that uses differentiable activation functions and supervised training. The optimization procedure in the program is based on Levenberg–Marquardt (L–M) algorithm that adjusts weights to reduce the system error or cost function (*Esfahani et al, 2009*). As illustrated in Figure 4.2, the forward connections are used for both the learning and the operational phases, while the backward linkages are used only for the learning phase. Each training pattern is propagated forward layer by layer until an output pattern is computed. The computed output is then compared to a desired or target output and an error value is determined. The errors are then used as inputs to feedback connections from which adjustments are made to the synaptic weights layer by layer in a backward direction. For the trend line method, the whole curve were fitted with a polynomial trendline and each indentation curve was represented by the coefficients. The output is the material parameters, μ and α . The work in Chapter 3 with the direct analysis, 2nd order polynomial fitting is sufficient to represent the P-h curves, However, in an inverse process, there is a situation that two input parameters are used to fit two parameters. Another approach is to use 3rd order fitting as illustrated in Figure 4.3. This will generate a situation where three input and two output which may potentially enhance the performance of the ANN program. Figure 4.4 shows the structure of the multilayer layer feed-forward neural network for trend line method (b). In each case, there are three layers in the neural networks: input layer hidden layer and output layer.

Figure 4.5 shows the main data used in the evaluating the effect of ANN. As explained in section 4.1, the development of ANN can be used in two ways. One is to predict trained data, which can be used in materials testing by using a training data with high density, so

the properties determined will in certain way represent the material data set within a certain range of error. Another more ideal situation is to develop an ANN which is able to predict the properties of untrained data. This is technically ideal, but not necessarily able to achieve full homogenisation, this has to be investigated to be certain with the prediction results. Different form of data sets used in Chapter 3 for the P-h curve prediction, apart from materials data sets 1-3 (same as the data in Chapter 3), one additional high density (Figure d) has been developed by combining materials data set-1 and materials data set-3. Figure 4.6 shows typical curve fitting illustrating the accuracy of fitting with 3rd order polynomial fitting. Both 2nd order and 3rd are used, the results for the second order fitting is not shown as it is the same as the result in Chapter 3. In all cases, all the FE data of P-h curves can be fitted by 3rd order polynomial with a correlation coefficient over 98%. This suggests that the curve can be represented by the 3rd order polynomial fitting.

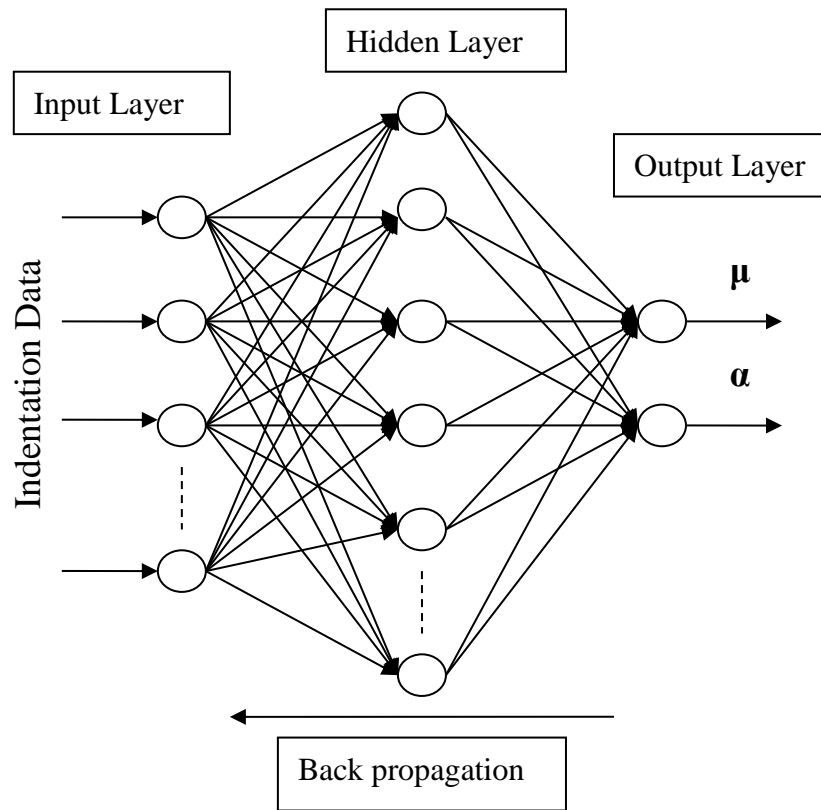


Figure 4.2 Proposed feed-forward neural network with back propagation Algorithm for estimating the material parameters (μ and α) based on indentation test data.

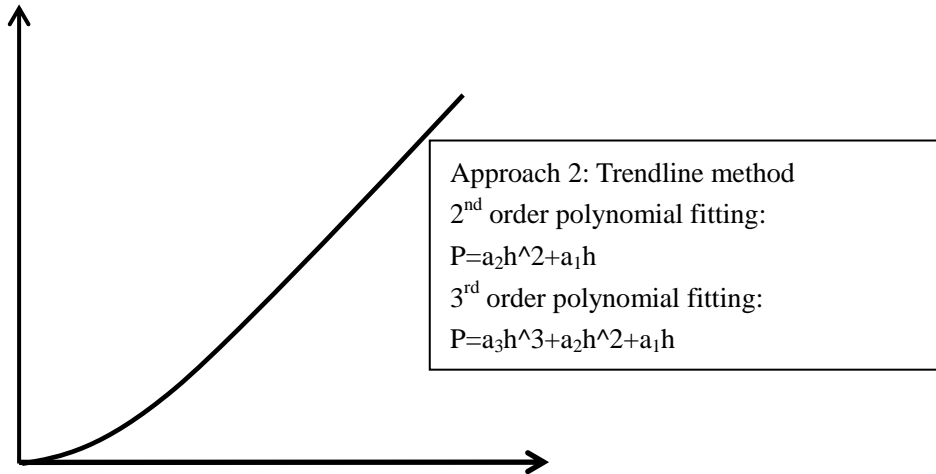


Figure 4.3 Schematic to show the two polynomial fitting approach.

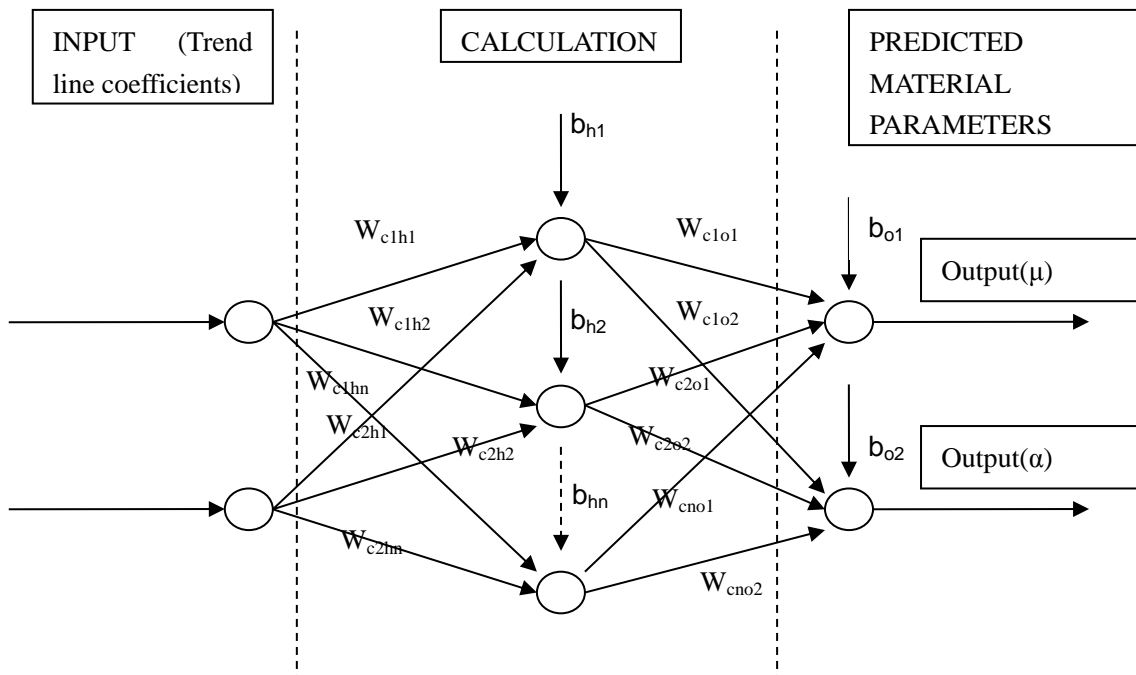
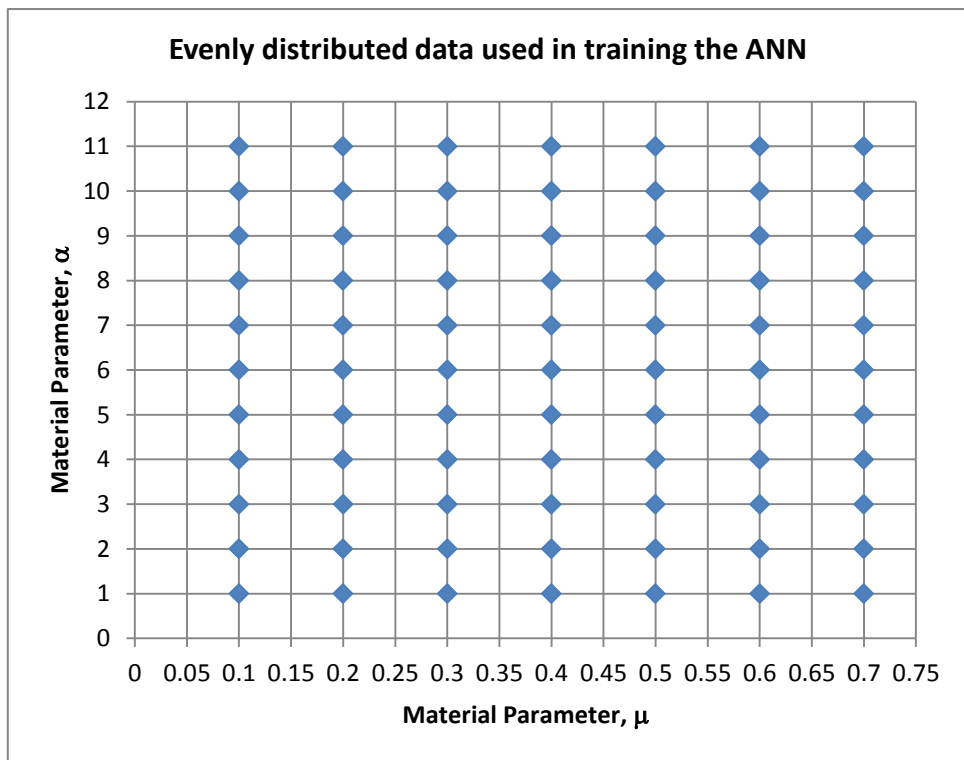
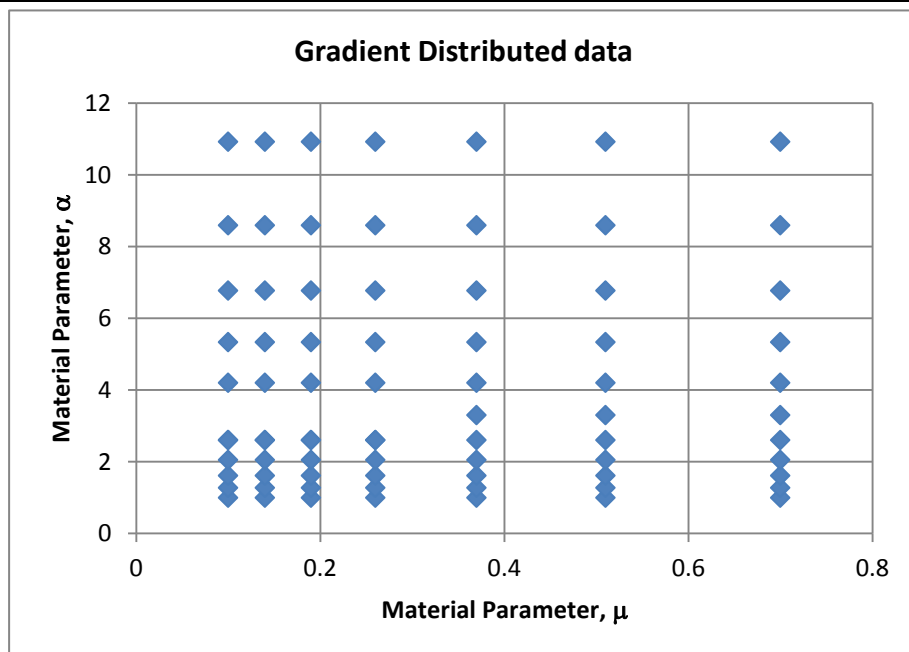


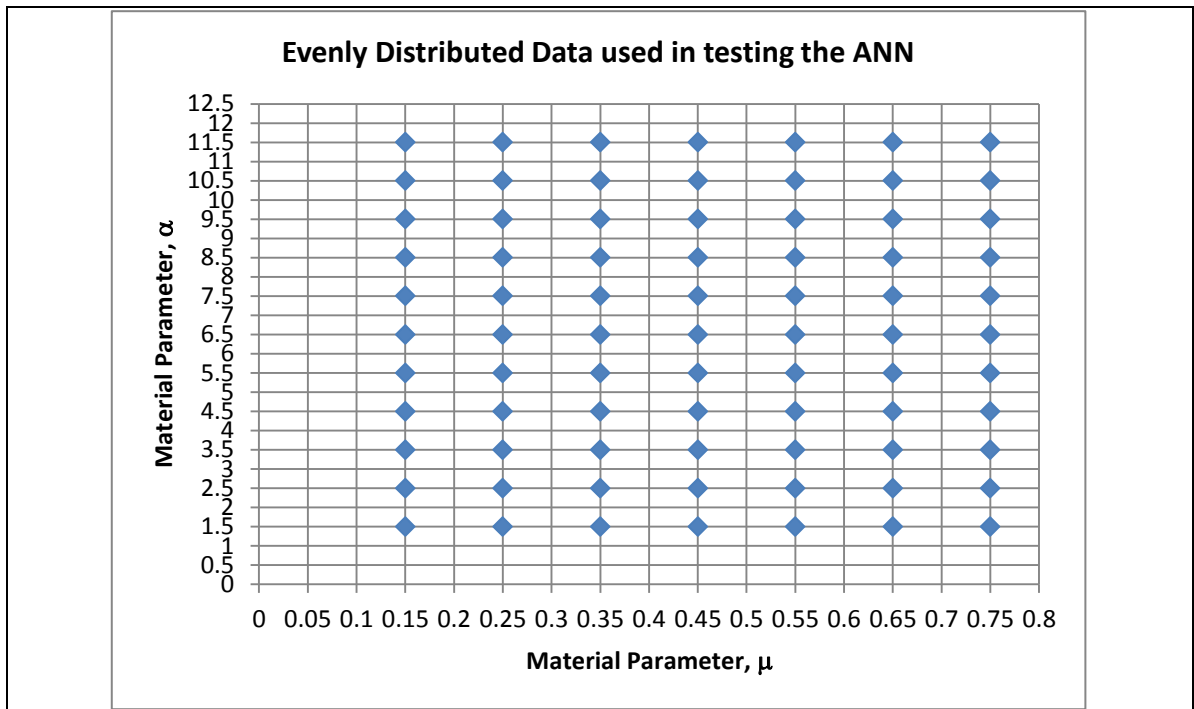
Figure 4.4 The structure of the multilayer neural networks for the trend line method.



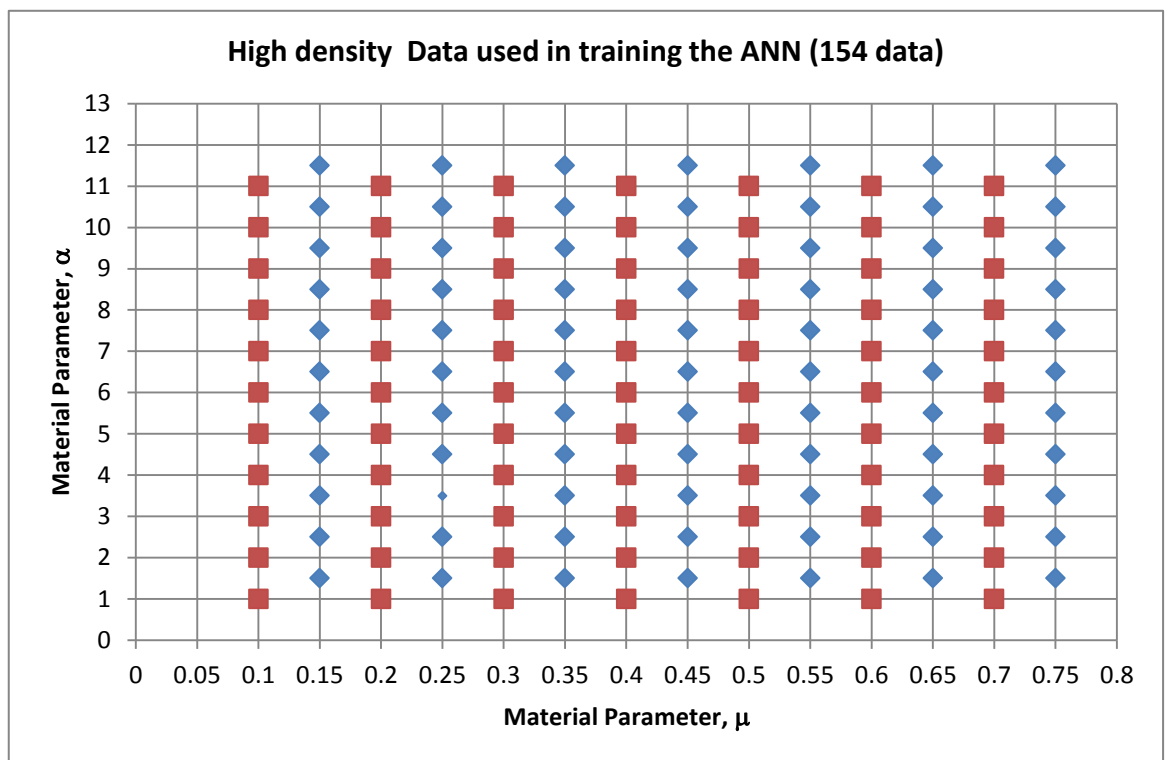
(a) Materials data set-1 (μ and α) used generate the training and validation data. The number and arrow shows numbering system used. The data is evenly distributed. Detailed values and numbering can be found in Table 3.1.



(b) Materials data set-2 (μ and α) used in the training and testing data. Detailed values and numbering can be found in Table 3.1.

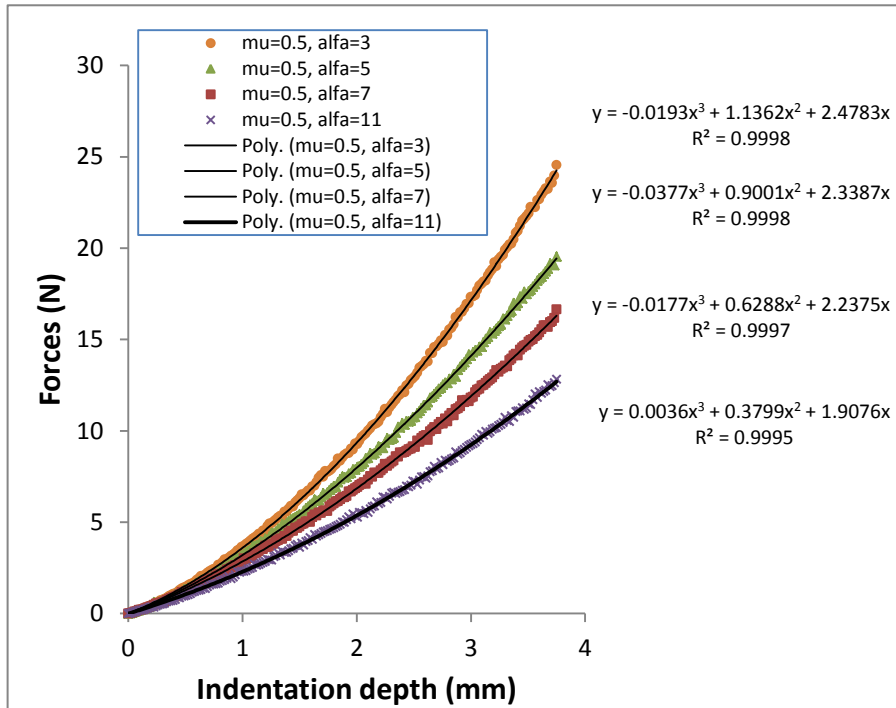


(c) Materials data set-3 (μ and α) used as the main testing data. Data used in testing and evaluate the accuracy and robustness of the ANN as untrained data. Detailed values and numbering can be found in Table 3.1.

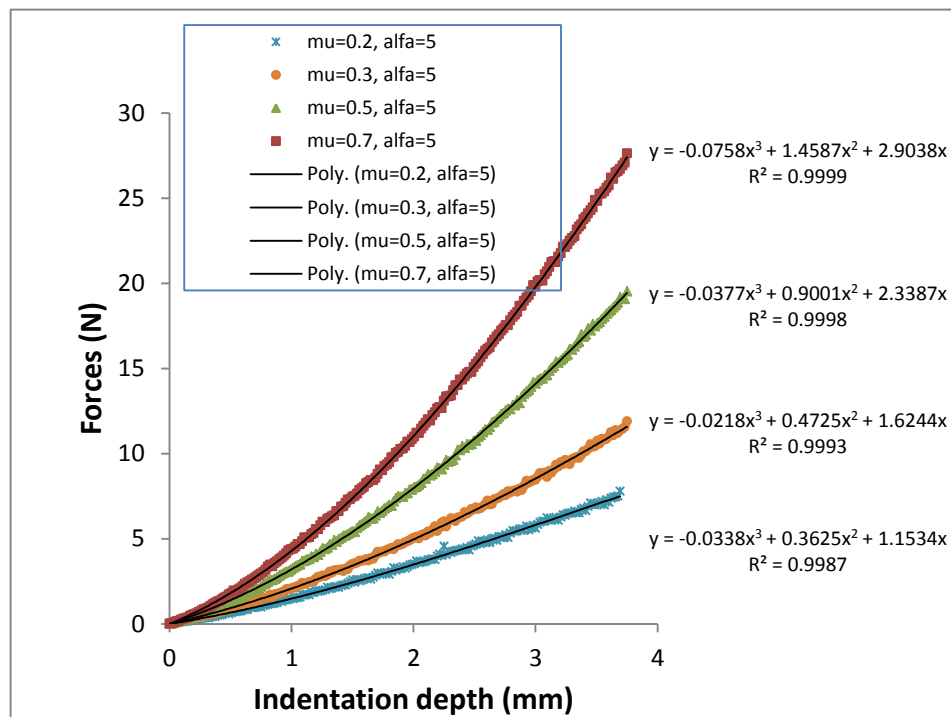


(d) High density data (data set-1 and data set-3)

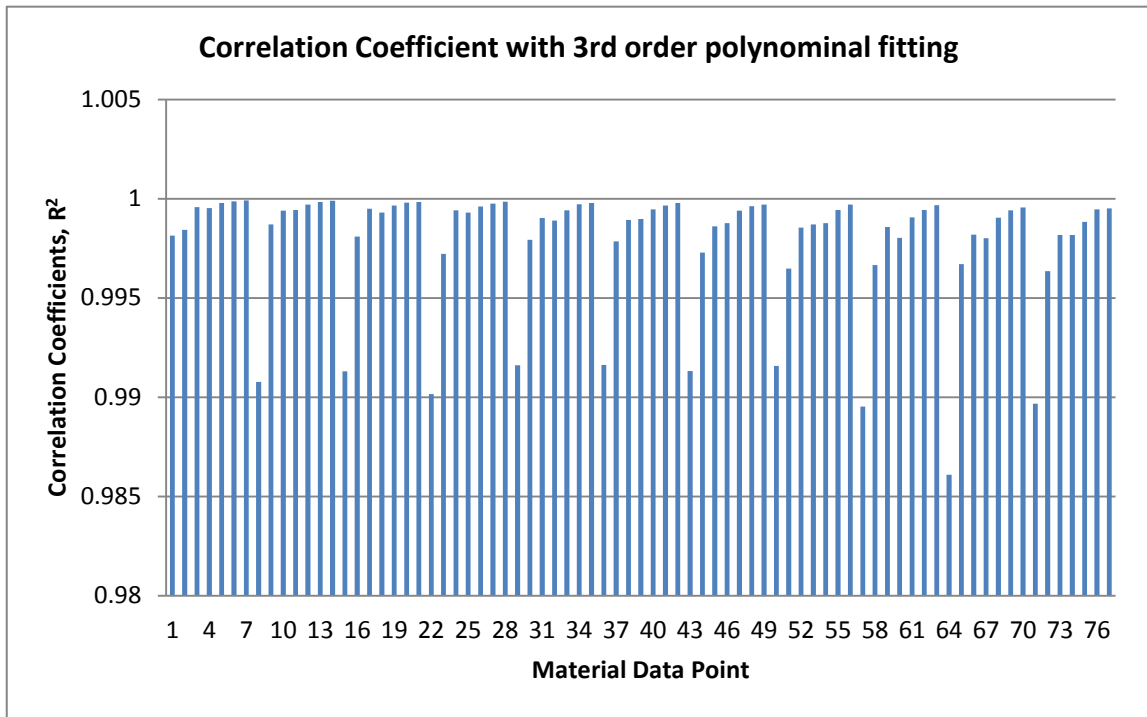
Figure 4.5 The matrix of training data for the ANN program.



(a) Typical FE indentation curves ($\mu=0.5, \alpha=1,3,5,7,9,11$) fitted with 3rd order trendline.



(b) Typical FE indentation curves ($\mu=0.2, 0.3, 0.5, 0.7, \alpha=5$) fitted with 3rd order trendline.



(c) Correlation coefficients of with 3rd order polynomial fitting (Material data set -1, distributed data as in Figure 4.6(a). (77 data)

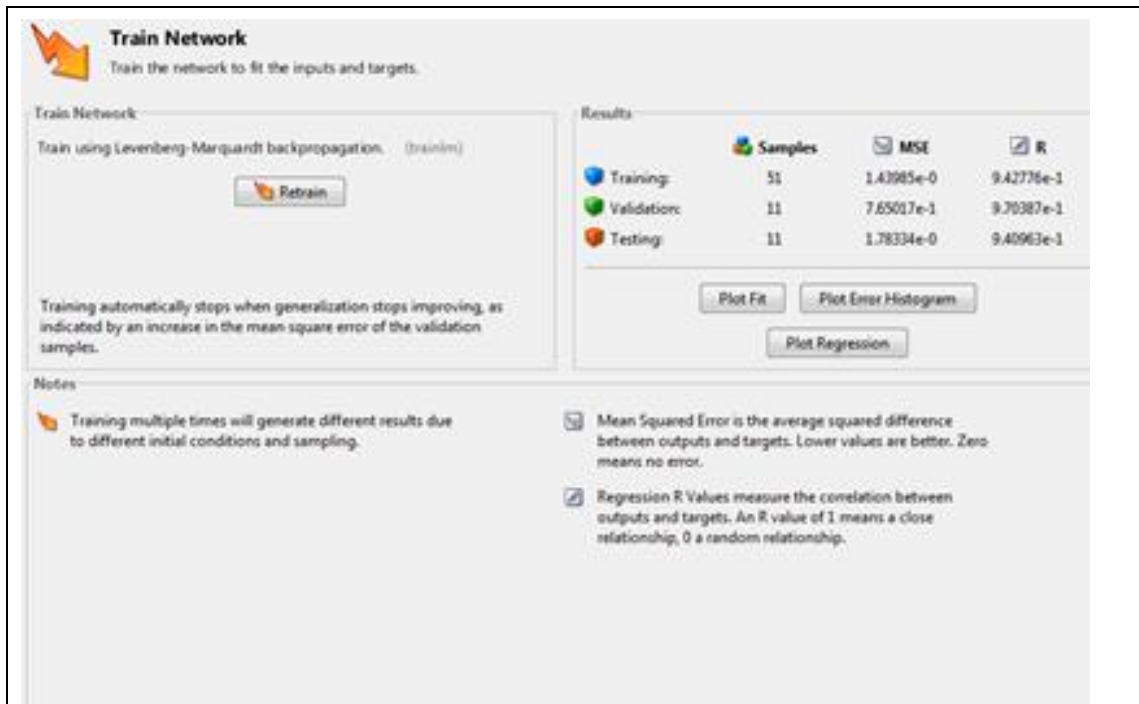
Figure 4.6 Typical FE p-h curves fitted with 3rd order polynomial equation. (2nd order polynomial fitting was shown in Figure 3.10)

4.2.2 Preliminary evaluation of the ANN using nftool and comparison between 2nd and 3rd order polynomial fitting.

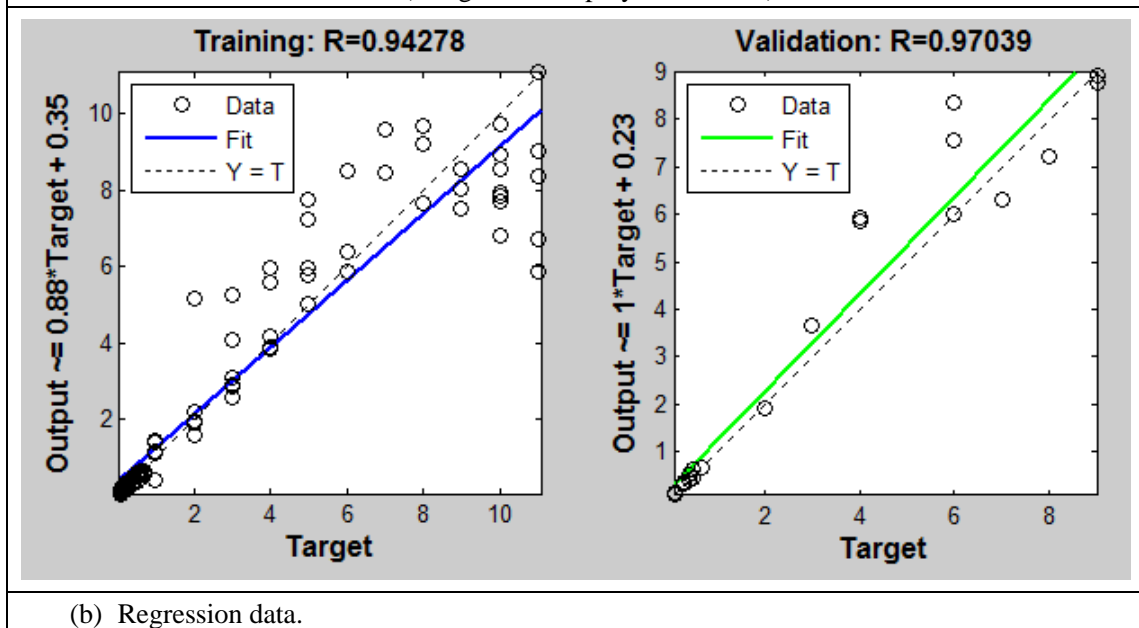
Due to the uncertainty of potential outcome of the inverse program, the nftool in MATLAB is used to evaluate the potential outcomes. nftool offers some useful function such as automatic partition of the data between training, testing and validation. It also has a direct re-training function, which will allow the determination of an optimum/best MSE for each situation. This suits the work as the two main purposes in using ANN for prediction with trained data and untrained data rather than going through a complex process using ANN code. Some typical results are used to demonstrate the characteristics of the nature of inverse prediction.

Figure .4.7 shows a typical fitting performance with material data set-1 (77 data, 70% training, 15% validation and 15% testing) based on data of second order polynomial coefficients. The data clearly showed that the regression is very poor, which suggest that the ANN could not be used for this. Further trials have been made to increase the number of neurons, but the MSE remains very high, as shown in Figure 4.8. Each of these data of MSE is determined by repeatedly re-training the ANN (at least 10 times) and the minimum value of MSE is used to represent the best possible conditions. The data clearly suggests that the 2nd order curve fitting coefficient approach could not be used. Also plotted in Figure 4.8 are the best MSE for trials where the P-h curves are represented by the 3rd order polynomial curve fitting coefficients. It is clearly shown that the output of the 3rd order fitting results are much better in particular in training with high number of neurons. A typical set of data is shown in Figure 4.9. With neuron number of 10, the regression is of very poor quality for both training and validation. But with neuron of 100, the regression quality of the training has been dramatically increased; but the regression of the validation data is still very poor. This work used relatively low number of data for validation (5%). If we increase the data percentage for validation, the performance will be even poorer. These work shows that 2nd order polynomial fit is not suitable for representing the P-h curves in the inverse parameters identification process, but potentially, the 3rd order coefficients

potential can be used to predict trained data. This is further checked by running an ANN with 100 neurons using the trained data (Material data set-1) as the input. The relative error of the predicted material parameters ' μ ' and ' α ' is plotted in Figure 4.10(a), most of the error for the 77 data are within 0.05 (less than 5%), with a few data lower than 0.1. While the error for the case to predict untrained data is all very high between up to 50% or 100%. Most likely, this is an over fitting situation, in which predicted data has been converged to the closest trained data, so the error in the data are very high. These results confirms that the ANN could only be used to predict trained data.



(a) Screenshot showing the function of the partition of data between training, validation and test and retrain functions (using 2nd order polynomial data).



(b) Regression data.

Figure 4.7 Typical result data when using nftool function in NN box with second order curve fitting coefficients. (Materials data set-1, Training data 70%, Validation data: 15%, Testing data: 15%).

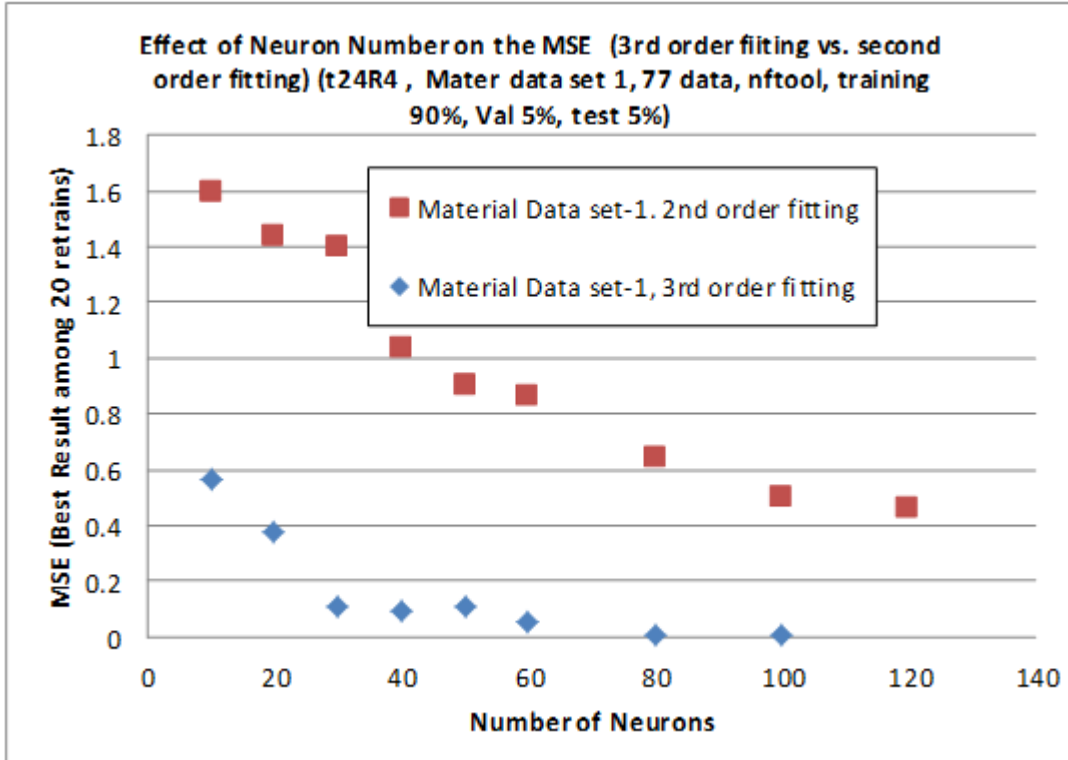


Figure 4.8 Effect of neuron number on the training MSE. (nftool) based on 2nd and 3rd order fitting data.

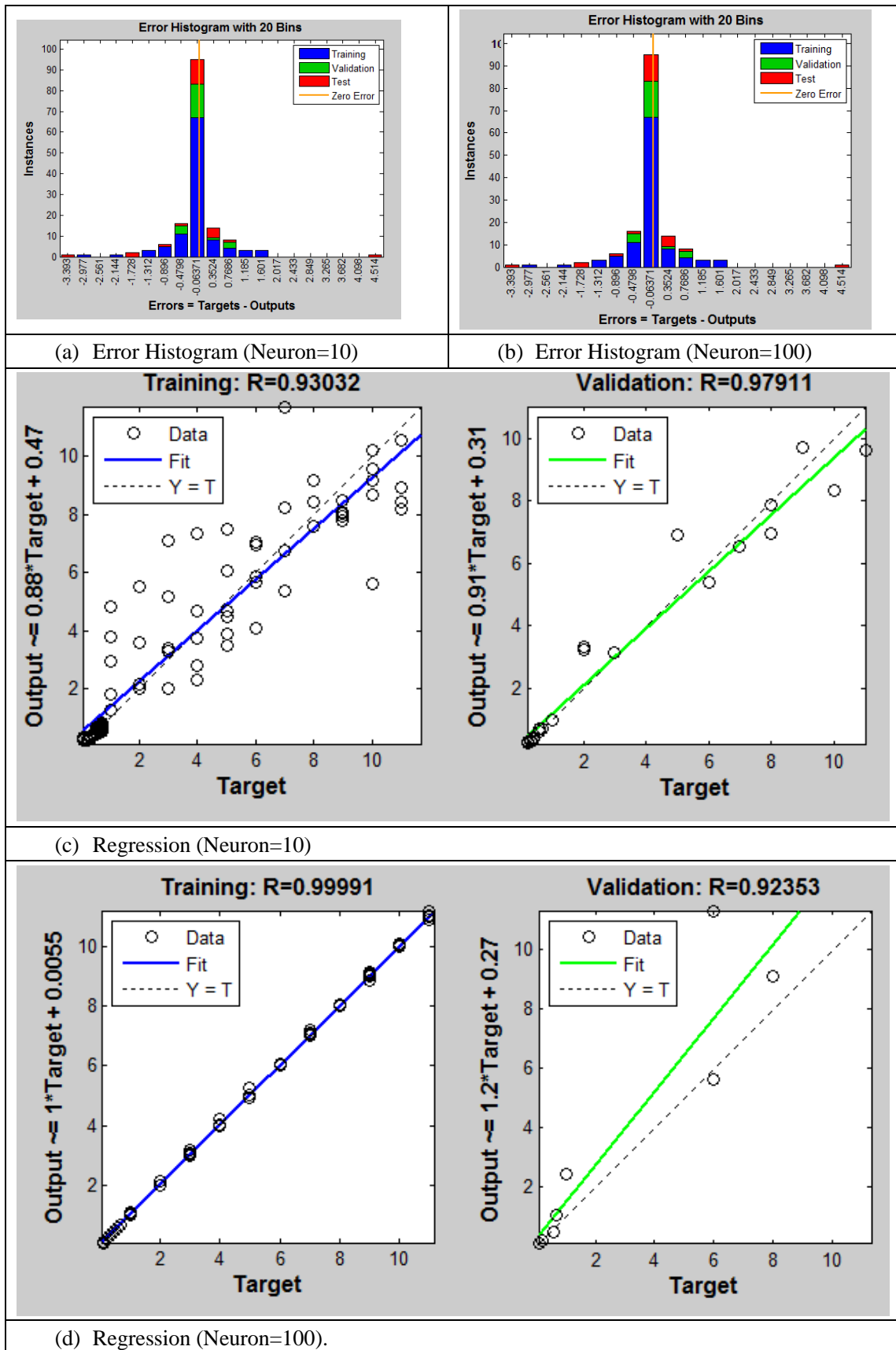
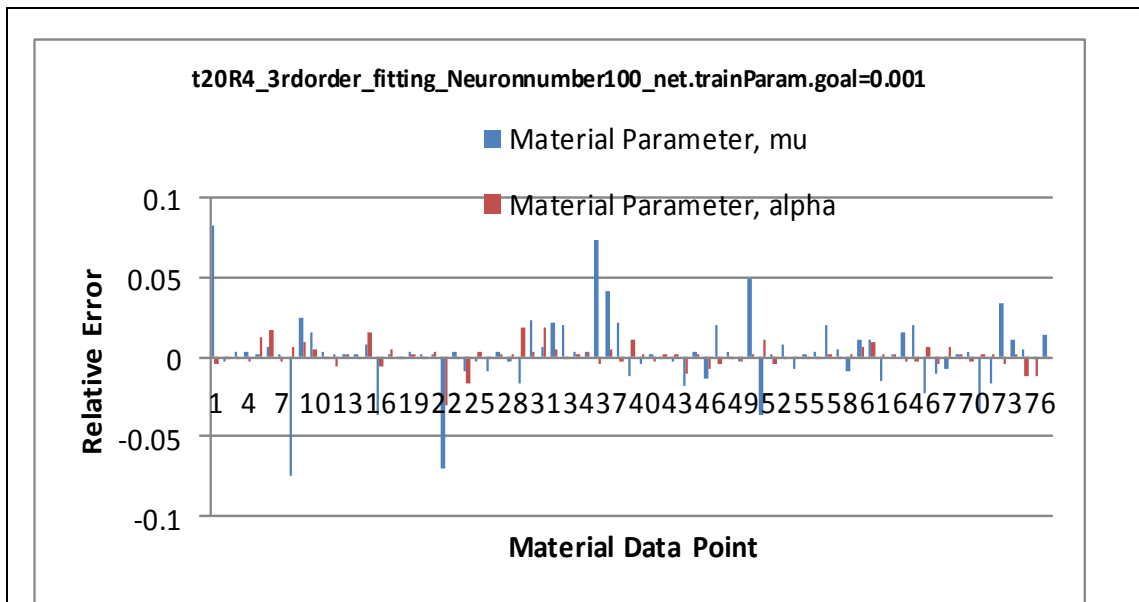
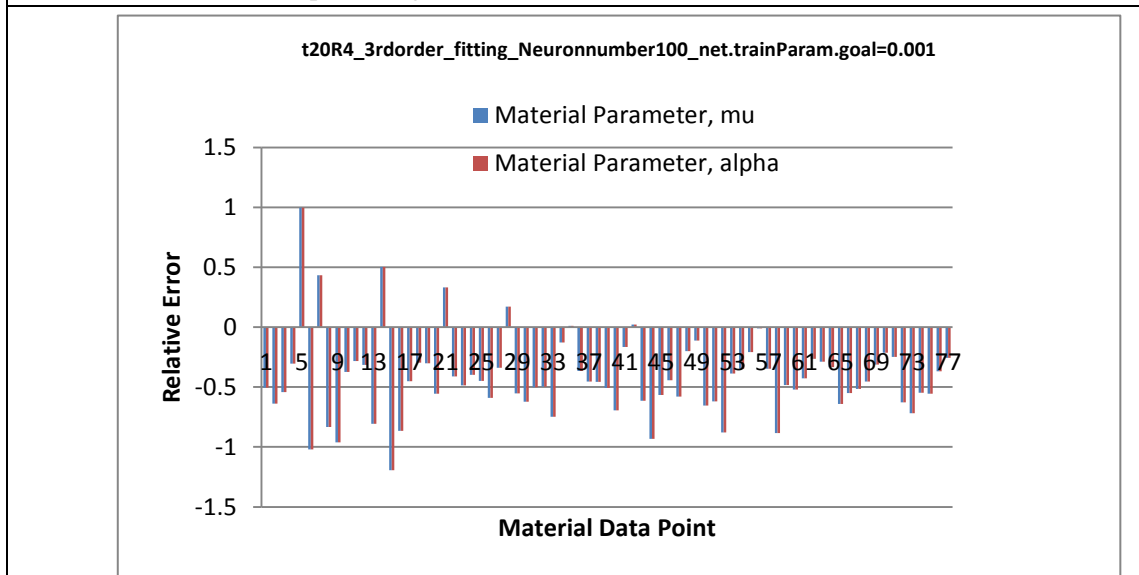


Figure 4.9 Typical data showing the effect of neuron numbers on the training results with 3rd order polynomial fitting showing the training accuracy can be improved but the validation accuracy is not improved.



(a) Typical ANN prediction data of trained data (materials data set 1) showing the prediction is reasonable for predicting trained data.



(b) Predict the untrained data showing that the prediction is not accurate.

Figure 4.10 Typical results with Material data set-1 as the training data (Neuron 100) to show that it can be used to predict train data (a) but can't be used for untrained data (b).

4.2.3 ANN based inverse with different data density.

The preliminary works shows that with 3rd order fitting, the prediction of trained data is possible while inverse with data not used in the training is not feasible. When using the function of ANN in predicting trained data in material properties identification, the density of the data has to be fine/dense enough to make this meaningful. The training data has to effectively cover the material data range (within a predefined error), then the ANN can be used as a prediction tool for new data. These are assessed by using material data set-4 (Figure 4.5d) in the ANN program; It was used as training data first, then used as the test data. The relative error between the predicted parameters and the target material parameter is calculated. Figure 4.11 (a) shows the regression results of the training and validation (5%) with neuron of 100. The x-axis is the material data point, the vertical axis is the relative error of the predicted material parameters. It shows that the regression with dense data set (154 data) is not as good as the one with 77 data (Figure 4.9). Figure 4.11(b) compared the relative errors with a ANN using 100 neurons, most of the material data showed lower error but there are a few with higher error range (over 10%). Similar results can be observed/repeated when re-run the ANN. The number of neuron is further increased for the dense data, Figure 4.11(c) shows the relative error of the predicted material properties when the neuron number is increased to 200. It is clearly shown that the quality of the prediction has been increase; with only one predicted material point has an error of over 10%. This clearly shows that the number of neuron is critical when using the ANN to predict trained data.

These results with different material data sets (Figure 4.10(a) and Figure 4.11(c)) suggest that it is potentially feasible to train the ANN with high density data and then use the trained ANN (without re-run of FEA) to predict the material parameters through a proper selection/matching process. To this aspect, the gradient data process may represent a better way to provide the training data as it can clearly control the relative error range of the material properties. Figure 4.12 (a) shows the MSE change with the number of neurons using materials data set -2 as the training data. With lower neurons, the MSE is very high,

and it reaches a reasonable level with Neuron number of 60-100. Figure 4.12(b) shows the relative error with neuron number of 100. Most of the predictions are within 5%. Further increasing the goal (from 0.01 to 0.0001) shows little improvement in terms of the accuracy. Further work has been conducted on training data with finer materials properties. A typical set is shown in Figure 4.13(a), in which both the parameter ' μ ' and ' α ' is increased by an increment of 10%. (as compared to ~30% in increment in Material data set-2). Figure 4.13(b) shows the ANN predicted trained data. Most of the prediction is within 5%, this suggests that the prediction is accurate even with high density data. With such data, it is possible to use the data to predict the materials properties within 10% or even finer.

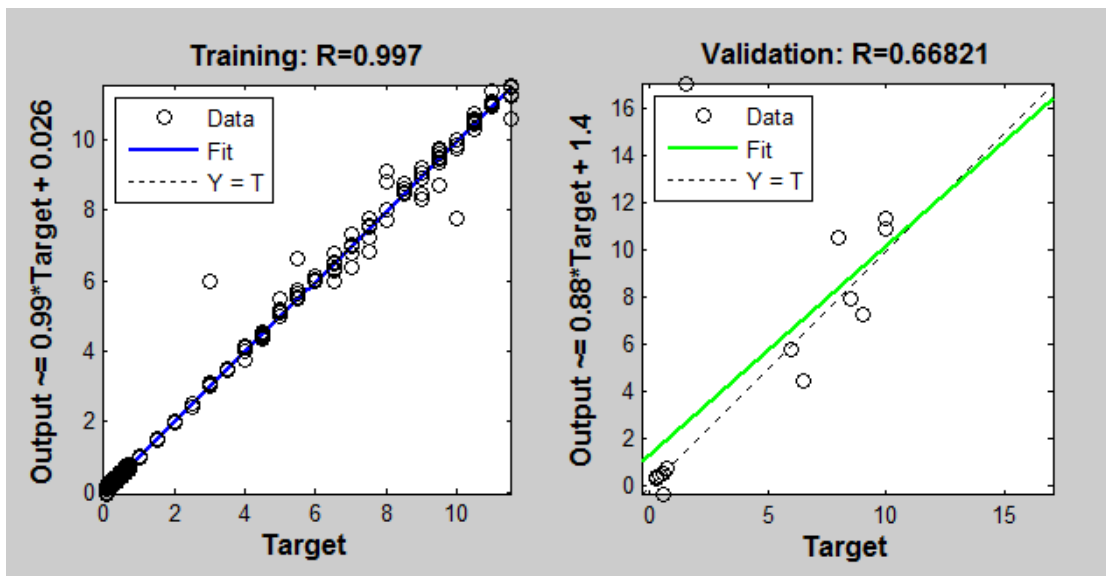


Figure 4.11(a) Typical regression for training with high density data (Materials data set 4, 154 point, 90% used in training, 5% used in validation and 5% used in testing). (Neuron 100).

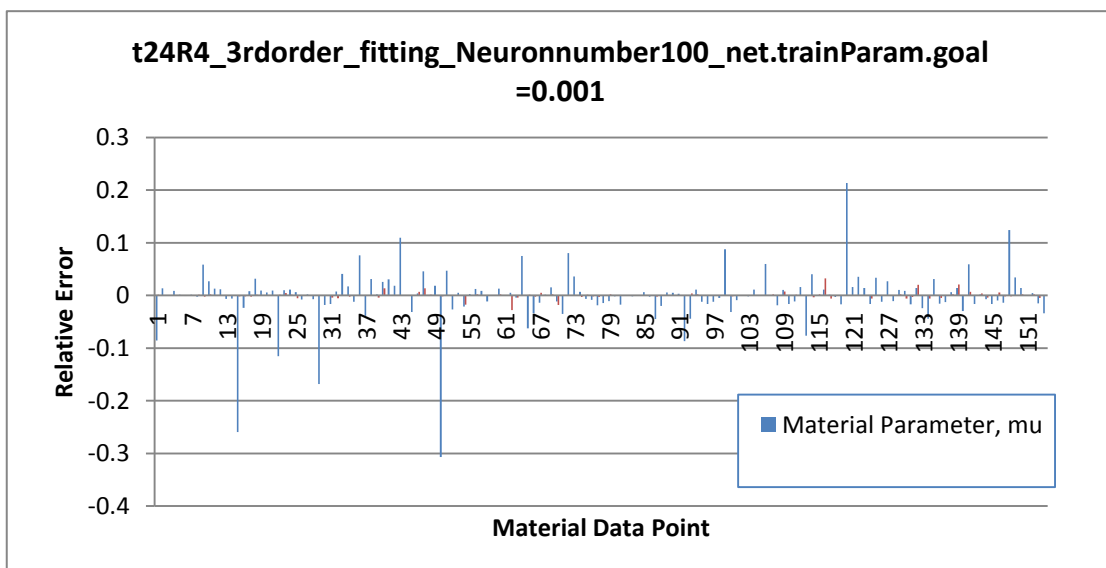


Figure 4.11(b) Typical ANN prediction data of trained data with high density data. (Materials data set 4, Neuron =100).

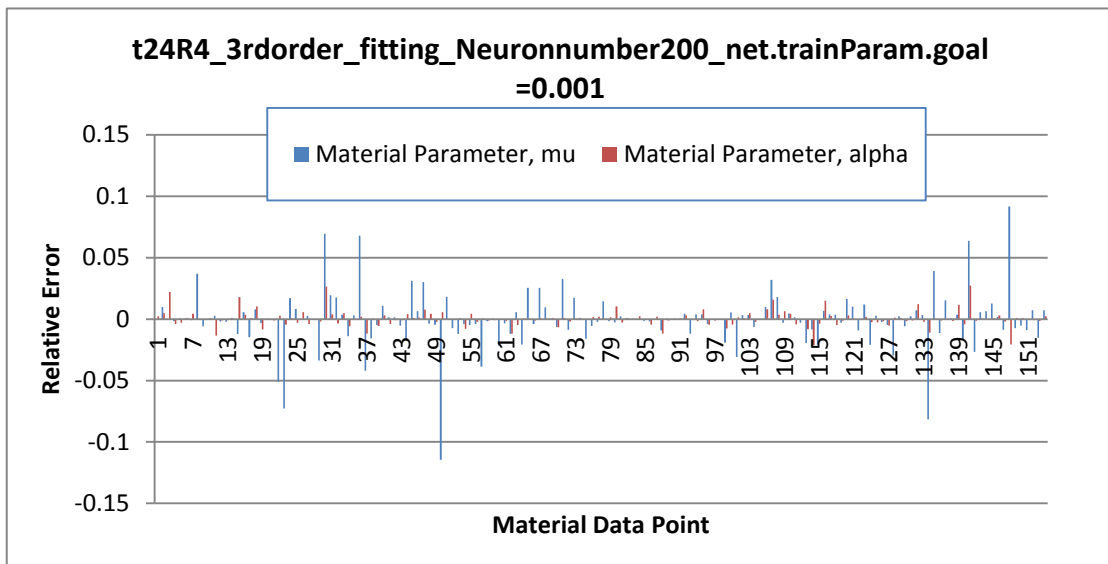
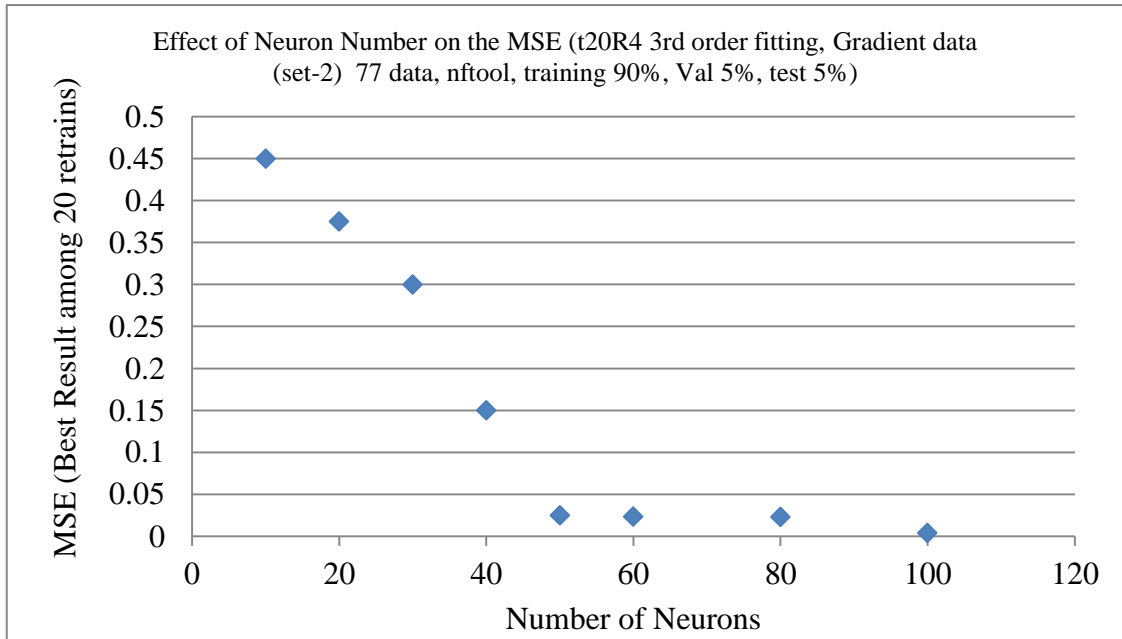
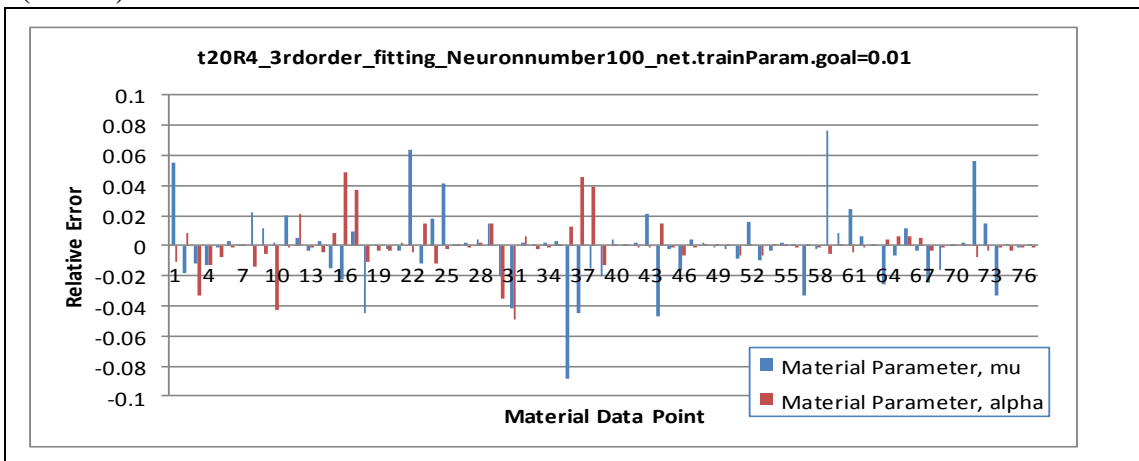


Figure 4.11(c) Typical ANN prediction data of trained data with high density data. (Materials data set 4, Neuron =200).

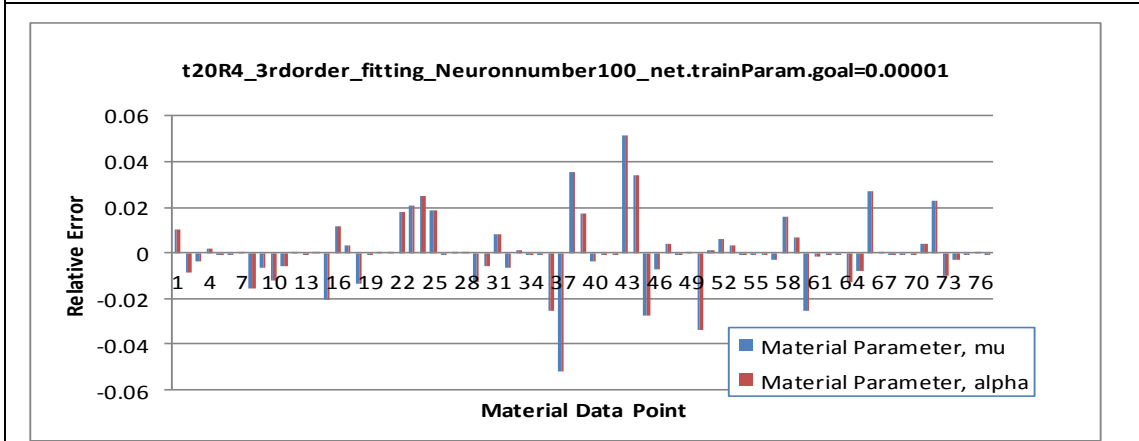
Figure 4.11 Typical ANN prediction results with trained high density data (Materials data set 4) and different neuron number showing that the neuron number needs to be increased when use high density data.



(a) Effect of neuron number on the training MSE with gradient data (material data set2). (nftool).

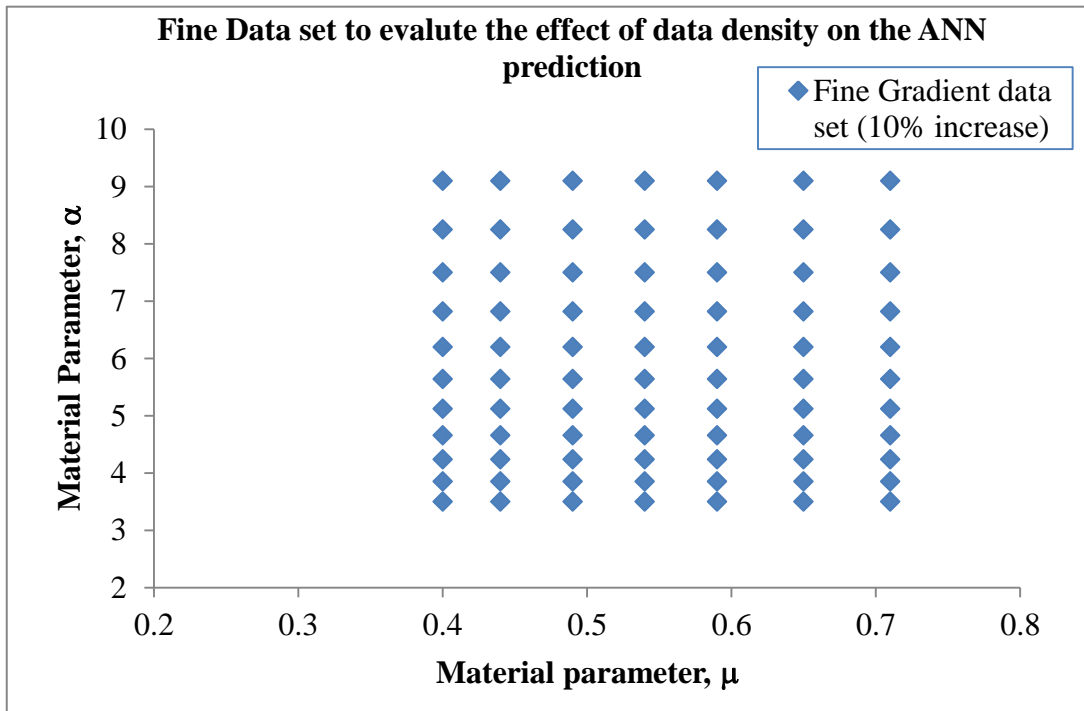


(b) Typical relative error when using gradient data as the training data. (neuron100, goal=0.01)

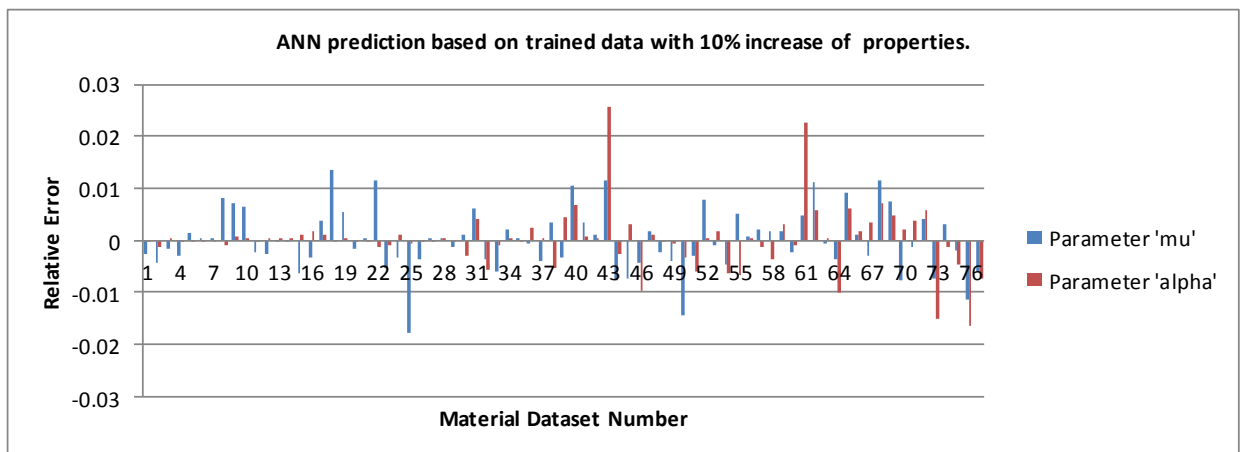


(c) Typical relative error when predict training data. (neuron100, goal=0.00001)

Figure 4.12 Typical results of ANN using the gradient data (Materials data set-2) in predict trained data showing the effect of neuron number on MSE and the value of goal on the prediction accuracy.



(a) Typical fine data with 10% increase of materials properties.

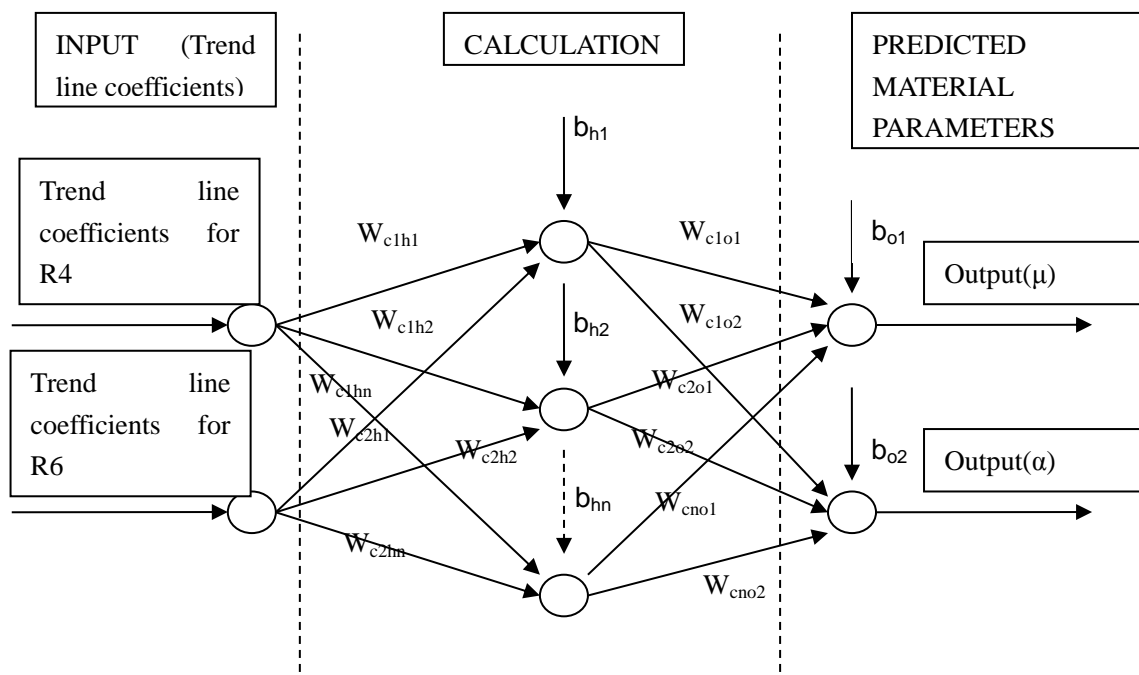


(b) Relative error of the predicted properties using trained data.

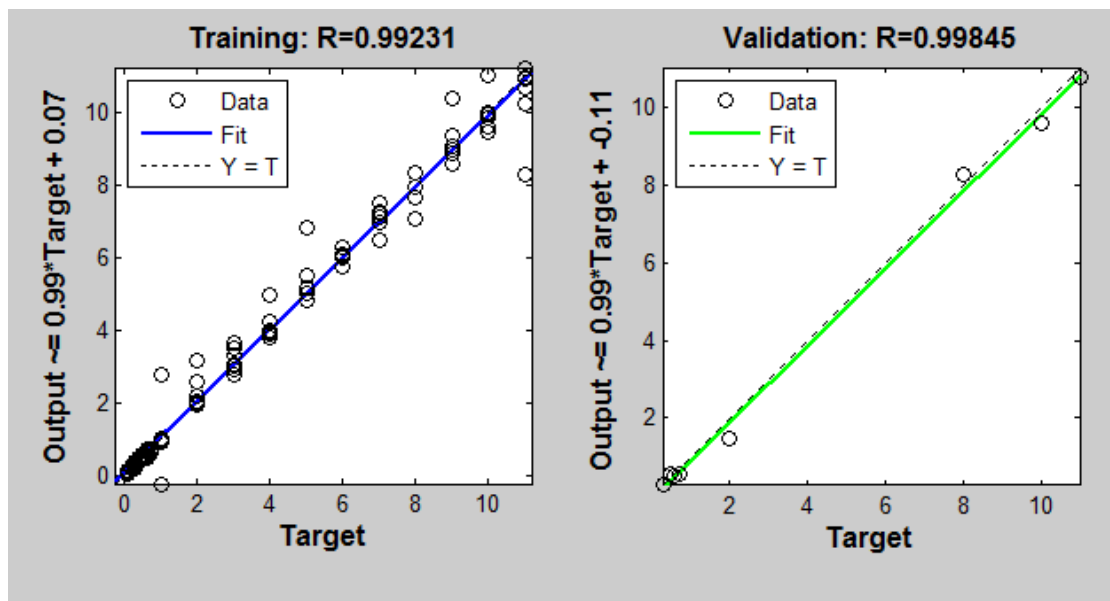
Figure 4.13 Typical fine training data with 10% increase and ANN prediction results showing this approach could be used to inversely predict the material parameters based on trained data.

4.2.4 ANN prediction of material parameters based on dual indenter approach

Most of the data reported in the last few section is based on data from single indenter (R4mm in radius) data. As discussed in 4.1, using data from additional indenter size as input may potentially improve the results. Figure 4.14(a) shows the ANN structure with dual indenters. In this process, the input includes the 3rd order polynomial curve fitting parameters for two indenter sizes, one is radius of 4mm (designated as R4) and one is radius of 6mm (designated R6). The predicted outcome is material parameter ' μ ' and ' α '. Figure 4.14(b) shows a typical regression data with nftool. Compared to the single indenter approach (Figure 4.9), the regression of the training data is not as good as the single indenter approach, but the regression of the test data is much better. Figure 4.15(a) shows the MSE of ANN with different number of neurons with the dual indenter approach. Different from the single indenter approach, there is no clear trend showing the effect of number of neurons. Figure 4.15(b) shows typical relative error of the ANN predicted of the training data. Compared to the results with the ANN data for the single indenter approach (Figures 4.10, 4.11, 4.12 and 4.13) in predicting trained data, the accuracy is not as good, several of the data has error over 10%. Figure 4.15(c) shows the prediction of untrained data, the error is still high (maximum value over 30%), but it is much better than the single indenter approach (Figure 4.11(b)) where the error is as high as 100%. However, even though the accuracy is increased, it is still not accurate enough to be used for material testing and characterisation. A new approach is required to use ANN or related method to predict untrained data.



(a) The schematic diagram of multilayer neural network for the trend line method with dual indenters (R4 and R6).



(a) Typical regression data.

Figure 4.14 The structure of the multilayer neural networks for dual indenter approach (a) and typical regression data (b). (Materials data set-1).

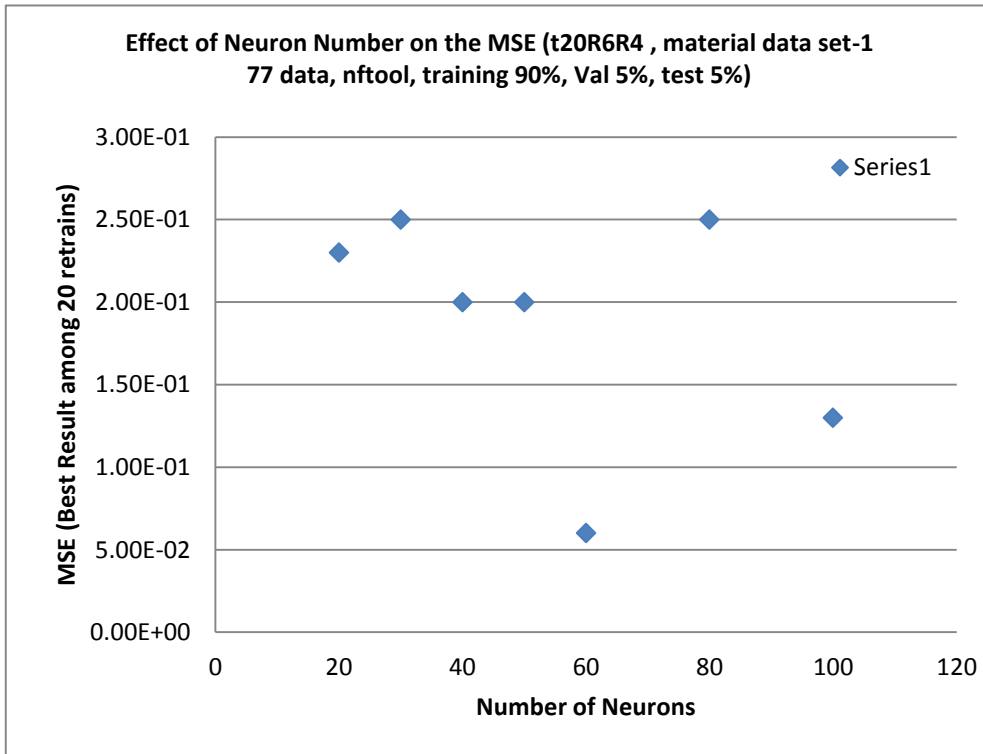


Figure 4.15 (a) Effect of neuron on MSE based on dual indenter approach.

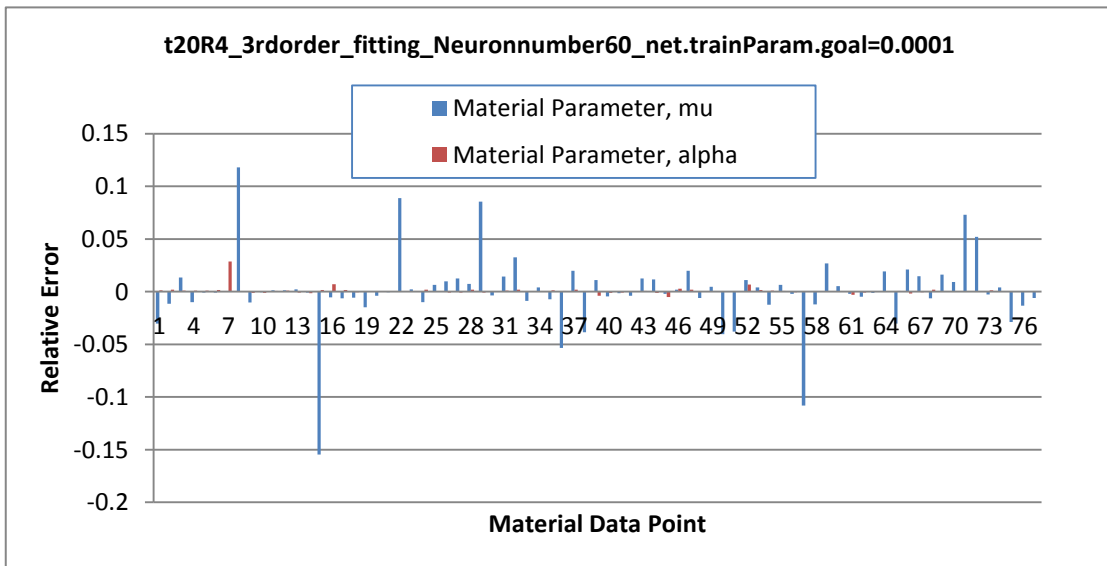


Figure 4.15(b) Predict trained data with dual indenter (3rd order training data, neuron 60).

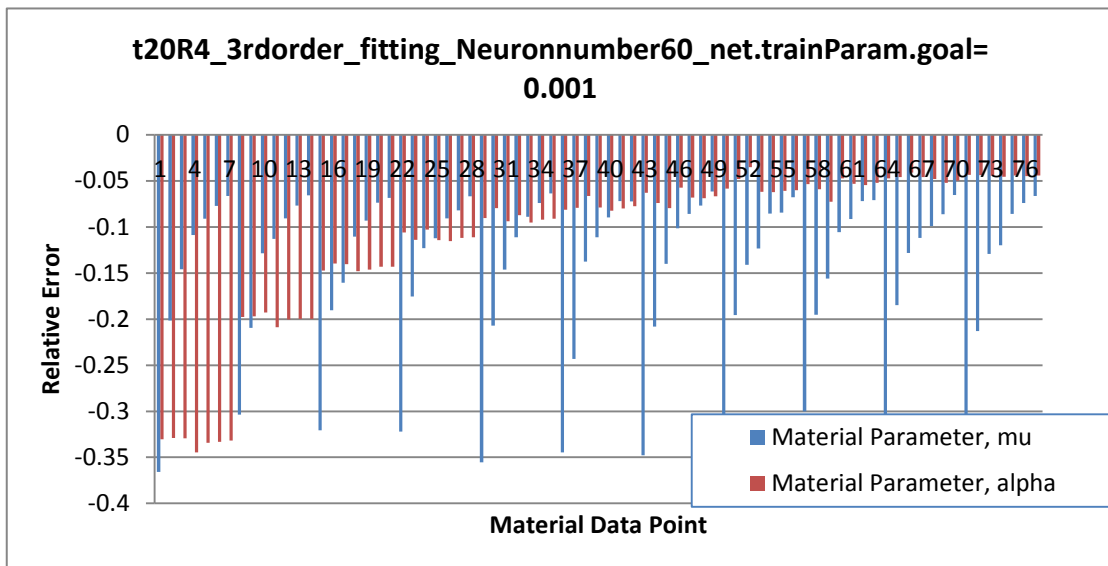


Figure 4.15 (c) Predict untrained data with dual indenter (3rd order training data, neuron 60) showing that dual indenter approach could improve the accuracy than single indenter but the results are still not good enough.

4.3 Material properties identification based on data mapping approach, computer program and results

To be able to identify all the potential material parameters for a P-h curve and develop a method to determine unique material parameter by combining data of different testing conditions, a new computer based approach is proposed and designed. The program used the function of direct ANN method established (chapter 3) to generate detailed data over a wide range, then search the database to establish potential material properties that produce P-h curves close to the target. This allows the mapping out of any potential materials sets. Further work is conducted to establish a proper method of filtering/matching data when indentation data from indenters of different sizes or sample of different dimensions.

4.3.1 Structure of the inverse materials parameter identification approach and computer program.

Figure 4.16 is a flow chart showing the inverse material properties identification process based on ANN predicted P-h curve and fitting parameters. The program consists of three main parts. In the first part, a range of materials parameters are used as input to the direct ANN program to predict P-h curve parameters as detailed/validated in Chapter 3. The range of μ and α can be changed by the user through a computer interface. The P-h curves are automatically analysed, and stored in a database forming a simulation space. A program is developed based on an objective function comparing the P-h curves based on input data (curve fitting coefficients) and the p-h curves of all the data in the simulation space. The simulation space included a group of *P-h* curves from the ANN prediction covering a wide range of material properties. Given the calculation speed of ANN is very fast, so the data can be as fine as possible (very small increment of material properties can be used). This is a significant advantage of ANN based P-h curve generation than FE based approach. In the searching process, the program calculates the difference between the P-h curve of the input data and all the *P-h* data in the simulation. In other words, it maps out all the materials data. In each case the optimum material parameters (for a user input error range), which

produces the *P-h* curves matching the input results within a certain error range were determined by mapping the objective function. In this case, the absolute value of relative error averaged over a large number of different indentation depth is used.

$$G = \sum_{i=1}^n ABS \left(\frac{Fi,e - Fi,n}{Fi,e} \right) / (n) \quad (4.1)$$

where :

- *G* is the objective function that needs to be minimised.
- *Fi,e* is the experimental force of the indenter at the observation *i* and *Fi,n* is the numerical model force of the indenter at the observation *i*.
- The number of observation (*indentation depth*) is *n*.

The simulation space (i.e. all the *P-h* curves) was produced using the established ANN program presented in Chapter 3. Compared to FE modelling, the process is much quicker with lower requirement on computational resources, allowing the development of much dense data (i.e. data with close properties or small increment). The predicted outcome from the ANN is the curve fitting parameters, which were then recorded and stored into a database to form a simulation space. Several computing language is used for different function in the program including effective searching and data storage technique. In the searching process, the *P-h* data was transformed into a discrete form with evenly spaced points against the indentation depth (termed indentation points). At each indentation point, the objective function values are calculated. The inverse program was evaluated using blind tests with numerical experimental data (numerical results with known material properties). This is a commonly used practice in developing inverse programs (Delalleau *et al*, 2006). It allows the uniqueness, accuracy and sensitivity of these inverse methods to be systemically investigated.

Figure 4.17&18 shows the interface of the program defined. In the first part, the user is able to produce the *P-h* curves using the ANN program. The user can decide the range as well as density (i.e. increment) of the material property data. The data is then stored in a

searchable database/space In the searching part, the user needs to define the 2nd order polynomial curve fitting coefficients of the input P-h curve, and the error range for the property prediction. The program will automatically identify all the materials data set which gives P-h curves close to the input/target within the error range as illustrated in Figure 4.18. The advantage of this specially developed program is to give the user the ability to deal with all the potential materials rather than just give one final value of the lowest error; this will produce a more comprehensive picture for the situation. This can be useful for material testing to produce all potential material parameters, further research is then conducted to establish a proper procedure to process data when using testing data form different conditions. In this work the use of data from single indenter, dual indenter or dual thickness are to be explored.

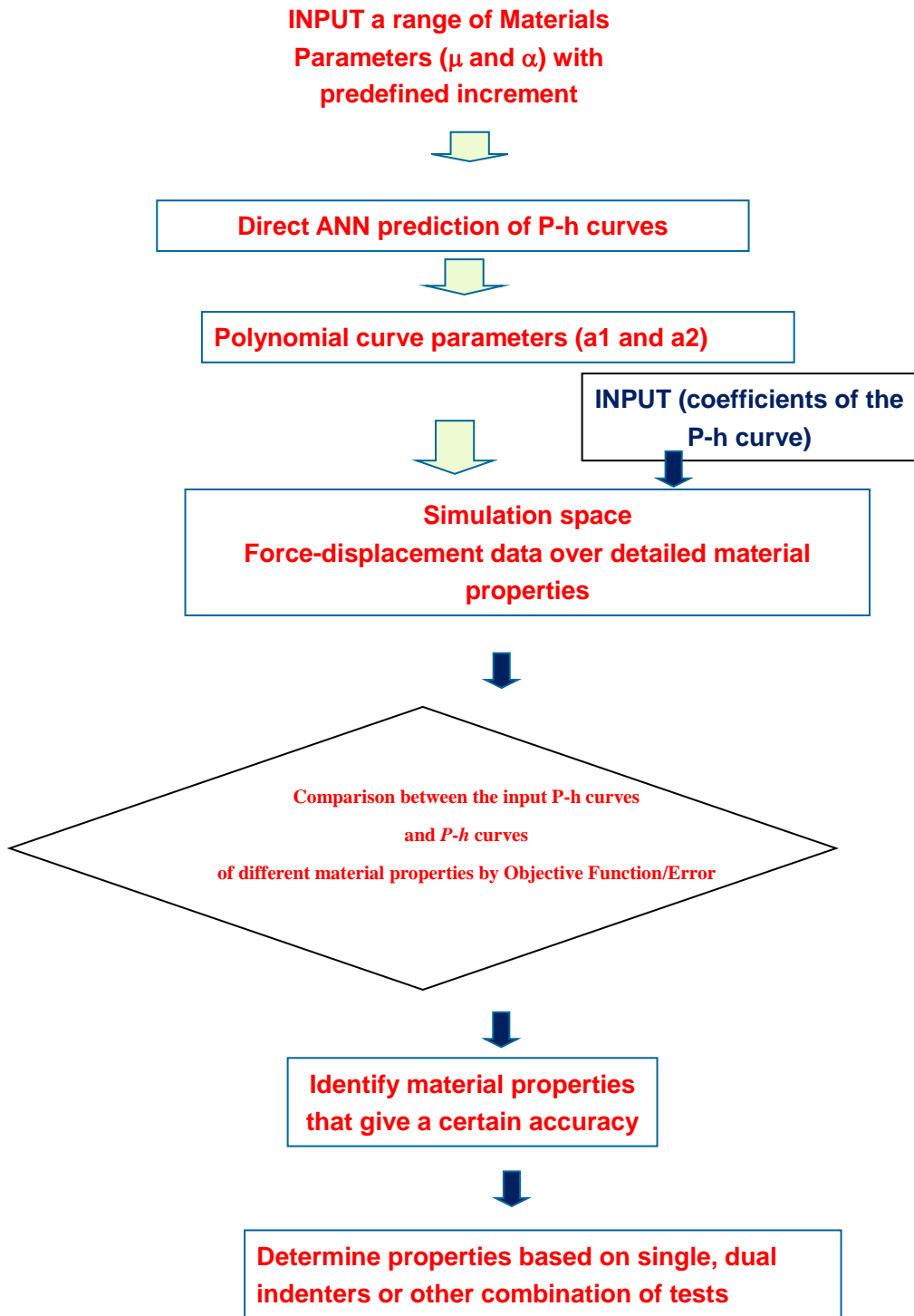


Figure 4.16 Flow chart showing the inverse FE modelling approach based on the data from ANN direct p-h curve prediction.

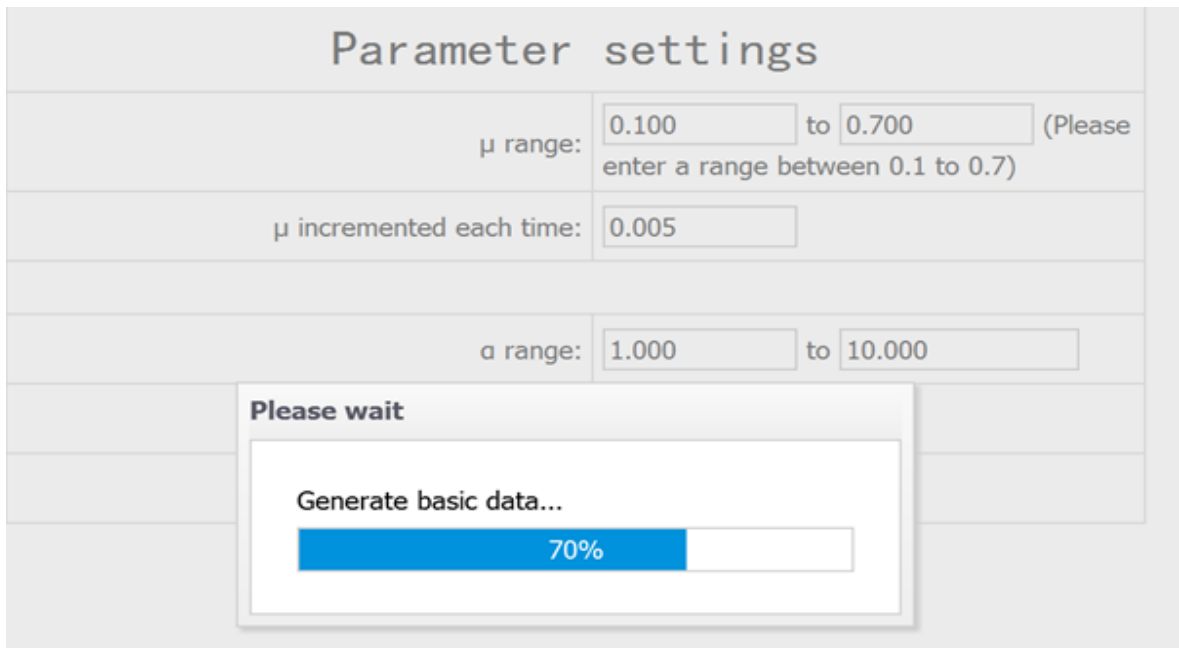


Figure 4.17 Screen shot to illustrate the data generating function of the computer program developed based on the ANN direct p-h curve prediction.



Figure 4.18 Screen shot to show the structure, input and error setting of the computer program developed.

4.3.2 Inverse FE modelling based on the test data of a single indenter

This section briefly present the process and results when using the single indenter approach. In the simulation space, the parameter ' μ ' was varied from 0.1 to 0.7 with an increment of 5% each time. The parameter ' α ' used were from 1 to 11, with an increment about 5%. The program can produce data of any density, but this relative large increment (upper limit of acceptable material variation for EVA foams based on experience) could test the accuracy of the program effectively. The input data was transformed into a discrete form with evenly spaced points against the indentation depth (termed indentation points). In this work the input numerical experiment curve was divided into 100 points. For each indentation depth, there is a corresponding simulation space (force) over a potential range of material properties. At each indentation point, the objective function value is calculated using predefined program in the database for each set of material properties (σ_y , n), then the average of the objective function averaged over the whole indentation curve was determined.

Figure 4.19(a) is a typical numerical $P-h$ curve with known material properties ($\mu=0.3; \alpha=6$) used as numerical experimental data in the blind test. Figure 4.19 (b) plots the material points with lower objective function values (relative error) of different range. As labelled by the legends, the material data are grouped based on the relative error between the numerical $P-h$ curve and the input data within 1% (not including 1%); within 1-3% (not including 1%); 3-5% then 5-10%. The error used is average error for all the depth points. It is clearly shown that the data with lower objective error are distributed along a stripe with μ and α increasing/decreasing at the same direction. Please note that as shown in Figure 4.6, the force will increase with increasing ' μ ', while decrease with increasing ' α '. So such a trend shown in Figure 4.19(a) is reasonable. As the effect of these two parameters may cancelled each out, so there are material properties totally different in value but could produce similar $P-h$ curves. Multiple FE models have been developed with the three different material properties with relative error lower than 1% (as circled on the figure) and the $P-h$ curves are compared with the input numerical experiment data. As

shown in Figure 4.19 (c), these $P-h$ curves are very close to the input data. This suggests that these material sets have different material properties but very close $P-h$ curves, in other words, the material property could not be determined uniquely using single indenter data only.

The same approach has been applied to other indenter sizes with the same sample thickness ($t=20\text{mm}$). A typical example is shown in Figure 4.20 with the same input ($R6$, $\mu=0.3$, $\alpha=6$). Figure 4.20 shows the properties which give relative error within different ranges for $R6$. Similar to the case for $R4\text{mm}$, there are several material data points which has lower relative error. One difference is that the number of material properties which have a very low error (e.g. within 1%) is different from that for $R4$. There is only one point has error below 1% while for $R4$ (Figure 4.19), there are several points producing relative error within 1%. But there are still a large number of material data have relative error within 3% for $R6$, which will all have $P-h$ curves very close to the target. It could not be proper/practical if only pick the one with lowest error. Similar to the practice for the $R4$ data, a few points with lower relative error has been picked to compare the $P-h$ curve directly and the result is shown in Figure 4.20(b). All the curves are very close to the input/target $P-h$ curves suggesting that the prediction is not unique. In other words, it is difficult to pick the optimum property based on a single indenter data. Similar approach has been performed on several other material properties, similar output was obtained; this suggests that the use of single indenter is not unique, difficult to be conclusive in deciding a single property.

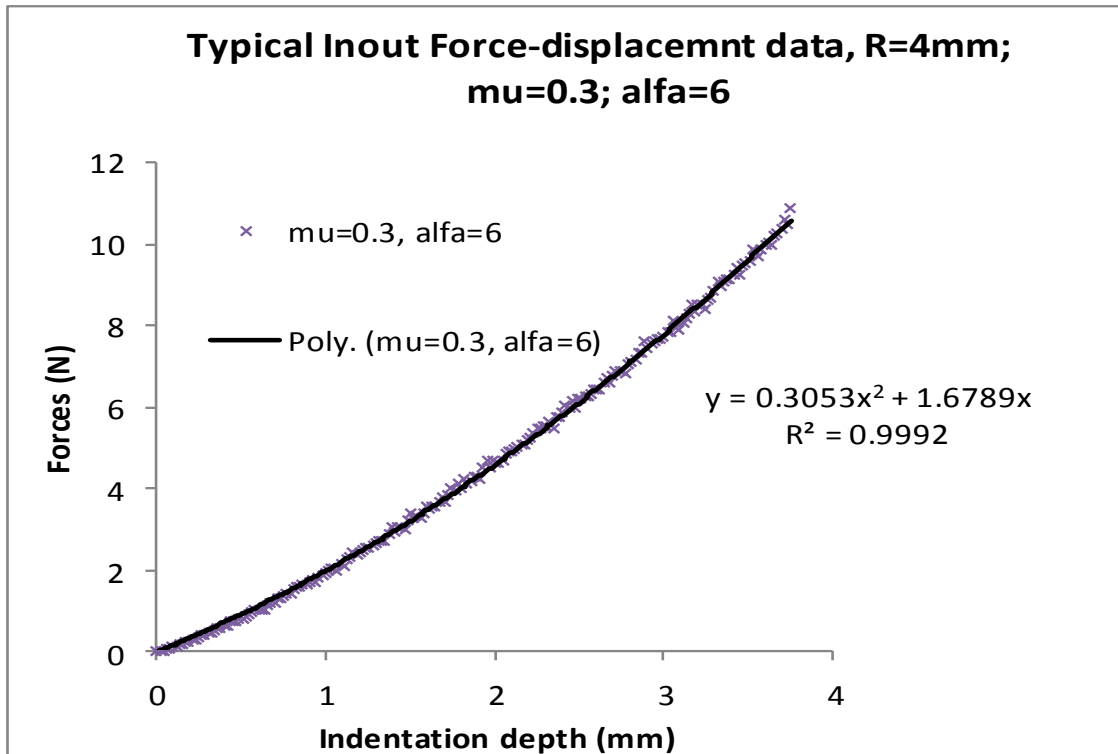


Figure 4.19 (a) Typical input data and curve fitting coefficients used to evaluate the inverse computer program.

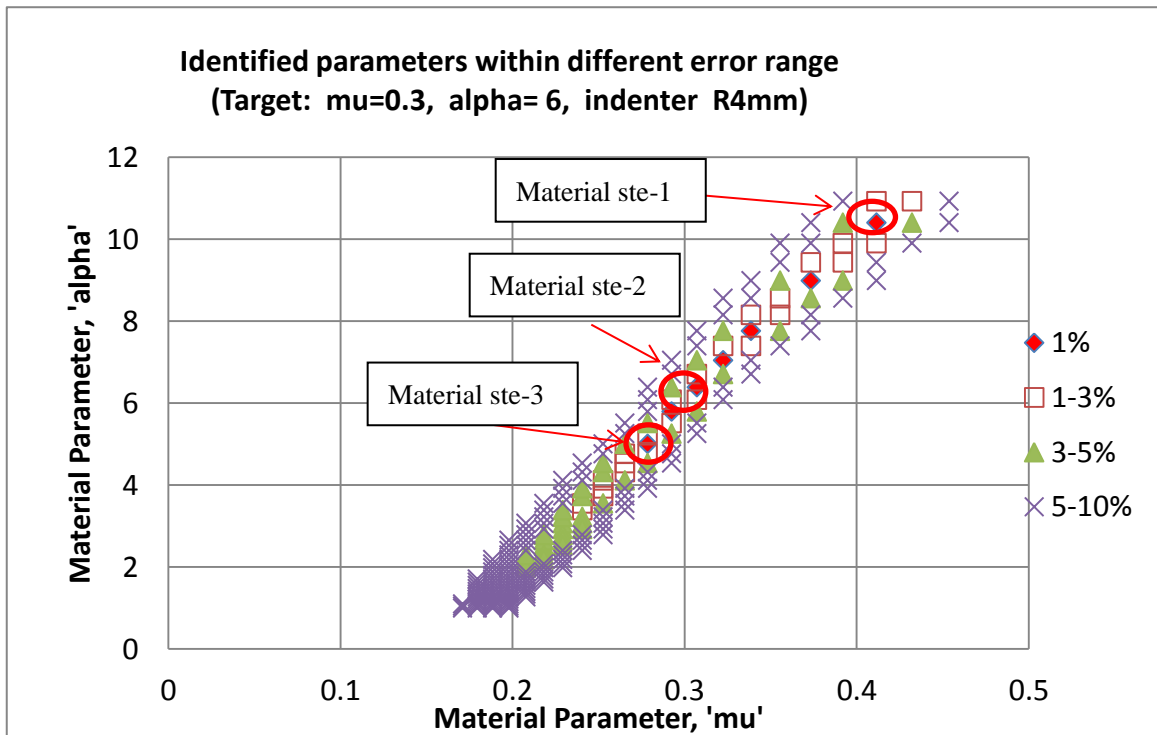


Figure 4.19(b) Data with different relative error. The labelled data are used to compare indentation curves.

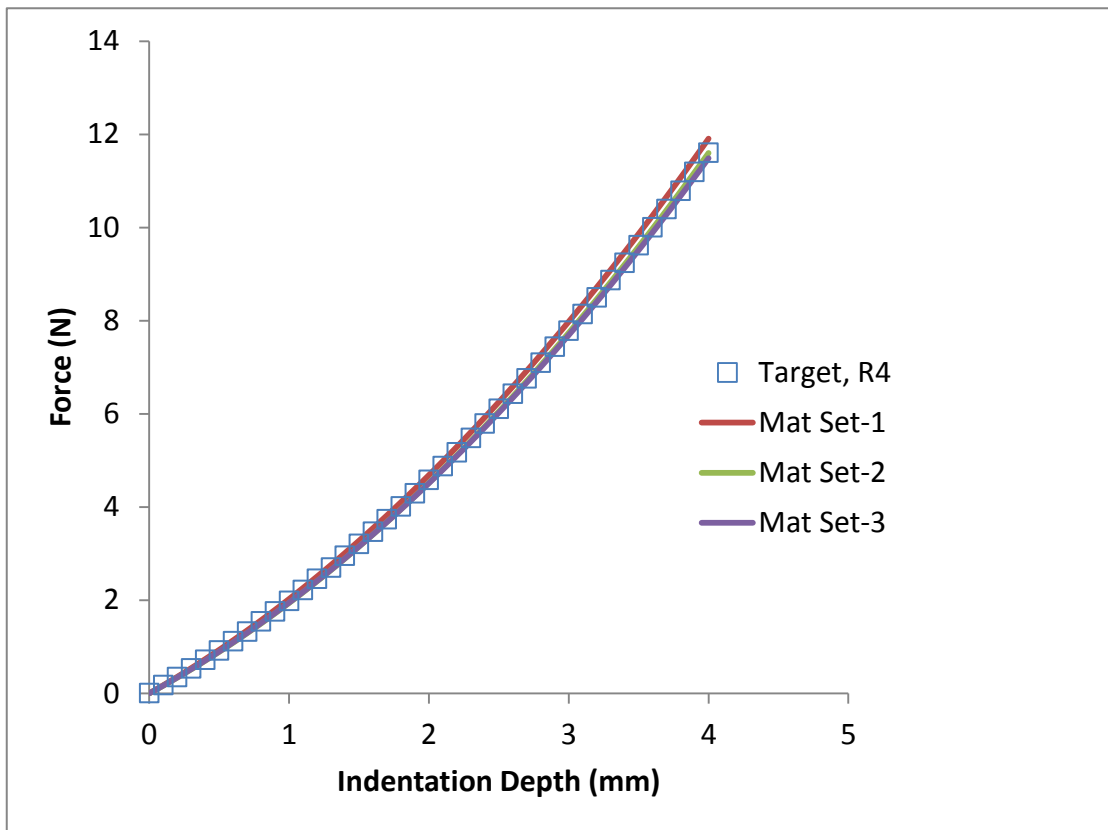
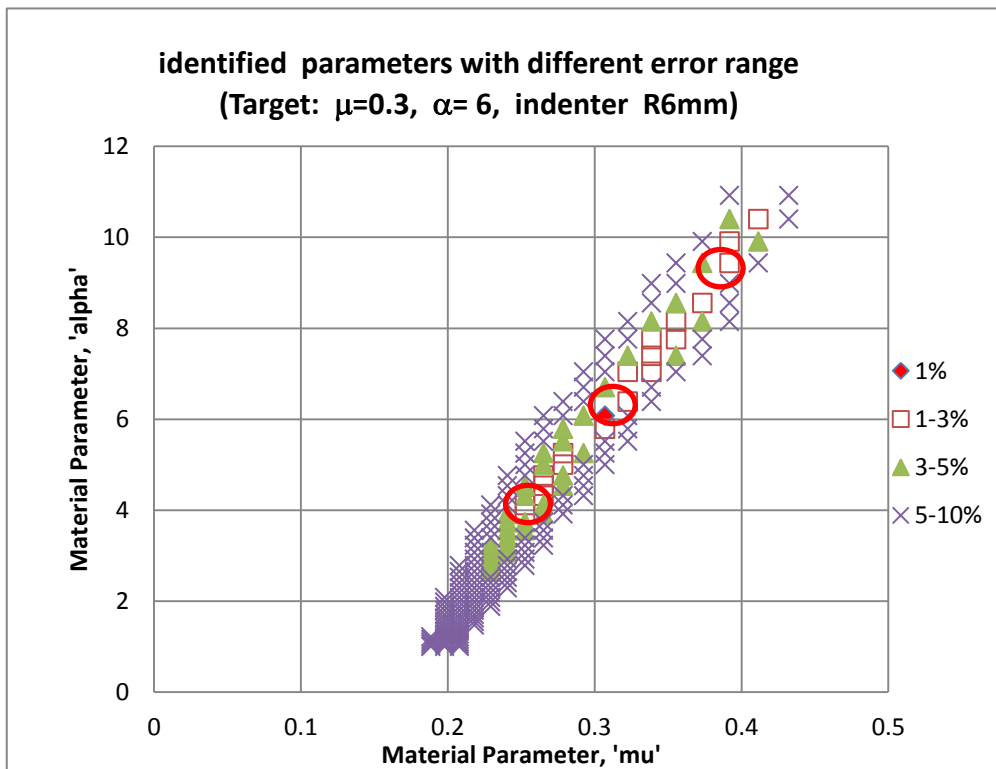
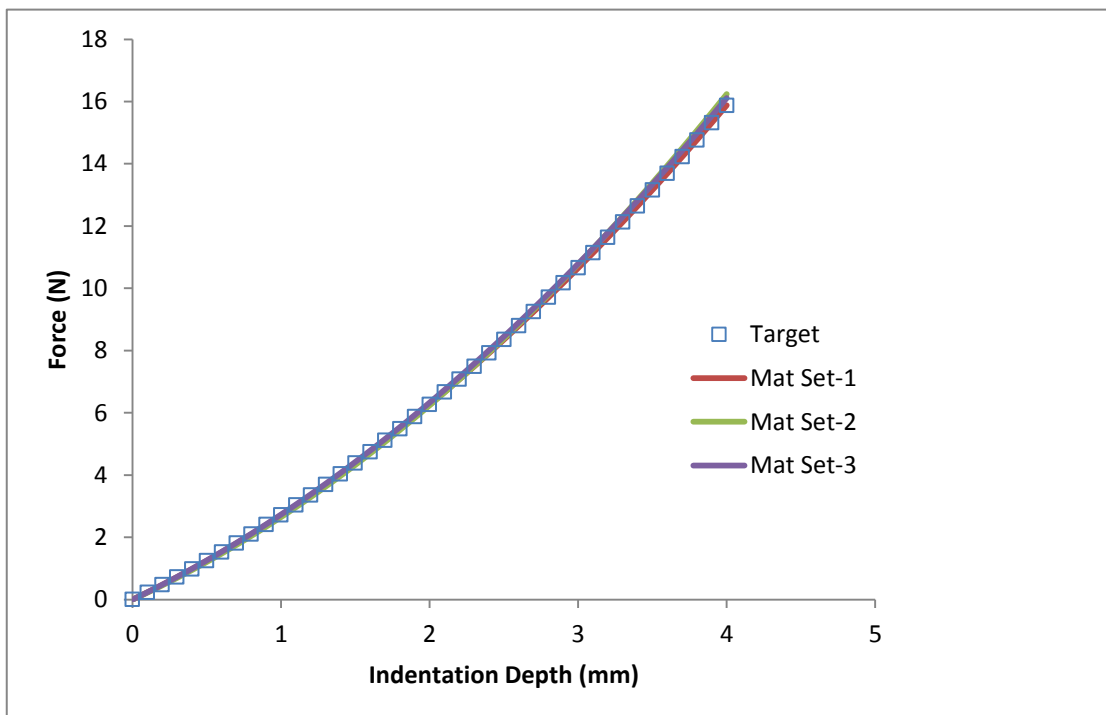


Figure 4.19 (c) Comparison of the P-h curves of the materials sets with lower relative error (labelled in Figure 4.19(b) to show that the P-h curves are very close to each other and the prediction is not unique.

Figure 4.19 Typical prediction data with $R=4\text{mm}$ using a FE data as input ($\mu=0.3$, $\alpha=6$).



(a) Data with different relative error. The labelled data are used to compare indentation curves.



(b) Comparison of the P-h curves of the materials sets with lower relative error (labelled in Figure 4.20(a) to show that the P-h curves are very close to each other and the prediction is not unique.

Figure 4.20 Typical prediction data with R=6mm using a FE data as input ($\mu=0.3$, $\alpha=6$).

4.3.3 Inverse FE modelling based on data from dual indenters of different sizes

One approach potentially could improve this is to use data from different testing conditions. For indentation, a easy way is to use indenter of different sizes. As the indenter size changed, the deformation of the material may change, which potentially could help generating data of different state. However, one main challenge is to establish a proper way to process the data. An optimum way of choosing the criteria of the data for comparison and the way to determine the final value will be critical. The methodology used will also influence the automation/programming progress to be able to do this with a computer program rather than rely on human judgement which may vary between subjects.

To achieve this goal, one natural approach is to plot the material data which have the same range of relative error in P-h curve, then try to look at the coincident data (i.e. data appeared in both cases). In an ideal situation, the true materials material property is more likely to appear in the materials sets with lower errors in both cases with the minimum error, but it will not be reliable if the choice of materials is decided on the only one data with the lowest error as there may be factor/noise that may accidentally influence the outcomes. So different approaches is to be tested. Figure 4.21 plots the material data with P-h curves within 3% of the target for R4 and R6. It is clearly shown that there is a zone (labelled in red circle) where more data matching/overlap between data for R4 and R6. But there is still another zone (blue circle) where there are obviously overlapping points. The data in the most likely zone (red zone) is close to the target ($\mu=0.3$, $\alpha=6$), but it difficult to be conclusive, as it is difficult to eliminate several data in the blue circle. This probably due to the fact that the as far as the error is within 3%, the material data will appear on the chart then it is difficult to distinguish the closeness of the predicted P-h to the target P-h curves. For example the way the data has been plotted could not tell 1% from 3% error. One approach might be to plot much smaller error range, but this will cause another problem. If there is any noise in one or both input data, then there may be no data with very low error. If the input is experimental data, it will be even more difficult to ensure that there will be any material that give error as low as 1 or 2%. Based on this analysis, 3% is a much reasonable range.

To avoid this problem with fixed error range, another approach is explored. In this case, rather than picking data based on the relative error range, the data is going to be picked based on those that has a relatively lower error rather than the absolute value. The relative error value will be influenced by factors such as materials, indenter size and noise. For example, the indentation force in R6 is higher than for R4, all these will influence the relative error directly. Since we are using 2nd polynomial curve fitting, it is still an approximation process, then this may introduce systematic noise due to the fitting process, the noise may in turn influence the level of calculated relative error. To avoid these uncertainties, the data to be picked will be based on their relative performance. It is reasonable to say that, irrespective of any factors influencing the level of relative error, the true material properties should have a relatively low relative error among the other material properties for the same condition (for example, same indenter size). This assumption would always be reliable rather than saying that the data must produce an error within certain range. Once the more likely material property set(s) is identified, it can then be further assessed easily to confirm if it is the true material property. Following this model, Figure 4.22 (a, b and c) plots the top 15, 10 and 5 material properties that has lower relative error. The outcome becomes much clearer with much less number of materials shown on the figure than the cases based on the 3% error rule. Based on the frequency of overlapping, it is reasonable to say that materials region 1 on Figure 4.22b is most likely to be the predicted value, which is very close to the target. To work out the value of the material, one approach is to average all the coincidental data within a focused region to determine the material properties, which will give a value close to the target. However, in all the three cases (Figure 4.22a-c), there conclusion could not be 100% certain, as there are still another property (blue circle, materials region-2) that match both indenter size. As shown in Figure 4.23, analysis show that the P-h curve of material data-2 (point in the blue circle in figure (b)) are almost the same as the input P-h curve for R4 and R6. This suggest that the material data is different from the target in value, but the P-h curves are very close. This situation will cause uncertainty in the approach, but the extra set of material point could not be identified when using other inverse programs such as the Kalman filter method. A more robust approach is required.

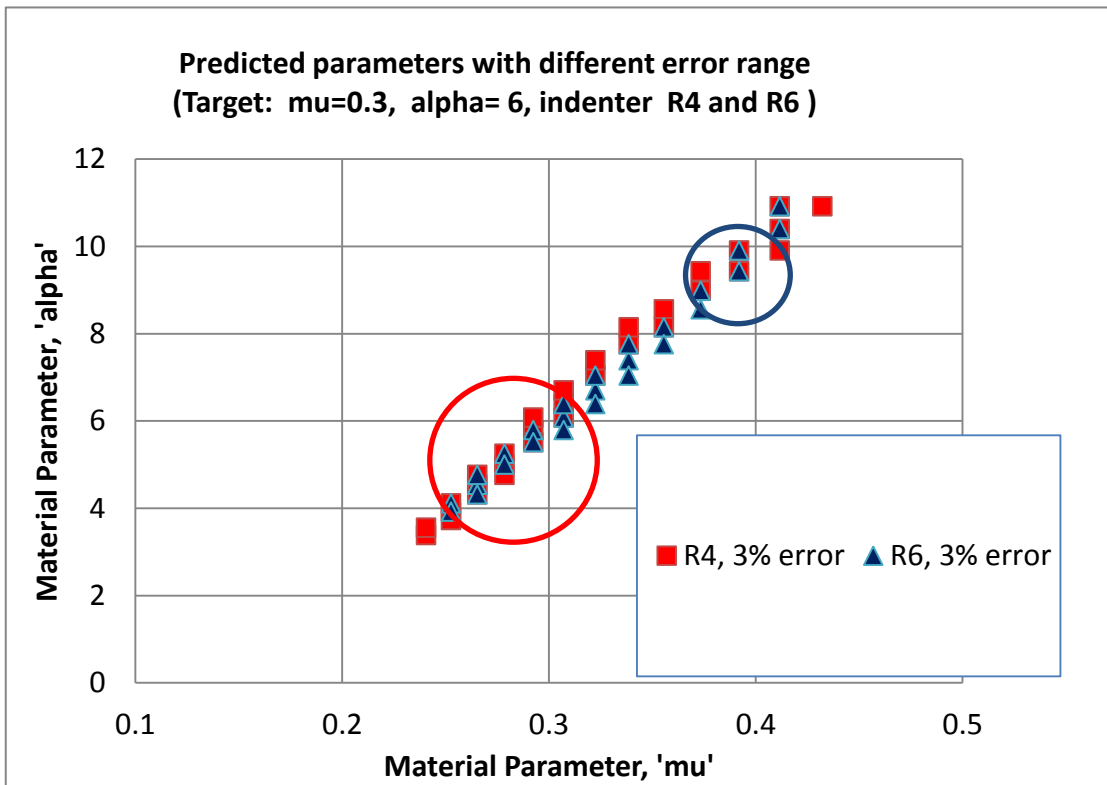
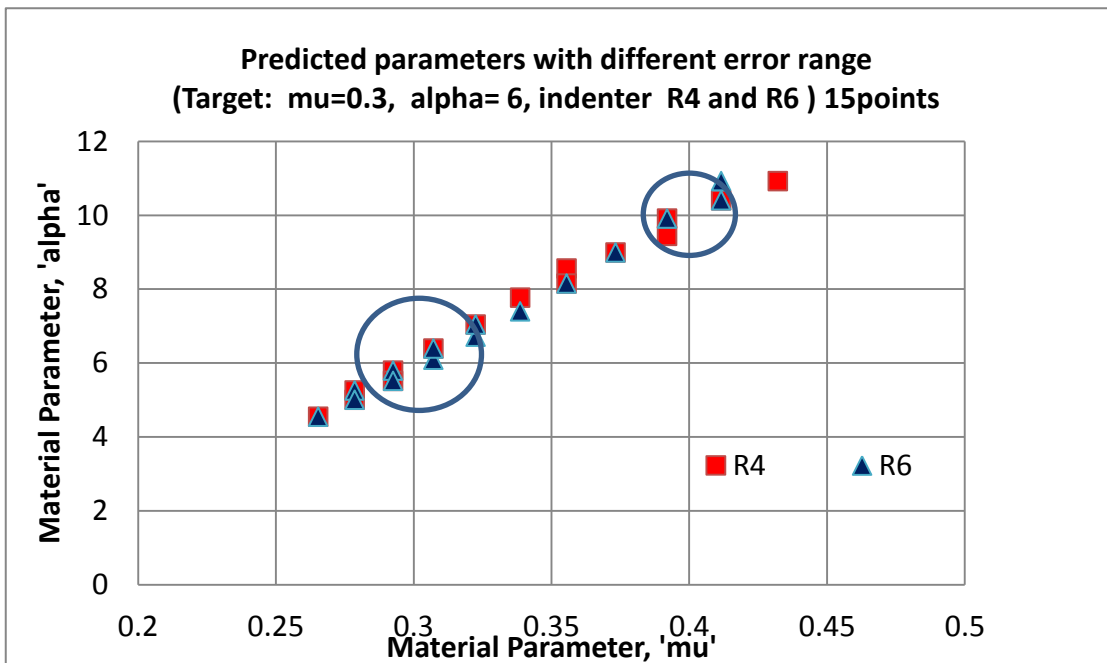
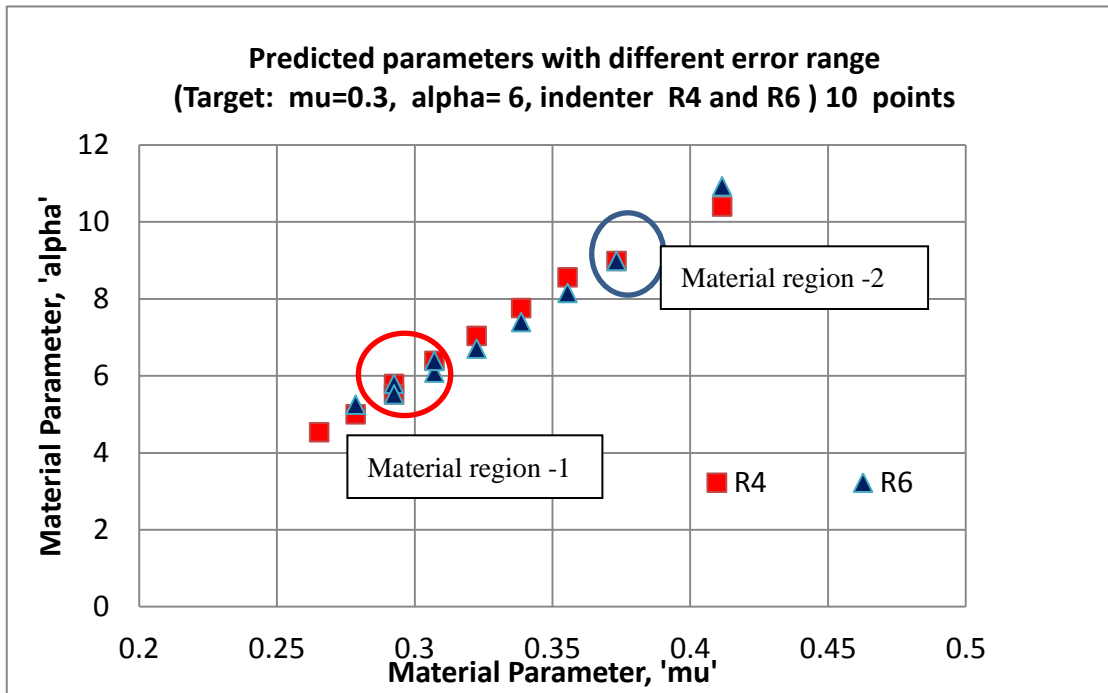


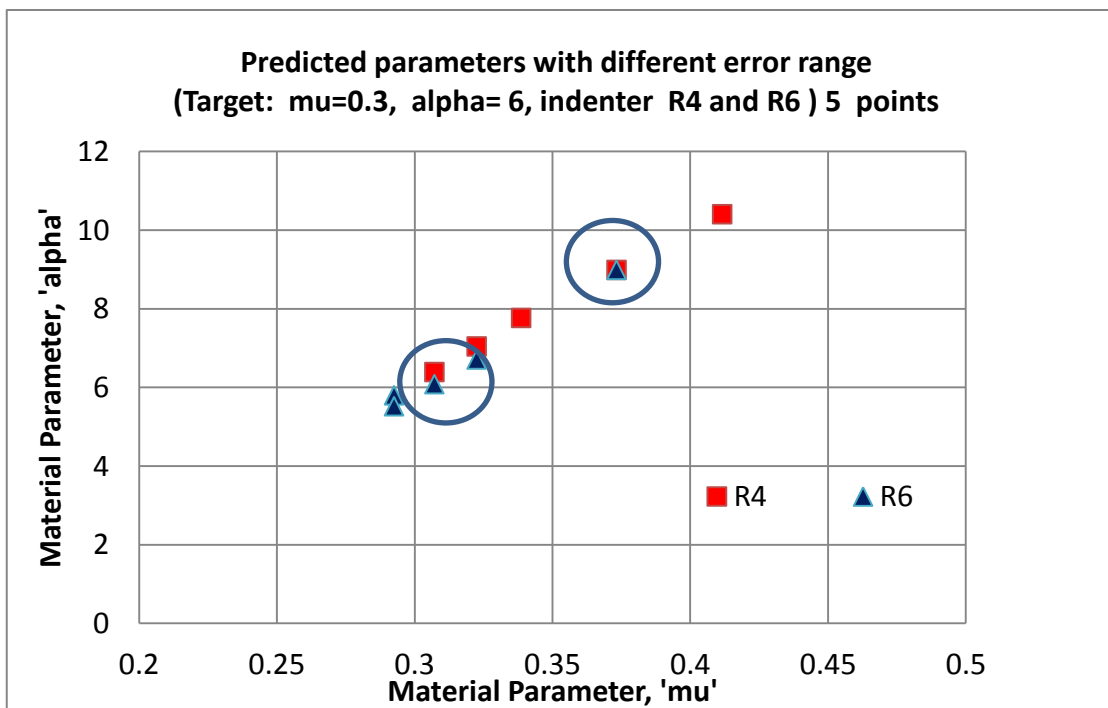
Figure 4.21 Dual Indenter approach (R4+R6) using data within predefined error (within 3%) showing that it is difficult to be predict the best material data set which match both indenter data.



(a) Data showing the dual indenter approach using the first 15 points with lower relative error to identify the optimum material property sets.



(b) Data showing the dual indenter approach using the first 10 points with lower relative error to identify the optimum material property sets.



(c) Data showing the dual indenter approach using the first 5 points with lower relative error to identify the optimum material property sets.

Figure 4.22 Typical result with approach using limited number of material point with lower error for the dual indenter approach showing that it works better than using the data within a given error range (in comparison with Figure 4.21). It shows that based on frequency of overlapping, the target can be predicted, but there are still multiple material property sets match both indenter data.

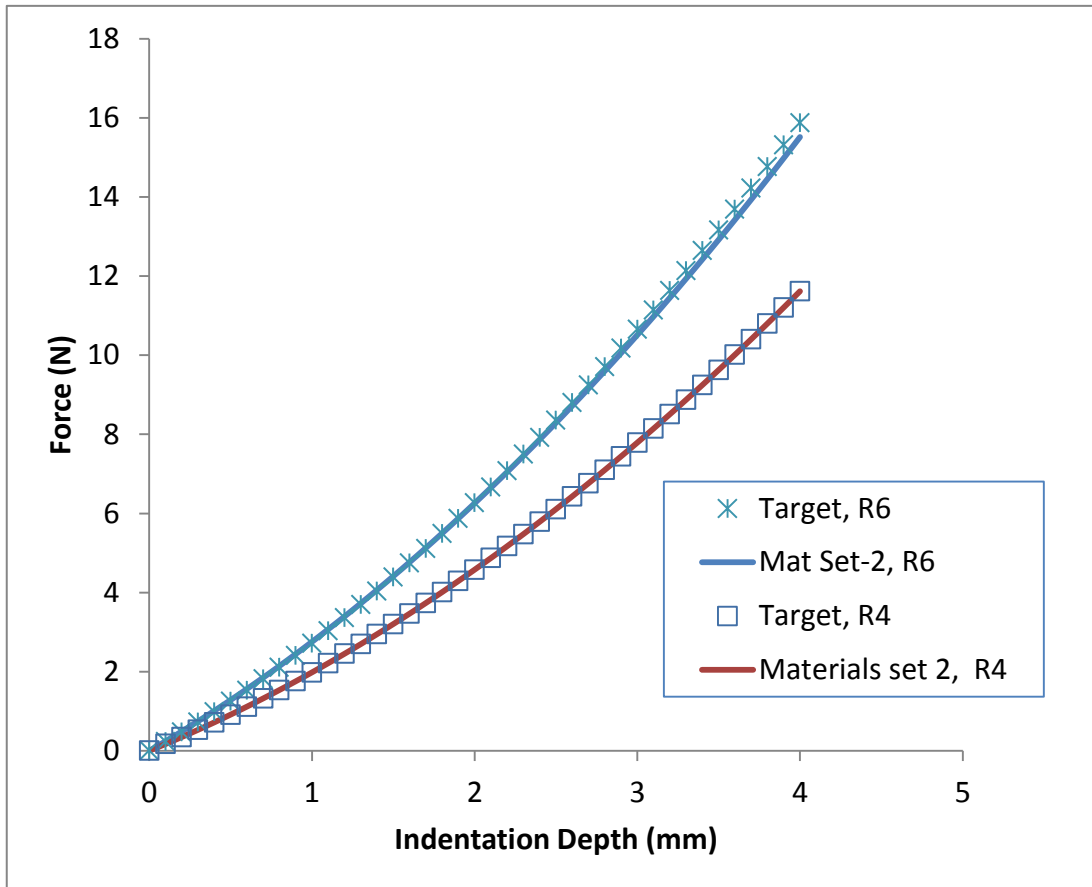


Figure 4.23 FE P-h curves using materials data point 2 in Figure 4.22 showing that there is still an additional materials property sets (not the target) that can match both indenter indentation data showing that it is not 100% unique.

4.4 Inverse FE modelling based on the tests data on samples of different thickness and dual thickness approach

A new approach explored in this work is to use data from test of different thickness. Many types of foam are supplied with limited thickness. When testing a thin foam, the supporting base may affect the force data, this may help to provide an condition to extract the material parameters if tests on thicker foam and thin foam is combined. This could potentially be an improved alternative to the dual indenter approach, which were found not able predict the property in a unique way. In addition, the use of dual indenter requires re-calibration with the change of indenters, which could be technically complicated; while change of sample with different thickness is much easier. To test the dual thickness approach, a new FE model corresponding to the new thickness needs to be produced and the suitability of using curve fitting needs to be researched using the ANN program reported in Chapter 3.

The procedure for producing the simulation space of the thin sample involves firstly developing FE model of a thinner model, in this case $t=12\text{mm}$ (the thicker sample used is $t=20\text{mm}$ data). A typical example of FE model is shown in Figure 4.24(a). The inp file used in the modelling allows the change of thickness in the program by setting the thickness values (Table 3.1). The boundary condition is similar to the model with thicker samples. As shown in Figure 4.24(a), a 2-D axial symmetric model was used due to the symmetry of the spherical indenter. The indenter was assumed to be analytically rigid body as it is much harder than the indented material. The element type of the material used is CAX4R (an axisymmetric element) and finer meshes have been applied around the indenter to improve the accuracy. The thickness and width of the model is 12 mm and 25mm, respectively. The bottom face of the material was fixed in all degrees of freedom (DOF). Contact has been defined between the indenter surface and sample surface with an coefficient of friction of 0.5. The material of interest is allowed to move and the contact between the indenter surface and the material surface was maintained at all the times. Mesh sensitivity tests has been performed to ensure that the results are consistent. Figure 4.24 (b) shows the strain field, which shows that the supporting base is interacting with the materials as the sample

is much thinner.

A typical force-displacement data ($\mu=0.3$, $\alpha=6$) is shown in Figure 4.24(c). The P-h data can be fitted with 2nd order polynomial equation with high correlation coefficients. Figure 4.25 shows the correlation coefficients for 2nd order polynomial fitting for all the 77 material data (Materials set-1, Figure 4.22(b)), which shows that 2nd order polynomial fitting is suitable to represent the curves. The lowest coefficient is over 99.5%. The data used in training the ANN and validation is similar to the work presented in Chapter 3. The whole process and results for using ANN to predict P-h curves of the thin sample are not shown to preserve clarity and avoid repeating.

The inverse process followed a similar procedure as that for the thick samples. The ANN program to predict P-h curves from known material properties are incorporated in the inverse program and database. Figure 4.26 (a) shows a typical prediction results based a known materials set (0.3, 6). Similar to the case of thicker sample (Figures 4.19 and 4.20), there are several material property sets producing P-h curves close to the target data. Figure 4.26 (b) plots the P-h curves based a few selected material data sets in Figure (b) and the target P-h curves. It is clearly shown that all these properties could produce P-h curves close to the target input.

Figure 4.27 (a&b) plots the materials properties with P-h curves of relative error of 3% for sample of thickness of 20 and 12 mm. As highlighted in the circle, the main region with high frequency of data overlapping, as circled on the figure, is close to the range of the target property. But there are data over other region also showing some overlapping to a limited extent. Figure 4.27 (b) plots the first 10 material data with lower relative errors for the two thickness cases, the data show that this approach is more effective/clearer as there is only one main region with high data overlapping frequency, which is close to the target value point. This shows that the dual thickness approach is a viable method. Comparing to the dual indenter size approach, only one region exist in the dual thickness approach, which is an improvement from the dual indenter approach. Figure 4.28 shows the situation

when plotting data with lower error from different thickness and indenter size. It is clearly shown that the method can be used to predict the properties. The average of these data point is close to the target data.

Several different material properties have been used as input data to assess the capacity of the program in dealing with different materials. Typical results were listed in Table 4.1. The results clearly show that the dual indenters could produce accurate results. In the case of the dual indenter approach, only the high overlapping frequency region is picked.

Table 4.1 Typical predicted results by inverse FE modelling based on the dual thickness and dual indenter approach on hyperfoam materials.

| Target value | | Dual thickness approach | | Dual indenter approach* | | Thickness and dual indenter approach | |
|-----------------|--------------------|-------------------------|----------|-------------------------|----------|--------------------------------------|----------|
| μ_{\square} | α_{\square} | μ | α | μ | α | μ | α |
| 0.5 | 1.6 | 0.49 | 1.55 | 0.48 | 1.63 | 0.48 | 1.59 |
| 0.7 | 1.6 | 0.69 | 1.50 | 0.58 | 1.60 | 0.73 | 1.54 |
| 0.1 | 3.7 | 0.09 | 3.60 | 0.12 | 3.75 | 0.11 | 3.66 |
| 0.3 | 3.7 | 0.28 | 3.68 | 0.28 | 3.70 | 0.28 | 3.48 |
| 0.5 | 3.7 | 0.51 | 3.68 | 0.52 | 3.68 | 0.53 | 3.43 |
| 0.7 | 3.7 | 0.70 | 3.70 | 0.72 | 3.73 | 0.69 | 3.65 |
| 0.1 | 5.8 | 0.11 | 5.81 | 0.11 | 5.87 | 0.09 | 5.74 |
| 0.5 | 5.8 | 0.51 | 5.79 | 0.49 | 5.81 | 0.58 | 5.60 |
| 0.7 | 5.8 | 0.70 | 5.80 | 0.67 | 5.59 | 0.71 | 5.54 |
| 0.1 | 7.9 | 0.09 | 7.83 | 0.085 | 7.95 | 0.085 | 7.82 |
| 0.3 | 7.9 | 0.29 | 7.68 | 0.29 | 7.95 | 0.32 | 7.78 |
| 0.7 | 7.9 | 0.69 | 7.93 | 0.68 | 7.94 | 0.67 | 7.85 |
| 0.1 | 10 | 0.10 | 9.97 | 0.09 | 10.06 | 0.09 | 9.81 |
| 0.3 | 10 | 0.31 | 9.85 | 0.30 | 9.92 | 0.28 | 9.86 |
| 0.5 | 10 | 0.49 | 9.78 | 0.55 | 9.9 | 0.53 | 9.62 |
| 0.7 | 10 | 0.70 | 10.00 | 0.69 | 10.10 | 0.71 | 9.94 |

*Pick the region with high overlapping frequency only.

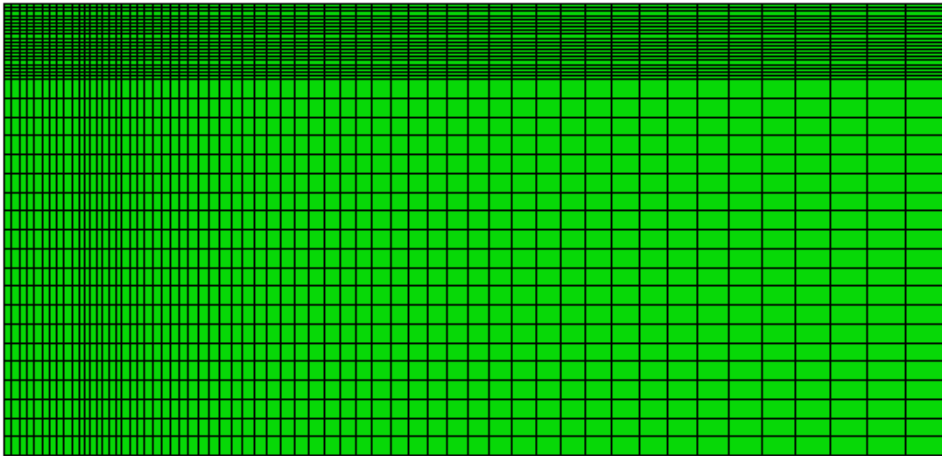


Figure 4.24 (a) FE model of thinner foams ($t=12\text{mm}$).

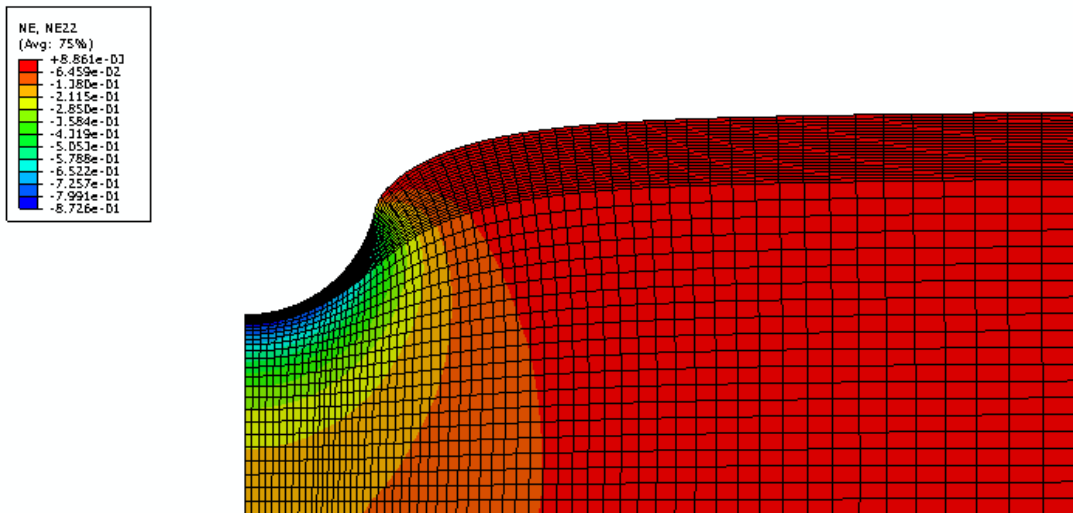


Figure 4.24(b) Strain field of the deformed model of thin EVA foam ($t=12$).

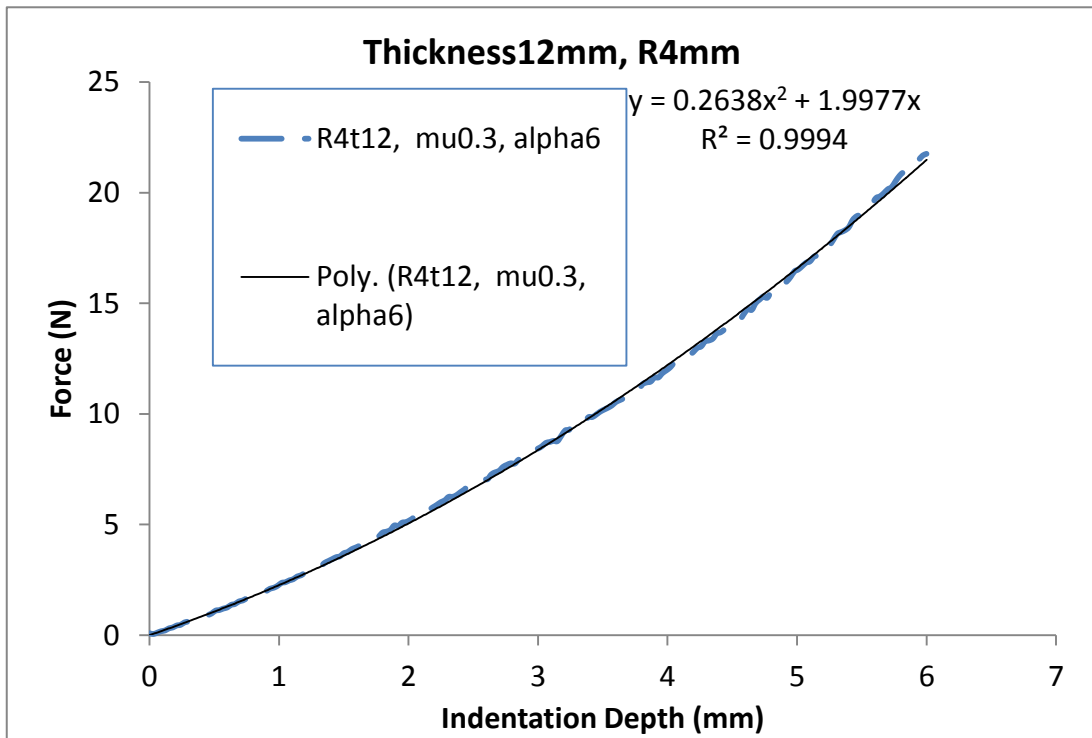


Figure 4.24 (c) Typical indentation force depth data (FE data). This is used as the input.

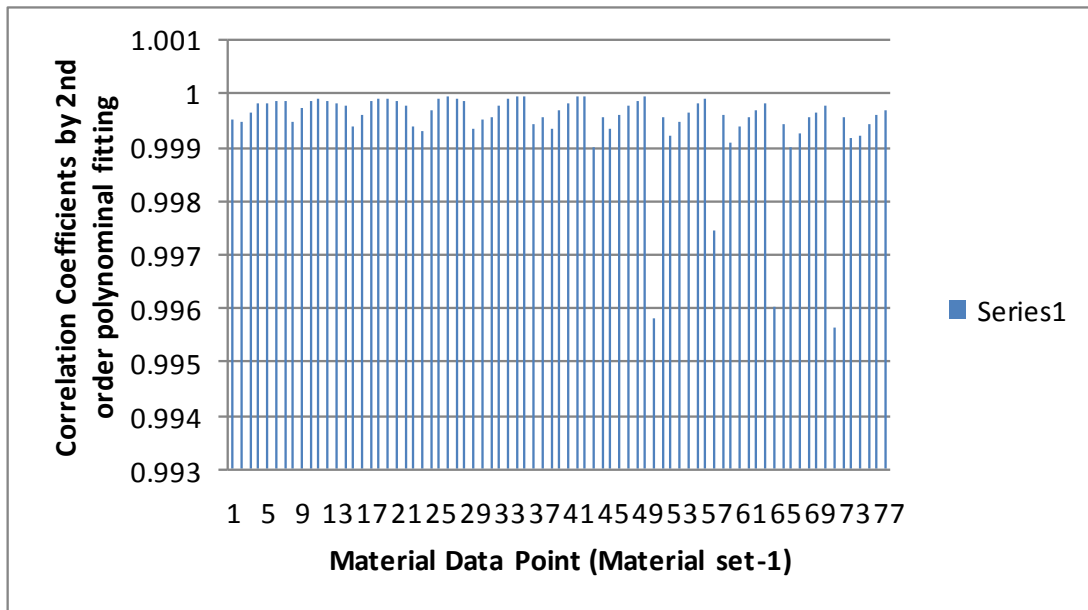


Figure 4.25 Correlation coefficients for 2ndorder polynomial fitting of force-displacement curves of a thin EVA foam (t=12mm) showing that 2nd polynomial fitting is sufficient to fit the data) (Materials data ste-1, 77 data).

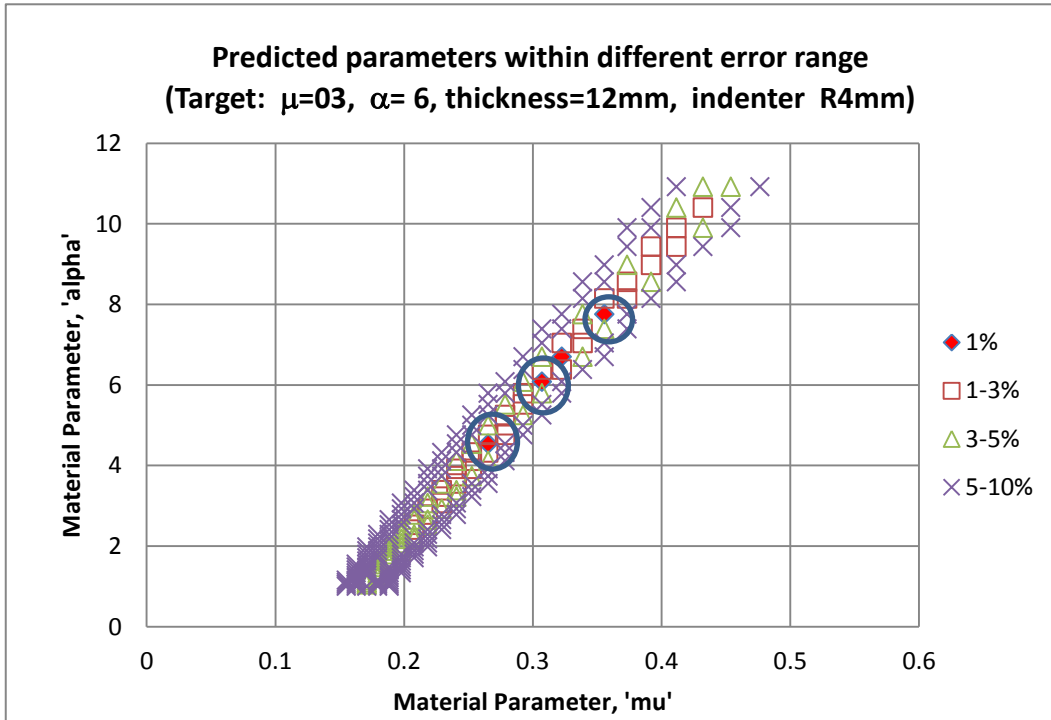


Figure 4.26 (a) Data with different relative error range of thin foam (t12mm, R4). The labelled data are used to compare indentation curves.

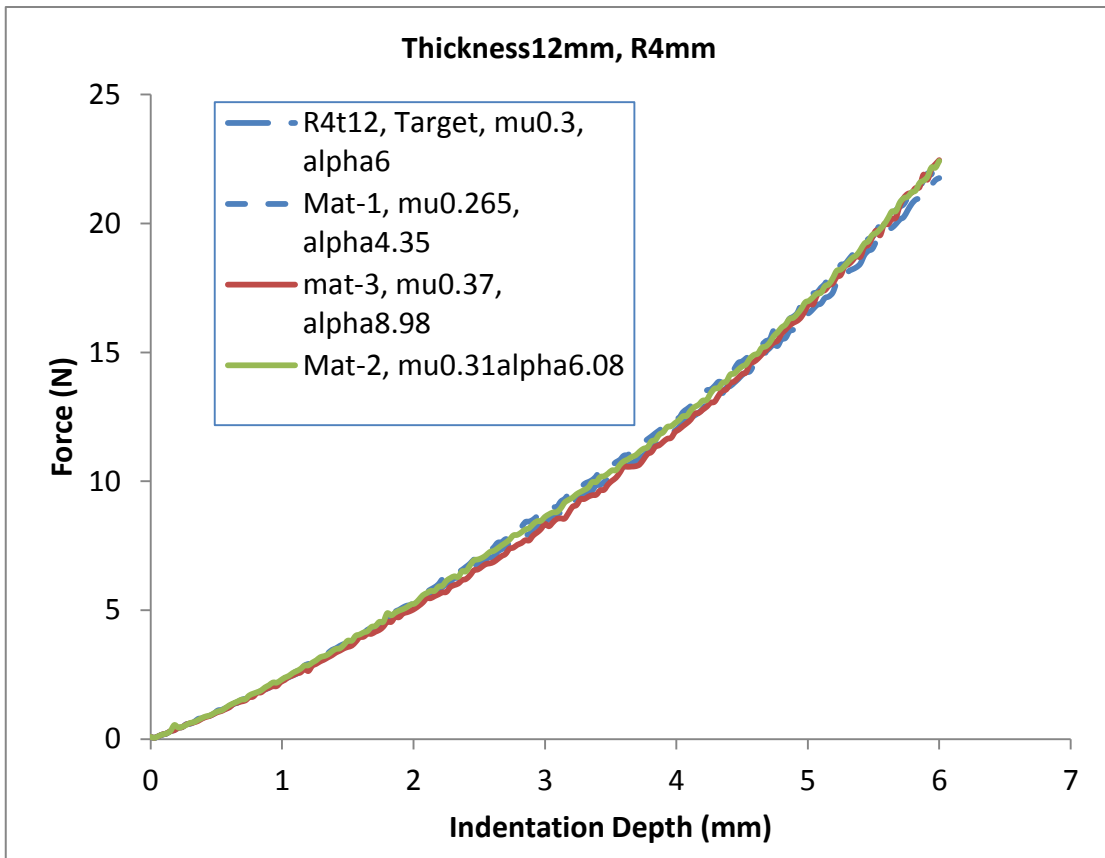
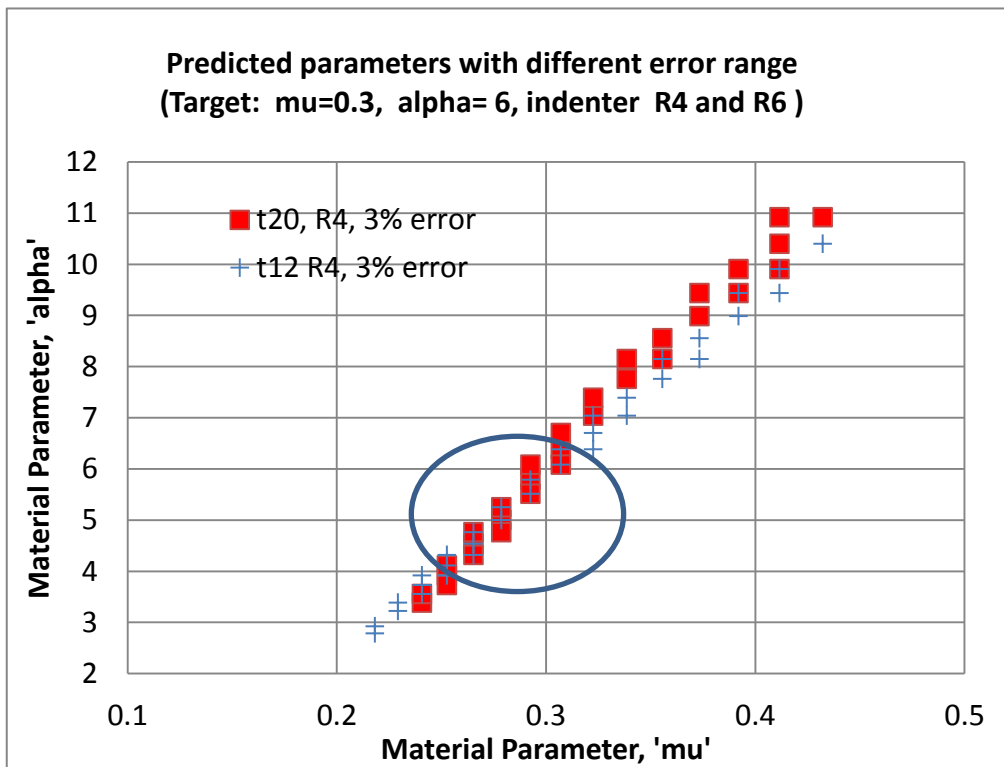
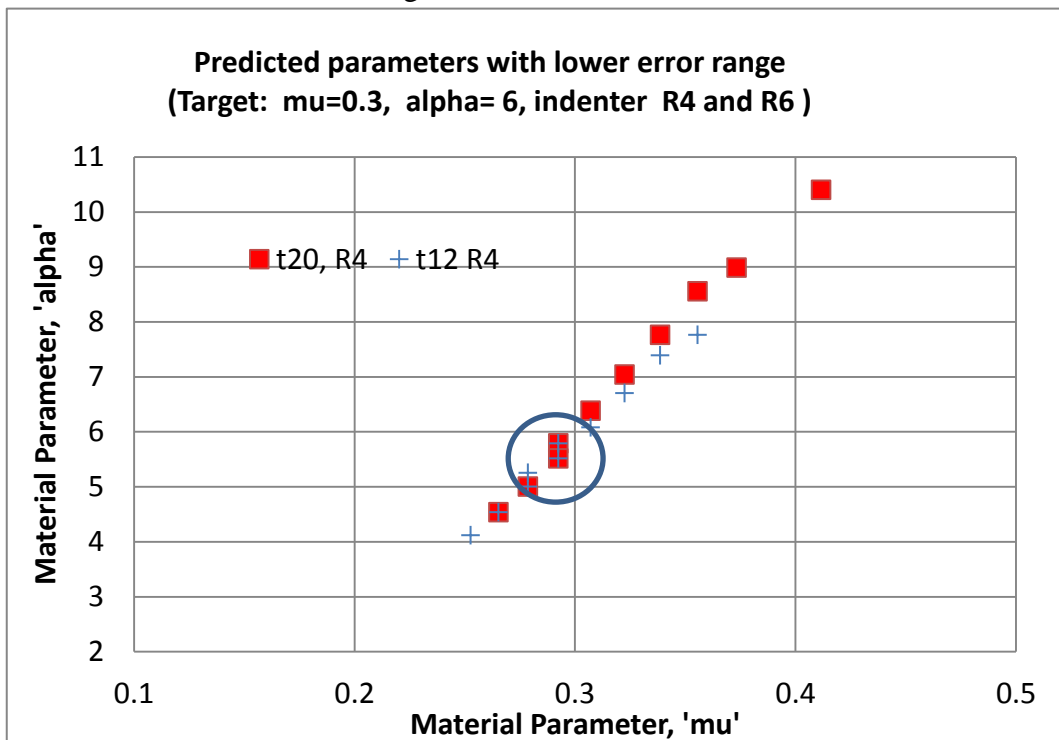


Figure 4.26 (b) Comparison between the FE P-h curves based on the material properties predicted and the target data.

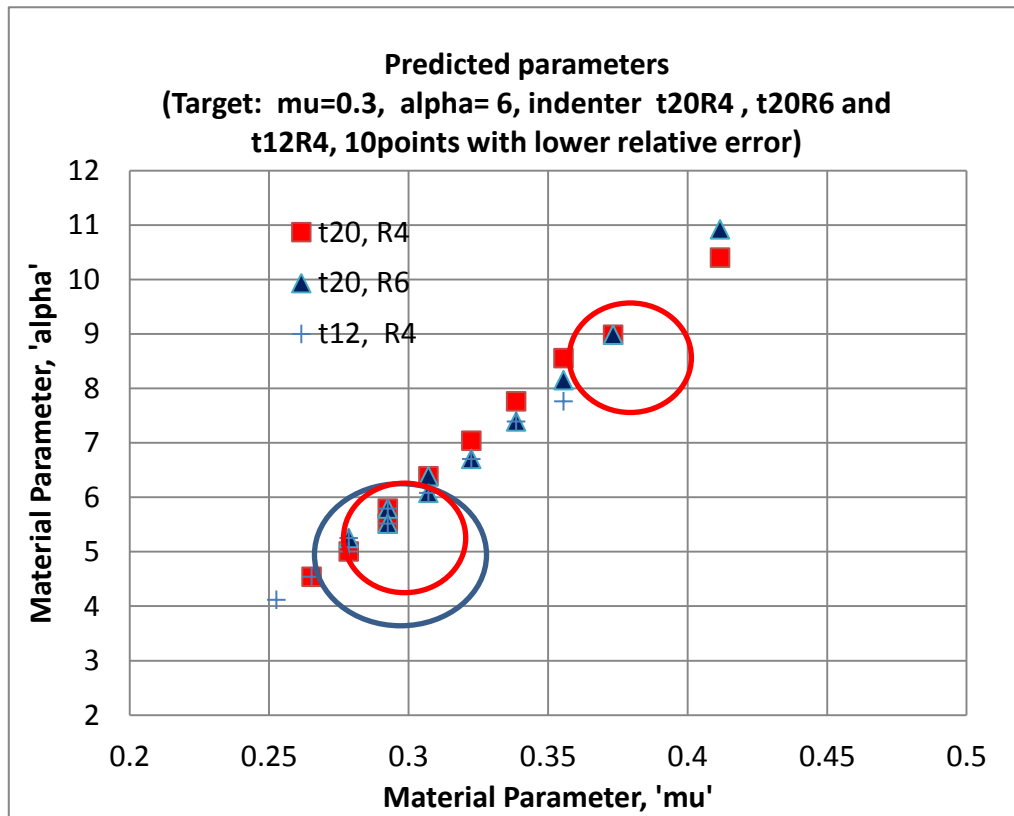


(a) Dual thickness approach (R4, t12 and t20mm), material data that produce P-h curves within 3% average error.

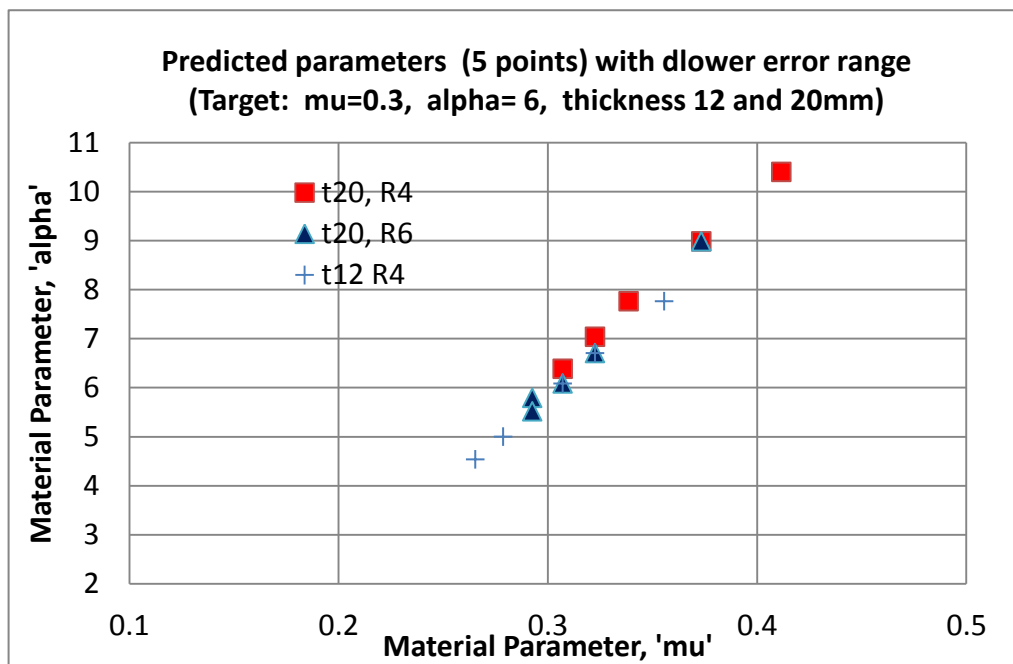


(b) Combination of t204R4 and t12R4, first 10 material data that produce P-h curves with lower average error.

Figure 4.27 Typical predicted results based on dual sample thickness data (t12 and t20mm) and two different approaches to identify the optimum material properties: fixed error range approach (a) and fixed data number approach.



(a) Combination of t20R4, t20R6 and t12R4, first 10 material data that produce P-h curves with lower average error.

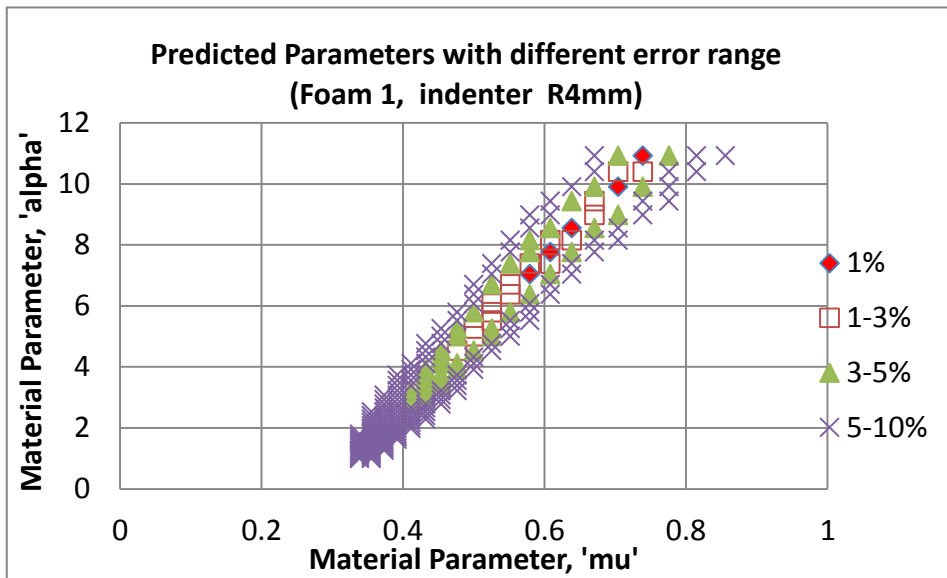


(a) Combination of t20R4, t20R6 and t12R4, first 5 material data that produce P-h curves with lower average error.

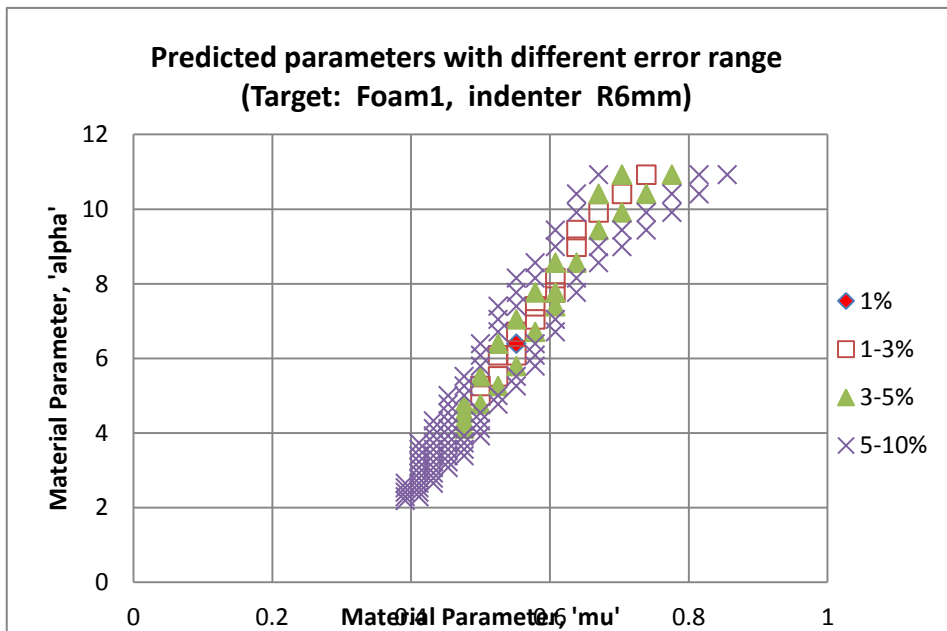
Figure 4.28 Combination of t24R4, t24R6 and t12R4 with different number of materials sets of lower relative error showing that the dual thickness approach is potentially more robust, but the 5 point approach is less conclusive.

4.5 Prediction of EVA foam properties based on experimental data

The ANN program is used in predicting the properties of EVA foams based on experimental data. A typical set of results are shown in Figures 4.29-30. Figure 4.29 shows the identified materials parameters for different indenter sizes (R4 and R6) for EVA foam 1. In both case, the material property sets with relative error of 1%, 1-3% 3-5% and 5-10% is plotted. It is clearly shown that there are multiple material property sets that have very low error. This confirms that the single indenter approach could not produce unique material properties. Figure 4.30 (a) plots the materials data for both R4 and R6 with the first 10 points with lower relative error. The region with overlapping data is marked by the circle. Figure 4.30(b) plots the identified materials data for t20 and t12 with the first 10 points with lower relative error. The region with high frequency of overlapping is highlighted by the circle. Figure 4.30(c) plots the data for R4t20, R4t12, R6t20, it is clearly shown that there is a region with high overlapping frequency, which represents the properties of the foam. Figure 4.31 compared the predicted properties based on different approaches in comparison with the standard experimental data (combination of compression and shear). Results shows that the properties predicted based the dual indenter (R4+R6) and dual thickness approach are in reasonable agreement with the standard test data. Also plotted is the dual indenter approach based on the Kalman filter method developed based on the work in a previous project. It shows that the new ANN based approach is more accurate. The property predicted by interception point of trendline approach also illustrated in Figure.31. The process of using the approach is shown in Figure 4.32, in which the interception point is treated as the predicted properties. This approach has been used by other researchers (Kong *et al*, 2009). However, in this case, the property predicted with the dual indenter approach is lower than the true value, while the value for the dual thickness method is higher (illustrated in Figure 4.32(b)). In some cases, the trendline is not applicable. An example is shown in Figure 4.33, where the data for Foam 2 could not be fitted with a trendline, but the prediction based the over lapping approach proposed in this work showed a good agreement with the experimental data. In addition, this overlapping method is also easier to be implemented in a computer searching progress, which is to be discussed in the next chapter and explored in future works.

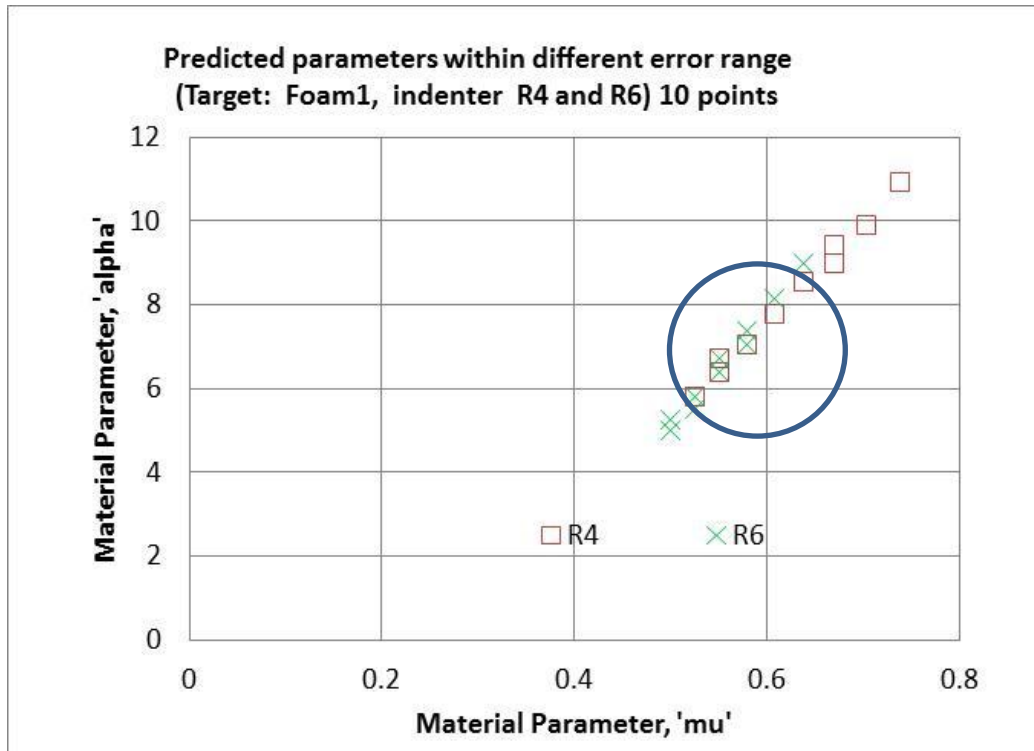


(a) Foam 1 R4

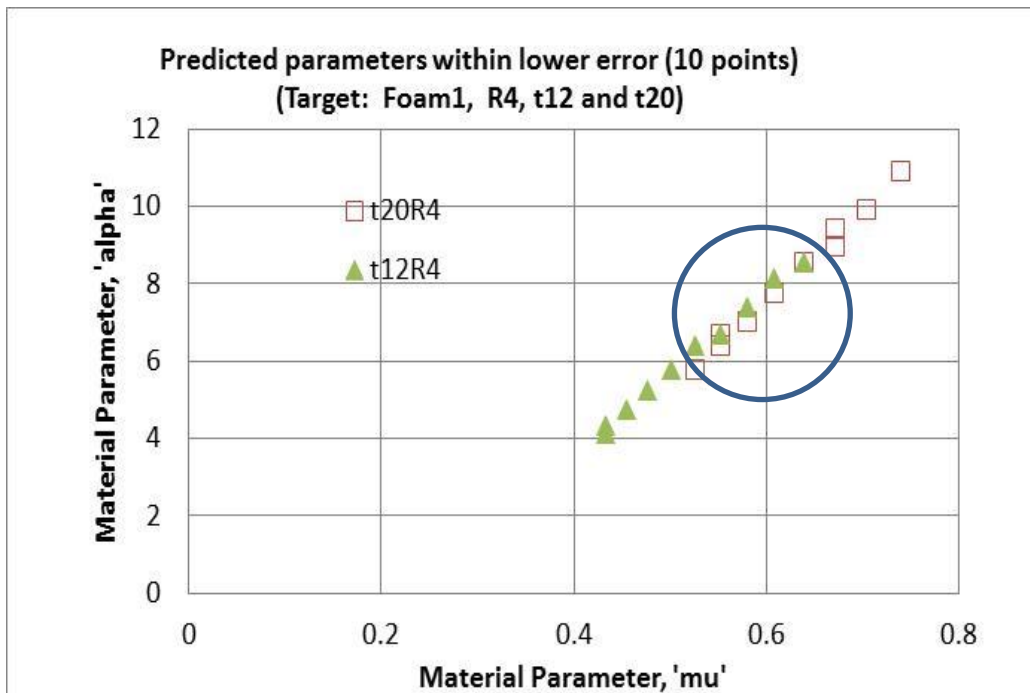


(b) Foam R6

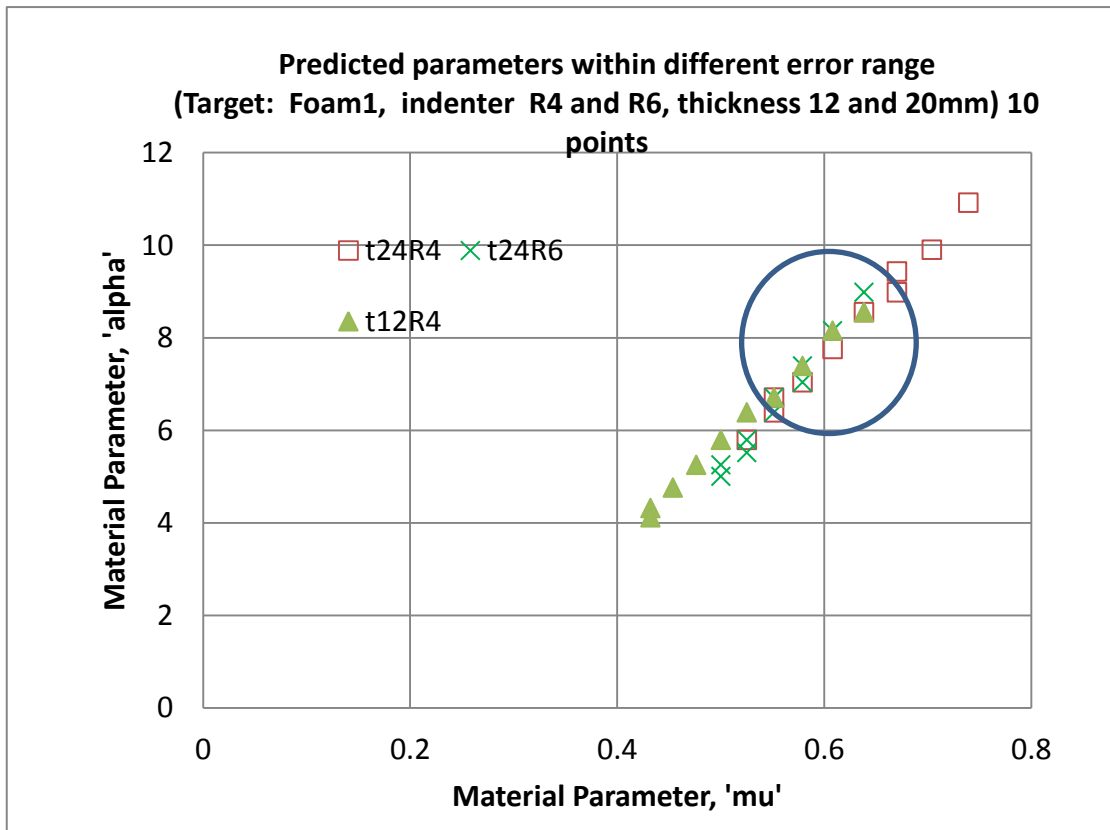
Figure 4.29 Material properties with different error range for Foam 1 using the experimental as input. (Target: $\mu=0.62$; $\alpha=8$).



(a) Dual indenter approach for Foam 1 (10 Material data with lower average error).

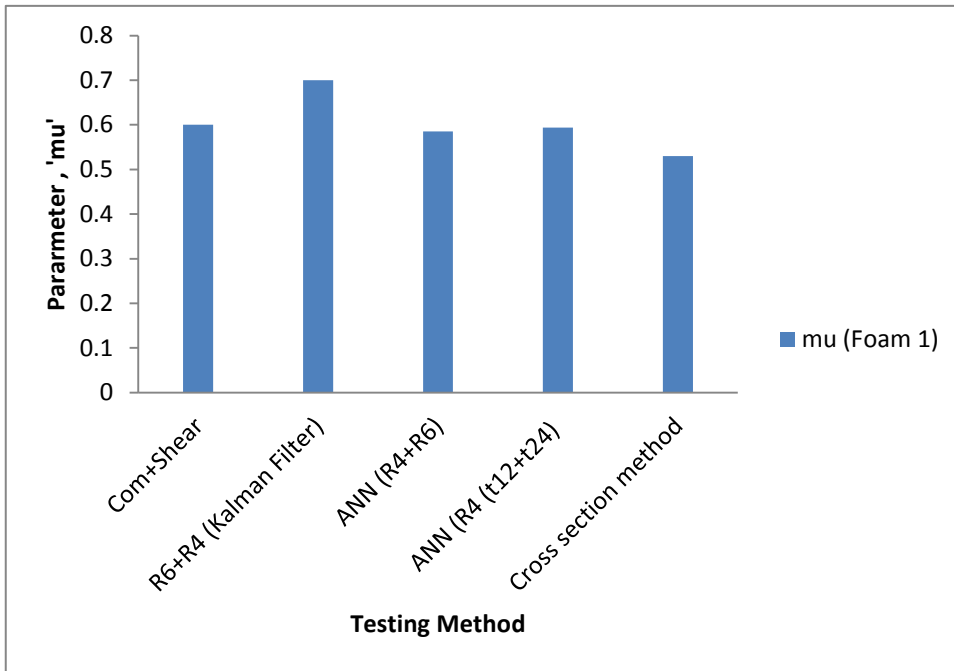


(b) Dual thickness approach for Foam 1 (first 10 points with lowest average error). The average within the range in the circle is identified as the predicted properties (Target: $\mu=0.62$; $\alpha=8$)

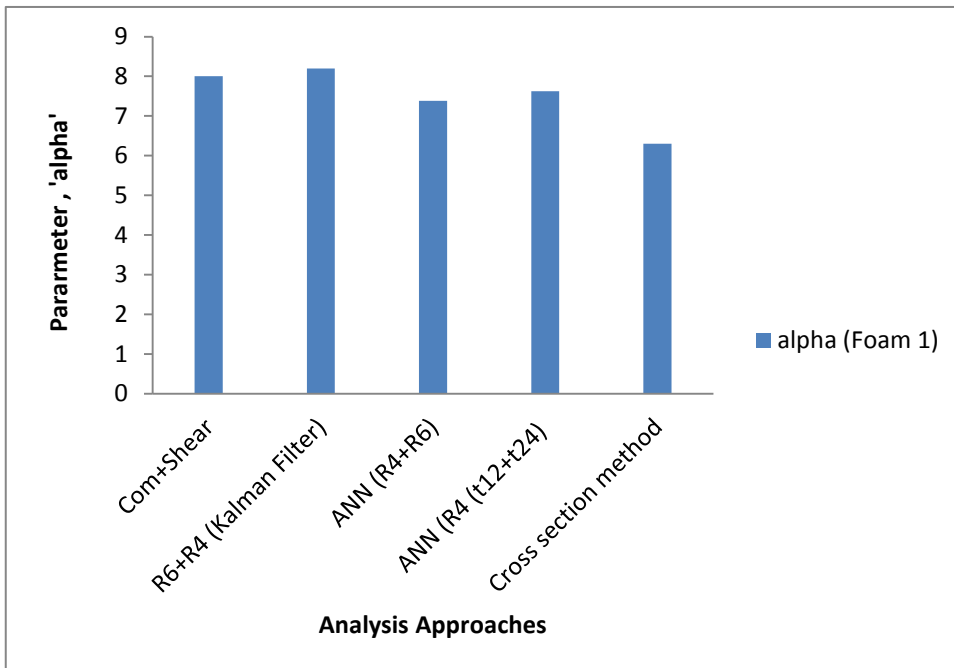


(c) Dual thickness and indenter approach for foam 1 with mixed indenter size and sample thickness.

Figure 4.30 Predicted results based on different range. (Target based on experimental tests: $\mu=0.62$, $\alpha=8$).

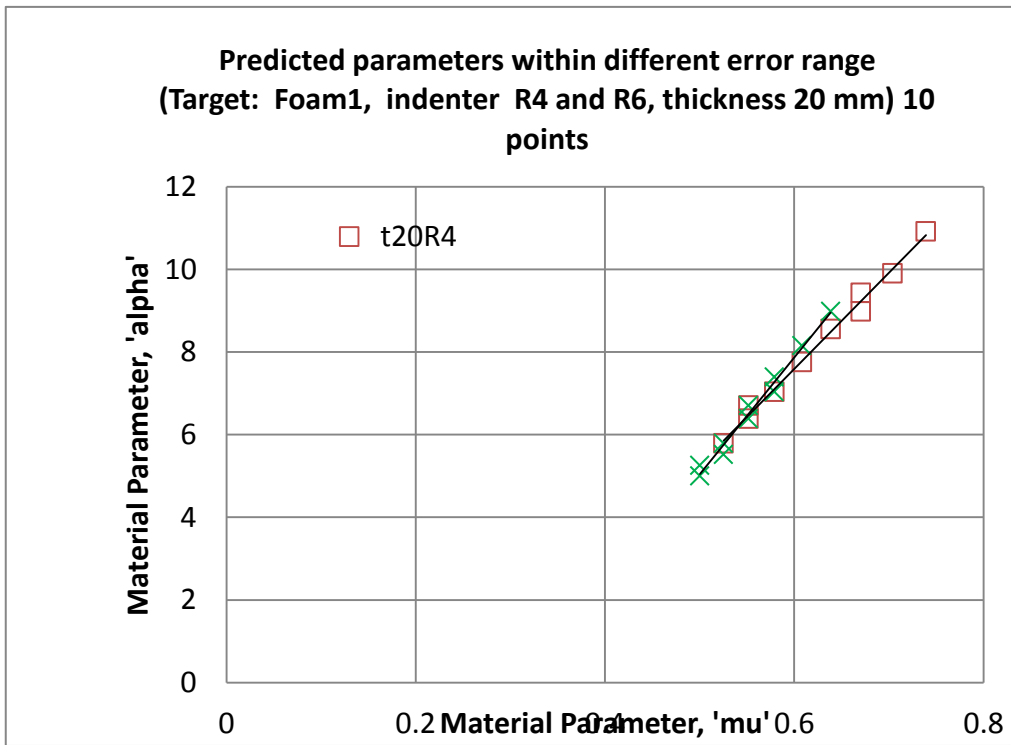


(a) Predicted parameter ' μ '

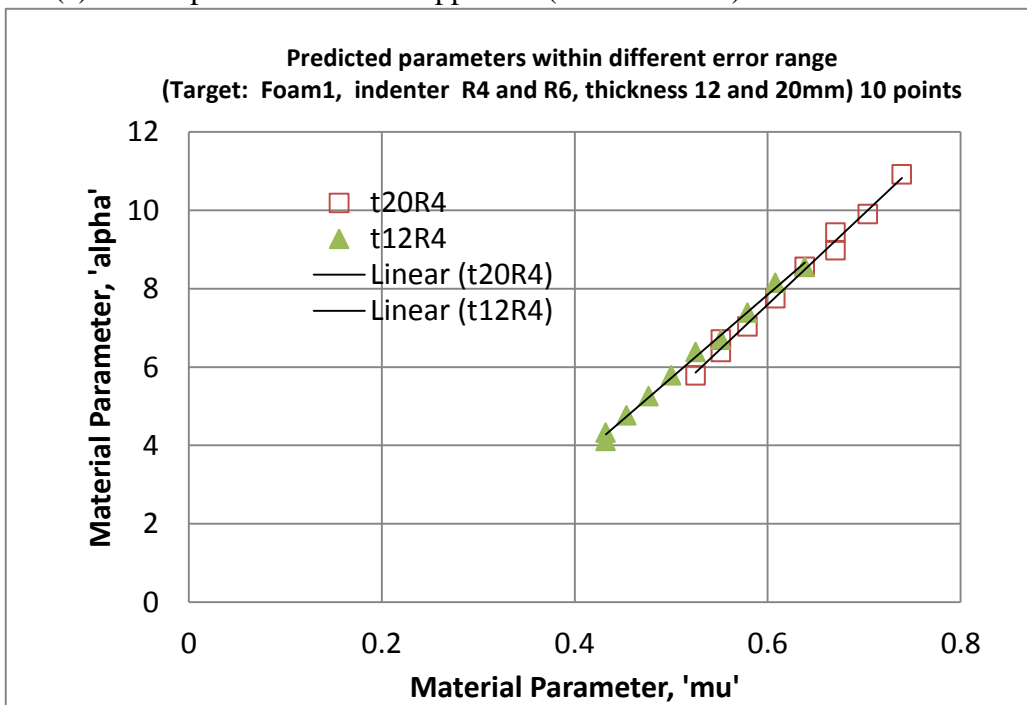


(a) Predicted parameter ' α '

Figure 4.31 Comparison between the predicted properties based on the ANN methods, experimental data and results from other methods.

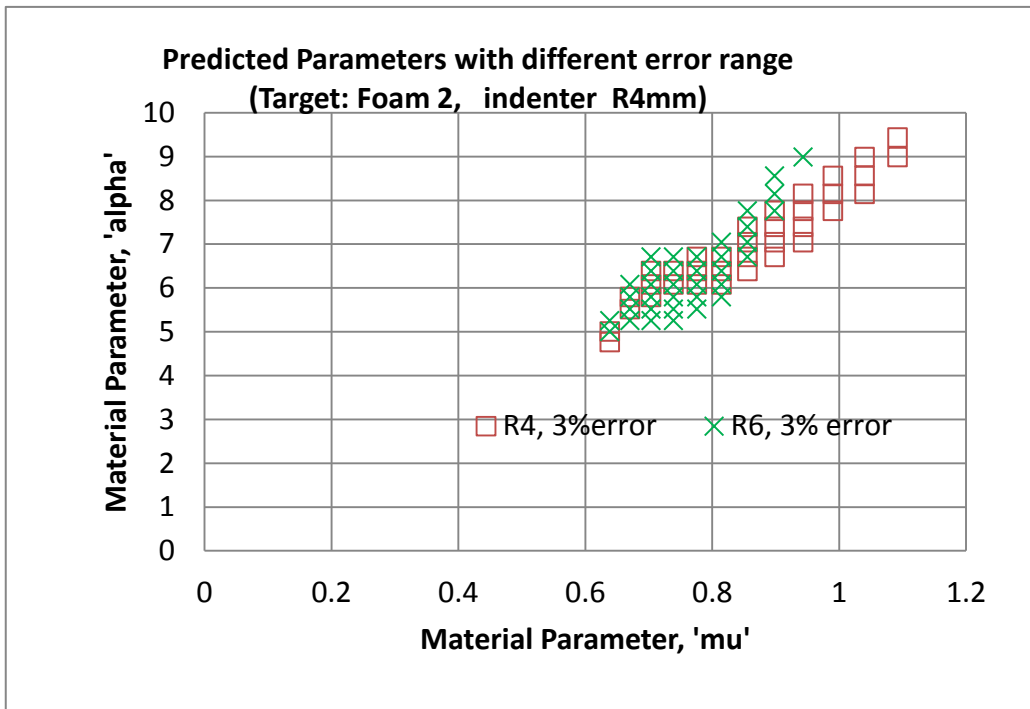


(a) Interception of trendline approach (Dual indenter)

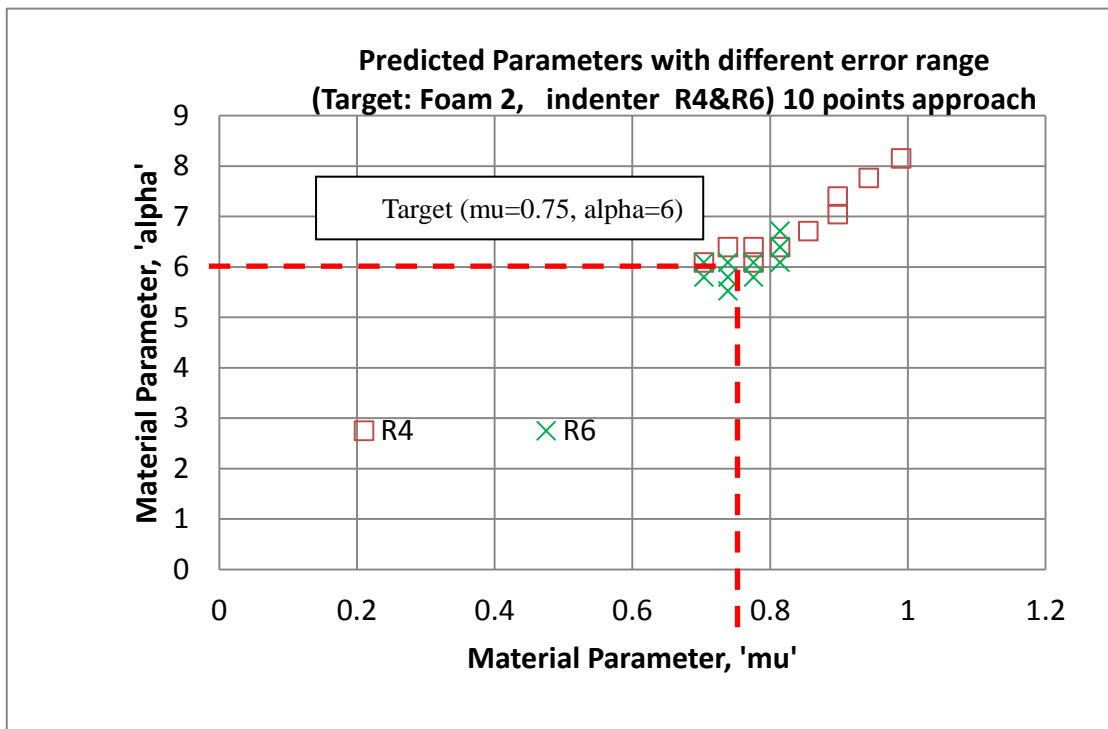


(b) Interception point of dual thickness approach. (R4, t20 and t12).

Figure 4.32 Typical Interception point of trendline approach for the dual indenter and dual thickness approach.



(a) Materials points with relative error within 3% (Foam 2, Dual indenter approach)



(b) First 10 points with lower relative error.(Foam 2, Dual indenter approach). Target ($\mu=0.75, \alpha=6$)

Figure 4.33 Sample property identification results showing a situation that the trendline approach is not feasible, while the prediction using overlapping point showed good agreement with standard experimental data.

4.6 Summary

In the first part of this chapter, the feasibility of using ANN to directly predict the material properties is evaluated including assessing its capacity to predict trained data and untrained data. The use of 2nd order and 3rd order polynomial curve fitting of the force displacement curve is compared. In addition, the use of single indenter approach and dual indenter approach is assessed. It was found that the approach with 2nd order polynomial fitting of the P-h curves is not able to predict the material parameters. Using 3rd order fitting showed some improvement and it is able to predict the trained data accurately but could not be used to predict untrained data. Works on dual indenter approach with R4 and R6 showed some improvement in predicting untrained data but could not produce data with reasonable accuracy of the full dataset.

In the second part of this chapter, a new approach utilising the direct ANN program developed is proposed. A computerised program (with web interface) has been developed including data generation through ANN, data storage, interface for input and viewing results. A searching program is developed which will enable the identification of any possible materials property sets that may match the experiment data within a predefined error range. The approach is applied to analyse single and dual indenter methods through blind tests with known material properties.. A new approach using foams of different thickness is also proposed. The results showed that, with the single indenter approach, there are multiple materials property sets that can produce similar P-h curves, thus the results are not unique. Dual indenter size approach showed a significant improvement, but the new program successful identify addition material property sets that can produce P-h curve that match both R4 and R6 data. This suggest the dual indenter method with hyperfoam model is not 100% unique, this new finding had not been identified with other inverse program. The new approach proposed of using the tested data on samples of different thicknesses showed that the uniqueness of the prediction can be improved. The accuracy and validity of the program is firstly assessed with blind tests (using numerical data as input/target) then used to predict the properties of the EVA foam samples. This is

not only further validating the program and method but also identify issue with real material test data as they are not as perfect as FE generated data. Some key results of the real foam data is compared to the target and prediction results from other programs and data processing method, the comparison showed that the new ANN base computer program has clear improvement in accuracy, robustness and efficiency in predicting the parameters of EVA foams.

Chapter Five Discussions

5.1 Use of ANN in prediction of P-h curves based on different approaches and its applications

In the first part of the work, an ANN based program has been developed and compared with the FE data and experimental data. The work is initially started with thick foam (chapter 3), then extended to thinner foam where the boundary condition will directly influence the force (Chapter 4). The prediction of P-h curve itself could be very useful as it can tell the resistance of the foam, which is associated with foam properties. In some cases, the P-h can be linked to the perception of foam performance (e.g. comfortness). With the ANN program large quantity data can be generated with limited computing time and resource, this can potentially help some other research work in materials, where such data is required. For example, [Ren and Su \(2014\)](#) is trying to use the data sets produced to develop an analytical solution based on effective Young's modulus.

The P-h curves prediction from known material properties using ANN is potentially a challenging process, in particular trying to develop a method which has to be 100% robust for material applications. There are 3 key aspects has been addressed in the work. 1) The key is to establish the approach to represent the experimental data (i.e. P-h curves); 2) how to assess the accuracy of the prediction; 3) Given this is a program aims at real application, so robustness is very important, while full generalisation is always a problem with ANN. A method has to be developed to ensure that the program will be able to produce consistent results.

Regarding to challenge (1), two approaches have been established, one is to use polynomial curve fitting, the other is to use force data at different depth. As shown in Chapter 3, both approaches showed a reasonable accuracy in predicting the results, with the 2nd Polynomial approach being a more practical approach. Advantage of the trendline method lies in its ability to represent the P-h curve with two simple coefficients, which is later proven to be very useful in developing a computerised database and searching program for inverse modelling. The simple curve coefficients make it easy to store the data with minimum requirement on computational resources. The coefficient for any experimental data can be processed using program Excel by the user or if the full indentation curve is input, then it can be processed through a program using C or java

using least square approach, it is easy to be coded in the program. The efficiency and accuracy of the ANN has been compared with other approach such as 3D surfacing, and interpolation approach and showed better performance, the results is to be present in section 5.2.

The challenge (2) is mainly relevant to the trend line fitting approach. The work systematically analysed the use of MSE in assessing the performance of the ANN program. It was found that MSE could be used as a primary indication but could not directly tell the performance of the ANN program with different neuron numbers. In addition, the direct use of the error in the polynomial coefficient (a_1 and a_2) is also not physically meaningful, as for polynomial fitting, the coefficients is not necessarily unique, i.e. different combination of a_1 and a_2 may produce similiar P-h curves, so the closeness of the prediction to the target value is not necessarily represents a physical condition why the force at a depth close to the true value. As shown in Figures 3.14-16, the most effective way is to directly use the P-h curves based on polynomial coefficients predicted to assess the performance of the prediction. This is the most valid one to determine the outcome including establishing the optimum number of neurons as shown in Figure 3.14. The advantage of using 2nd order polynomial fitting lies that fact it is easy to program to calculate the force at different depth automatically, thus make the comparison very easy to achieve through averaging the relative error.

Regarding to challenge (3), as pointed out in the literature review (section 2.5.2) and other publications (Masters, 1993; Lawrence et al, 1996; Finlay 2004; Wan et al, 2009), it is difficult to achieve full generalisation with ANN. An approach has to be developed that is statistically robust for material related works. From the frequency analysis (Figure 3.19 and 3.22), each ANN prediction could produce around 95% of prediction of acceptable accuracy (within 5%). The work showed that if the ANN is run more than 5 times, then the result could be fairly accurate and repeatable. The average can be done either by averaging the coefficients or average the force directly as shown in Figure 3.20. The new approach proposed and assessed is based on the fact that ANN produces discrete results for the different input data and ANN simulation, so it is unlikely that the inaccurate results will repeatedly appear at the same material data point. Based this understanding, the accuracy

of the predication can be improved by running the ANN several times. The program is set to clear all initial value and start completely from a new set of initialised data. This method is able to produce prediction data with consistence accuracy (e.g. Figure 3.16). This has laid a good frame work in predicting P-h curves based known material properties. The detailed results for ANN P-h curve prediction with other condition (such as R6, thickness t12mm, etc.) was not shown to preserve clarity and avoid repeat, but all the tests have showed similar trend in terms of accuracy, repeatability.

The ANN program is an important development as it can produce P-h curves over a wide range of properties in a quick and convenient way, which in itself could give the user a direct perception of the indentation resistance of the foam (thick or thin). The approach has been tested on several thicknesses (10, 12, 15, 20, 30mm) and indenter size (including R6, R4 and R2mm) has been tested, in all cases the ANN is able to predicted the P-h curves close to the FE simulation. Most of the work reported in this thesis has been focused on R4 and R6 as these two testing conditions are easier to control in the test. With R2, the results become much more sensitive to the testing condition as the indenter is small. The ability of predicting the indentation curve of foam with different thickness is also useful as foam can be supplied/used in a variety of thicknesses. As detailed in Chapter 3, the performance of ANN is evaluated through a detailed process in particular the effect of neuron number including using MSE, the relative error, neuron number of 20 was found to be the optimum number. This was found to be applicable to all the thickness case. The frequency analysis is found to be an effective way to analyse the data, as for material testing, robustness is crucial. In a real test case, maybe only the P-h for one material property is needed, it has to be 100%. The approach tested using the average of 5 ANN test showed consistent results. This has make use of the fact that ANN prediction is discontinuous.

One typical application of the ANN program is shown in Chapter 4 in developing inverse material property identification programs. The ANN direct program has provided a much quicker way to provide extensive data for the development of a new computerised inverse modelling approach (post FE modelling) to map/predict material parameter from multiple indentation tests. This allowed the dual indenter approach to be extensively investigated to establish the data distribution to given user a full picture thus improve the confidence in

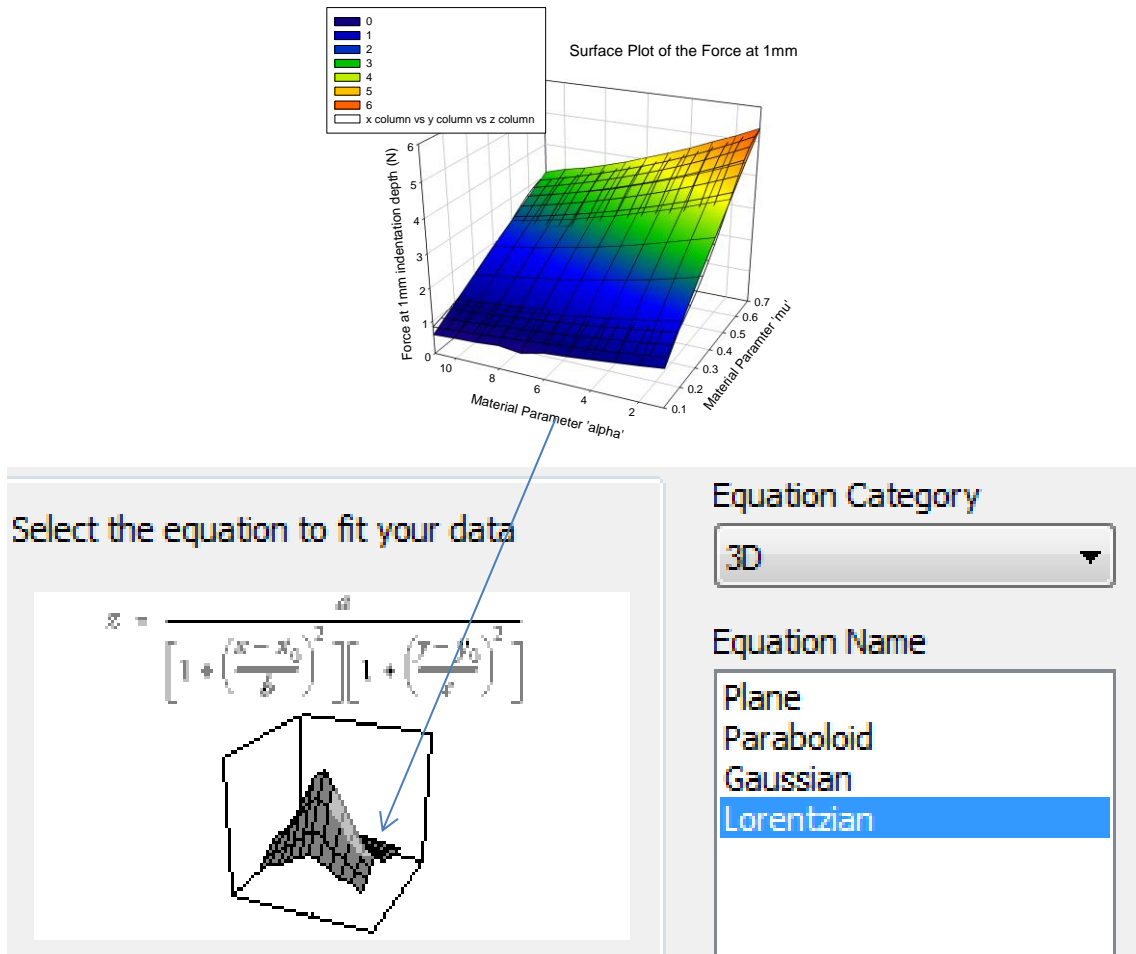
the inverse results. As a new finding, it was found that with dual indenter, the majority of predicted data will be confined to a local zone close to the target data, but there are other areas where the material parameter can match both R4 and R6. This is a key fact that was not identified by other approach such as interactive searching or Kalman filter (Li, 2009; Aw et al, 2014). Based on ANN program, a new approach has been developed to use samples of different thicknesses rather than different indenter sizes, which could effectively avoid the requirement on change of indenters that is complex and requires calibration of the system. Both approaches (i.e. dual indenter size or dual thickness) are fully validated against blind tests (using numerical data as target) and experimental data (Chapter 4). The approach is currently being assessed to be used in testing the effects of temperatures of on EVA foam and rubber like materials, which is difficult with other approaches.

5.2 Comparison of the ANN approach with other methods (data file: EVA_Foam_3)

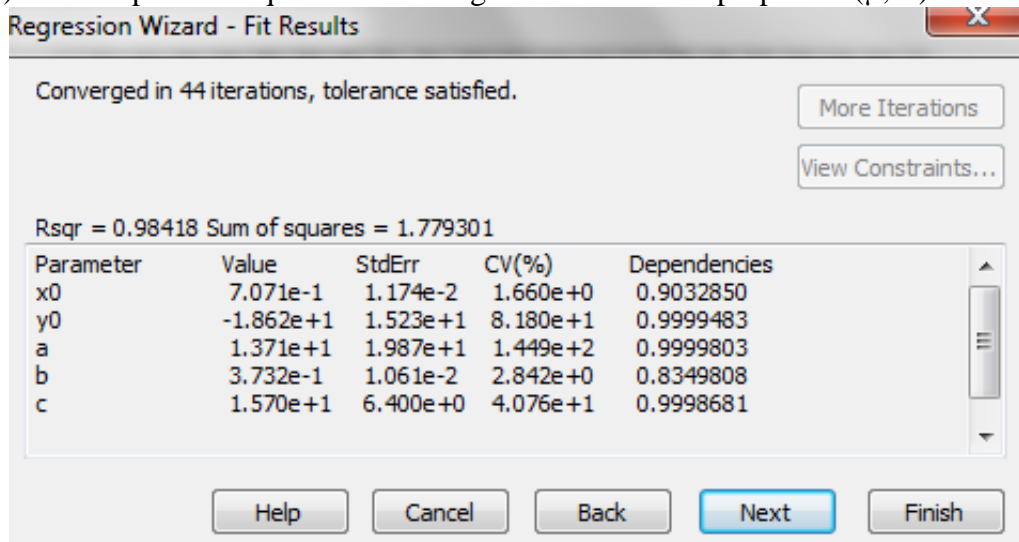
For predicting P-h curves, preliminary work has been conducted using surface plotting approach (sigma plot) and interpolation approach (Matlab). In the surface mapping approach, the force at different depth were fitted with an equation using simgplot, then P-h curve is predicted. Figure 5.1 shows a typical surface plot at depth of 1mm based on materials data set 1 (μ 0.1-0.7, α 1-11) with the Lorentzian equation. Several other equations are available, including Paraboloid, Gaussian and Lorentzian. As shown in the figure, the Lorentzian equation is not able to fit the data as the standard deviation of some coefficient is very high. For example, the parameter 'y0' and 'a' and 'c' in the equation are all very high which suggest that the approach is not feasible.

Another approach explored in the early stage of the project is using line interpolation rather than surface fitting. The concept is illustrated in Figure 5.2(a). In this process, the P-h curve was divided into 100 evenly distributed points along its depth. In the second stage, at each alpha value used in the matrix (in this case $\alpha=1, 2, 3, 4, 5, 6, 7, 8, 9, 10, 11$), the force vs ' μ ' is fitted with a high order polynomial function; then the force for material with a given ' μ ' value (same as the input data) but different ' α ' can be determined ($\mu, 1$ to 11) with 11 points. Then another fit with polynomial function can be determined, which can be used to predict the value for the input ($\mu=x1, \alpha=y1$). This process is repeated over all the depth point, then the full P-h curve can be determined. Figure 5.2(b) shows a typical results with materials parameter ($\mu=0.5, \alpha=6$), the program used the same number of P-h curves and data range as the ANN program (Material data set-1 with 77 data). As shown in the figure, the predicted P-h curve is reasonably close to the target (FE data), but not as good as the ANN prediction. During the process of exploring this method, it was found that more data has to be used in the building the simulation space to further improve the accuracy. In addition, the simulation speed of the polynomial fitting is much slower than the ANN process. The polynomial program typically need a few minutes to simulate one curve, while the ANN can produce thousands of data in a few minutes. This clearly shows that the ANN approach is a better option. In terms of comparison between ANN and FE, the ANN is post modelling method which doesn't require re-run of the FE model, this is a significant advantage in terms demand on FE related resource, which can be costly in

terms time and resource. An FE job of similar nature typically runs typical 2-5 minutes, which is much slower the ANN program established.



(a) Surface plot and equation for fitting force vs material properties (μ , α).



(b) Typical results and error data.

Figure 5.1 Sample figure to illustrate the process of 3D surface mapping and typical data showing the error range. The data shows that the process is not suitable for predicting indentation curve of hyper foam model.

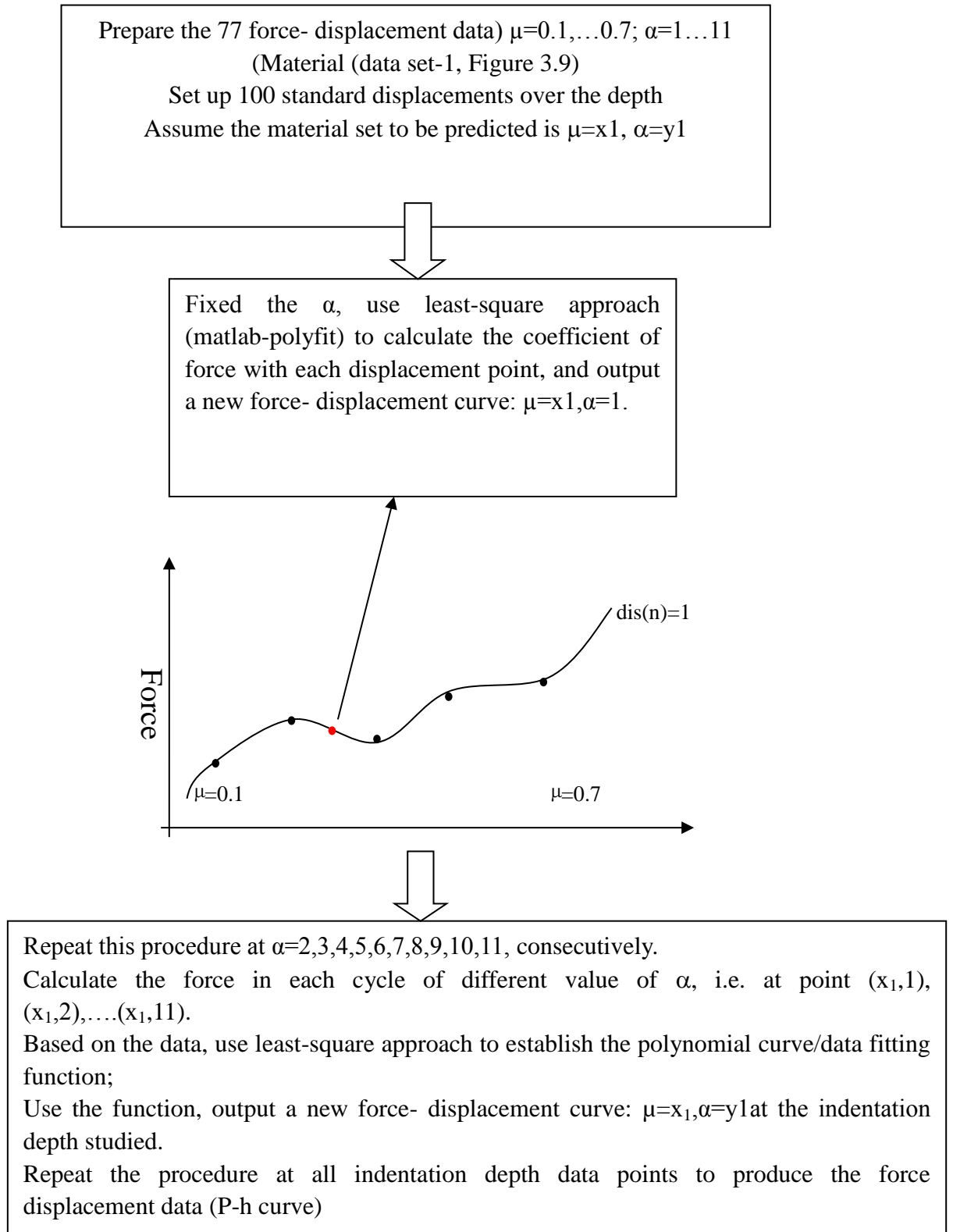


Figure 5.2 (a) Program for polynomial point fitting.

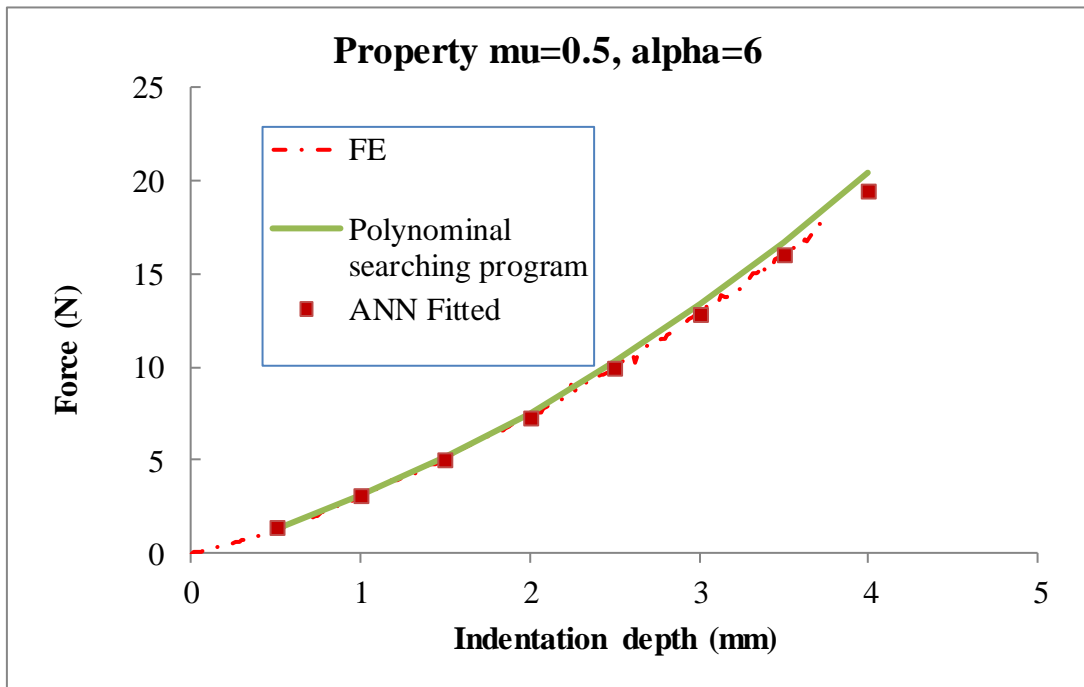


Figure 5.2(b) Comparison between the original FE P-h curve, ANN predicted and curve predicted directly though polynomial point fitting.

5.3 Inverse modelling and data analysis method

As shown in Figures 4.7-15, the use of ANN in inversely identifying the material properties are much more complicated than predicting the P-h curves. Given the uncertainty with inverse modelling, the use of nftool is shown to be very effective in establishing/exploring the possibility/feasibility when using P-h curves to identify the material parameters. The use of 2nd order polynomial and 3rd order polynomial and depth data are all explored. The results show that using polynomial curve fitting coefficients could not explicitly predict the material data for untrained data. This is probably due to the fact that the relationship between the curve and properties are not unique. i.e. one P-h curve (or force at a given depth) could be closely correlated to many different set of properties; this is approved by later program mapping through detailed materials. As shown in Figures 4.19, 4.20 and 4.26, for one input P-h curve parameters, there are many material property sets that can produce P-h curve closely matching the input data. This made is not possible to produce a working ANN to predict untrained data. In a direct ANN prediction process, each material set only corresponds to one p-h curve, so the direct process works OK. The results show that only way to use ANN is to train the ANN with extensive training data of very small increment of properties and large number of neurons, then the program can be used as an inverse tool. In some cases, this can be a useful feature; however, this requires the running of large amount of FE models, which will be time and resources consuming and not practical.

The new approach proposed and evaluated made use the function of ANN in direct P-h curve prediction, then use a computer searching program to effectively identify all the possible materials property sets that can produce P-h curve within a certain error range. The work on blind tests (using FE data) and experimental works showed that the method is an effective approach. The focus of the approach is to identify any possible materials properties set rather than only using limited data. The advantage of the approach in comparison with other methods such as interactive methods lies in the fact that it can identify/map out all potential material properties set, to give the user a full confidence. While interactive method may end up converge to a local minimum rather than a global minimum (Aw 2014). The new approach developed in this work, is also improvement from

some post modelling approach. For example, in the work on using Kalman filter approach (Li, 2009), several initial input value (over 10) has to be assigned to repeat the inverse program to avoid ill conditioning, which is time and resource consuming and could not achieve full confidence. So ANN program fits the situation for indentation and material related research better than for these situation where the identification of the full range is crucial, then the property search can be further improved through combination of tests (such dual indenter size, dual thickness etc.) or through pre-knowledge.

The idea behind using tests under different conditions is an effective way to improve the robustness of the prediction. The establishment of using ANN to predict the P-h curves opened up a new way of enhancing the use of this method through combining different tests. Dual indenter method is widely regarded as a good approach (Luo and Lin 2008; Tho et al, 2004), which is easy to implement. However, it do require the change of indenter, for some tests on soft material (in particular in testing at different environments, such as temperature, humidity), change of indenter can be complicated and requires calibration the system each time. The new approach proposed using dual thickness is much simpler. Once the potential material sets have been identified using the computer program, it is still a challenging task to combine the data from different conditions (such as indenter size or thickness). The results in this work showed that the material sets can be identified by plotting the material with lower objective function/relative error, then identify the overlapping points. This is probably better than some other methods. Other approaches assessed is to use the sum of the objective functions for different condition. For example for dual indenter, the average/sum of the error or objective function for indenter size 4 and 6 can be used. The use of sum of the objective functions is easier to implement mathematically, however, since the force value could be quite different in some situation (e.g. indenter size), then error in one condition may become much higher than the other condition, so one set of data become more dominant, thus cause error in the prediction. For example, the force in R6 is much higher than R4. As presented in Chapter 3 as a comparison to the approach using overlapping points, another approach is to plot the trendlines for the material sets with lower objective functions, the cross point between the

two set of data is assumed to be the true/best material properties. This method has been used in studying the combination of dual sharp indenters on metal materials (e.g. Luo and Lin 2007). However, this method is not suitable for hyperfoam materials. As shown in Figure 4.32, the data for R4 and R6 can be approximated as linear line and there is clear cross point. The point is close to the target value but not very accurate (Figure 4.31). In some case with experimental data, the trendline intersection point is not always available as shown in Figure 4.32(b) or Figure 4.33. To this aspect, the new approach by using overlapping point is a better methodology. From programming point of view, this approach is much easier to implement in computerised program.

Based on detailed research, the ANN program and the inverse program can be directly used in material research works. For example, the direct P-h prediction ANN is currently used to help the development of analytic models of hyperfoam P-h curves (Ren and Su, 2014). The inverse approach is also being transferred to other material testing processing and engineering problems, for example indentation bending tests of rubber (Aw, 2013), prediction of the temperature in the heat affected zones of spot welded joints (Norbury, 2013). Work is also to be conducted to use the program to test EVA foam at different temperatures using different indenter sizes and thicknesses with the program established.

Chapter Six

Conclusions and Future Works

6.1 Summary and conclusions

In this project, an ANN program has been developed to predict the indentation P-h curves with known properties (hyperfoam material parameter, μ and α). An interactive parametric FE model and python programming based data extracting program has been developed and used to develop data for the ANN program. Two approaches have been proposed and evaluated to represent the P-h curve. One is using 2nd order polynomial trendline approach ($P=a_2h^2+a_1h$), the other is to use the forces at different indentation depth. The ANN program is developed with early stopping mechanism, the effect of the transfer function and number of neurons was systematically analysed using three set of material matrix data. The performance of the ANN based on the trendline approach is evaluated with MSE and relative error of the coefficient 'a2' and 'a1' and then, the average error in forces over different depths. A frequency method is used to analyse the data, which provided important data/base to further enhance the accuracy of the P-h curve prediction based on averaging multiple ANN tests. This approach effectively taking use of the fact that ANN prediction is not continuous around any property point. Sensitivity tests with purposely introduced error in the input to ANN showed that the approach is accurate and robust. The ANN program with the depth based approach showed similar accuracy in predicting P-h curves of hyperfoam materials. The work is initially developed based on indenter size of 4mm, it was then transferred to an indenter size of 6mm, both were used to predict P-h curves and compared directly to experimental data of two EVA foams with known properties. Comparison with other approaches (including surface mapping and direct data space fitting process) showed that the ANN program is accurate and much quicker than some other commonly used approach and direct FE modeling. This will provide an important tool in analysis of foam testing and development of new computerized inverse program.

The feasibility of using ANN to directly predict the material properties was evaluated including assessing its capacity to predict trained data and untrained data. The use of 2nd order and 3rd order polynomial curve fitting of the force displacement curve is compared. In addition, the use of single indenter approach and dual indenter approach is assessed. It

was found that the approach with 2nd order polynomial fitting of the P-h curves is not able to predict the material properties. Using 3rd order fitting showed some improvement and it is able to predict the trained data accurately but could not be used to train untrained data. Works on dual indenter approach with R4 and R6 showed some improvement in predicting untrained data but could not produce data with reasonable accuracy of the full dataset.

A new inverse material parameter identification approach utilising the direct ANN program established is developed. A computerised program (with web interface) has been developed including data generation through ANN, data storage, interface for input and viewing results. A searching program is developed which enables the identification of possible materials property sets that match the experiment data within a predefined error range. The approach is applied to analysis single and dual indenter data through blind tests with model materials (with known material properties). A new and novel approach using foam of different thickness is also proposed to further improve the robustness of the program. The results showed that in a single indenter approach, there are multiple materials property sets that can produce similar P-h curves suggesting that the results are not unique. Dual indenter size approach showed a significant improvement but the new program successful identify additional material property sets that can produce P-h curve that match both R4 and R6 data. This suggests the dual indenter method with hyperfoam model is not 100% unique, this was not identified previously with other inverse program. With the new approach proposed, using the tested data on samples of different thickness showed that the uniqueness of the prediction can be improved. A new approach to identify materials properties through analysing overlapping data is also analysed and showed clear improvement than other approaches (e.g. sum of objective function methods, and trendline intercepting point method) when dealing with data from different testing conditions. The accuracy and validity of the program is firstly assessed with blind tests (using numerical data as input/target) then used to predict the properties of the EVA foam samples. This is not only further validating the program and method but also identify issue with real material test data in comparison with blind tests, as experimental data are not as perfect as FE generated data. Some key results of the real foam data is compared to the target and

prediction results from other approaches and data processing method, the comparison results showed that the new ANN base computer program has clear improvement in accuracy, robustness and efficiency in predicting the parameters of EVA foams.

The outcome of work has contributed new knowledge in materials characterisation and inverse modelling in particular in the development of a new ANN approach to predict the indentation P-h curves of hyperfoam materials and establishment of a new computerised program to inversely predict the material parameters from indentation tests of different conditions. The program and the results on EVA foams have laid a solid platform for future works.

6.2 Recommendations for future works

One area is to use the approach to study other material systems and testing method such as rubber, PU foam etc, All these materials are widely used. The methodology developed represents a general approach which can be used in many other materials testing systems. One particular test of interest is indentation bending tests in which an indenter is pressed onto a thin film (e.g. rubber, biological tissues) clamped onto a tube; In another project, the frame work of ANN has helped with predicting the temperature history of the heat affected zones in resistance spot welding using remote thermal couples.

One area is to apply the method in testing foam at different environments such temperature effects, as mentioned in the literature review, it is difficult to be performed the standard shear tests at different environments. Another area to be explored is to use the program as a quick way of identifying the sample properties in material development of foam or rubber with different composition. With this method, many small samples can be made with different thickness, and then the property can be estimated using the program developed. This could represent significant cost and time saving. In situations like these, the range change of property can be further narrowed/estimated through pre-knowledge. A special function can be incorporated in the computer program to allow the user to do it.

Some of the practical techniques in programming and data analysis established have made it easier to convert the program into a computer system. Future work will incorporate more material systems in the computer program to cover different types of indenter shape and tests.

References

- ABAQUS 6.10 User's Manual, ABAQUS, Inc, Providence, RI.
- Adeloye AJ and De Munari A, 2006, Artificial neural network based generalized storage–yield–reliability models using the Levenberg–Marquardt algorithm, *Journal of Hydrology*, 362, 215–230.
- Aldrich C, 2002, *Exploratory Analysis of Metallurgical Process Data with Neural Networks and Related Methods*, Elsevier, London.
- Altun F, Kis IO, Aydın K, 2008, Predicting the compressive strength of steel fibre added lightweight concrete using neural network. *Computer Material Science*, 42(2), 259–65.
- Aw J, 2013, Inverse properties prediction of blow moulded plastic, PhD Project (In process). Liverpool John Moores University.
- Baldi P, 1995, Gradient descent learning algorithm overview: a general dynamical systems perspective, *IEEE Transactions on Neural Networks*, 6/1, 182-194.
- Barnard E and Wessels L, 1992, Extrapolation and interpolation in neural network classifier, *IEEE Control; Systems*, October, 50-53.
- Benchebra D, 2008, *Artificial Neural Network-Based Control for process Tomography Applications*, Phd Thesis, Manchester Metropolitan University.
- Budiarsa N, Norbury A, Su X, Bradley G and Ren XJ, 2013, Analysis of Indentation Size Effect of Vickers Hardness Tests of Steels, *Advanced Materials Research*, 652-654, 1307-1310.
- Bishop CM, 2006, *Pattern Recognition and Machine Learning*, Springer, London.
- Bolzon G, Maier G and Panico M, 2004, Material model calibration by indentation, imprint mapping and inverse analysis. *International Journal of Solids and Structures*, 41, 2957-2975.
- Brescia M, 2012, DAME – Data Mining & Exploration - Quasi Newton Learning Method for Multi Layer Perceptron, March, 30.

- Briody C, Duignan B, Jerrams S and Tiernan J, 2012, The Implementation of a Visco-hyperelastic Numerical Material Model for Simulating the Behaviour of Polymer Foam Materials, *Computational Materials Science*, 64, 47–51.
- Coulibaly P, Ancti F and Bobee B, 2000, Daily reservoir inflow forecasting using artificial neural networks with stopped training approach. *Journal of Hydrology* 230, 244–257.
- Dao M, Chollacoop N, Van Vliet KJ, Venatesh TA and Suresh S, 2001 Computational modelling of the forward and reverse problems in instrumented sharp indentation, *Acta Mater*, 49, 3899–3918.
- Davidon WC 1968, Variance algorithm for minimization. *Computer Journal*, 10, 406.
- Davidon Wc, 1991, Variable Metric Method For Minimization, *Siam J Optimization*, 1/1, 1-17.
- Delalleau A, Josse G, Lagarde, JM, Zahouani, H, Bergheau, JM, 2006, Characterization of the mechanical properties of skin by inverse analysis combined with the indentation test, *Journal of Biomechanics*, 39/9, 1603-1610.
- Demir F, 2008, Prediction of elastic modulus of normal and high strength concrete by artificial neural network, *Construction Build Mater*, 22/7, 1428–35.
- Demuth H and Beale M, 2008, *Neural Network Toolbox for use with Matlab*. The Mathworks, Inc Natick.
- Esfahani MB, Toroghinejad MR and Yeganeh AR, 2009, Modelling the yield strength of hot strip low carbon steels by artificial neural network, *Material and Design*, 30, 3653-3658.
- Finlay JP, 2004, Numerical methods for the stress analysis of pipe-work junctions, PhD Thesis, Liverpool John Moores University, UK.
- Gerard JM, Ohayon J, Luboz V, Perrier P and Payan Y, 2005, Non-linear elastic properties of the lingual and facial tissues assessed by indentation technique Application to the biomechanics of speech production, *Medical Engineering & Physics*, 27, 884–892.
- Giannakopoulos AE, 2006, Elastic and viscoelastic indentation of flat surfaces by pyramid indenters, *Journal of the Mechanics and Physics of Solids*, 54, 1305-1332.

Gilbert JC and Lemareichal C, 1989, Some Numerical Experiments With Variable-Storage Quasi-Newton Algorithms, *Mathematical Programming*, 45, 407-435.

Gong L; Liu C, Li Y and Yuan F, 2012, Training Feed-forward Neural Networks Using the Gradient Descent Method with the Optimal Stepsize, *Journal of Computational Information Systems*, 8/4, 1359-1371.

Gu Y, Nakamura T, Prchlik L, Sampath S and Wallace J, 2003, Micro-indentation and inverse analysis to characterize elastic-plastic graded materials. *Materials science and Engineering*, A345, 223-233.

Gu YD, 2010, Biomechanical Investigation of the Human Foot Deformation under Different Landing Conditions Using Finite Element Analysis, PhD thesis, Liverpool John Moores University, UK.

Gu YD, Ren XJ, Lake M and Li JS, 2010, Heel skin stiffness effect on the hind foot biomechanics during heel strike, *Skin Research and Technology*, 5, 1–6.

Gu YD, Li JS, Lake MJ, Zeng YJ; Ren XJ, Li ZY, 2011, Image-based midsole insert design and the material effects on heel plantar pressure distribution during simulated walking loads. *Computer Methods in Biomechanics and Biomedical Engineering*, 14/8, 747-753.

Gualano L, 2008, Development of Artificial Neural Network Techniques for Prediction of Wheel-Rail Forces, PhD Thesis, The Manchester Metropolitan University, UK.

Hagan MT and Menhaj M, 1999, Training feed-forward networks with the Marquardt algorithm. *IEEE Trans Neural Network*, 5/6, 989–93.

Harkin S, 1994, *Neural Networks: A Comprehensive Foundation*. Prentice Hall PTR, USA

Harsono E, 2009, Material Characterization *Via* Simulated Indentation Test Including Effect Of Friction, Phd Thesis, National University Of Singapore.

Hendriks FM, Brokken D, Oomens CWJ, Bader DJ, Baaijens FTP, 2006, The relative contributions of different skin layers to the mechanical behavior of human skin in vivo using suction experiments. *Medical Engineering & Physics*, 28, 259-266.

Huber N, Tsagrakis I and Tsakmakis C, 2007, Determination of constitutive properties of thin metallic films on substrates by spherical indentation using neural networks,

- International Journal of Solids and Structures, 37, 6499-6516.
- Ince R, 2004, Prediction of fracture parameters of concrete by artificial neural networks, Eng Fract Mech, 71/15, 2143–59.
- Jordan P, Socrate S, Zickler T E, Howe RD, 2009, Constitutive modeling of porcine liver in indentation using 3D ultrasound imaging, Journal of the mechanical Behaviour of Biomedical materials, 2, 192-201.
- Karlik B and Olgac AV, 2005, Performance Analysis of Various Activation Functions in Generalized MLP Architectures of Neural Networks, International Journal of Artificial Intelligence And Expert Systems (IJAE), 1/4, 111-122.
- Kavzoglu T, 2009, Increasing the accuracy of neural network classification using refined training data, Environmental Modelling & Software, 24, 850–858.
- Khin Z, Liu GR, Deng B and Tan KBC, 2009, Rapid identification of elastic modulus of the interface tissue on dental implants surfaces using reduced-basis method and a neural network. Journal of Biomechanics, 42, 634-641.
- Kong X, Yang Q, Li B, Rothwell G, English R, Ren XJ, 2008, Numerical study of strengths of spot-welded joints of steel. Materials and Design, 29, 1554-1561.
- Kong X, Shi Y, Li B, Rothwell G, English R, Yang Q and Ren XJ, 2009, Effect of Indenter Shapes on Inverse Plastic Parameters Identification of Metals on Dual Indenters Method", International Journal of Materials Research, 7, 950-953.
- Kunz J and Studer M, 2006, Determining the Young's Modulus with shore hardness test, Kunststoffe International, June, 92-94.
- Lawrence S, Giles CI and Tsoi CA, 1996, What Size Neural Network Gives Optimal Generalization? Convergence Properties of Backpropagation, Report, Institute for Advanced Computer Studies, University of Maryland
- Lee JA, 1998, Fatigue-life prediction of fibre-reinforced plastics by using artificial neural networks, PhD Thesis, The University of Bath, UK.
- Lek S and Guegan JF, 1999, Artificial neural networks as a tool in ecological modelling, an introduction. Ecological Modelling 120, 65–73.
- Li B, 2009, Development of An Inverse FE Modelling Method for Material Parameters Identification Based on Indentation Tests. PhD Thesis, Liverpool John Moores

University.

Likas A and Stafylopatis A, 2000, Training the random neural network using quasi-Newton methods, *European Journal of Operational Research*, 126,331-339.

Lippman R, 1987. An introduction to computing with neural nets. *IEEE ASSP Mag.* 4, 4–22.

Lippmann R, 1987. An introduction to computing with neural nets, *IEEE ASSP Mag.* 4, 4–22.

Liu H, 2010, On the Levenberg-Marquardt Training Method for Feed-Forward Neural Networks, *Sixth International Conference on Natural Computation (ICNC 2010)*, 456-460.

Luo J and Lin J, 2007, A study on the determination of plastic properties of metals by instrumented indentation using two sharp indenters, *International Journal of Solids and Structures*, 44, 5803–5817.

Maier HR and Dandy GC, 2000, Neural networks for the prediction and forecasting of water resources variables: a review of modelling issues and applications. *Environmental Modelling & Software*, 15, 101–124.

Mansour MY, Dicleli M, Lee JY and Zhang J, 2004, Predicting the shear strength of reinforced concrete beams using artificial neural network. *Eng Struct*, 26/6, 781–99.

Masters T, 1993, *Practical Neural Network Recipes in C++*, NY: John Wiley and Sons,

Matlab Manual, <http://www.mathworks.co.uk/help/matlab/ref/menu.html> (accessed JAN 2014)

Meng Y and Lin B, 2008, A feed-forward artificial neural network for prediction of the aquatic ecotoxicity of alcohol ethoxylate, *Ecotoxicology and Environmental Safety*, 71, 172–186.

Meuwissen, MHH, Oomens, CWJ, Baaijens, FPT, Petterson, R and Janssen, JD, 1998, Determination of the elasto-plastic properties of aluminium using a mixed numerical–experimental method'. *Journal of Materials Processing Technology*, 75, 204–211.

Mills N and Zhu H, 1999. The high strain compression of closed cell polymer foam. *Journal of the Mechanics and Physics of Solids*, 47, 669-695.

- Mills NJ, Fitzgerald C, Gilchrist A and Verdejo R, 2003, Polymer foams for personal protection: cushions, shoes and helmets, *Composites Science and Technology*, 163, 2389–2400.
- Mirzaee 2009 Long-term prediction of chaotic time series with multi-step prediction horizons by a neural network with Levenberg–Marquardt learning algorithm, *Chaos, Solitons and Fractals*, 41, 1975–1979.
- Moreu YM and Mills NJ, 2004, Test method-rapid hydrostatic compression of low density polymeric foams. *Polymer Testing*, 23, 313-322.
- Nakamura T, Wang T and Sampath S, 2000, Determination of properties of graded materials by inverse analysis and instrumented indentation, *Acta materialia*, 48, 4293-4306.
- Neaupane KM and Sugimoto M, 2003, An inverse boundary value problem using the extended Kalman filter. *Science Asia*, 29, 121-126.
- Norbury A., 2013, Prediction of the thermal history of HAZ in resistance spot welding usingin remote thermal couples, PhD project, Liverpool John Moores University, UK.
- Pal S, Pal SK and Samantaray AK, 2008, Artificial neural network modeling of weld joint strength prediction of a pulsed metal inert gas welding process using arc signals. *Journal of materials processing technology*, 202, 464–474.
- Pala M, Ozbay E , Ahmet Oztas A and Yuce M, 2007, Appraisal of long-term effects of fly ash and silica fume on compressive strength of concrete by neural networks, *Construction and Building Materials*, 21, 384–394
- Pala M, Ozbay E, Oztas A and Yuce MI, 2007, Appraisal of long-term effects of fly ash and silica fume on compressive strength of concrete by neural networks, *Construction Build Mater*, 21/2, 384–94.
- Partheepan G, Sehgal DK, and Pandey RK, 2011, Quasi-Non-Destructive Evaluation of Yield Strength Using Neural Networks, *Advances in Artificial Neural Systems*, 1-8.
- Petre MT, Ahmet EE and Peter CR, 2005, Determining Foam Parameters for Complex Biomechanical Loading Simulations. Summer Bioengineering Conference, Vail, Colorado.
- Petre MT, Erdemir A and Cavanagh PR, 2007, Determination of elastomeric foam

parameters for simulations of complex loading, *Computer Methods in Biomechanics and Biomedical Engineering*, 9, 231-242.

Prechelt L, 1994, A set of neural network benchmark problems and benchmarking rules, Technical report 21/94, University of Karlsruhe, Karlsruhe, Germany.

Ren XJ, Hooper RM, Griffiths C and Henshall LJ, 2002, Indentation size effect (ISE) in single crystal MgO. *Philosophical Magazine A*, 82/10, 2113-2120.

Ren XJ, Silberschmidt VV, 2008, Numerical modelling of low-density cellular materials'. *Computational Materials Science*, 43, 65-74.

Ren XJ, Smith CW, Evans KE, Dooling P, Burgess A, Wiechers J, Zahlan N, 2006, Experimental and numerical investigations of the deformation of soft materials under tangential loading. *International Journal of Solids and Structure*, 43, 2364-2377.

Rumelhart DE, Hinton GE, and Williams RJ, 1985, Learning internal representations by error propagation. Report, University of California.

Rumelhart DE, Hinton GE, and Williams RJ, 1985, Learning internal representations by error propagation. *Nature*, 323, 533-536.

Shanno DF, 1970, Conditioning of quasi-Newton methods for function minimization. 1970, *Mathematics of Computation*, 24, 647-656.

Sibi P, S Allwyn Jones Sa And Siddarth P, 2013, Analysis of different activation functions using back propagation neural networks, *Journal of theoretical and applied information technology*, 47/3, 1264-1268.

Tho KK, Swaddiwudhipong S, Liu Z S and Hua J, 2004, Artificial neural network model for material characterization by indentation. *Modelling and Simulation In Materials Science and Engineering*, 12, 1055-1062.

Tho KK, Swaddiwudhipong S, Liu ZS, Zeng K and Hua J, 2004, Uniqueness of reverse analysis from conical indentation tests. *Journal of Material Research*, 19/8, 2498-2502.

Tong J, Lim CS. Goh OL, 2003, Technique to study the biomechanical properties of the human calcaneal heel pad'. *The Foot*, 13, 83-91.

Ullner C, Beckmann J and Morrell R, 2002, Instrumented indentation test for advanced technical ceramics. *Journal of the European Ceramic Society*, 22, 1183-1189.

Verdejo R and Mills N, 2004, Heel-shoe interactions and the durability of EVA foam

- running-shoe midsoles. *Journal of Biomechanics*, 37,1379-1386.
- Verdejo R and Mills NJ, 2004, Simulating the effects of long distance running on shoe midsole foam, *Polymer Test*, 23/4, 567-574.
- Wan W, Mabou S, Shimada K and Hirasawa K, 2009, Enhancing the generalization ability of neural networks through controlling the hidden layers, *Applied Soft Computing*, 9/1, 404–414
- Wu MH, Lin W and Duan S, 2006, Developing a neural network and real genetic algorithm combined tool for an engine test bed, *Proceedings of the institution of mechanical engineers, Part D: Journal of Automobile Engineering*, 220L 1737-1753.
- Zaw K, Liu GR, Deng B and Tan KBC, 2009, Rapid identification of elastic modulus of the interface tissue on dental implants surfaces using reduced-basis method and a neural network. *Journal of Biomechanics*, 42, 634-641.
- Zhao W, Li K, and Irwin GW, 2013 (Feb), New Gradient Descent Approach for Local Learning of Fuzzy Neural Models, *IEEE transactions on fuzzy systems*, 21/1, 30-44.